Investigating novel pathways in B cell mediated autoimmunity in the context of the disease juvenile dermatomyositis

Meredyth Grace Llewellyn Wilkinson

A thesis submitted for the degree of Doctor of Philosophy to University College London

Supervisors

Dr. Elizabeth Jury

Prof. David Isenberg

Dr. Kiran Nistala

Centre for Adolescent Rheumatology

University College London

5 University Street

London

WC1E 6JF

January 2018

Declaration

I, Meredyth Wilkinson, confirm that the work presented in this thesis is my own. Where information has been derived from other sources, I confirm that this has been indicated in this thesis.

……..

Meredyth Wilkinson

Date

Dedication

I would like to dedicate my thesis in loving memory of my Nana, Ann Richardson, who peacefully passed away on the 18th September 2017.

Abstract

The Inflammatory Idiopathic Myopathies (IIM) are a rare group of myopathic autoimmune diseases diagnosed in both adults and children. Patients present with proximal muscle weakness and Gottron's papules. Immunohistochemical analysis of muscle tissue from these patients has identified immune cell infiltrate and the expression of pro-inflammatory cytokines however, little is known about the peripheral immunological profile in juvenile and adult patient groups.

There are three aims: Firstly, to investigate mechanisms driving B cell lymphocytosis and define pathological features of B cells in the blood of Juvenile Dermatomyositis (JDM) patients. Secondly, to identify specific immune cell signatures and cytokine profiles for myositis disease subtypes and correlate this data with measurements of disease activity. Finally, to delineate a correlation between the up-regulated type I interferon signature and dysfunction of cholesterol homeostasis in immune cells.

Using a combination of cell culture, flow cytometry, RNA-seq, q-PCR and ELISA techniques this study has assessed the immune cell signature, B cell biology and IFN related mechanisms in patients with IIM. The results identified that JDM patients with active disease have a significantly expanded immature B cell population which was correlated with a type I IFN signature. Activation through TLR7 and IFN-α may drive the expansion of immature B cells in JDM and skew the cells towards a more pro-inflammatory phenotype. There are unique immune signatures in adult disease sub-types, one example was an expanded Th17 population seen in adult dermatomyositis

(ADM). Lastly, IFN-α stimulation of T and B cells does change the expression of some genes that are part of the Hallmark cholesterol homeostasis pathway.

In conclusion, the work undertaken during my thesis provides further evidence that anti- IFNα biologics could be efficacious in the treatment of JDM. Also, the need for further investigation for the use of IL-17A inhibitors in the treatment of IIM.

Impact statement

This body of work has begun to delineate the peripheral immunological profile found in juvenile and adult IIM. The results identified that JDM patients with active disease have a significantly expanded immature B cell population which was correlated with a type I IFN signature. Activation through TLR7 and IFN-α may drive the expansion of immature B cells in JDM and skew cells towards a more pro-inflammatory phenotype. Novel immunophenotyping signatures have been identified in adult-disease subgroups, by disease activity and the presence of different auto-antibodies. Lastly, lipid rafts and cholesterol homeostasis may be altered by the up-regulation of type I interferon pathway in IIM patient immune cells. These findings paint a broader picture of the heterogeneity of IIM but also the importance of the re-occurring interferon theme found in many autoimmune diseases.

I have identified notable immune cell signatures that may impact the stratification of patients and inform the choice and response to treatment. My work substantiates a building body of evidence for the use of anti-IFN-α biologic agents and IL-17A inhibitors in the treatment of IIM.

This work has already resulted in the submission of a manuscript for publication in a peer-reviewed journal, and another is in preparation. Dissemination at National and International conferences have enabled my work to be critiqued an acknowledged by the scientific community.

Interaction with patients at clinics has fostered a relationship where I have been able to inform them about the broad aims of the research, and reciprocally they have been able to contribute with issues that concern them about the disease. I have developed a pipeline to recruit and process samples from child control volunteers from UCLH clinics in collaboration with the ARUK Centre for Adolescent Rheumatology at UCL, GOSH and UCLH. This experience also involved explaining my research and the impact it would have on patients to a wide public audience.

My PhD studies have introduced me to the area of translational medicine. With rare diseases, the concept of 'bench to bedside' can be extremely challenging with barriers including financial commitment, demand for the drug, suitable cohort size for clinical trials and the potential response to the drug within heterogenic disease groups. My work has implored to bridge the gap in IIM and highlighted the importance of this research to both the public and scientific communities.

Acknowledgements

The work presented in this thesis would not have been achieved without the support and assistance of so many people. Firstly, I would like to thank my supervisors Prof. David Isenberg and Dr. Liz Jury for their un-failing support and invaluable insights throughout my PhD. I would also like to thank Dr. Kiran Nistala for his guidance and motivation during the first year of my studies.

I have been fortunate to work across multiple laboratory groups including: Prof. Claudia Mauri, Dr. John Ioannou, Dr. Liz Jury and Prof. Lucy Wedderburn. I would like to thank all the fore-mentioned principle investigators. I have worked in close collaboration with Chris Piper and owe him a great debt of gratitude for all he has taught me and assisted me with laboratory work and preparing a body of work for publication. I would like to thank; Dr Claire Deakin for her assistance and expertise in bioinformatics; UCL genomics for RNA-sequencing, in particular Dr. Georg Otto and Dr. Dan Kelberman; the Juvenile Dermatomyositis Research Group (JDRG), including Dr. Raquel Marques, Stephanie Simou and Lucy Marshall, and the Center for Adolescent Rheumatology for patient recruitment and sample collection, including Ania Radziszewska, Dr. Kate Webb, Dr. Laura Hanns, Dr. Corinne Fisher, Hema Chaplin, Hannah Peckham, Linda Suffield, and Francesca Josephs. I would also like to thank Jamie Evans and Dr. Ayad Eddaoudi for their support with flow cytometry.

I would like to pay special thanks to the Jury group, Dr Claire Bradford, Kirsty Waddington, George Robinson, Nicolyn Thompson and Lucia Martin, for assisting

with sample collection and sharing their expertise on immunophenotyping and lipids. During the final year of my PhD I supervised David Ashby's BSc dissertation project, I would like to thank him for his hard work and contribution to my results.

I would not have been able to produce this body of work without the extremely generous sample donations from adult and juvenile patients and healthy volunteers, as such I am extremely grateful to all of them.

The patient samples were collected in conjunction with relevant patient information. I would like to thank Dr Jessica Manson, Dr Chris Wincup and Eve McLoughlin for all their help in obtaining and interpreting this information.

I would like to thank the Rheumatology Discretionary Fund UCL charity and the Centre for Adolescent Rheumatology who provided the funding for this PhD project.

The undertaking of a PhD is no mean feat and has an impact on those around you. With these thoughts, huge thanks go to Jonny Harries, my parents Lisa and Jonathan Wilkinson, my sisters Millicent and Dorothy Wilkinson, but also to my extended family and friends who have supported and inspired me along the way.

Table of contents

List of figures

List of tables

List of abbreviations

5NT1A	Cytosolic 5'nucleotidase 1A
Ag	Antigen
AHC	Adult healthy control
AM	Adult myositis
ANCA	Anti-neutrophil cytoplasmic antibodies
ANOVA	Analysis of variance
anti-PmScl	Anti-75-and 100kDa polymyositis/systemic sclerosis proteins
APC	Antigen presenting cell
APM	Adult polymyositis
BAFF	B cell activating factor
BCR	B cell receptor
Be1	B effector 1 cell
BILAG	British Isles Lupus Assessment Tool
BLK	B lymphoid tyrosine kinase
BM	Mature B cell
BSA	Bovine serum albumin
CCL	C-C motif chemokine ligand
CCL21	Chemokine (C-C motif) ligand 21
CCR7	CC chemokine receptor 7
CD62L	L-selectin
cDC	Classical dendritic cell

cDNA	Complementary DNA
CHC	Child healthy control
CHO	Chinese hamster ovary
CK	Creatine kinase
CM	Central memory
CMAS	Childhood myositis assessment scale
cMYC	MYC proto-oncogene, BHLH transcription factor
CRP	C-reactive protein
CSR	Class switch recombination
CTB	Cholera toxin-B subunit
CTD	Connective tissue disease
CV	Cardiovascular
CVB	Coxsackievirus B2/B4
CVD	Cardiovascular disease
CXCL	Chemokine (C-X-C motif) ligand
DAPI	4,6 diamidino-2-phenylindole
DC	Dendritic cell
°C	Degrees Celsius
DHCR7	7-Dehydrocholesterol reductase
DM	Dermatomyositis
DMARDs	Disease modifying anti-rheumatic drugs
DMSO	Dimethyl sulfoxide
DNA	Deoxyribonucleic acid
dNTP	Deoxynucleotide triphosphate
dTTP	Thymidine triphosphate

dUTP	Deoxyuridine triphosphate
EDTA	Ethylenediamine tetra-acetic acid
(Anti-)EJ	Glycol-tRNA synthetase
ELOVL5	ELOVL fatty acid elongase 5
EM	Effector memory
EMG	Electromyogram
EMRA	Effector memory CD45RA+ T cells
ER	Endoplasmic reticulum
ERK	Extracellular signal-regulated kinases
ESR	Erythrocyte sedimentation rate
FACS	Fluorescence-activated cell sorting
FASN	Fatty acid synthase
FBS	Foetal bovine serum
FBX06	F-box 06
FCS	Foetal calf serum
FDR	False discovery rate
FO	Follicular
FoxP3	Forkhead box P3
FSC	Forward scatter
Fv	Variable domain
G1P2	ISG15 ubiquitin-like modifier
GC	Germinal centre
GM1	Monosialotetrahexosylganglioside
GSEA	Gene set enrichment analysis
GSL	Glycosphingolipid

GWAS	Genome-wide association study
Gy	Gray
(Anti-)Ha	Tyrosyl tRNA synthetase
HLA-DQA1	Human leukocyte antigen -major histocompatibility complex, class II, DQ alpha 1
HLA-DRB1	Human leukocyte antigen -major histocompatibility complex, class II, DR beta 1
HMGCR	3-hydroxy-3methylglutaryl-coenzyme A reductase
Hr	Hour(s)
IBM	Inclusion Body myositis
IC	Immune complexes
IFIH1	Interferon induced with helicase C domain 1
IFIT1	Interferon induced protein with tetratricopeptide repeats 1
IFN	Interferon
IFNAR	Type I IFN receptor
Ig	Immunoglobulin
IIM	Idiopathic inflammatory myopathies
IL-10	Interleukin-10
IL-17	Interleukin-17
IL-6	Interleukin 6
ILD	Interstitial lung disease
IU	International units
iNKT	Invariant killer T cells
iNOS	Inducible nitric oxide synthase

IP-10	Interferon gamma-induced protein 10
IQR	Interquartile range
IRF	Interferon regulatory factor
ISGs	IFN-stimulated genes
IVIG	Intravenous immunoglobulin G
JAK	Janus kinase
JDCBS	JDM Cohort and Biomarker study and repository
JDM	Juvenile dermatomyositis
JDRG	Juvenile Dermatomyositis Research Group
JIIM	Juvenile idiopathic inflammatory myopathies
(anti-) Jo-1	Histidyl-tRNA synthase
KREC	Kappa-deleting recombination excision circles
(anti-) KS	Asparaginyl-tRNA synthetase
LAMP	Lysosome-associated membrane protein
LCPUFA	w-6 long-chained polyunsaturated fatty acid
LDL	Low-density lipoprotein
LXR	Liver X receptor
M1	M1 macrophage
MAAs	Myositis associated autoantibodies
MAC	Membranolytic attack complexes
MACS	Magnetic-activated cell sorting
MCP-1	Monocyte chemoattractant protein 1
MDA5	Melanoma differentiation-associated gene 5
ME1	Malic Enzyme 1
MFI	Median fluorescence intensity

$MgCl_2$	Magnesium chloride
MHC	Major histocompatibility complex
(anti-) Mi-2	Nucleosome-remodelling deactylase complex
µg	Microgram
µl	Microlitre
mg	Milligrams
ml	Millilitre
mM	Milli Molar
MIP	Macrophage inflammatory proteins
MITAX	Myositis disease activity assessment tool
MMF	Mycophenolate mofetil
MMT8	Manual muscle testing of 8 groups
MRI	Magnetic resonance imaging
MRP	Multidrug resistance-associated protein
MS	Multiple sclerosis
MSAs	Myositis specific autoantibodies
MXA	MX dynamin like GTPase 1
MZ	Marginal zone
nM	Nano Molar
NCBI	National centre for biotechnology information
NES	Normalized enrichment score
NF-κB	Nuclear factor kappa-light-chain-enhancer of activated B cells
NK	Natural killer
dNTPs	Deoxyribonucleotide triphosphate

NXP-2	Nuclear matrix protein
(anti-) OJ	Isoleucyl-tRNA synthetases
PB	Peripheral blood
PBMC	Peripheral blood mononuclear cells
PBS	Phosphate-buffered saline
PCR	Polymerase chain reaction
pDCs	Plasmacytoid dendritic cells
PFA	Paraformaldehyde
PGA	Physicians global assessment
PI3K	Phosphatidylinositol-4,5-bisphosphate 3-kinase
(anti-) PL-12	Alanyl-tRNA synthetase
PL7	Threonyl-tRNA synthetase
PLCL1	Phospholipase C-like 1
PLSCR1	Phospholipid scramblase 1
PM	Polymyositis
PMA	Phorbol 12-myristate-13-acetate
(anti-) PmSCL	Anti-75-and 100kDa polymyositis/systemic sclerosis proteins
PRR	Pattern recognition receptor
RA	Rheumatoid arthritis
RNA	Ribonucleic acid
RNP	Ribonucleoprotein
Ro	Sjogren's-syndrome-related antigen A
ROS	Reactive oxygen species
RPKM	Reads per kilobase per million mapped reads

SAE	Small ubiquitin-like modifier activating enzyme
SCD	Stearoyl-CoA desaturase
SLE	Systemic lupus erythematosus
snRNP	Small nuclear ribonucleic protein
SREBP	Sterol regulatory element-binding transcription factor
SRP	Signal recognition particle
SSC	Side scatter
SSc	Systemic sclerosis
STAT3	Signal transducer and activator of transcription 3
STING	Stimulator of interferon genes
STX5	Syntaxin 5
SYBR	Synergy brands, Inc.
TCR	T cell receptor
TfH	Follicular T helper cell
Tfreg	T follicular regulatory cell
TGF	Transforming growth factor
Th1	T helper 1
Th17	T helper 17 cell
Th2	T helper 2
THC	Teenage healthy control
TIF1-γ	Transcriptional intermediary factor 1
TLR	Toll-like receptor
TNF	Tumour necrosis factor
TNFR	Tumour necrosis factor receptor

TRAC	T cell receptor alpha constant
TREC	T cell receptor excision circles
Treg	T regulatory cell
UCLH	University College London Hospital
UGCG	UDP-glucose ceramide glucosyltransferase
UKB	Unknown bands
(anti-) Zo	Phenylalanyl-tRNA synthetase

Chapter I

Introduction

Idiopathic inflammatory myopathies

Idiopathic Inflammatory Myopathies (IIM) are rare diseases that are heterogeneous in terms of pathology and age of onset, but share a common target, namely skeletal muscle. Juvenile dermatomyositis (JDM) is the most common subtype of the juvenile idiopathic inflammatory myopathies (JIIM); however, it is still rare with an annual incidence of three in every million children (Shah et al., 2013, Pachman et al., 2005). Children present with a symmetrical proximal and axial muscle weakness and characteristic skin changes including Gottron's papules and heliotrope rash. In severe cases, JDM patients can present with skin ulceration, severe pharyngeal weakness necessitating nasogastric feeding and rarely gut vasculitis that may be fatal. Long-term complications of the disease include lung fibrosis, lipodystrophy and calcinosis (McCann et al., 2006, Guseinova et al., 2011, Ravelli et al., 2010, Sato et al., 2009, Christen-Zaech et al., 2008). Adults, adolescents and children can all develop dermatomyositis, but the clinical pathology can differ depending on the age of onset as shown in ***Table I.1***.

Table I.1 Similarities and differences between juvenile and adult myositis

	Similarities	Differences	
	Juvenile and Adult	**Juvenile Myositis**	**Adult Myositis**
Epidemiology	Female predilection	7.6 years	30-50 years
Clinical features	Share most.	- Calcinosis - Lipodystophy	- Interstitial lung disease - Myocardial involvement
Autoantibodies (most common)	The same for both, including association with clinical features.	- Anti-p155/140 (TIF-1γ) - Anti-MJ (NXP2)	- Antisynthetases
Immunogenetic risk factors	- MHC gene regions (HLA-DRB1* 0301-DQA1*0501 and TNF-α-308A	- DQA1*0301 (Caucasians) - Gm phenotypes - HLA alleles (protective)	- Other cytokine polymorphisms have not been studied
Pathogenesis	- Humoral attack on muscle capillaries - Up-regulation of MHC I on myofibres - Infiltration of pDCs - Type I interferon response	Increased in JDM compared to adult DM: -Neovascularization of capillaries - Up-regulation of MHC I on myofibres - Type I interferon response	- PM is mediated by CD8+ T cell attack on non-necrotic myofibres resulting in destruction.
Treatment response	- Prednisolone and immunosuppress-ive agents	- Greater response	- Lower response
Outcome	- Long-term functional disability - Disease damage - Predictors of mortality (antisynthetase autoantibodies, ILD, older age at diagnosis)	- Lower mortality (≤3%) - 28-41% with functional disability - 37-41% with monocyclic course.	- Higher mortality (10-26%) - 10-year survival (53-89%) - 35-60% with functional disability 17-20% with monocyclic course.

(Rider et al., 2016)

Dermatomyositis (DM), polymyositis (PM), and cancer-associated myositis are the most common forms of IIM diagnosed in adults. These diseases share a similar clinical and pathological phenotype to that of juvenile IIMs (JIIM). The peak age of onset in adult IIM is 30-50 years. Adult IIM have a higher incidence than juvenile IIM at approximately 9.6 per million adults diagnosed annually (Bendewald et al., 2010). Adults with DM have a more chronic disease course and a higher mortality rate than children with DM (Rider et al., 2016). A set of five criteria was developed by Bohan and Peter to aid diagnosis in both childhood and adult disease (***Table I.2***) (Bohan and Peter, 1975a, Bohan et al., 1977). Four of these criteria are required for a definite diagnosis of dermatomyositis and three for a probable diagnosis (Rider et al., 2016).

Table I.2 Bohan and Peter criterion for myositis

1	Progressive proximal symmetrical weakness
2	Elevated levels of muscle enzymes
3	An abnormal finding on electromyography
4	An abnormal finding on muscle biopsy
5	Compatible cutaneous disease (only in dermatomyositis)

Environmental risk factors

Dermatomyositis can be triggered by environmental risk factors in individuals genetically susceptible to the disease. This condition is characterised by immune dysfunction and specific tissue pathology. Some studies have reported an antecedent infection prior to the onset of JDM suggesting that infectious pathogens could trigger the disease, such as coxsackievirus B2/B4 (CVB) and enterovirus associated with both upper respiratory and gastrointestinal symptoms (Pachman et al., 2005,

Christensen et al., 1986). Non-infectious environmental exposures have been linked with the development of myositis including medications, immunizations, ultraviolet light exposure and stressful life events (Neufeld et al., 2013).

Immunopathology found on muscle biopsy

According to the Bohan and Peter criteria for myositis, the positive findings on muscle biopsy include; necrosis, phagocytosis, regenerative activity reflected by basophilia, atrophy and degeneration of both type I and II muscle fibres, internal migration of nuclei, vacuolization, fibre size variation, and mononuclear cell infiltrate (Bohan and Peter, 1975b). Detailed studies have investigated the immunopathology of the diseased tissue from myositis patients. An early event to occur in the muscle fibres of dermatomyositis patients is complement activation and formation of membranolytic attack complexes (MAC) that cause muscle ischaemia, lysis of endothelial cells and destruction of capillaries (Dalakas, 1991, Mastaglia and Phillips, 2002, De Visser et al., 1989, Kissel et al., 1986, Dalakas, 2006). Complement activation triggers immune cell recruitment and pro-inflammatory cytokines, these include CD4+ T cells, B cells, macrophages, plasmacytoid dendritic cells, interferon-γ and interferons-α/β (Dalakas and Hohlfeld, 2003, Greenberg et al., 2005b). Polymyositis and inclusion body myositis (IBM) share the T-cell-mediated autoimmune process of CD8+ cytotoxic T cells attacking non-necrotic muscle fibres that express MHC-I antigen. These T cells can persist over many years due to clonal expansion (Benveniste et al., 2004, Amemiya et al., 2000). The T cells are drawn to the tissue by a pro-inflammatory environment of cytokines and chemokines. PM and inclusion body myositis (IBM) are unique in the IIM group of diseases as they ubiquitously over express MHC-I on the surface of muscle fibres as first shown by

Isenberg and colleagues (Karpati et al., 1988, Emslie-Smith et al., 1989, Rowe et al., 1981). Muscle biopsies should clearly differentiate between DM, PM, IBM and non-immune myopathies due to presence or absence of the CD8+/MHC-I complex.

Genetics

Familial autoimmunity has been reported in some patients with JDM, most frequently type I diabetes mellitus or SLE (Andreoli et al., 2011). JDM is a complex genetic disorder that has been explored by a large cohort Genome-wide association study (GWAS). Polymorphisms of the major histocompatibility complex (MHC) class II region on chromosome 6 have been linked to a strong risk of developing myositis in a Caucasian population (Miller et al., 2013). Three of the haplotypes linked to a higher risk factor of developing JDM are HLA-B*08, DRB1*0301 and DQA1*0501. Protective haplotypes have also been found these include, DQA1*0201 (OR0.37), *0101 (OR0.38) and *0102 (OR0.51) (Mamyrova et al., 2006). Examination of 141 non-MHC single-nucleotide polymorphisms (SNPs) previously linked with other autoimmune diseases found three SNPs to be associated significantly with JDM/DM. These genes include phospholipase C-like 1 (PLCL1), B lymphoid tyrosine kinase (BLK) and chemokine (C-C motif) ligand 21 (CCL21) (Miller et al., 2013). In a separate study of JDM, TNF-α-308A allele was associated with the development of calcinosis and ulceration, and prolonged disease (Pachman et al., 2000, Mamyrova et al., 2008).

Autoantibodies

Myopathies in both adults and children can be split into subgroups according to their clinical and autoantibody phenotype (Deakin et al., 2016b). There are two classes of myositis autoantibodies: myositis specific autoantibodies (MSAs) that are unique to

myositis, and myositis associated autoantibodies (MAAs) that are detected in myositis and other autoimmune diseases. Approximately 70% of JIIM patients have an identifiable autoantibody phenotype. The main myositis specific autoantibodies detected in juvenile IIMs are anti-p155/140 (TIF1-γ) and anti-MJ (NXP-2) (Rider et al., 2013). In adult myositis, the most frequent group of myositis autoantibodies detected are the anti-synthetase enzymes. The anti-synthetases are present in 25-40% of adult patients compared to 5% of juvenile patients (Shah et al., 2013).

The autoantibody profiles are associated with patient demographics and clinical phenotype (***Table I.3*** and ***Figure I.1***). The anti-p155/140 (TIF1-γ) and anti-MJ (NXP-2) autoantibodies are predominantly associated with JDM in Caucasian patients. Anti-p155/140 autoantibodies are present in 23-30% of JDM, in particular patients that have extensive photosensitive skin rashes. Anti-p155/140 autoantibodies have been associated with lipidystrophy and a chronic disease course (Bingham et al., 2008). Anti-MJ autoantibodies are present in 12-23% of JDM patients and are associated with calcinosis, muscle cramps, muscle atrophy, joint contractures, dysphonia and absence of a truncal rash (Tansley et al., 2014b). The MDA5 autoantibody in juvenile cases is associated with mild muscle disease, but strongly associated with interstitial lung disease (ILD). In adult IIM anti-Jo-1 is the most common of the anti-synthetase autoantibodies and is associated with ILD, arthritis, fevers, Raynaud's phenomenon and mechanics' hand. The anti-Jo-1 autoantibody subgroup in adult IIM has the highest mortality rate predominantly due to its strong association with ILD. The majority of mortality in adult and children IIM patients is due to ILD (Rider et al., 2013).

Table I.3 Myositis-specific autoantibodies; frequencies and clinical associations

Autoantibody	Target	Prevalence in JDM	Prevalence in Adult myositis	Clinical association
Jo-1	Histidyl-tRNA synthase	2-4%	9-24%	ILD, mechanics' hand, arthritis, Raynaud's phenomenon
TIF1-γ	Transcriptional intermediary factor 1	22-29%	13-31%	Cancer - adults
NXP-2	Nuclear matrix protein	23-25%	1-17%	Cancer - adults Calcinosis - JDM
MDA5	Melanoma differentiation-associated gene 5	7-38%	0-13% Caucasian 10-48% Asian	Amyopathic, Rash, ILD
Mi-2	Nucleosome-remodelling deactylase complex	4-10%	9-24%	Rash
SRP	Signal recognition particle	<2%	5% Caucasian 8-13%Asian/African	>CK, necrotizing myopathy, dysphagia, cardiac, arthritis
HMGCR	3-hydroxy-3methylglutaryl-coenzyme A reductase	<1%	6%	>CK, necrotizing myopathy, Statins

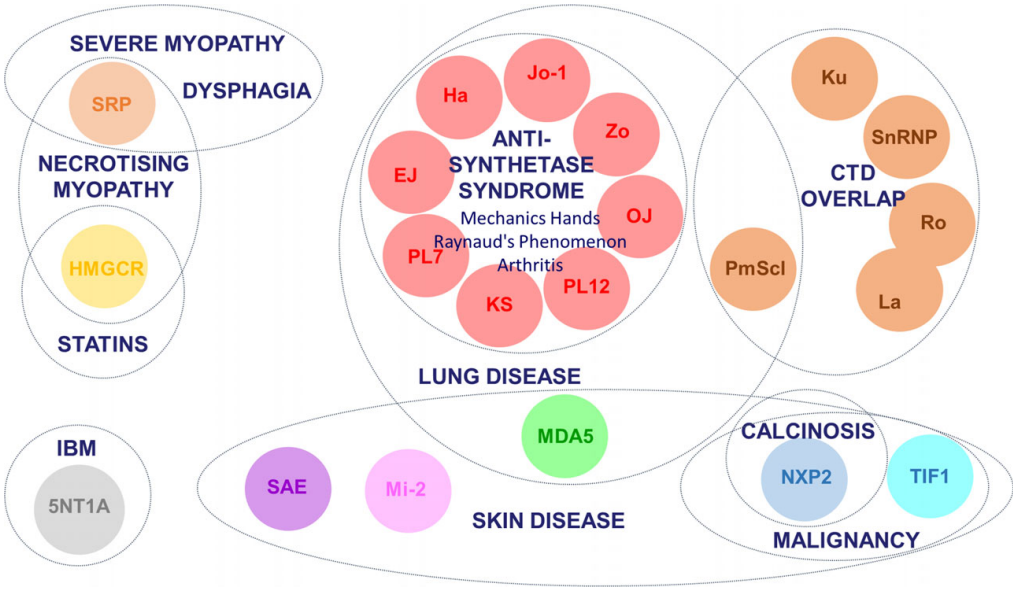

Figure I.1 Myositis autoantibodies and their key clinical associations. *IBM, inclusion body myositis; CTD, connective tissue disease; SRP, signal recognition particle; HMGCR, 3-hydroxy-3methylglutaryl-conenzyme A reductase; TIF1, transcription intermediary factor 1; NXP2, nuclear matrix protein 2; MDA5, melanoma differentiation-association gene 5; SAE, small ubiquitin-like modifier activating enzyme; 5NT1A, cytosolic 5'nucleotidase 1A; Mi-2, nucleosome-remodeling deacetylase complex, Jo-1, histidyl tRNA synthetase; PL7, threonyl tRNA synthetase; PL12, ananyl tRNA synthetase; OJ, isoleucyl tRNA synthetases; EJ, glycyl tRNA synthetase; KS, aspararginyl tRNA synthetase; Zo, phenylalanyl tRNA synthetase, Ha; tyrosyl tRNA synthetase; snRNP, small nuclear ribonucleic protein.* (taken with permsission from Betteridge and McHugh, 2016)

Not only are MSAs associated with particular disease phenotypes, they have also been found to aid the prediction of the risk of remaining on treatment. Specifically, anti-Mi-2 autoantibodies have a protective effect reducing the time to remain on treatment. Unlike anti-nuclear matrix protein 2, anti-transcription intermediary factor 1γ autoantibodies, or no detectable autoantibody that were all associated with more severe histopathology and prolonged time remaining on treatment (Deakin et al., 2016a).

Calcinosis

Amongst IIM, JDM have the highest frequency of calcinosis (12-47%). Patients typically present with subcutaneous calcinotic lumps 1-2 years after disease onset. Calcinosis is defined as the presence of dystrophic calcification in subcutaneous, myofascial, or muscle tissue (Sato et al., 2009). It is distinct from bone in its mineral composition and matrix as the mineral is deposited in fragments and becomes solid over time (Rider et al., 2016). Anti-MJ (NXP-2) autoantibodies are strongly associated with the presence of calcinosis (Tansley et al., 2014b).

Cancer and myositis

Adult patients with DM and PM have an increased risk of cancer compared to a control cohort, and can have up to a 10-fold increased risk (Chen et al., 2010). Cancer is most commonly detected within the first year of IIM diagnosis with about two-thirds of comorbid cancers occurring after diagnosis (Huang et al., 2009). Population based epidemiological studies of IIM conducted around the world have shown different types of cancer are prevalent among defined populations and ethnic groups. Studies in Denmark, Sweden and Finland identified that IIM was associated with an increased comorbidity of ovarian, lung, pancreatic, stomach, urinary tract and haemolytic cancers (Hill et al., 2001, Chow et al., 1995). Asian population studies of IIM conducted in Korea, Singapore, Hong Kong, South East China and Taiwan have demonstrated an increased comorbidity of cancers of the breast, stomach and nasopharynx, the last being the most common (Lee et al., 2006, Peng et al., 1995, Chan, 1985, Chen et al., 2001, Wang et al., 1993).

As shown in ***Figure I.1*** the MSA TIF1-γ has a strong correlation to cancer-associated myositis but only in adult disease (Betteridge and McHugh, 2016). In JDM cohorts there is no known association between the presence of anti-TIF1-γ autoantibody and risk of cancer (Gunawardena et al., 2008). Trallero-Araguas et al demonstrate by meta-analysis that the sensitivity of using anti-TIF1-γ to detect cancer-associated myositis in adults is 78% [95% confidence interval(CI) 45-94%] with a specificity of 89% (95% CI 82-93%) (Trallero-Araguas et al., 2012). The difference between juvenile and adult cancer association is thought to be age related, the older the patient the higher the risk of developing cancer (Fiorentino et al., 2015). Anti-NXP2, a MSA mainly associated with calcinosis in JDM, has been detected in a small percentage (~17%) of the adult IIM population (Gunawardena et al., 2009, Ichimura et al., 2012). Additionally, there is a growing body of evidence that anti-NXP2 is associated with malignancy in adult disease (Fiorentino et al., 2013).

Interstitial lung disease

Interstitial lung disease (ILD) is the most common respiratory disease associated with IIM (Fathi et al., 2004). In adult disease, the prevalence has been reported between 17-36%, and in large cohort studies of JDM ILD is thought to occur in 8-13% of patients. Patients with IIM-associated ILD have a 50% mortality risk from respiratory failure (Connors et al., 2010, Shah et al., 2013). ILD can be diagnosed before or after the onset of the myositis and does not differ from idiopathic disease (Cottin et al., 2003). The signs and symptoms related to IIM-associated ILD include dyspnoea on exertion, cough, decreased exercise tolerance, digital clubbing and asthenia (Lega et al., 2015). In adult disease, there is a strong association to the anti-synthetase syndrome autoantibodies (anti - Jo-1, PL7 and PL-12) with ILD (Lega et al., 2014).

These autoantibodies have a high prevalence of HLA-DRB1*03, DQA1*05 and DQB1*02 haplotypes and a determining factor of IIM-associated ILD is the presence of the HLA-DRB1*03 haplotype (Oddis et al., 1992, Chinoy et al., 2006, Rider et al., 2013). Anti-MDA5 autoantibodies have also been shown to have a strong association with interstitial lung disease especially in juvenile disease (Tansley et al., 2014a). A 'gain of function' mutation in the *IFIH1* gene that encodes for the MDA5 protein has been reported and leads to enhanced type 1 interferon production. This finding suggests that type I interferon production may link anti-MDA5 to ILD (Rice et al., 2014). The treatment of ILD depends on the severity and progression at diagnosis and is similar to that of IIM. Treatment includes high-dose corticosteroids with additional immunosuppressive drugs such as azathioprine, mycophenolate mofetil, methotrexate, cyclosporine and cyclophosphamide (Lega et al., 2015). A better understanding of the pathophysiology underlying ILD will lead to more targeted therapy.

Pathophysiology

JDM can be defined as an autoimmune angiopathy characterised by chronic inflammation in a genetically susceptible individual after exposure to an environmental trigger. Both humoral and cell mediated mechanisms cause vascular and muscle damage in dermatomyositis. Key events that contribute to the pathogenesis of JDM are: the immune attack on muscle capillary endothelium, up regulation of MHC class I expression on the surface of myofibres, and infiltration of plasmacytoid dendritic cells (pDCs) initiating a type I interferon (IFN) response (Rowe et al., 1981). These central events are consistent in both adult and juvenile DM, but are more prominent in juvenile disease (Huizinga et al., 2005).

The main type I interferons are IFN-α and IFN-β. The IFNs bind to the IFN-α receptor and activate the Janus kinase (JAK)-signal transducer and transcription (STAT) pathway that in turn leads to the transcription of IFN-stimulated genes (ISGs) (Ivashkiv and Donlin, 2014). The over production of IFN in the blood and muscle is an abnormality in the pathogenesis of dermatomyositis (Walsh et al., 2007, Greenberg et al., 2005b). SLE is another autoimmune disease where overproduction of type I interferons has been implicated in disease (Baechler et al., 2003). The release of type I IFNs leads to immune cell activation and vasculopathy. The main source of type I IFNs is from pDCs after activation by either self-DNA or viral nucleic acid (Mauri and Menon, 2015, Menon et al., 2016). pDCs have been identified in JDM muscle, but IFN is rarely detected in the serum of JDM patients as it is tightly regulated by the immune system (Baechler et al., 2011, Niewold et al., 2009). Due to the difficulties in measuring IFN directly, the genes induced by IFN, interferon-induced protein with tetratricopeptide repeats 1 (IFIT1), ISG15 ubiquitin-like modifier (G1P2), and interferon regulatory factor 7 (IRF7), are measured to ascertain the levels of IFN signalling *in vivo* (Bilgic et al., 2009, Menon et al., 2016). Another indirect measure of IFN is the IFN chemokine signature that measures serum levels of interleukin 6 (IL-6), monocyte chemoattractant protein 1 (MCP-1), monocyte chemoattractant protein 2 (MCP-2) and interferon gamma-induced protein 10 (IP-10); the chemokine signature has correlated with disease activity in JDM (Nistala et al., 2013).

Blockade of the IFN pathway could be a useful therapy in DM. A phase 1b clinical trial of sifalimumab, a fully human immunoglobulin G_1 κ monoclonal antibody that binds to and neutralizes the majority of IFN-α subtypes, has been carried out in patients with DM and PM using the outcome measures of IFN gene signature

suppression against disease improvement. Sifalimumab suppressed the IFN gene signature in blood and muscle tissue of the IIM patient cohort; this suppression correlated to clinical improvement. These initial results have identified that targeting the IFN pathway with sifalimumab achieves a good level of disease suppression in DM and PM, but blockade of the type I IFN receptor (IFNAR) may offer superior clinical benefit (Higgs et al., 2014). Other potential biomarkers of DM have been identified that include interferon gamma-inducible protein (IP)-10, galectin 9 and tumour necrosis factor (TNF) receptor type II (Bellutti Enders et al., 2014).

Mouse model experiments have shown that overexpression of HLA class I on muscle cells is sufficient to drive muscle damage, leukocyte recruitment, and muscle weakness. Therefore, HLA class I overexpression is not necessarily a response to inflammatory processes (Nagaraju et al., 2000). Further studies have shown that overexpression is due to misfolding of excessive class I protein in the endoplasmic reticulum (ER) that triggers cellular damage responses and leads to immune activation (Nagaraju et al., 2005). This misfolding is referred to as the ER stress pathway.

Treatment

The mainstay treatments for IIM are prednisolone and methotrexate. Other immunosuppressive treatments are used including mycophenolate mofetil and azathioprine. Advances in the understanding of the immunopathology and genetics underlying IIM have led to clinical trials of the biological therapies sifalimumab and rituximab (Oddis et al., 2013, Higgs et al., 2014). Investigating the functions of B cells in IIMs may provide an insight into the mechanisms of the disease and lead to novel therapeutic pathways.

Immunopathogenesis of IIM

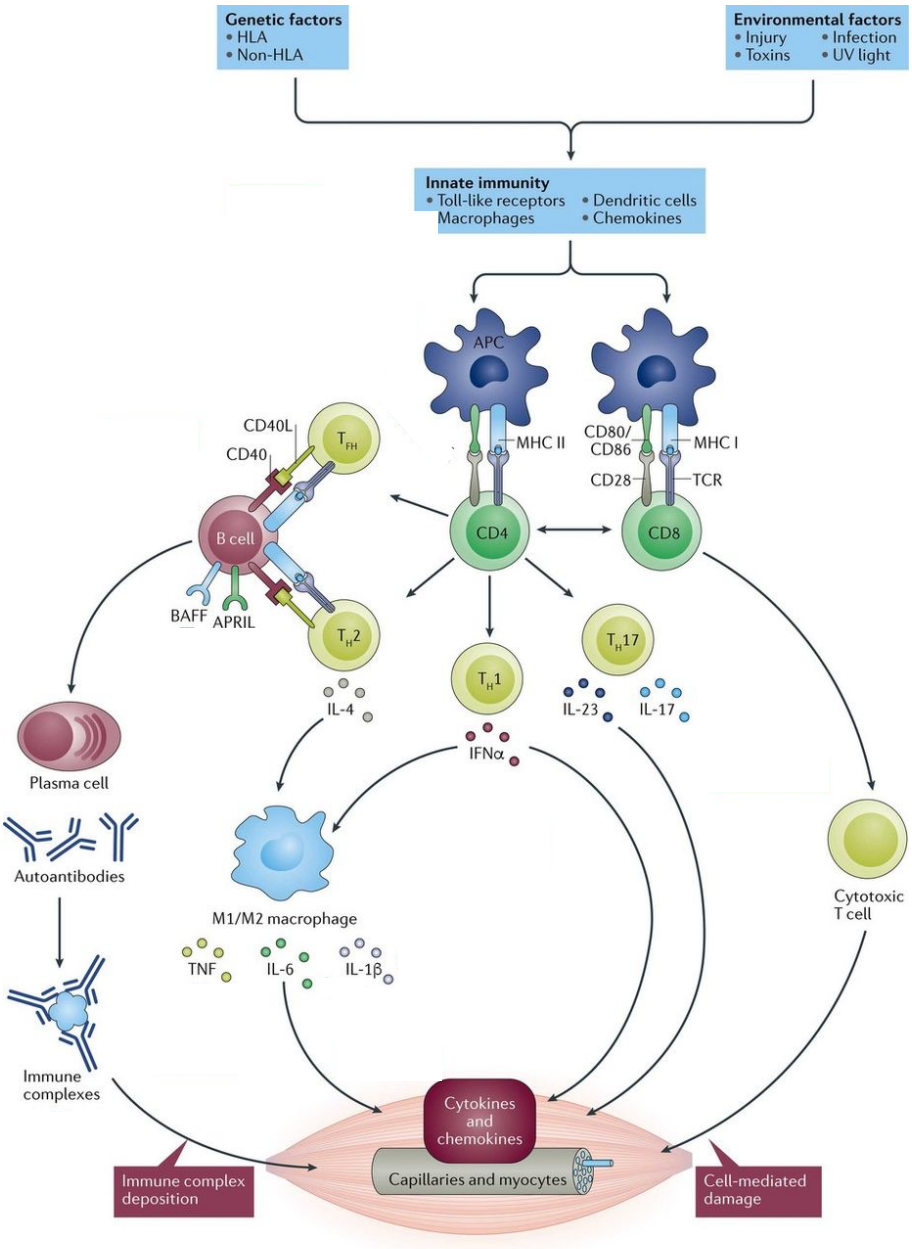

Figure I.2 Immune cells and cytokines involved in the pathogenesis of IIM. *There have been many identified factors involved in the pathogenesis of myositis that can lead to the recruitment of both arms of the innate and the adaptive immune system. It has been proposed that genetic and environmental factors can trigger an innate immune response by the recruitment of antigen presenting cells (APC) which in turn activate CD4+ and CD8+ T cells. These T cells upregulate the expression of B cell activating factor (BAFF) and a proliferation-inducing ligand on B cells through the engagement of CD40-CD40 ligand and T cell receptor (TCR) to major histocompatibility complex (MHC) II. T-helper (T_H) and T follicular helper cells (T_{FH}) drive cytokine production and recruitment of macrophages, immune complexes and cytotoxic T cells to the muscle tissue. Adapted from (Oddis and Aggarwal, 2018)*

Pathogenesis of IIM summary

The IIM group share common features of immune-mediated muscle injury. There are clear clinical and histopathological differences between the IIM sub-groups (ADM, APM, JDM and IBM), this suggests that there are different underlying pathogenic mechanisms. DM appears to be driven by a type I IFN response with myofiber injury resulting from specific antibody and complement-mediated microangiopathy. In JDM the most common MSAs are anti-TIF1γ and anti-NXP-2, whereas in adult disease anti-Jo-1 is the most prevalent. PM also has a distinct autoantibody profile with links to a type I IFN-inducible transcript, but the cellular infiltrate is confined to the fascicle within the muscle with diffuse muscle fibre injury. This injury seems to be mediated by CD8+ cytotoxic T cells and increased expression of MHCII from muscle fibres.

B cells

T and B lymphocytes work in unison to generate an adaptive immune response. The ability to produce variable T or B cell receptors (TCR/BCR) is key to this response.

B cells originate from haematopoietic stem cells in the bone marrow. At this stage, pro-B cells express a unique antibody, the immunoglobulin (Ig) variable domain (Fv). Re-arrangement of the heavy and light chains of this immunoglobulin (V-D-J and V-J recombination) is supported by stromal-cell derived interleukin-7 (Nutt et al., 1999, Brack et al., 1978). Ig recombination leads to the development of the pre-B cell receptor (BCR). When a pre-B cell acquires antigen specificity by the expression of a unique BCR and surface IgM, it can then migrate from the bone marrow as an immature B cell (LeBien and Tedder, 2008, Lam et al., 1997). Although immature, these B cells are able to execute a rapid antibody response against type-I antigens.

Immature B cells migrate to secondary lymphoid structures, such as the spleen and lymph nodes, unless they encounter antigen-presenting cells including macrophages and dendritic cells. On reaching a lymphoid structure a B cell can either differentiate into a plasma cell or enter the germinal centre (GC). To mature into a plasma cell a naïve B cell must form either a follicular (FO) or marginal zone (MZ) B cell in the spleen after antigen engagement. Short-lived plasma cells secrete IgM, but also other Ig subtypes by class switch recombination (CSR).

A GC is formed of mature B cells and T-helper cells. Within a GC antigen presentation promotes expansion of the B cells with antigen-specific BCR. The GC produces memory and high affinity antibody-producing plasma B cells as a result of somatic hyper mutation, clonal expansion and class switch recombination (CSR) (Illera et al., 1993, Jacob et al., 1991). Terminally differentiated plasma cells migrate back to the bone marrow where they can reside for up to one year (Shapiro-Shelef and Calame, 2005). Memory B cells from a GC will not produce antibody unless they encounter a secondary antigen (Klein and Dalla-Favera, 2008). T cells aid the adaptive immune response performed by memory B cells. The BCR is used to recognise, bind and internalize specific antigens. The immune response to a foreign antigen is T-cell independent and performed by MZ B cells by the activation of innate receptors such as toll-like receptors (TLRs) (Gray et al., 2007).

B cell subsets

Human B cell subsets can be defined by the expression of the surface markers CD19, CD24 and CD38. CD19 positive PBMC co-express CD24 and CD38 whereas CD19 negative PBMC do not express CD24. Mature B cells are $CD38^{pos}$ and $CD24^{low}$.

Memory B cells are $CD38^{neg}$ and $CD24^{hi}$. Immature B cells are $CD38^{hi}$ and $CD24^{hi}$. Studies showed that the frequency of immature B cells was higher in the bone marrow compared to peripheral blood confirming the origins of B cell development (Carsetti et al., 2004). The expression of CD27 can also be used to separate mature and memory B cells. Memory B cells are predominantly CD27 positive, while mature B cells are predominantly CD27 negative. Definition of early B cells subsets, pro- and pre- B cells, can be measured via CD10 and IgM with these subsets having a $CD10^{hi}$ and IgM^{neg} phenotype. Immature and transitional B cells have increasing amounts of IgM and decreasing amounts of CD10. The individual roles in the adaptive immune response played by each B cell subset are beginning to be defined.

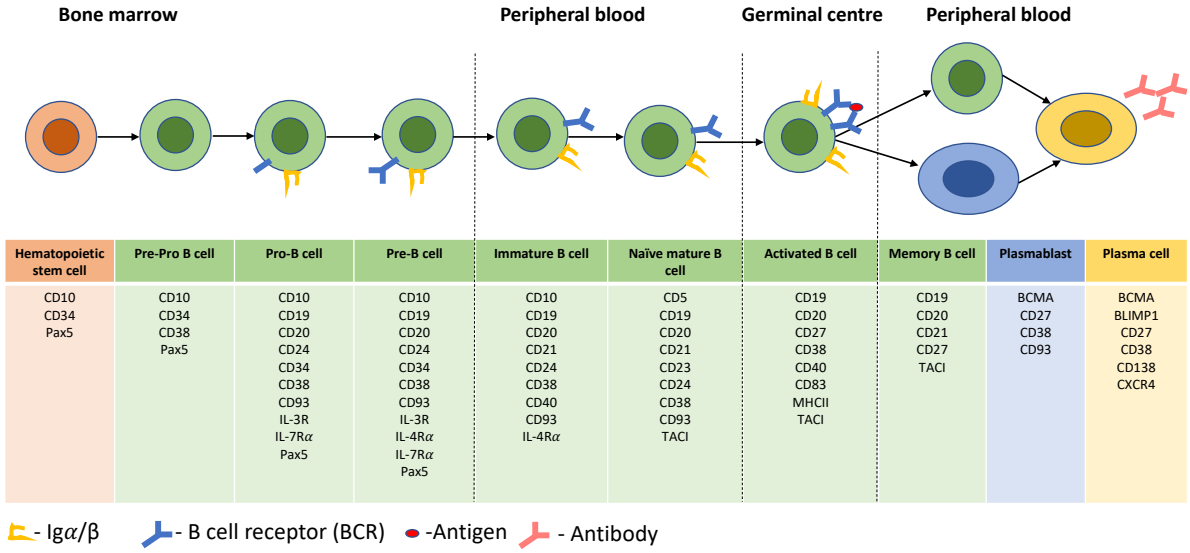

Figure I.3 ***B cell development pathway in humans.*** *B cells develop from hematopoietic stem cells generated in the bone marrow. They proceed into the peripheral blood expressing surface markers, B cell receptor (BCR) and Igα/β. In the germinal centre they become activated and develop into memory B cells or plasmablasts to re-enter the blood.*

B cells in IIM

The precise cause of inflammatory muscle disease including adult and childhood onset polymyositis (PM) and dermatomyositis (DM) remains uncertain. However, B-

lymphocytes have been strongly associated with the disease pathogenesis especially in DM (Miller et al., 2013). B cells are thought to contribute primarily towards autoimmune pathology through the production of autoantibodies. In approximately a third of Juvenile DM (JDM) cases B-lymphocytes have been detected in inflamed muscle, and almost 50% of patients have detectable myositis-specific (MSAs) or myositis-associated autoantibodies (MAAs) (Shah et al., 2013, Nistala and Wedderburn, 2013). MSAs and MAAs have been identified in the serum of myositis patients and closely correlate to specific clinical phenotypes. Therefore, B cells are important in the pathogenesis of myositis as producers of autoantibodies. B cells have long been detected in the inflamed muscle of myositis patients (Arahata and Engel, 1984). The B cell muscle infiltration has not been determined as pro-inflammatory or regulatory. The anti-CD20 antibody, rituximab, which depletes B cells has been trialed in JDM and adult DM (Oddis et al., 2013). Although the primary end point of the trial was not met, Oddis et al showed that a higher proportion of JDM (87%) patients treated with rituximab met the definition of improvement more quickly compared to adult DM (78%). These results might imply that B cells in JDM are either more pathogenic than in adult DM, or have a greater regulatory role in adult DM compared to JDM.

Other functions of B cells in the immune system

The most well-defined function of B cells is their ability to produce antibodies as part of an adaptive immune response. Other defined roles of B cells in the immune system have emerged. These include peptide and lipid antigen presentation and cytokine production. Activated B cells require immune cell stimulation to differentiate into cytokine producing B effector cells. B effector cells are classified as Be1 or Be2, pro-

inflammatory or regulatory respectively. Naïve B cells can differentiate into Be1 or Be2 cells when co-cultured with polarized T helper 1 (Th1) or T helper 2 (Th2) cells (Harris et al., 2000). It has been demonstrated that B cell secretion of cytokines depends on the stimulus. B cells stimulated with CD40L and BCR signalling produced the pro-inflammatory cytokines TNF-α, lymphotoxin, and IL-6. The regulatory cytokine, IL-10, was produced with CD40L stimulation without BCR signalling. A study in multiple sclerosis (MS) highlights the dysregulation of cytokines in the context of autoimmunity. Duddy et al showed that naïve B cells from patients with MS could be polarized *in vitro* to Be1 cells that produce pro-inflammatory cytokines, or Be2 cells that produce regulatory cytokines (Duddy et al., 2004). B cells are an integral component of the adaptive response and it is their ability to secrete both pro-inflammatory and regulatory cytokines that make them an important target for investigation in autoimmune disease.

T cell development

T cells develop in the thymus which provides a microenvironment directing differentiation, positive and negative selection. Hematopoietic stem cells from the bone marrow develop into lymphoid progenitors and migrate to the thymus where they complete antigen-independent maturation into functional T cells. It is in the thymus that T cells gain expression of specific cell surface markers including TCR, CD3, CD4 or CD8 (Zuniga-Pflucker, 2004).

Progenitor cells start by expressing CD3, but are double negative (DN) for CD4 and CD8 as their TCR genes have not yet rearranged (Ceredig and Rolink, 2002). Once the rearrangement of the β chain of the TCR stops, the cells become double positive

(DP) for both CD4 and CD8 losing their CD25 and CD44 (CD117) expression (Godfrey et al., 1993). Interactions with the Notch receptor-expressing thymocytes and Notch ligand expressing thymic stromal cells induce T cell maturation, resulting in the generation of singular positive T cells (Godfrey et al., 1993, Huang et al., 2003, Harman et al., 2003). This process generates CD4+ helper T cells and CD8+ cytotoxic T cells which migrate to the peripheral blood from the thymic medulla (***Figure I.3).***

Before a T cell can leave the thymus, it must pass through positive and negative selection. Firstly, double positive T cells that have rearranged αβTCR must bind to self-peptides and cortical epithelial cells expressing Class I or Class II MHC with high affinity to produce a survival signal, allowing positive selection. If the double positive T cell instead binds to self-peptides and Class I and Class II MHC expressed on bone-marrow derived antigen-presenting cells, such as macrophages and dendritic cells, negative selection will occur due to apoptotic signals (Alberola-Ila et al., 1996).

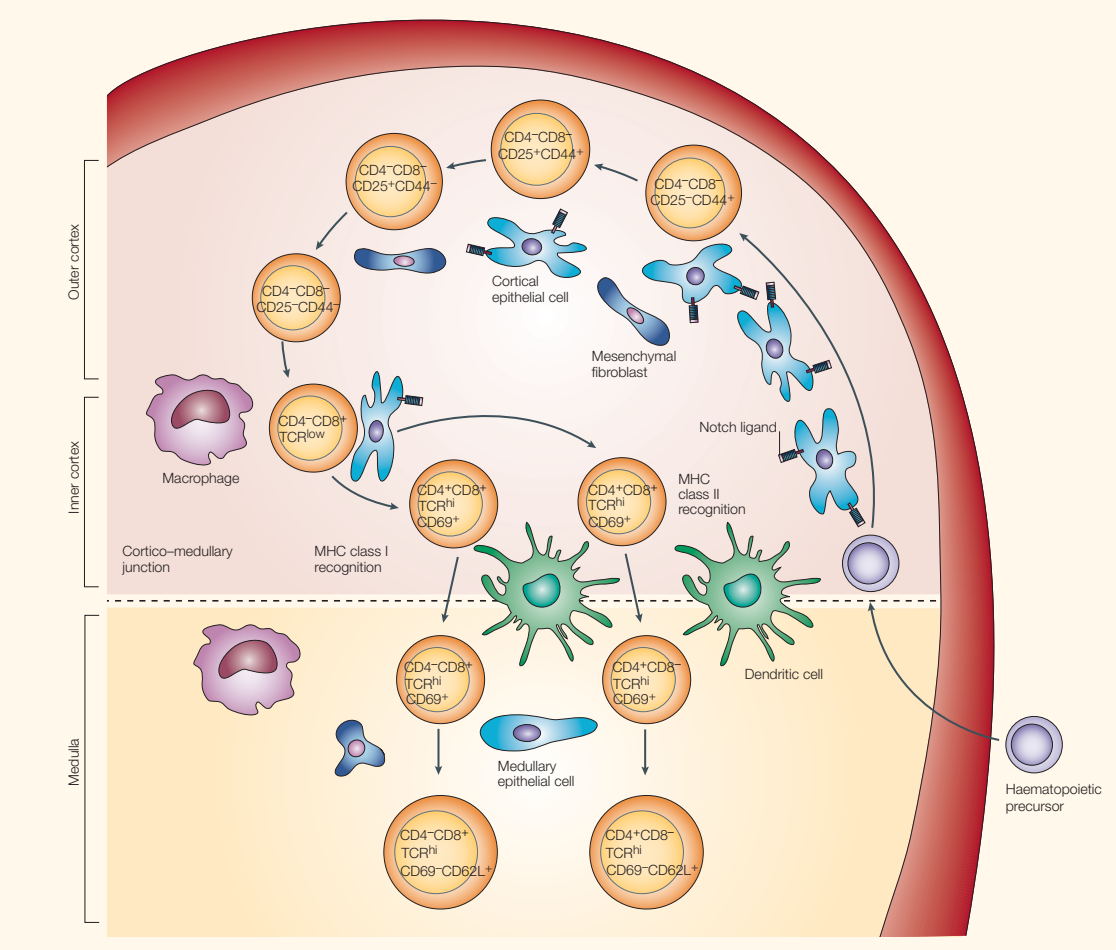

Figure I.4 ***Intrathymic T-cell development.*** *T cell differentiation is characterised by specific surface markers, including; CD4, CD8, CD44, CD25 and the stability of the of the T-cell receptor (TCR). The programme of T-cell maturation in the thymus results in the generation of self-tolerant CD4+ helper T cells and CD8+ cytotoxic T cells which in turn migrate into the peripheral blood.* (Zuniga-Pflucker, 2004)

T cell subsets

Mature T cells emerging from the thymus are known as naïve T cells as they have not yet encountered foreign antigen (Ag). These cells express multiple surface markers including CC chemokine receptor 7 (CCR7), L-selectin (CD62L), CD45RO, CD45RA, CD127 and CD28. Naïve T cells circulate through the blood and the lymphatic system to reside in secondary lymphoid organs where antigen is presented to them by dendritic cells (DC). TCR engagement via the APC triggers a cascade of intracellular signaling events activating the naïve T cell. Proliferating activated T cells

mature into cytotoxic CD8+ T cells and CD4+ T helper cells. Cytotoxic CD8+ T cells perform direct lysis of infected or malignant cells expressing the antigen, whereas CD4+ T helper cells produce cytokines, can be directly toxic, stimulate T cell effector functions, B cell antibody production and induce other inflammatory mechanisms. Effector T cells (CD45RO+, CD95+, Granzyme B +, CD25+) tend to disappear once the antigen has been removed, but can form memory T cells (CCR7+, CD62L+, CD45RO+, CD127+, CD28+) which can survive in the lymphoid organs and peripheral tissues for many years unlike effector and naïve T cells. Memory T cells are rapidly activated to effector function (CD45RO+, CD95+) in response to a recognised antigen and quickly eliminate the pathogen at an early stage (***Figure I.4***).

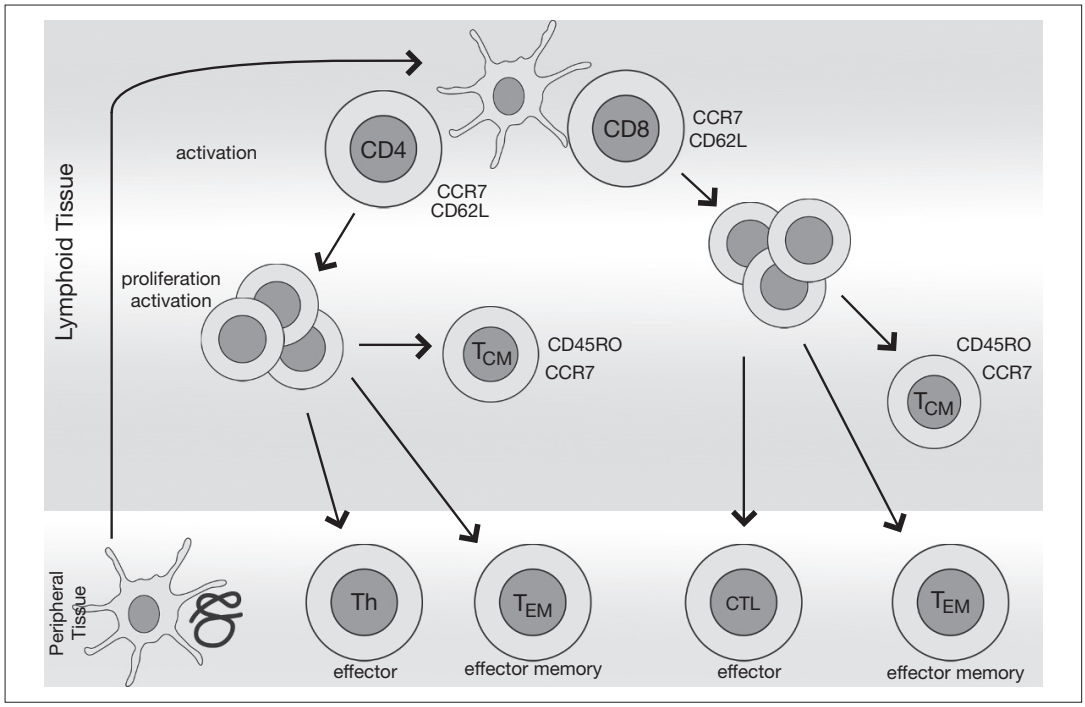

Figure I.5 Development of T cells upon activation. *T cells are activated by antigen presenting cells (APC) by the recognition of major histocompatibility complex (MHC)-peptide. On activation they proliferate and differentiate into effector and memory T cells. Both CD4 T-helper (Th) effector and CD8 cytotoxic T lymphocytes (CTL) migrate to the peripheral tissue to exert their function. Memory T cells can develop into C-C chemokine receptor type 7 (CCR7) negative effector memory cells (EM) that migrate to peripheral tissue or CCR7+ central memory T cells (CM) circulating in lymphoid tissue.* (Broere, 2011)

Sub-populations of CD4+ T helper cells are defined by cytokine profiles. Th1 produce IFN-γ but also IL-2, TNF-α and lymphotoxin. Th2 cells secrete IL-4, -5, -6, -10 and -13. Th1 cells mediate a pro-inflammatory response whereas Th2 promote a more non-inflammatory immunity. Both instigate B cell production of IgG but Th2 are also essential for IgA and IgE. A third type of T helper cell, Th17, secretes the pro-inflammatory cytokine IL-17 in response to IL-23. In the immunogenesis of autoimmune diseases such as rheumatoid arthritis, psoriasis and Crohn's disease, Th17 cells are considered to contribute as a pro-inflammatory effector lineage (Miossec and Kolls, 2012, Miossec et al., 2009). Follicular T helper cells (Tfh) have been defined by their development in the presence of IL-6 and transcription factor Bcl-6.

T regulatory cells (Treg) can express TGF-β, Il-10 and IL-35 which are key immunosuppressive cytokines that contribute to the critical role of Tregs in the maintenance of peripheral tolerance, down-modulation of the amplitude of an immune response, and prevention of autoimmune disease. It is thought that Tregs can fall under CD4+ and CD8+ subsets and are characterized by the expression of CD25 and the transcription factor forkhead box P3 (Foxp3). It is Foxp3 that is key for Treg development and without it severe systemic autoimmune disease can arise in both human and mouse (Buckner, 2010, Abdulahad et al., 2011).

T cell pathogenesis in IIM

The main clinical manifestation of IIM is muscle weakness and fatigue. When investigated by muscle biopsy most patients have immune cell infiltrates within the muscle fibres. These immune cell infiltrates can consist of both CD4+ and CD8+ T

cells. One pathway of T cell migration to inflamed muscle tissue has explored the expression of the alpha and beta chemokines acting as chemoattractants. This group of chemokines includes CXCL9/10 and CCL2/3/4/19/21 that can be expressed by immune cells and muscle fibres alike (Malmstrom et al., 2012). A positive expression of CCL2 on muscle biopsies has been demonstrated by immuno-histochemistry (Baird and Montine, 2008, De Paepe et al., 2007). CCL2 is a chemoattractant for CCR2- and CCR4- expressing cells such as monocytes, memory T cells, and dendritic cells. A significant up-regulation of CCL3 has been detected at mRNA level on IBM myofibres, and muscle infiltrating mononuclear cells from DM, PM and IBM patients. This chemokine can regulate Th1 cells and acts as a chemoattractant for macrophages and T cells (Schmidt et al., 2008). Within the affected muscle tissue the immune cell infiltrates can have a focal distribution which is thought to reflect a chemokine pro-inflammatory feed-back loop. In regard to the type of T cells found in muscle tissue the literature suggests that it is dependent on disease type. CD8+ T cells were more common in PM and IBM whereas in patients with DM CD4+ T cell populations were more prevalent (Salajegheh et al., 2007, Hofbauer et al., 2003).

Skin-infiltrating T cells

Dermatomyositis is a sub-type of the IIM group and affects both muscle and skin. Previous studies have concluded that CD4+ T cells drive DM more than in PM and IBM. Granzyme B-expressing T cells and FOXP3+ T cells have been found to be low in DM, which contrasts to findings in patients with RA and SLE who have skin involvement (Grassi et al., 2009, Solomon and Magro, 2008). In contrast, CXCR3+ lymphocytes are enriched in the skin of DM patients, which suggests a strong type I interferon involvement. In the peripheral blood of JDM patients a population of

CXCR5+ T helper helper cells has been detected. This population was found to display Th2 and Th17 functionality and correlated to disease activity.

Interstitial lung disease and Th1 cells

Myositis-associated ILD is most common in those patients that express autoantibodies against Jo-1 (Mammen, 2011). The Jo-1 antigen is highly expressed in the lung compared to other organs (Casciola-Rosen et al., 2005). The cleavage of Jo-1 antigen by granzyme B in the lung is believed to trigger T cell activation by antigen-presenting cells (Danoff and Casciola-Rosen, 2011). Jo-1 antigen has been shown to trigger chemokine receptors on immature dendritic cells and T cells, in particular the expression of CCR5 (Levine et al., 2007, Howard et al., 2002). The main type of T cell found to infiltrate lung tissue of ILD patients are pro-inflammatory Th1 cells (Kurasawa et al., 2002). The presence of Th1 cells has been associated with elevated serum levels of CXCL9 and CXCL10, anti-Jo1 antibodies and ILD (Richards et al., 2009). Therefore, emphasizing a role for Th1 cells in the pathogenesis of myositis-associated ILD.

Monocyte development – macrophages and dendritic cells

Monocytes are derived from hematopoietic stem cells that leave the bone marrow and circulate in the blood stream and spleen as mononuclear phagocytes (van Furth and Cohn, 1968). Monocytes are immune effector cells that express chemokine and adhesion receptors that enable the migration from blood to tissue during infections. They can engulf cells and toxic molecules, but also express inflammatory cytokines (Auffray et al., 2009, Swirski et al., 2009). When these cells become resident in tissue they become macrophages and dendritic cells, these cells are heterogenic in

homeostatic turnover, phenotype and function (Geissmann et al., 2010). Macrophages are found resident in lymphoid and non-lymphoid tissue acting as phagocytic cells during steady-state tissue homeostasis. Their role is to remove apoptotic cells via pattern-recognition receptors (PRR) and the induction of inflammatory cytokines. Macrophages also excrete growth factors (Gordon, 2002). There are two type of dendritic cells; classical (cDCs) and plasmacytoid (pDCs). cDCs present and process antigen and as immature cells, they have high phagocytic activity whereas on maturity they produce inflammatory cytokines (Banchereau and Steinman, 1998, Mellman and Steinman, 2001). cDCs are short-lived, migratory cells that regulate T cell responses in homeostasis and infection (Waskow et al., 2008). pDCs have a longer life span than cDCs and some have immunoglobulin rearrangements. They are found in the bone marrow and peripheral organs (Corcoran et al., 2003). Their main function is to respond to viral infection with the production of type I IFNs, they also control T cell responses and act as antigen-presenting cells [APC] (Colonna et al., 2004).

Monocyte subsets

Circulating monocyte sub-populations can be defined by their expression of the surface markers CD16 and CD14 (Passlick et al., 1989). The nomenclature for types of monocytes was agreed upon in 2010 (Ziegler-Heitbrock et al., 2010). The largest population is known as classical monocytes, these are defined by being $CD14^{high}$. The smaller population, known as non-classical monocytes, are $CD14^{low}$ and $CD16^{high}$. More recently an intermediate population has been defined by $CD14^{high}$ $CD16^{high}$ (Ziegler-Heitbrock, 2015). Studies have shown that the intermediate monocyte population is expanded in inflammatory disease (Rogacev et al., 2012).

Pathogenesis of macrophages and dendritic cells in IIM

Both dendritic cells and tissue resident macrophages have been found in DM and PM biopsies (Rayavarapu et al., 2013). DCs can be divided into immature and mature subtypes. Mature DCs express DC-LAMP, this subtype is enriched in perivascular inflammatory sites in both adult and juvenile DM (Nagaraju et al., 2006). Both myeloid and plasmacytoid DCs have been implicated in the pathogenesis of DM through their association with the up-regulated type I IFN signature (Facchetti and Vergoni, 2000, Bilgic et al., 2009). Monocytes and macrophages are pathogenic in inflammatory myopathies and undergo morphological and functional change during inflammation. Studies have indicated that both M1 and M2 macrophages can be found in the muscle from myositis patients. It has been found that the detected macrophages express both early, MRP14 and 27E10 (M1) and late activation 25F9 (M2) markers in addition to the inflammatory markers iNOS and transforming growth factor (TGF)-beta (Rostasy et al., 2004, Rostasy et al., 2008). The proportion and ratio of M1 and M2 macrophages depends on the stage of the disease. The presence of different macrophages within the perimysium or endomysium reflects a diagnosis of either PM (increased M1) or DM (increased M2) and could contribute as a diagnostic tool (Rostasy et al., 2004).

Cytokines

Cytokines are a group of proteins and glycoproteins involved in signalling between lymphocytes, phagocytes and other cells of the body during an immune response. There are several sub-categories of cytokines. The interferon family includes type I and II IFN including; IFNα, IFNβ and IFNγ. The main role of the type-I IFN family is to induce a state of antiviral resistance in uninfected cells. The interleukin family

can be produced by many cells types and mainly stimulate cell division and differentiation. The colony stimulating factors direct the division and differentiation of haematopoietic stem cells in the bone marrow. Chemokines direct leukocyte recruitment to different tissues and can activate particular functions in leukocytes. Finally, there are the tumour necrosis factors (TNF) and the TGFs that are mainly involved in mediating inflammation and cytotoxic reactions.

Cytokines are key communication molecules of the immune system and play a vital role in autoimmunity (Schett et al., 2013). Pro-inflammatory cytokines such as IL-6 and TNF-α have been associated with disease pathology in many conditions, and are considered suitable therapeutic targets (Ogata et al., 2012). In rheumatoid arthritis IL-6 is expressed in excess at sites of inflammation and is considered to have an important function in inducing chronic inflammation (Hashizume and Mihara, 2011). Monoclonal antibodies against the IL-6 receptor and TNF-α bound receptor complex have been developed to block the signaling pathways of these cytokines (Jones et al., 2011, Tanaka and Martin Mola, 2014). Drugs such as tocilizumab (a humanized monoclonal antibody against the IL-6 receptor) and infliximab (a chimeric monoclonal antibody against TNF-α) have been very successful in suppressing inflammation in autoimmune diseases such as RA.

Type I IFN signature

Many autoimmune diseases have been found to have an up-regulated type I IFN signature, including SLE, RA and DM (Crow, 2014, Baechler et al., 2011, Bilgic et al., 2009). The type I IFNs comprise of thirteen types including IFN-α, IFN-β, IFN-κ, IFN-ω and IFN-ν, these bind to a common receptor, IFN-α receptor (IFNAR), but the

differences in induction of cellular responses is poorly defined (Crow, 2016). There are three proposed mechanisms behind this signature. The first mechanism is that pDCs are activated by endogenous IFN inducers to produce IFN-α. These inducers include autoantibodies and autoantigens that contain immune complexes (IC) that activate Toll-like receptor (TLR) 7 or 9 (Ronnblom and Eloranta, 2013). The second mechanism is that genes associated with autoimmune disease risk lie within the type I IFN signaling pathway that in turn affect the production and response of IFN-α. IFN-regulatory factor (IRF) 5 was identified as a SLE risk gene as it has increased expression and is activated in SLE patients (Sigurdsson et al., 2005, Feng and Barnes, 2013). Other autoimmune diseases have their own risk genes that associate with the IFN signature (Stone et al., 2012). The third identified mechanism proposes that the regulation and control of pDCs and the expression interferon regulatory genes (IRG) is not functioning correctly. The normal homeostatic negative feedback loop to switch off the production of IFNα does not work correctly in the context of SLE. B cells and natural killer (NK) cells induce pDC function after IC stimulation, and the NK cells are inhibited by monocytes (Berggren et al., 2012, Eloranta et al., 2007). This inhibition is deficient in SLE as the monocytes produce less reactive oxygen species (ROS). These are just three mechanisms that contribute to the type I IFN signature seen in autoimmunity, the relative contribution of each may differ between autoimmune disease, severity and patient.

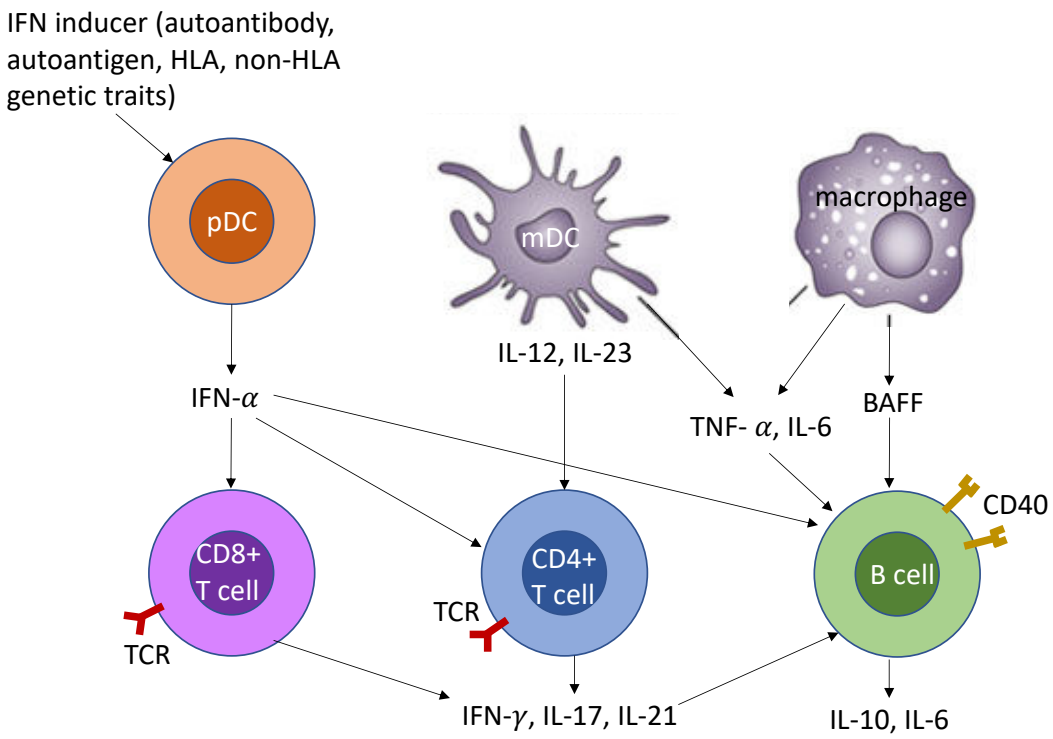

Figure I.6 The role of type I IFN and the interaction with other cytokines in the immune system.. *This is a simplified diagram of the cells involved and cytokines produced in an autoimmune disease, highlighting the wide-reaching effects of IFN-α. Arrows indicate a major producer or target cell. B-cell activating factor (BAFF), interleukin (IL), myeloid dendritic cell (mDC), plasmacytoid dendritic cell (pDC), T-cell receptor (TCR) and tumour necrosis factor (TNF). Adapted from (Ronnblom and Elkon, 2010)*

IL-6

The pleiotropic cytokine IL-6 acts as both a pro-inflammatory cytokine and an anti-inflammatory myokine. T helper 2 (Th2) cells and macrophages are the predominant producers of IL-6 but other sources include monocytes, B-lymphocytes, muscle and vascular tissue. The receptor complex mediates the biological activities of IL-6. The complex consists of IL-6 binding to the type I trans membrane glycoprotein IL-6 receptor (CD126) and the type I transmembrane signal transducer protein gp130 (CD130). IL-6 first binds to the membrane-bound non-signaling IL-6Rα (mbIL-6R). The IL-6/ IL-6Rα complex binds to two molecules of gp130. This leads to a signal

transduction pathway activating JAK/STAT, ERK and P13K (Scheller et al., 2011). Activation of the signal transduction pathway by IL-6 leads to acute phase protein synthesis, production of neutrophils in the bone marrow and supports B cell growth (Hunter and Jones, 2015).

TNF-α

TNF-α is an endotoxin-induced glycoprotein that is mainly produced by activated macrophages and T-lymphocytes. B-lymphocytes, NK cells, neutrophils, mast cells, endothelial cells, osteoclasts, fibroblasts, smooth and cardiac muscle cells are also sources of endogenous TNF (Bradley, 2008). There are two main types of TNF-α; membrane bound 26kDa protein and the 17kDa soluble form. The two forms are active in their trimeric forms and are suggested to have distinct biological activities (Black et al., 1997). The signalling pathway acts through the two receptors; TNFR1 (CD120a) and TNFR2 (CD120b). Both receptors act on the transcription factor NF-ϰB. Regulation of NF-ϰB is a principle component of the TNF signal pathway (Bouwmeester et al., 2004). TNFR1 has been shown to mediate pro-inflammatory pathways associated with programmed cell death and tissue injury. An opposite affect has been shown for TNFR2 that mediates signals that promote tissue repair and angiogenesis.

Interleukin-10

Interleukin-10 (IL-10) is an anti-inflammatory cytokine that plays a vital role in the prevention of inflammatory and autoimmune pathologies. Many cells of the innate and adaptive immune system are capable of IL-10 production regardless of

stimulation (Saraiva and O'Garra, 2010). Recent findings show that a regulatory subset of B cells produce IL-10. This B cell production of IL-10 is believed to contribute to the differentiation and maintenance of a regulatory T cell population and for the inhibition of T helper 17 and Th1 cells (Mauri and Bosma, 2012). IL-10 was found to be increased in the sera of patients with PM and DM, and positively correlated with an increase of disease activity (Gono et al., 2014).

Interleukin-17

The interleukin-17 (IL-17) family of cytokines are pro-inflammatory in nature and are produced to protect the body from infection. IL-17 works synergistically with TNF- α to induce inflammation (Bartlett and Million, 2015). During chronic inflammation and within autoimmune diseases IL-17 contributes to tissue destruction. It was discovered that IL-17 producing T cells (Th17) played a central role in autoimmune inflammation, making IL-17 an important therapeutic target (Miossec and Kolls, 2012). IL-17 expressing cells have been detected in the muscle of IIM patients, but there is a much higher proportion of IFN-γ producing Th1 cells than Th17 cells (Tournadre and Miossec, 2012, Tournadre et al., 2009). Again, the mRNA expression of IL-23 and IL-17 were detected in muscle tissue from IIM patients, but absent from healthy muscle (Kondo et al., 2009). IL-23 promotes the differentiation of the Th17 population from naïve CD4+ T cells in conjunction (Bettelli et al., 2006). These findings support an activation of the IL-23-Th17 pathway in the muscle tissue of IIM patients and identify it as a potential therapeutic target.

Cytokines in IIM

Cytokines are important mediators in chronic inflammation and in immune regulation. The type I IFN-α and –β are involved in the immunopathology of IIM. Analysis of cytokine expression in muscle tissue from patients with IIM showed increased expression of IL-1α, IL-1β, TNF-α, macrophage inflammatory proteins (MIP)-1α and TGF-β (Lundberg, 2000). As well as elevated expression in muscle tissue, TNF-α is increased in the serum of patients that have the TNFα-308A allele (Pachman et al., 2000). Another cytokine that has been detected in the muscle of patients with IIM is IL-6 (Salomonsson and Lundberg, 2006). Studies have shown that IL-6 is elevated in JDM serum and closely relates to disease activity (Bilgic et al., 2009, Yang et al., 2013). Other autoimmune diseases, such as RA, have elevated levels of serum IL-6. The therapeutic use of the monoclonal antibodies against the IL-6 receptor, tocilizumab is effective in many patients with RA (Okuda, 2008).

Lipid rafts and cell signalling

Lipid rafts are located within the plasma membrane, they are enriched with glycosphingolipid (GSL) and cholesterol (Pike, 2003, Sezgin et al., 2017).They are dynamic in nature instigating the formation of larger domains through protein-protein and protein-lipid interaction. Lipid rafts range in size from 10-200nm, but are too small to identify by optical microscopy (Gupta and DeFranco, 2007). The accumulation of lipid rafts within a plasma membrane is quantified by the stain for monosialotetrahexosylganglioside (GM1), cholera toxin-B subunit (CTB) (Blank et al., 2007). These areas of the plasma membrane accumulate high densities of signalling molecules. When the BCR binds to an antigen it associates with a lipid raft

which in turn enhances B cell signalling. Lipid rafts have been associated with atherogenesis and T–cell hyper-responsiveness (Jury et al., 2007). In SLE, it has been shown that CD4+ T cells display an alternative lipid-raft associated glycosphingolipid profile when compared to healthy control T cells. The main finding was increased levels of GM1 in the lipid rafts (McDonald et al., 2014). Restoration of the lipid rafts to normal levels comparative of healthy controls may contribute to restoration of T cell function in SLE and other autoimmune diseases (Kidani and Bensinger, 2014).

Cholesterol

Cholesterol is a vital component of all cell membranes and as such is biosynthesised by every cell, providing structural integrity and maintaining fluidity of the membrane. There are two transcription families that control cholesterol; sterol regulatory element-binding protein (SREBP) and liver X receptor (LXR). SREBP ensures a regulatory feedback loop between the biosynthesis and the uptake of cholesterol. LXR controls a feedback loop to remove excess cholesterol. Both these transcription factor families are additionally involved in regulating cytokine production and phagocytosis (Spann and Glass, 2013).

IIM and dyslipidaemia

A study by Tisseverasinghe et al suggested that patients with DM and PM have a significantly increased risk of incurring a cardiovascular event (CV). They also showed that CV events were strongly associated with dyslipidaemia (Tisseverasinghe et al., 2009). Treatment of dyslipidaemia in patients with IIM is challenging as there are no advisory treatment guidelines. The main lipid-lowering agents used are 3-hydroxy-3-methylglutaryl-coenzyme A reductase (HMGCR) inhibitors (statins), these

drugs have known myopathic side effects. Patients with IIM are considered to be at a higher risk of statin-related toxicity, but research is ongoing (Charles-Schoeman et al., 2012). Patients that are treated for CVD without an IIM can develop self-limited myopathies that resolve with discontinuation of the statin (Mohassel and Mammen, 2013). In rare cases treatment with statins can trigger an immune-mediated necrotizing myopathy that can be characterised by the presence of an autoantibody against HMGCR, the pharmacological target of statins. Anti-HMGCR myopathies require immunosuppressive treatment (Mammen, 2011).

Chapter II

Hypothesis and aims

Hypothesis 1:

Immature B cells are pathogenic in JDM

Aims:

1. Investigate the mechanisms driving B cell lymphocytosis
2. Define pathological features of B cells in JDM patients

Hypothesis 2:

Subsets of IIM have unique immune signatures

Aims:

1. Immunophenotype adult and adolescent-onset IIM PBMC samples
2. Define immune signatures by disease subtype and disease activity

Hypothesis 3:

The up-regulated type I IFN signature dysregulates cholesterol homeostasis in IIM

Aims:

1. Explore the relationship between type I IFN and cholesterol homeostasis in JDM
2. Investigate the effect of IFN-α on plasma membrane-associated lipid glycosphingolipids and cholesterol-related genes.

Materials and methods

Ethical approval

Adult myositis, adult healthy control, adolescent onset juvenile dermatomyositis, teenage healthy control and child healthy control samples were donated under the North Harrow ethics committee approval REC11/0101.

Juvenile dermatomyositis samples were donated under the London-Bloomsbury and Yorkshire research ethics committee approval REC 99RU11.

Sample collection

JDM peripheral blood mononuclear cells (PBMC), serum, plasma and DNA samples were collected through the Juvenile Dermatomyositis Research Group (JDRG) from patients recruited to the UK JDM Cohort and Biomarker study and repository (JDCBS). The JDCBS consists of 16 centres across the UK and Ireland that collect serial blood samples and clinical data from patients with JDM. Adolescent onset JDM, adult myositis (AM), teenage healthy control (THC), child healthy control (CHC) and adult healthy control (AHC) PBMC, serum and plasma samples were collected and stored in the Centre of Adolescent Rheumatology Biobank. JDM patients were recruited on the basis that they met the Bohan and Peter criteria for probable or definite disease (Bohan and Peter, 1975a). AM patients were recruited on the basis that they had a positive diagnosis by a clinician from the University College London Hospital (UCLH) with positive myositis findings on Electromyogram (EMG), magnetic resonance imaging or muscle biopsy. Child HC and adult HC

volunteers were recruited on the criteria that they did not have an immunological related condition, were not taking any medications and were healthy on the day that the samples were taken.

Recruitment pipeline

I developed a pipeline to recruit and process samples from adult myositis patients and child control volunteers (patients having elective surgery for dental caries or hernia repair, but otherwise healthy) from University college London hospital (UCLH) clinics in collaboration with the Arthritis Research UK (ARUK) Centre for Adolescent Rheumatology at University College London (UCL) Great Ormond Street Hospital (GOSH) and UCLH. I identified each patient and child control volunteer from clinic lists, recruited them in clinic, collected the blood samples and processed to be stored for experimental use.

Measurements of disease activity

The disease activity score tools described below were used to ascertain disease activity for adult and juvenile IIM.

MITAX score

Clinical assessment of the adult and juvenile myositis patients was undertaken using a myositis disease activity assessment tool (MITAX). The MITAX tool was found to be reliable and valid in an international study (Sultan et al., 2008).This activity assessment tool was developed using the same principles as the British Isles Lupus Assessment Tool (BILAG) for lupus. They are both based on the principle of the

physician's intention to treat. In each of the different organs and systems assessed a patient deemed sufficiently active to require at least 20mg of steroids +/- an immunosuppressive drug is assessed as a grade A; a patient with moderately active disease requiring a lesser amount of steroid/immunosuppressive is assessed as a B; a patient with mild disease requiring topical treatments only or Hydroxychloroquine/non-steroidal anti-inflammatories is assessed as a C; a patient whose disease was once active in the individual organ system but is no longer active is assessed as a D; and a patient whose organ systems were never previously involved is assessed as an E.

In a study involving 369 patients with lupus, the optimal numerical scoring system for the BILAG-2004 index was determined to be an A = 12 points; B = 8 points; C = 1 point; D & E = 0 points (Yee et al., 2010). As the principles on which the MITAX index were developed are identical to those for lupus, the same numerical conversion has been applied to the patients with myositis that were studied. It should be noted however that no formal proof of the validity of this methodology in patients with myositis currently exists.

Clinicians decision to treat

In addition to calculating the MITAX for each individual adult and juvenile myositis patient, the clinicians' decision on treatment was also recorded. At each sample point it was determined whether the patient had an increase, decrease or no change (stable) in their treatment. This information also informed the categorisation of patient into the disease activity groups; active, mildly active, remission on treatment and remission off treatment.

Manual muscle testing of 8 groups (MMT8)

The MMT8 scoring tool is a set of 8 designated muscles tested unilaterally. The potential maximum score demonstrating full muscle strength is 80 and the minimum score is 0 (0-80). The muscle groups tested include; deltoid, biceps, wrist extensors, quadriceps, ankle dorsi-flexors, neck flexors, gluteus medius and gluteus maximus. This scoring tool was validated in adult and juvenile IIM (Rider et al., 2010).

Childhood myositis assessment scale (CMAS)

The CMAS is a 14-item observational, performance-based tool that was developed to evaluate muscle strength, physical function, and endurance in children with juvenile IIM. The scores for the 14 items add up to form a total score ranging from 0 (very poor physical function and strength) to 52 (normal physical function and strength). This scoring tool was validated in juvenile IIM (Huber et al., 2004).

Physicians global assessment (PGA)

PGA is an accumulation of scores that represent the ways an illness affects disease activity or general health (Rider et al., 1997). The global assessment of disease activity is scored by a physician using all the information available to them on the day of appointment including the subject's appearance, history, physical examination, diagnostic laboratory testing and the resultant medical therapy. The score range is 0-10 and is marked as a vertical line on a 10cm scale. The left hand of the scale bar is equal to zero and refers to no evidence of disease activity. The midpoint line is equal to five and refers to moderate disease activity. The far-right end is equal to 10 and refers to extremely active or severe disease activity.

PBMC isolation

JDM samples:

Whole blood samples (~5ml) were collected into a universal containing ~35µl of preservative free sodium heparin (Monoparin, 1000IU/ml) or into a 7.5ml S-Monovette Na-Heparin vacutainer (Sarstedt). Equal volumes of whole blood to medium (RPMI 1640 containing L-Glutamine supplemented with Penicillin (final concentration 100 IU/ml), Streptomycin (final concentration 100µg/ml) Gibco) were diluted in a universal. Peripheral blood mononuclear cells (PBMC) were isolated by density centrifugation using Lymphoprep (Stemcell technologies). Cell count was calculated using a haemocytometer with Trypan Blue (Sigma-Aldrich), a dye that stains the nuclei of dead cells. To calculate the total number of cells; the number of cells counted in the central 5 by 5 square of the haemocytometer was multiplied by the dilution factor, 10,000 and the cell suspension volume. The PBMC were frozen in cryovials at a cell concentration of 5-10x10^6 live cells per vial re-suspended in 0.5-1ml of sterile freezing medium (90% heat inactivated foetal calf serum (FCS) plus 10% dimethyl sulfoxide (DMSO). Cryovials were labelled with allocated sample code, date and number of cells and frozen at -80°C in a Nalgene® Mr.Frosty® freezing container (controlled rate of freezing of 1°C/minute with isopropyl alcohol). The samples were stored in liquid nitrogen (-196°C) no later than 72 hours after initial freezing for future use.

AM, THC, CHC and AHC samples:

Whole blood samples (~15ml) were collected in sodium heparin coated vacutainers. PBMC were isolated by density centrifugation using Ficoll-Paque Plus (GEHealthcare). The PBMC pellet was re-suspended at 5-10x10^6 cells/ml of freezing media. The samples were aliquoted into labelled cryovials and frozen at -80°C in a Nalgene® Mr.Frosty® freezing container. The samples are stored in liquid nitrogen (-196°C) for future use.

Serum isolation

JDM samples:

Whole blood was collected in vacutainers free from coagulant. The blood was allowed to clot for 30 minutes at room temperature. The supernatant was transferred to sterile Eppendorf's and sera was isolated by micro-centrifugation (10,000xg for 10 minutes at room temperature). Supernatant was frozen and stored in labelled aliquots at -80°C.

ADM, THC, CHC and AHC samples:

Serum samples were collected in vacutainers primed with silicon clotting agents (BD vacutainer SST II advance). 30 minutes after collection the sera were isolated by density macro-centrifugation. The separated serum samples were labelled, aliquoted, frozen and stored at -80°C.

PBMC thawing and counting

PBMC samples were thawed in a water bath at 37°C, washed and re-suspended in media (RPMI-1640 with L-glutamine and $NaHCO_3$ (Sigma Aldrich) plus 10% FBS and 1% penicillin-streptomycin (10,000 units penicillin and 10mg/ml streptomycin in 0.9% NaCl working solution – Sigma Aldrich)). Cell count was calculated using a haemocytometer with Trypan Blue (Sigma-Aldrich).

Cell sorting

Magnetic bead purification

CD3+ T cells, CD14+ monocytes and enriched B cells were isolated from PBMC suspensions by magnetic bead purification using EasySep positive selection or enrichments kits (StemCell technologies), according to manufacturer's instructions. Positive selection is where the cell of interest is bound to a magnetic particle recognised by a specific antibody complex and isolated by magnetic selection. Negative selection is where all other cells apart from the cell of interest are bound to a magnetic particle recognised by a specific antibody cocktail complex and isolated by magnetic selection, leaving the negative fraction in the supernatant.

Positive selection of T cells

PBMC were thawed and then washed twice with ice-cold magnetic-activated cell sorting (MACS) buffer (PBS (Sigma-Aldrich) containing 0.5% FCS and 2mM ethylenediamine tetra-acetic acid (EDTA; Gibco, Invitrogen)) in a 50ml falcon tube and centrifuged at 500xg at 4°C for 8 minutes. The PBMC were re-suspended in MACS buffer at an indicated concentration of $1x10^8$ cells/ml in a 5ml polystyrene

round-bottom tube. The EasySep Human CD3 positive selection cocktail (tetrameric antibody complexes recognizing CD3 and containing an antibody to human Fc receptor to minimize nonspecific binding) was added at 100µl/ml of sample, mixed and incubated for 15 minutes at room temperature. The dextran-coated magnetic particles were mixed and added to sample at 50µl/ml of sample, mixed and incubated for 10 minutes at room temperature. The sample was topped up to a volume of 2.5ml with MACS buffer, mixed and placed in a cold magnet (chilled to 4°C) without a lid for 5 minutes. After the incubation the magnet was picked up and the supernatant (containing the negative fraction) was poured off in one continuous movement into a new falcon. The round-bottom tube inside the magnet was topped up to 2.5ml of MACS buffer and the magnetic incubation step was repeated twice, each time pouring off the supernatant (containing the negative fraction). After the final magnetic incubation step the isolated CD3+ T cells were re-suspended in MACS buffer and counted prior to subsequent use.

Positive selection of Monocytes

PBMC were thawed and then washed twice with ice-cold MACS buffer (PBS (Sigma-Aldrich) containing 0.5% FCS and 2mM EDTA and centrifuged at 500xg at 4°C for 8 minutes. The PBMC were re-suspended in MACS buffer at an indicated concentration of $1x10^8$ cells/ml in a 5ml polystyrene round-bottom tube. The EasySep Human CD14 positive selection cocktail (tetrameric antibody complexes recognizing CD14) was added at 100µl/ml of sample, mixed and incubated for 15 minutes at room temperature. The dextran-coated magnetic particles were mixed and added to the sample at 50µl/ml of sample, mixed and incubated for 10 minutes at room temperature. The sample was topped up to a volume of 2.5ml with MACS buffer,

mixed and placed in a cold magnet (chilled to 4°C) without a lid for 5 minutes. After the incubation the magnet was picked up and the supernatant was poured off in one continuous movement into a new falcon. The round-bottom tube inside the magnet was topped up to 2.5ml of MACS buffer and the magnetic incubation step was repeated twice, each time pouring off the supernatant. After the final magnetic incubation step the isolated CD14+ cells were re-suspended in MACS buffer and counted prior to subsequent use. ***Figure II.1B*** depicts the CD14+ monocyte cell purity before and after magnetic purification.

Negative selection of B cells

PBMC were thawed and then washed twice with ice-cold MACS buffer (PBS (Sigma-Aldrich) containing 0.5% FCS and 2mM EDTA in a 50ml falcon tube and centrifuged at 500xg at 4°C for 8 minutes. The PBMC were re-suspended in MACS buffer at an indicated concentration of $5x10^7$ cells/ml cell/ml in a 5ml polystyrene round-bottom tube. The EasySep Human B cell enrichment cocktail (tetrameric antibody complexes recognizing non-B cells) was added at 50µl/ml of sample, mixed and incubated for 10 minutes at room temperature. The EasySep D magnetic particles were vortexed and added to sample at 75µl/ml of sample, mixed and incubated for 5 minutes at room temperature. The sample was topped up to a volume of 2.5ml with MACS buffer, mixed and placed in a cold magnet (chilled to 4°C) without a lid for 5 minutes. After the incubation the magnet was picked up and the supernatant was poured off in one continuous movement into a new falcon tube. Isolated B cells in the supernatant were counted prior to subsequent use. ***Figure II.1C*** depicts the B cell purity before and after magnetic purification.

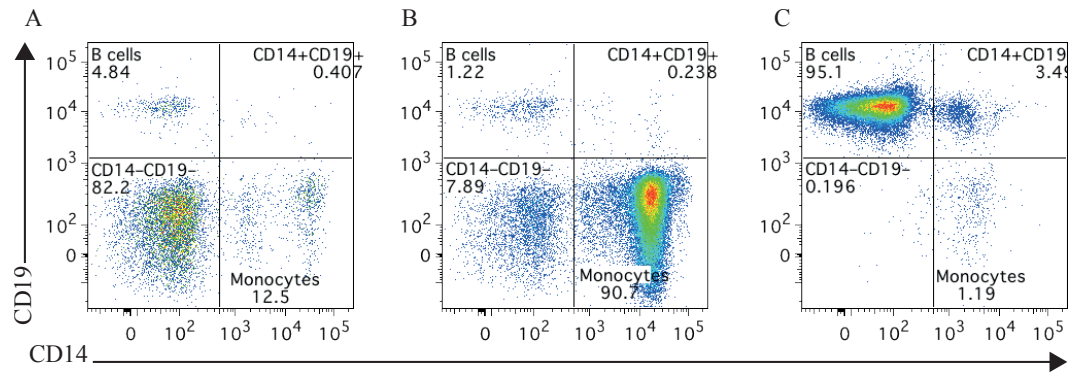

Figure II.1 Monocyte and B cell purification plots before and after isolation. *Flow cytometry plots demonstrating CD19+CD14-, CD19+CD4+, CD19-CD14+ and CD19-CD14- populations. (A) PBMC before purification. (B) PBMC after CD14+ monocyte isolation. (C) PBMC after B cell enrichment isolation.*

Flow cytometry

Staining

PBMC samples were plated in a 96 well plate at 300,000 per well. The PBMC were washed with 1xPBS and incubated at room temperature for 20 minutes with Live/Dead fixable cell stains (Life Technologies) [1:500 dilution] that were used to exclude dead cells from flow cytometric analysis (***Table II.1***). Flow cytometry was performed with directly conjugated antibodies (***Table II.2***). Surface markers were diluted in FACS buffer (500ml 1x PBS (Sigma Aldrich), 1%FBS, 0.01% sodium azide). The PBMC were washed with FACS buffer and then incubated at 4°C for 20 minutes in the presence of surface markers. All samples were fixed with intracellular fixation buffer for 20 minutes at 4°C (eBiosciences). For the measurement of *ex-vivo* intra-nuclear Ki-67, cells were fixed with FOXP3 fixation buffer (eBiosciences). Intracellular markers were diluted in Perm buffer (10% 10x permeabilisation buffer (eBiosciences), 90% FACS buffer). The PBMC were washed with Perm buffer and then incubated in the presence of intracellular or intra-nuclear markers for 45 minutes at 4°C.

For samples that were stained for CTB and filipin. All samples were stained with 50µL of CTB (1:100) (Sigma Life Sciences) in FACS buffer for 20 minutes at 4°C. Samples were next washed with 150µL of FACS buffer and spun at 800xg, for 3 minutes at 4 °C. Samples were fixed with 100µL 2% paraformaldehyde (PFA) (Sigma-Aldrich) in foil at room temperature (RT) for 1hour. The samples were washed with 100µL of FACS buffer and spun at 800xg, for 3 minutes at 4°C. The samples were re-suspended in 200µL of 1xPBS and left overnight in the fridge. The samples were washed with 100µL of FACS buffer and spun at 800xg, for 3 minutes at 4°C. The samples were stained with 100µL of filipin (1:200 in 1 xPBS) for 2hours at RT in foil. The samples were washed with 100µL of FACS buffer and spun at 800xg, for 3 minutes at 4°C. The samples were re-suspended in 200µL of FACS buffer and placed in FACS tubes to be run on LSRII flow cytometer.

Flow cytometry cell sorting

The PBMC subsets CD4, CD8, CD14 and CD19 were sorted by flow cytometry (FACS Aria III), after staining for 30 minutes with CD4 BV711 (1:25), CD8 APC (1:200), CD14 FITC (1:100) and CD19 Pe-Cy7 (1:25) in sort buffer (50ml 1x sterile PBS, 1ml FBS, 400µl 0.5M EDTA) (***Table II.2***). Dead cells were excluded by using 4,6 diamidino-2-phenylindole (DAPI; Sigma) at 1µ/ml. Sorted cells were collected in collection media (RPMI+1%penicillin-streptomycin + 20% FBS). A purity check was completed on each sorted cell type collecting 500 events for each.

Analysis

Data were collected on an LSRII flow cytometer (BD Pharmingen) using FACS Diva software. Application settings were created to begin with and Cytometer Setup and Tracking (CS&T) beads were run on the flow cytometer before each session. Application settings were applied to panel templates each time prior to compensation to ensure that all immunophenotyping data is comparable over time. Data were analysed with Flowjo (Tree Star).

List of antibodies

Table II.1 List of live/dead fixable stains

Live/dead	Fluorochrome	Manufacturer
Live/dead fixable blue	Live/dead blue	Life technologies
Live/dead fixable yellow	QDOT 605	Life technologies
4,6-diamidino-2phenylindole (DAPI)	DAPI	Sigma

Table II.2 List of conjugated antibodies used for flow cytometry

Surface marker	Fluorochrome	Clone	Isotype	Manufacturer
CD3	BUV396	UCHT1	Mouse BALB/c IgG1, κ	BD
CD185	BV605	J252D4	Mouse IgG1, κ	Biolegend
CD4	BUV737	SK3	Mouse BALB/c IgG1, κ	BD
CD4	BV711	OKT4	Mouse IgG2b, κ	Biolegend
CD45RA	BV421	HI100	Mouse IgG2b, κ	Biolegend
CD27	BV785	O323	Mouse IgG1, κ	Biolegend
CD127	BV711	A019D5	Mouse IgG1, κ	Biolegend
CD25	PE-Cy7	M-A251	Mouse IgG1, κ	Biolegend
TCR V a24-Ja18	APC	6B11	Mouse IgG1, κ	Biolegend
CD8	APC-cy7	RPA-T8	Mouse IgG1, κ	Biolegend
CD8	APC	SK1	Mouse IgG1, κ	eBioscience
CD69	BV510	FN50	Mouse IgG1, κ	Biolegend
PD-1	PE	NAT105	Mouse IgG1, κ	Biolegend
CD278	AF488	C398.4A	Armenian Hamster IgG	Biolegend
CD19	BV786	HIB19	Mouse IgG1, κ	Biolegend
CD19	Pe-Cy7	SJ25C1	Mouse IgG1, κ	eBioscience
CD38	BUV737	HB7	Mouse IgG1, κ	BD
CD24	BV421	ML5	Mouse IgG2a, κ	Biolegend
CD27	BV711	O323	Mouse IgG1, κ	Biolegend
CD14	BV605	M5E2	Mouse IgG2a, κ	Biolegend
CD14	FITC	61D3	Mouse IgG1, κ	eBioscience
CD16	APC-cy7	B73.1	Mouse IgG1, κ	Biolegend
IgD	FITC	IA6-2	Mouse IgG2a, κ	Biolegend
CD69	PE-cy7	FN50	Mouse IgG1, κ	Biolegend
HLA-DR	BV510	L243	Mouse IgG2a, κ	Biolegend
CD24	APC	SN2 A5-2H10	Mouse IgG1, κ	eBioscience
CD27	PECy7	O323	Mouse IgG1, κ	eBioscience
CD38	BV605	HIT2	Mouse IgG1, κ	Biolegend
IgM	Pacific Blue	MHM-88	Mouse IgG1, κ	eBioscience
Cholera Toxin b subunit (CTB)	FITC			Sigma
Filipin	INDO-1 violet			

Table II.3 List of conjugated intracellular and intra-nuclear antibodies used for flow cytometry

Intracellular/nuclear	Fluorochrome	Clone	Isotype	Manufacturer
IL-6	PE	MQ2-13A5	Rat IgG1,k	eBioscience
IL-17A	AF 488	N49-653	Mouse IgG1, k	BD
Ki-67	PE	B56	Mouse IgG1, k	BD
IL-10	APC	JES3-9D7	Rat IgG1,k	BD

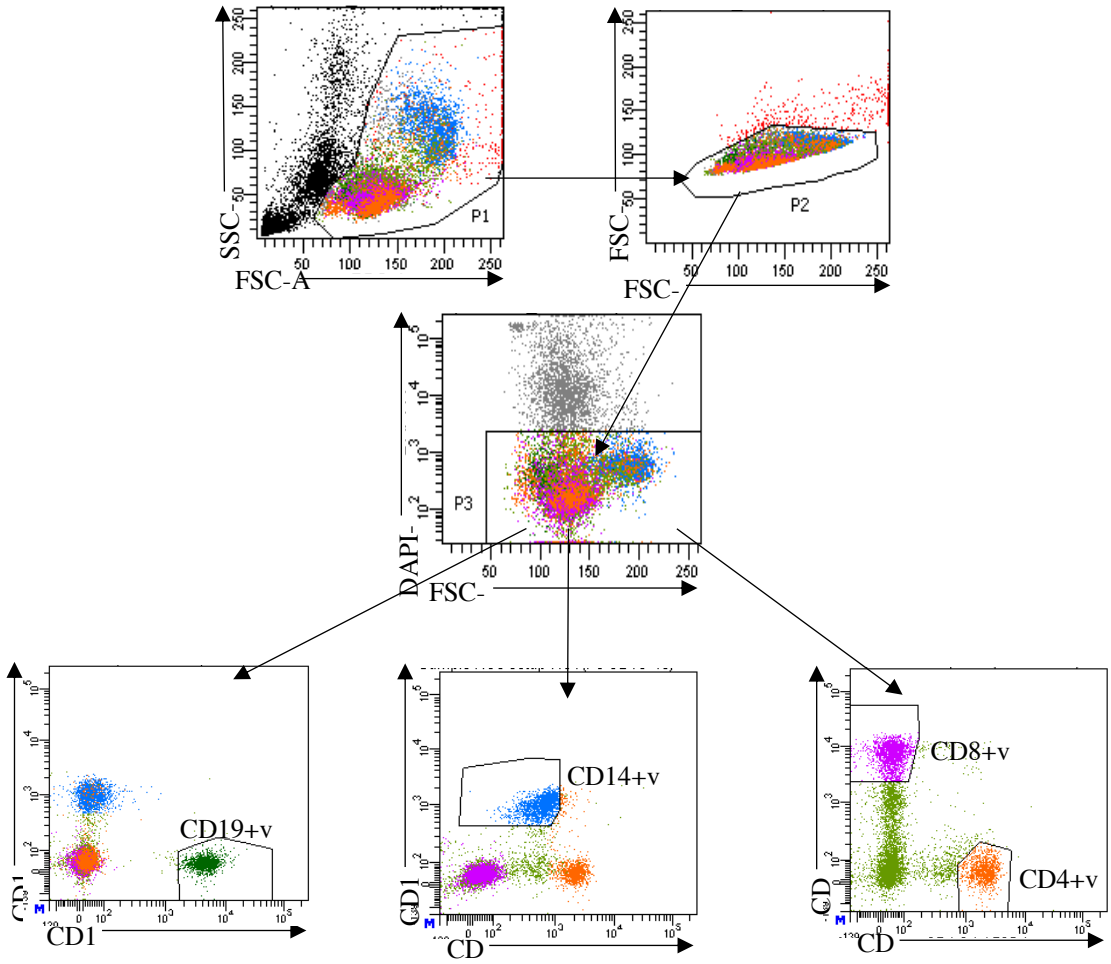

***Figure II.2 FACS gating strategy**. Representative flow cytometry gating strategy plots for sorting CD19+ve B cells, CD14+ve monocytes, CD8+ve and CD4+ve T cells from PBMC sample. Gate P1 selects PBMC by size. Gate P2 selects singularly stained cells. Gate P3 selects live DAPI negatively stained PBMC.*

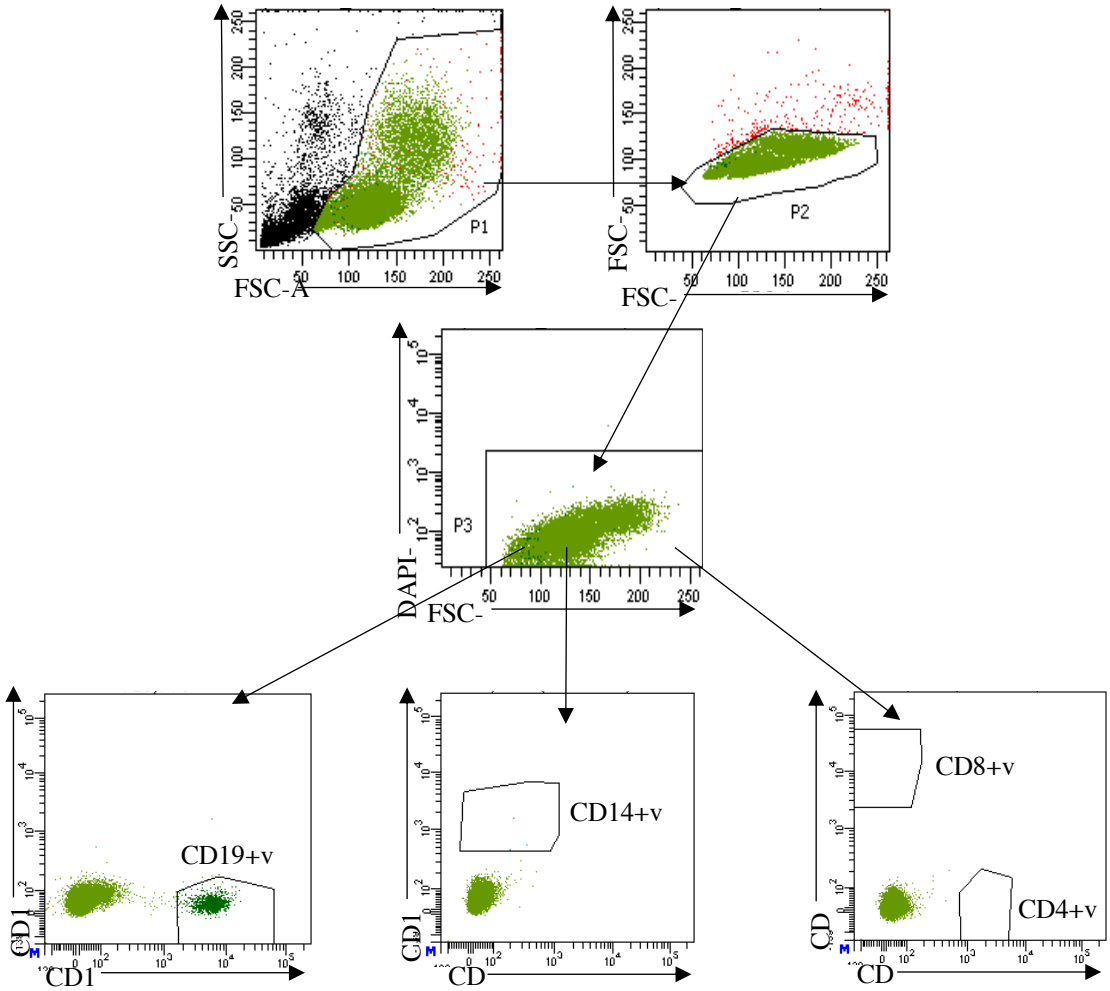

Figure II.3 Purity check for CD19+ve sorted cells. *Gate P1 selects PBMC by size. Gate P2 selects singularly stained cells. Gate P3 selects live DAPI negatively stained PBMC.*

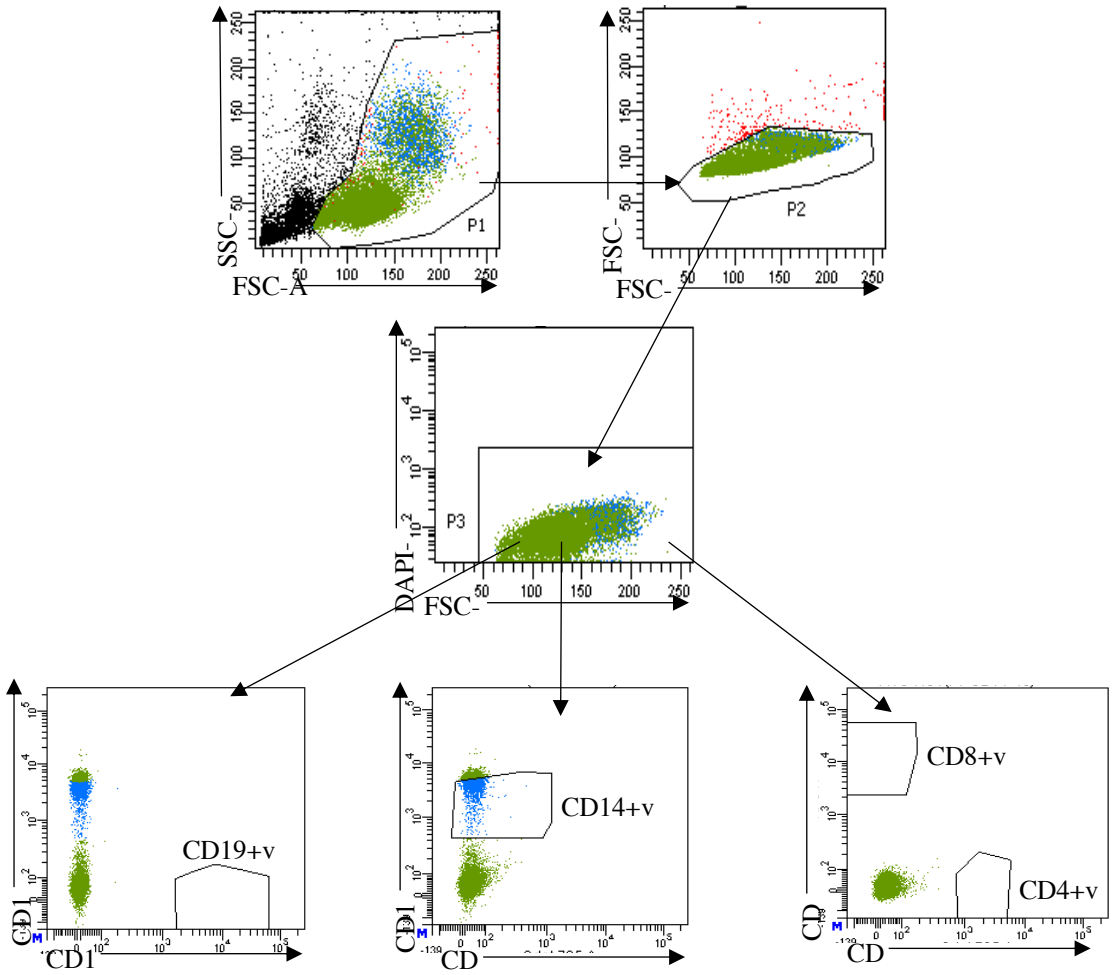

Figure II.4 Purity check for CD14+ve sorted cells. *Gate P1 selects PBMC by size. Gate P2 selects singularly stained cells. Gate P3 selects live DAPI negatively stained PBMC.*

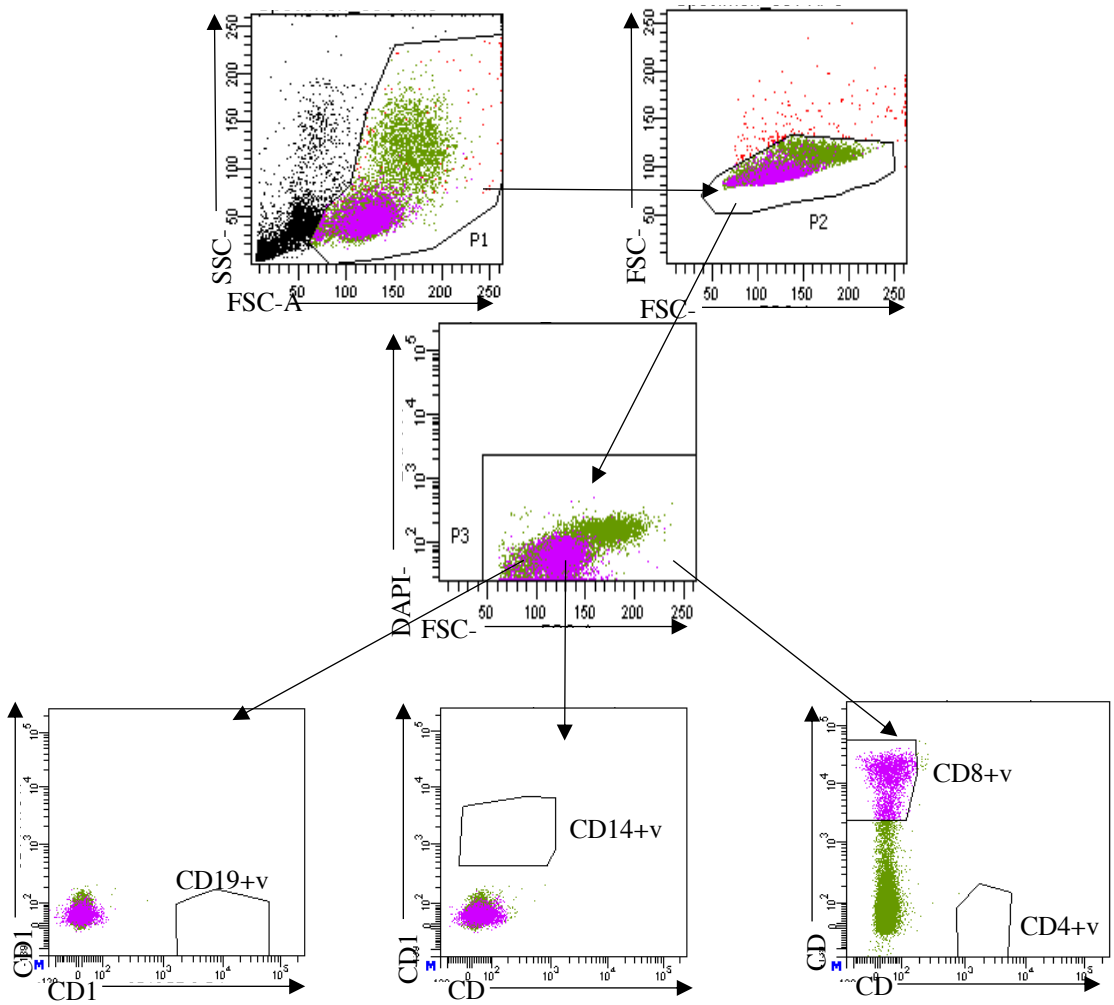

Figure II.5 Purity check for CD8+ve sorted cells. *Gate P1 selects PBMC by size. Gate P2 selects singularly stained cells. Gate P3 selects live DAPI negatively stained PBMC.*

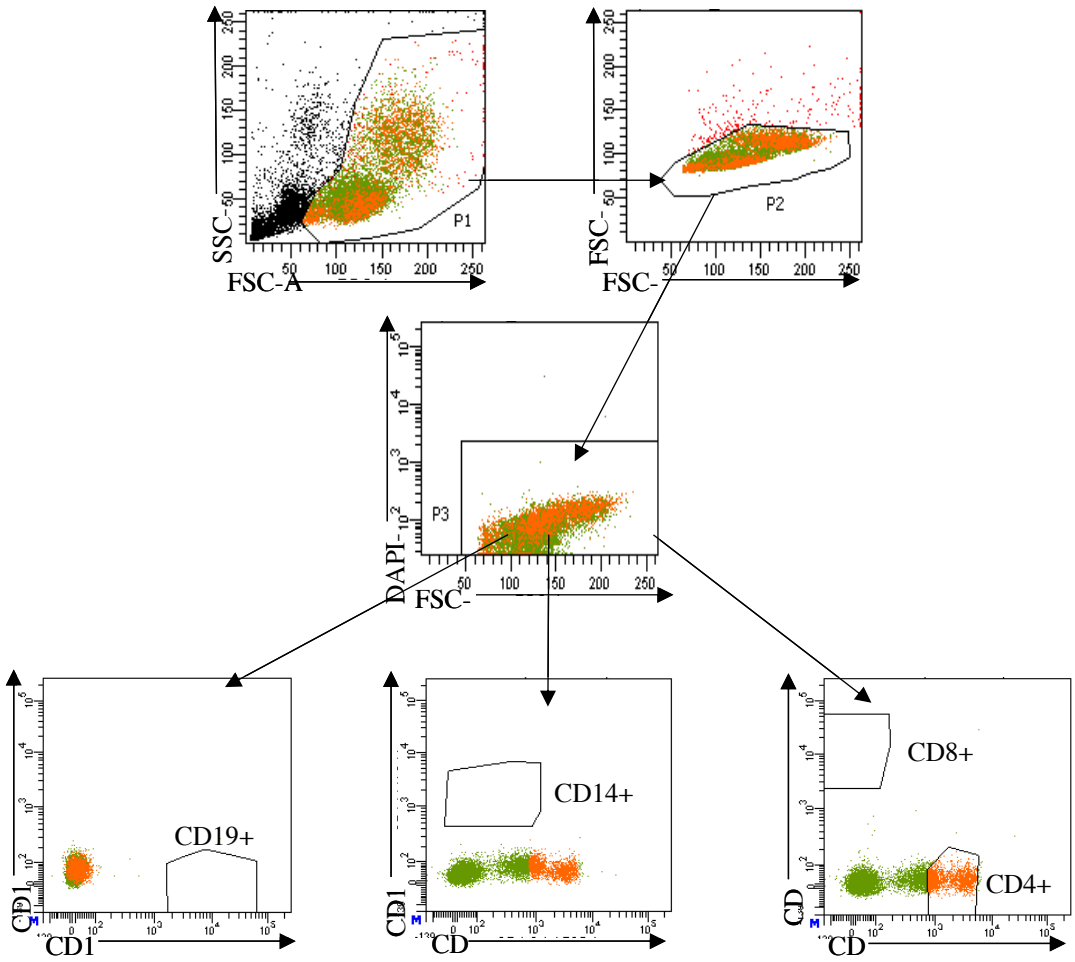

Figure II.6 Purity check for CD4+ve sorted cells. *Gate P1 selects PBMC by size. Gate P2 selects singularly stained cells. Gate P3 selects live DAPI negatively stained PBMC.*

Cell culture

PMA/I/GP

To detect intracellular cytokines PBMC were stimulated for 4 hours; with 50ng/ml PMA and 250ng/ml Ionomycin (both Sigma Aldrich) in the presence of Golgi plug (BD Bioscience).

IFN-α and R848

For the detection of intracellular IL-6 and IL-10; 300,000 PBMC/B cells were cultured for 48/72 hours with R848 at 1μg/ml (Invivogen) +/- recombinant IFN-α at

1000 IU/ml (PBL assay Science) in media (RPMI 1640 containing L-Glutamine supplemented with 10% FCS and Penicillin (final concentration 100 IU/ml)). To detect changes in lipid regulated genes in response to IFN-α, 300,000 sorted monocytes, B and T cells were cultured with IFNα for 2/6/24hours.

Chinese hamster ovary (CHO) cells expressing human CD154 (CD40L)

One million CD154 transfected CHO cells and un-transfected control cells (donated by Prof. R. Mageed, Queen May University London) were grown in Dulbecco's Modified Eagle's Medium (DMEM; Sigma-Aldrich) containing 4500 mg/ml glucose, 110 mg/ml sodium pyruvate and 2nM L-glutamine, supplemented with 5% FCS and 100U/ml penicillin and streptomycin in T25 flasks. When the CHO cells were adherent and confluent they were washed with ice-cold phosphate-buffered saline (PBS), and detached using Trypsin-EDTA (Sigma-Aldrich) and were seeded in new culture flasks after each passage. Routinely through the growth period of the CHO cells the CD154 expression was checked by flow cytometry. The CHO cells received gamma-irradiation via a caesium source for 10 minutes (250kV, 11.6mA, 7 Gy/minute) in 25cm^2 culture flasks with a minimal covering of culture media prior to use in an experiment, this was to prevent further proliferation. The irradiated CHO cells were then washed with RPMI 1640, detached using Trypsin-EDTA as previously and counted using a haemocytometer. A ratio of 1:10 CHO:B cells was used in experimental cell cultures. The CHO cells were incubated for 2 hours prior to addition of human B cells to allow adherence.

Analysis of Kappa-deleting recombination excision circles (KREC) content

Immature, mature and memory B cells were sorted and DNA was extracted using a QIAamp Blood DNA Mini Kit (Qiagen), according to manufacturer's instructions. Quantitative real time PCR (qRT-PCR) was carried out on the DNA samples as previously described (Gaspar et al., 2011), with a standard curve method of analysis, using serial dilutions of a known quantity (10^6, 10^5, 10^4, 10^3, 10^2, 10 copies) of a linearised plasmid containing segments of T cell receptor alpha constant (TRAC), KREC and T cell receptor excision circles (TREC). The quantity of KREC per 10^6 cells were calculated by the following equation, whereby *n* is the total amount of KRECs per 10^6 cells; *k* is the mean quantity of KRECs and *t* is the mean quantity of TRAC.

$$n = \frac{k}{t/2}\ x10^6$$

Details of the plasmid and primer/probe sequences used were previously (Sottini et al., 2010).

ELISA

Human serum and PBMC culture supernatants (stimulated with CD40L CHO for 72 hours) were measured for concentrations of IL-10, IL-6 and soluble IL-6 receptor complex. IL-6 and soluble IL-6 receptor complex were measured separately using R&D systems human ELISA kits (DY206, DY8139-05) according to manufacturer's instructions. The Ready-set-go human IL-10 ELISA kit (eBioscience) was used according to manufacturer's instructions. Sera from patients were tested for CXCL10, CXCL11, MCP-1 and MCP-2 via multiplex cytokine array (Luminex) (Bellutti Enders et al., 2014).

RNA extraction

PicoPure

PBMC and sorted cell sample RNA were extracted following the Arcturus PicoPure RNA Isolation protocol, using cell suspension media (0.9ml 1xPBS/10%BSA, 0.1ml 0.5M EDTA) and extraction buffer (Arcturus PicoPure RNA Isolation Kit). The samples were frozen and stored at -80°C.

Within the lab benches, an RNA free zone with RNase was established. RNA was isolated following the Arcturus PicoPure RNA manufacturers protocol using reagents from the PicoPure RNA Isolation Kit (Thermo Fisher). 250µl of conditioning buffer was pipetted onto the purification columns filter membrane and incubated at room temperature for 5 minutes. The columns were spun at 16,000xg for 1 minute in a micro-centrifuge. The extracted PBMC and sorted cell RNA samples were thawed and 100µl of 70% ethanol was added and mixed. The samples were pipetted into the pre-conditioned purification columns and spun at 100xg for 2 minutes, followed by 1 minute at 16,000xg to bind the DNA. 100µl of wash buffer 1 was pipetted into each purification column and spun at 8,000xg for 1 minute. A mix of 10ul of DNase I stock solution and 30µl of Buffer RDD per sample was made, 40µl was added to each purification column and the incubated for 15 minutes. 40µl of wash buffer 1 was added to each column and spun at 8,000xg for 1 minutes. 100µl of wash buffer 2 was pipetted into each column and spun at 8,000g for 1 minutes. 100µl of wash buffer 2 was pipetted into the column and spun at 16,000g for 2 minutes. The column was transferred into new 0.5ml micro centrifuge tube and 11µl of elution buffer was directly pipetted onto each membrane. After being incubated for 1 minute at room

temperature each column and tube complex was spun at 1,000xg for a minute followed by 16,000xg for another minute to elute the RNA into the micro-centrifuge tube. The isolated RNA samples were labelled and stored at -80°C in preparation for RNA sequencing or polymerase chain reaction (PCR).

Trizol RNA extraction

PBMC and sorted cell sample RNA were extracted following the Trizol RNA isolation protocol developed within the lab group. The samples were aliquoted into RNA free labelled eppendorfs and spun at 400xg for 10 minutes in a micro-centrifuge. The supernatant was removed and the pellet re-suspended in 200µl of Trizol in a fume cupboard. The Trizol samples were stored at -80°C.

Extraction was carried out within the RNA free zone with RNase Zap ® and the protocol was carried out on ice. The extracted PBMC and sorted cell RNA samples were thawed and an identical set of labelled eppendorf's were placed in the fridge. 40µl of chloroform was added to thawed samples, vortexed and incubated at room temperature for 3 minutes. The samples were spun at 13,500rpm for 20 minutes at 4°C. Following centrifugation the mixture separates into lower red, phenol-chloroform phase, an interphase, and a colourless upper aqueous phase. RNA remains exclusively in the aqueous phase. The upper aqueous phase was transferred into the cold new eppendorf's, taking care not to disturb the interphase. The RNA was precipitated from the aqueous phase by mixing it with 100µl of cold isopropyl alcohol and 0.2µl of glycogen (10µg/L) (a carrier to ensure visible RNA pellets) and stored at -20°C overnight.

The samples were thawed and spun at 13,500rpm for 15 minutes at 4°C. The supernatant was removed completely and 500µl of cold 70% ethanol was added to each tube. The suspension was mixed and spun at 13,000rpm for 15 minutes at 4°C. The wash and spin was repeated. The supernatant was completely removed and the pellets were left to dry without lids for 5 minutes at room temperature. The RNA pellet was dissolved in 20µl of pre-heated (65°C) molecular water. The quantity and quality of the eluted RNA samples were analysed by nanodrop spectrophotometer and stored at -80°C.

cDNA synthesis

cDNA was synthesised using the qScripta cDNA synthesis kit (VWR). 4µl of 5x master mix (containing primer blend (oligo dT(20) and random hexamer), dNTPs and $MgCl_2$), and 1µl of enzyme (50x concentrated qScript reverse transcriptase) were added to 15µl of pre-diluted RNA. The samples were mixed and centrifuged for 30 seconds to collect the contents. The samples were placed in a thermal cycler programmed; one cycle at 22°C for 5 minutes, one cycle at 42°C for 30 minutes, one cycle at 85°C for 5 minutes and then stored at 4°C.

PCR

Primer design

Primers were designed to be intron spanning or flanking (to avoid amplification of genomic DNA) using Primer 3 (Koressaar and Remm, 2007). The specificity was checked with NCBI Primer Blast (Ye et al., 2012). The efficiency was validated by

amplifying a standard curve of DNA, and the dissociation curves were checked for primer dimers.

Table II.4 Primers used to measure gene expression by qPCR

Gene	Forward primer	Reverse primer
Cyclophilin	5'GCATACGGGTCCTGGCATCTTGTCC3'	5'ATGGTGATCTTCTTGCTGGTCTTGC3'
3-hydroxy-3methylglutaryl-coenzyme A reductase (HMGCR)	5'CAGCCATTTTGCCCGAGTTT3'	5'AGCGACTGTGAGCATGAACA3'
Fatty acid synthase (FASN)	5'CTGCTGCTGGAAGTCACCTA3'	5'GTGTGTGTTCCTCGGAGTGA3'
Sterol regulatory element-binding transcription 1 (SREBP1)	5'TCAGCGAGGCGGCTTTGGAG3'	5'CATGTCTTCGATGTCGGTCAG3'
Sterol regulatory element-binding transcription 2 (SREBP2)	5'CTGGAGACCATGGAGACCCT3'	5'GTCAGGGAACTCTCCCACTTG3'
UDP-glucose ceramide glucosyltransferase (UGCG)	5'CGTCCTCTTCTTGGTGCTGT3'	5'AGAGAGACACCTGGGAGCTT3'
Stearoyl-CoA desaturase (SCD)	5'GCAAACACCCAGCTGTCAAA3'	5'GCACATCATCAGCAAGCCAG3'
ELOVL fatty acid elongase 5 (ELOVL5)	5'CTTGGGCTAAAAGGTTTTCAAATGG3'	5'ATCTCGAGGGCCTAGCAATG3'
F-box 06 (FBX06)	5'TGGGGATCCCAGGCCA3'	5'TTCTCGGGCAGGTCGTTAAT3'
Syntaxin 5 (STX5)	5'GACAATCTTGGCAAAGCGCA3'	5'TCCTGGAGCTGAGCAATTTGT3'
Malic enzyme 1 (ME1)	5'TAGTTTGGTGTTTCGGAAGCC3'	5'CCACAATGGCCTTGATGACA3'

Quantative PCR (qPCR)

To measure the expression of the selected genes qPCR was used. SYBR green (Quanta Biosciences TM) was the reference dye and cyclophilin was the endogenous control (housekeeping) gene. qPCR was carried out using a 2-step protocol (the annealing and extension happen in the same step); 30s at 95°C, followed by 40 cycles of 5s 95°C (denaturation), 30s 60°C (annealing/extension), finishing with the dissociation curve (***Figure II.7***).

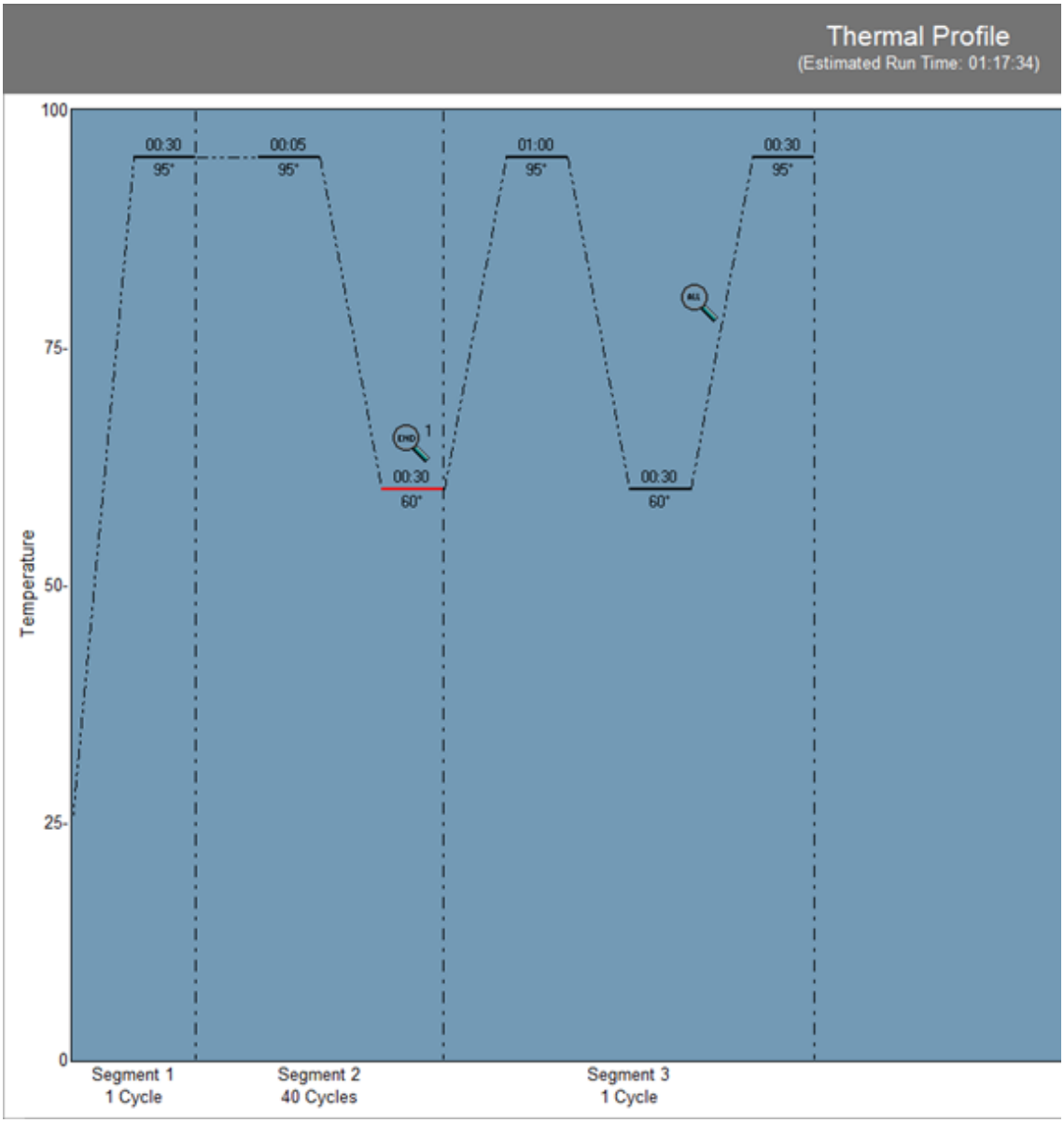

Figure II.7 Thermal profile for qPCR

RNA-sequencing

Library preparation

Samples were processed using Illumina's TruSeq Stranded mRNA LT sample preparation kit (p/n RS-122-2101) according to manufacturer's instructions with minor alterations. Products that were used that were not included in this kit have been stated.

PolyA select mRNA

250ng total RNA and nuclease free H_20 was mixed to a final volume of 50µl. RNA purification beads were vortexed and 50µl was added to each RNA sample. The sample was mixed by pipetting up and down until beads were in a homogenous suspension. Next the sample was incubated in a thermacycler to denature for 5 minutes at 65°C and hold at 4°C. Once the thermocycler reached 4°C the samples were removed and placed on the bench at room temperature for 5 minutes. The samples were placed in a magnetic rack for 5 minutes. The supernatant was removed and discarded. The samples were removed from the rack. 200µl of Bead Washing buffer was added to each sample and pipetted up and down until the beads were in a homogenous suspension. The samples were put back into the magnetic rack for 5 minutes, or until the beads had pelleted. The supernatant was removed and discarded. 50µl of Elution Buffer was added to each sample and pipetted up and down until beads were in a homogenous suspension. The samples were incubated in the thermocycler to elute the RNA for 2 minutes at 80°C for 2 minutes and then held at 25°C. The samples were removed from the thermocycler when they had reached 25°C and kept at room temperature. 50µl of Bead Binding Buffer was added to each sample and pipetted up and down until beads were in a homogenous suspension. The samples were incubated at room temperature for 5 minutes. The samples were placed in the magnetic rack for 5 minutes, or until the beads pelleted. The supernatant was removed and discarded. The samples were removed from the rack. 200µl of Bead Washing Buffer was added to each sample and pipetted up and down until the beads were in a homogenous suspension. The samples were placed in a magnetic rack for 5 minutes, or until beads pelleted. The supernatant was removed and discarded. 19.5µl of

Fragment, Prime, Finish mix was added to each sample and pipetted up and down until the beads were in a homogenous suspension. The samples were incubates in the thermocycler to prime for 10 minutes at 94°C and then hold at 4°C, then briefly spun and placed in a magnetic rack for 5 minutes. Lastly, 17µl of the supernatant was transferred to a new 0.2ml PCR tube.

First strand synthesis

8µl First Strand Synthesis ActD/Superscript II mix (SuperScript II, Life Technologies p/n 18064014) was added to each sample. The samples were incubated in the thermocycler for the fscDNA stage for 10 minutes at 25°C, then 15minutes at 42°C, 15 minutes at 70°C and held at 4°C.

Second strand synthesis

5µl of Resuspension buffer was added to each sample. 20µl of Second Strand Marking Master mix was added to each sample. The samples were incubated in the thermocycler with the lid open for the sscDNA stage for 60 minutes at 16°C and then held at 4°C. The samples were removed and left at room temperature.

Clean up cDNA

90µl of well vortexed AMPure XP beads (Ampure XP, Beckman Coulter p/n A63881) were added to each sample and mixed by pipetting up and down until the beads were in a homogenous suspension. The samples were incubated at room temperature for 5 minutes, then placed in a magnetic rack for 5 minutes, or until beads had pelleted. The supernatant was removed and discarded. The samples were kept in

the magnetic rack and 200µl 80% ethanol was added to each. The samples were incubated for 30 seconds. All supernatants were removed and discarded. The ethanol wash was repeated twice. All the residual ethanol was removed. The samples were left to stand at room temperature to dry for 5-15 minutes. 19.5µl Resuspension Buffer was added to each sample and pipetted up and down until the beads were in a homogenous suspension. The samples were incubated at room temperature for 2 minutes, and placed in a magnetic rack for 5 minutes, or until beads pelleted. 17.5µl of the supernatant was transferred to new 0.2ml PCR tube.

Perform A-tailing

12.5µl A-Tailing mix was added to each sample. The samples were incubated in the thermocycler for the ATAIL step for 30 minutes at 37°C, 5 minutes at 70°C and held at 4°C. The samples were removed from the thermocycler when they had reached 4°C.

Ligate adaptors

To each sample 2.5µl of Resuspension buffer, 2.5µl ligation mix, and 2.5µl of RNA Adaptor index was added. The samples were incubated in a thermocycler for the Ligate step for 10 minutes at 30°C. 5µl of Stop ligation mix was added to each.

Clean up Adaptor-ligated cDNA

42µl of well vortexed AMPure XP beads were added to each sample and mixed by pipetting up and down until the beads were in homogenous suspension. The samples were incubated at room temperature for 5 minutes. The samples were placed in a

magnetic rack for 5 minutes, or until beads had pelleted. The supernatant was removed and discarded. The samples were kept in the magnetic rack and 200µl 80% ethanol was added. The samples were incubated for 30 seconds. All supernatant was removed and discarded. The ethanol wash was repeated twice. All residual ethanol was removed. The samples were let to stand at room temperature to dry for 5-15 minutes. 52.5µl Resuspension buffer was added to each sample and pipetted up and down until the beads were in a homogenous suspension. The samples were incubated at room temperature for 2 minutes, and placed in a magnetic rack for 5 minutes, or until beads had pelleted. 50µl of the supernatant was transferred to a new 0.2ml PCR tube. 50µl of well vortex AMPure XP beads was added to each sample and mixed by pipetting up and down until the beads were in homogenous suspension. The samples were incubated at room temperature for 5 minute, and placed in a magnetic rack for 5 minutes, or until beads had pelleted. The supernatant was removed and discarded. The samples were kept in the magnetic rack and 200µl 80% ethanol was added to each. The samples were incubated for 30 seconds. All the supernatant was removed and discarded. The ethanol wash was repeated twice. All residual ethanol was removed. The samples were let to stand at room temperature to dry for 5-15 minutes. 22.5µl Resuspension buffer was added to each sample and pipetted up and down until the beads were in a homogenous suspension. The samples were incubated at room temperature for 2 minutes. The samples were placed in a magnetic rack for 5 minutes, or until beads had pelleted. 20µl of the supernatant was transferred to a new 0.2ml PCR tube.

Amplify library by PCR

A mastermix was prepared for each reaction; 5µl of PCR Primer cocktail and 25µl of PCR master mix. 30µl of the mastermix was added to 20µl adaptor ligated cDNA and mixed by pipetting up and down. The cDNA was amplified by the following PCR protocol; 30 seconds at 98°C, then for 14 cycles (10 seconds at 98°C, 30 seconds at 60°C, 30 seconds at 72°C), 5 minutes at 72°C and then held at 4°C.

Clean up PCR products

50µl of well vortexed AMPure XP beads was added to each sample and mixed by pipetting up and down until the beads were in homogenous suspension. The samples were incubated at room temperature for 5 minutes, then placed in a magnetic rack for 5 minutes, or until beads had pelleted. The supernatant was removed and discarded. The samples were kept in the magnetic rack and 200µl 80% ethanol was added. The samples were incubated for 30 seconds. All supernatant was removed and discarded. The ethanol wash was repeated twice. All residual ethanol was removed. The samples were let to stand at room temperature to dry for 5-15 minutes. 32.5µl Resuspension buffer was added to each sample and pipetted up and down until the beads were in a homogenous suspension. The samples were incubated at room temperature for 2 minutes, and placed in a magnetic rack for 5 minutes, or until beads had pelleted. 30µl of the supernatant was transferred to a new 0.2ml PCR tube. The library distribution was assessed on a Bioanalyser DNA 1000 and quantified using the Qubit DNA HS assay. The concentration was normalised to 10nM.

Briefly, mRNA was isolated from 250 ng total RNA using Oligo dT beads to pull down Poly-Adenylated transcripts. The purified mRNA was fragmented using

chemical fragmentation (heat and divalent metal cation) for 10 minutes and primed with random hexamers. Strand-specific first strand cDNA was generated using Reverse Transcriptase and Actinomycin D. This allows for RNA dependent synthesis while preventing spurious DNA-dependent synthesis. The second cDNA strand was synthesised using dUTP in place of dTTP, to mark the second strand. The resultant cDNA is then "A-tailed" at the 3' end to prevent self-ligation and adapter dimerisation. Full length TruSeq adaptors, containing a T overhang are ligated to the A-Tailed cDNA. These adaptors contain sequences that allow the libraries to be uniquely identified by way of a 6 base pairs Index sequence. Successfully ligated fragments were enriched with 14 cycles of PCR. The polymerase is unable to read tough uracil, so only the first strand is amplified, thus making the library strand specific.

Sequencing

Libraries to be multiplexed in the same run were pooled in equimolar quantities, calculated from Qubit and Bioanalyser fragment analysis. Samples were sequenced on the NextSeq 500 instrument (Illumina, San Diego, US) using a 43 bp paired end run resulting in >15million reads per sample.

iData Analysis

Run data were demultiplexed and converted to fastq files using Illumina's bcl2fastq Conversion Software v2.16. Sequencing reads (in fastq format) were aligned to the GRCh38 reference sequence using TopHat v2.1.0 (Kim et al., 2013). Alignments were processed using samtools version 1.2 and Picard tools version 1.140 (http://picard.sourceforge.net/)(Li et al., 2009). Aligned reads were filtered for

mapq >= 4, i.e. uniquely mapping reads, and putative PCR duplicates were removed. Read summarization was performed using featureCounts (Liao et al., 2014). Expression analysis was carried out using R version 3.2.2 (Team, 2015), and differential gene expression was analysed using edgeR (Robinson et al., 2010).

Gene Set Enrichment Analysis (GSEA)

GO term and pathway enrichment analysis was carried out using '*goseq'* which uses a test based on the Wallenius' noncentral hypergometric distribution (Young et al., 2010). Gene set enrichment analysis was carried out with "Hallmark" gene sets from databases (Subramanian et al., 2005). Normalized enrichment scores (NES) and multiple adjusted p-values (q values) were calculated.

Statistical analysis

Data, excluding RNAseq, were analysed using Graphpad Prism 6. Expression analysis was carried out using R version 3.2.2, and differential gene expression was analysed using edgeR (Team, 2015, Robinson et al., 2010). One way analysis of variance (Crow and Casanova) was used to assess significance of differences between group means (≥3 groups) and unpaired Student's t test was used to assess significance between 2 groups. Bonferonni, Dunnett's and Tukey's corrections were applied for multiple comparisons using ANOVA. Pearson's/ Spearman's correlation coefficients were used to assess correlations. Bar graph data represented as mean ± SEM. For all figures, *P* values are represented as followed: * $P < 0.05$; ** $P < 0.01$; *** $P < 0.001$.

Statistical analysis for chapter IV

Statistical analysis was performed in GraphPad Prism 6 software. Initially unpaired student t-tests were used to compare ex-vivo cell populations from patients and controls, this calculated p values from testing the significance of the difference. The fold change was also calculated to determine the directional change in the mean average. Each disease group was also analysed by comparing subsets of the disease; dermatomyositis (DM), polymyositis (PM), dermatomyositis with cancer (DM+C), dermatomyositis with overlap (DM+O), and polymyositis (PM+O). Also, comparing groups of disease activity. These comparisons were made using multiple *t* tests with Holm-Sidak method of correction or one-way ANOVA to calculate an adjusted p value by Tukey's multiple comparison test. SPSS version 24 software was used to produce correlation values by calculating Pearson's correlation between two sets of cell types. MultiExperiment Viewer (MeV) was used to produce heat maps and perform hierarchical clustering on large data sets.

Chapter III

Immature B cells are expanded in juvenile dermatomyositis and are skewed towards a pro-inflammatory phenotype by TLR7 and IFNα

Results (section 1)

This body of work was completed in collaboration with the following:

Experimental data and interpretation - Christopher JM Piper – [redacted]

RNA-seq data analysis and interpretation – Claire Deakin – [redacted]

RNA-seq pipeline and analysis - Georg W Otto – [redacted]

INTRODUCTION

Juvenile Dermatomyositis (JDM) a systemic autoimmune disease, is the most common idiopathic inflammatory myopathy (IIM) in childhood. Symptoms include proximal muscle weakness and heliotrope rash, which are pathognomonic for JDM (Nistala and Wedderburn, 2013). Other organ involvement in JDM is common, with a proportion of patients developing complications such as interstitial lung disease (ILD), gut involvement and calcinosis (Tansley et al., 2014b). Disease pathology is thought to stem from complement mediated vasculopathy and muscular atrophy. The inflammatory infiltrate typically seen in affected muscle, is composed of B cells, $CD4^{+}$ and CD8+ T cells, macrophages and dendritic cells (DC). DC are not normally present in healthy muscle tissue, however at the onset of myositis, muscle biopsies from these patients have an abundance of CD83+ plasmacytoid DCs (pDC) (Greenberg et al., 2005b, Lopez de Padilla et al., 2007), which are a major source of interferon alpha (IFN-α).

IFN-α-inducible chemokines, CXCL10 and CXCL11 associate strongly with mononuclear cell infiltration in JDM muscle (Fall et al., 2005), and disease activity (Bellutti Enders et al., 2014). Several reports also document a significant IFNα gene signature in peripheral blood samples from DM patients (Baechler et al., 2007, Bilgic et al., 2009). As well as increasing MHC class I expression (Rowe et al., 1981), and facilitating antigen presentation, IFNα also enhances autoantibody production and proliferation of B cells (Braun et al., 2002, Bekeredjian-Ding et al., 2005, Lau et al., 2005). Importantly, B cells are thought to play a role in JDM pathology tough the production of myositis specific autoantibodies (MSA). Although it is currently

unknown how autoantibodies contribute to disease pathology, specific MSA are associated with distinct clinical phenotypes and the frequency and types of MSA vary between adult and juvenile forms of DM (Tansley and McHugh, 2014). The type of MSA associates to particular muscle biopsy pathology as assessed by the standardized score tool (Wedderburn et al., 2007, Varsani et al., 2015), which is predictive of disease progression and outcome (Deakin et al., 2016b). To date, there is no information regarding whether IFN-α affects abnormal B cell responses in JDM.

As well as having pathogenic roles in autoimmune disease or protective roles in controlling infection, B cells have been shown to have suppressive function, tough the production of interleukin-10 (IL-10) (Fillatreau et al., 2002, Mizoguchi et al., 2002, Mauri et al., 2003). More recently, these IL-10 producing regulatory B cells been identified in the $CD19^{+}CD24^{hi}CD38^{hi}$ (immature B cell) population in humans (Blair et al., 2010). Regulatory B cells (Bregs) are known to be diminished and/or functionally impaired in a variety of autoimmune diseases, including SLE, systemic sclerosis, rheumatoid artitis and ANCA-associated vasculitis (Blair et al., 2010, Matsushita et al., 2015, Mavropoulos et al., 2015, Flores-Borja et al., 2013, Todd et al., 2014, Mavropoulos et al., 2016). Importantly, IFN-α is known to induce both the differentiation of Bregs and plasmablasts in a concentration dependent manner (Menon et al., 2016). This finding suggests that the type 1 interferonopathy observed in paediatric myositis may be influencing both regulatory and pathogenic B cell responses. However, previous studies have been limited to investigating changes in total CD19+ B cells in JDM (Behan et al., 1987).

In this thesis, in-depth phenotyping of B cell compartment in JDM was carried out. The results demonstrate that $CD19^{+}CD24^{hi}CD24^{hi}$ immature B cells are expanded in JDM patients prior to treatment and correlate with disease severity. The data also confirmed that the IFN signature previously observed in JDM extends to include the B cell compartment and that this IFN signature positively correlates with this expansion in immature B cells. Finally, the TLR7 agonist R848, which is known to be a potent inducer of IFN, can no longer induce IL-10 production by JDM B cells.

RESULTS

The JDM pre-treatment patients have more active disease than the on-treatment patients

66 patients who met the Bohan and Peter criteria for probable or definite JDM were included, with a median age of 9.9 years at time of sample (***Table III.1***). Blood was collected prior to and serially during treatment as indicated. Patient and CHC demographics were summarised in Table III.1. Patients were stratified into pre-treatment, <6 months, 7-30 months and >30 months on-treatment. This table showed that the JDM samples were age matched to the CHC samples, but the female predominance seen in the JDM cohort was not proportionally reflected in the CHC cohort. The JDM pre-treatment patients had worse disease than patients receiving treatment, which was confirmed by significantly higher PGA score and creatine kinase (CK) levels, but significantly lower MMT8 and CMAS scores. A broad spectrum of autoantibodies were represented in the JDM cohort. A high proportion of the 'on-treatment' samples were taken from patients on methotrexate and oral prednisolone, but other medications were recorded for some patients at longer time points including cyclophosphamide and azathioprine.

Table III.1 Demographic, clinical and serological features. *Serial samples were used from 37 patients, 15 patients of these patients had pre- and on-treatment samples. The median and interquartile range (IQR) was represented for patient characteristics and clinical features. Student t-test was used to test the significance between JDM pre- and on-treatment groups for PGA, manual muscle testing of 8 groups (MMT8), and childhood myositis Assessment Scale (CMAS). Mann-Whitney test was used to test the significance between JDM pre- and on-treatment groups for creatine kinase (CK). The number of patients and percentage of group were shown for autoantibody status and medication taken. Autoantibodies included; anti–transcription intermediary factor 1g (anti–TIF-1g), anti–nuclear matrix protein 2 (anti–NXP-2), anti-75-and 100kDa polymyositis/systemic sclerosis proteins (anti-PmScl), Nucleosome-remodelling deactulase complex (anti–Mi2), anti-small ubiquitin like modifier activating enzyme (anti-SAE), anti-melanoma differentiation associated gene 5 (anti-MDA5), anti-ribonucleoprotein (anti-RNP). Medications were recorded at the time of sample.*

	JDM patients			Controls
Patient characteristics	**Pre-treatment samples (n=20)**	**On- treatment samples (n=89)**	**All JDM samples (n=109)**	**Child healthy control (n=23)**
Number of patients	**20**	**46**	**66**	
Age at onset (years), median [IQR]			6.81 [4.17-10.06]	
Age at diagnosis (years), median [IQR]			5.86[4.86-9.31]	
Age at sample (years), median [IQR]	5.0 [4.0-8.9]	9.9[6.4-12.3]	9.9[8.4-12.9]	7.79[5.02-11.63]
Sex, (F/M) [p=0.081]	11/9	31/15	42/24	11/12
Clinical features, median [IQR]				
Physician's Global Assessment (PGA) - (0-10) [p<0.0001]	6.70 [5.73-7.68]	0.85 [0.20-1.63]		
MMT8 - (0-80) [p<0.0001]	29.00 [28.00-42.00]	80 [76-80]		
CMAS - (0-53) [p<0.0001]	11.5 [4.50-22.75]	51 [47-53]		
Creatine Kinase (CK) U/L - (>0) (meaured in serum at time of PBMC sample) [p<0.0001]	652.5 [265.00-3893.25]	80 [48.5-134]		
Myositis-specific autoantibodies, n (%)				
Anti-TIF1g			16 (24.24)	
Unknown bands			6 (9.09)	
Anti-NXP2			15 (22.73)	
Anti-Mi2			5 (7.58)	
Anti-MDA5			4 (6.06)	
Anti-SAE			1 (1.52)	
Anti-PmScl			1 (1.52)	
Anti-U3RNP			1 (1.52)	
Anti-U1RNP			1 (1.52)	
No-detectable autoantibodies			12 (18.18)	
Unknown			4 (6.06)	
Medications (at time of sample) n(%):				
Azathioprine		16(17.98)		
Cyclophosphamide		17(19.1)		
Oral Prednisolone		57(64.0)		
Methotrexate		56(62.92)		
IV Prednisolone		32(35.96)		
Other drugs		11(12.36)		

The Immature B cell compartment is significantly expanded in pre-treatment JDM patients

B cells have been reported to be expanded in the peripheral blood (PB) of JDM patients (O'Gorman et al., 1995). However, since the initial observations, further characterisation of B cell abnormalities in JDM has not been performed. To address this, the frequency and absolute number of total B cells and different B cell sub-populations were evaluated. Initial analyses showed a significant increase in the frequency of CD19+ B cells within PBMC of pre-treatment patients compared to age-matched CHC (***Figure III.1A***). However, no lymphocytosis was observed in these patients (***Figure III.1B***).

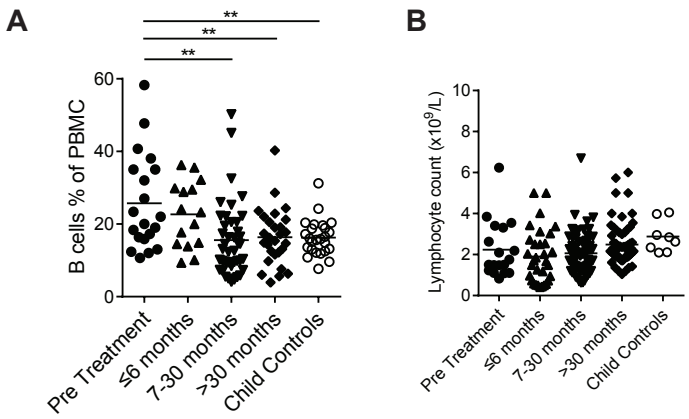

Figure III.1 Expansion of B cells from JDM patients prior to treatment*. PBMC from patients and age-matched controls were analysed by flow cytometry and B cell data compared across disease course and against clinical measures. (A) B cell (CD19+ cells within all PBMC) frequencies summarised according to time since treatment start in patients, compared to controls. (B) Lymphocyte counts x 10⁹ per litre of blood, for pre-treatment and on-treatment JDM patients and age matched child controls. *p<0.05, **p<0.01, ***p<0.001*

Expression of CD24 and CD38 was used to determine immature ($CD19^{+}CD24^{hi}CD38^{hi}$), mature ($CD19^{+}CD24^{int}CD38^{int}$) and memory

(CD19^{+}CD24^{hi}CD38^{hi}) B cell frequencies (Carsetti et al., 2004) (***Figure III.2A***). IgD, IgM and CD27 were used to confirm immaturity of CD19^{+}CD24^{hi}CD38^{hi} cells *(**Figure III.2B***). Pre-treatment, patients had an expansion of immature B cells, which significantly reduced in frequency and absolute number within the first 6 months of treatment. After 6 months on-treatment equivalent levels of immature B cells were seen in CHC and patients. Notably, memory B cells were reduced in pre-treatment patients (***Figure III.2C-D***). To confirm these findings, the same trend was also observed over time from patient serial samples (***Figure III.2E***).

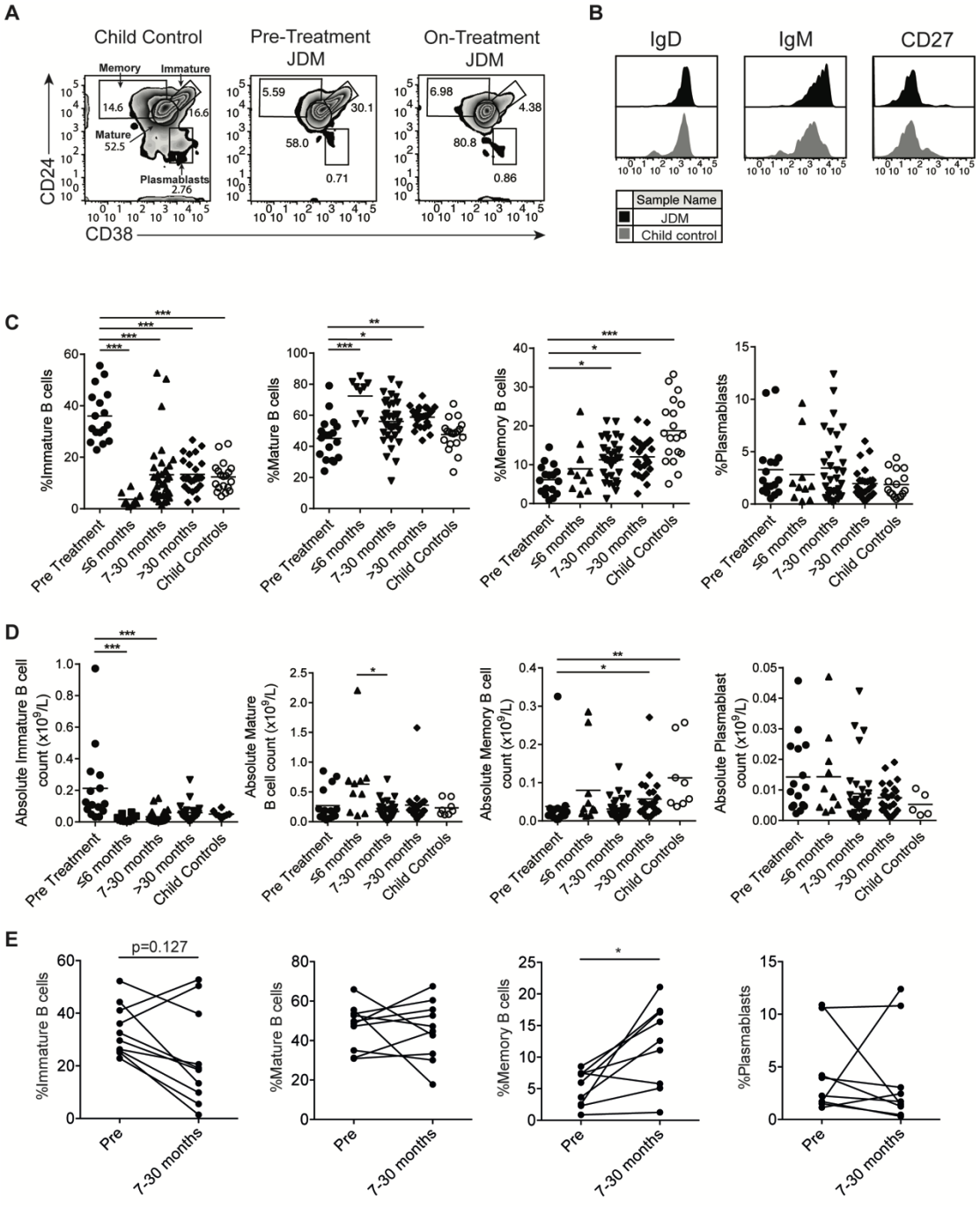

Figure III.2 Immature B cells are significantly expanded in JDM patients prior to treatment. *Immature B cells are significantly expanded in JDM patients prior to treatment. PBMC from patients and age-matched controls were analysed by flow cytometry and B cell data compared across disease course and against clinical measures.* ***(A)*** *Representative flow cytometry plots of B cell subsets, identified using expression of CD24 and CD38, shown for child controls (left plot), JDM pre-treatment (middle plot) and JDM (<6 months) on-treatment (right plot).* ***(B)*** *Representative histograms of IgM, IgD and CD27 expression (left to right) on immature B cells are shown for pre-treatment JDM patients (black outline) and child controls (grey outline). Summary graphs showing* ***(C)*** *frequency and* ***(D)*** *absolute numbers of immature, mature, memory B cells and plasmablasts (left-right) from JDM pre- treatment (n=20), JDM on-treatment (n=89) and CHC (n=23).* ***(E)***

*Frequencies of immature B cells, mature B cells, memory B cells and plasmablasts (left-right respectively) in patients with samples collected pre- (n=10) and on-treatment (7-30 months) [n=10]. For figures C-D line indicates mean, one-way ANOVA was used to measure significance. For figure E student t-test was used to measure significance. *p<0.05, **p<0.01, ***p<0.001*

Previous publications have shown that immature B cell frequency decreases with age, which we confirmed within our cohort of child controls (Morbach et al., 2010). Both CHC and pre-treatment patients were age-matched *(**Figure III.3A***). Immature B cells did not decrease with age in pre-treatment patients *(**Figure III.3B***). Furthermore, frequency and absolute numbers of immature B cells were found to correlate with Physicians Global Assessment (PGA) (***Figure III.4A-B***). This finding was specific to immature B cells (***Figure III.4C-D***). Autoantibody status did not influence the frequency of immature B cells in pre-treatment patients (***Figure III.4E***).

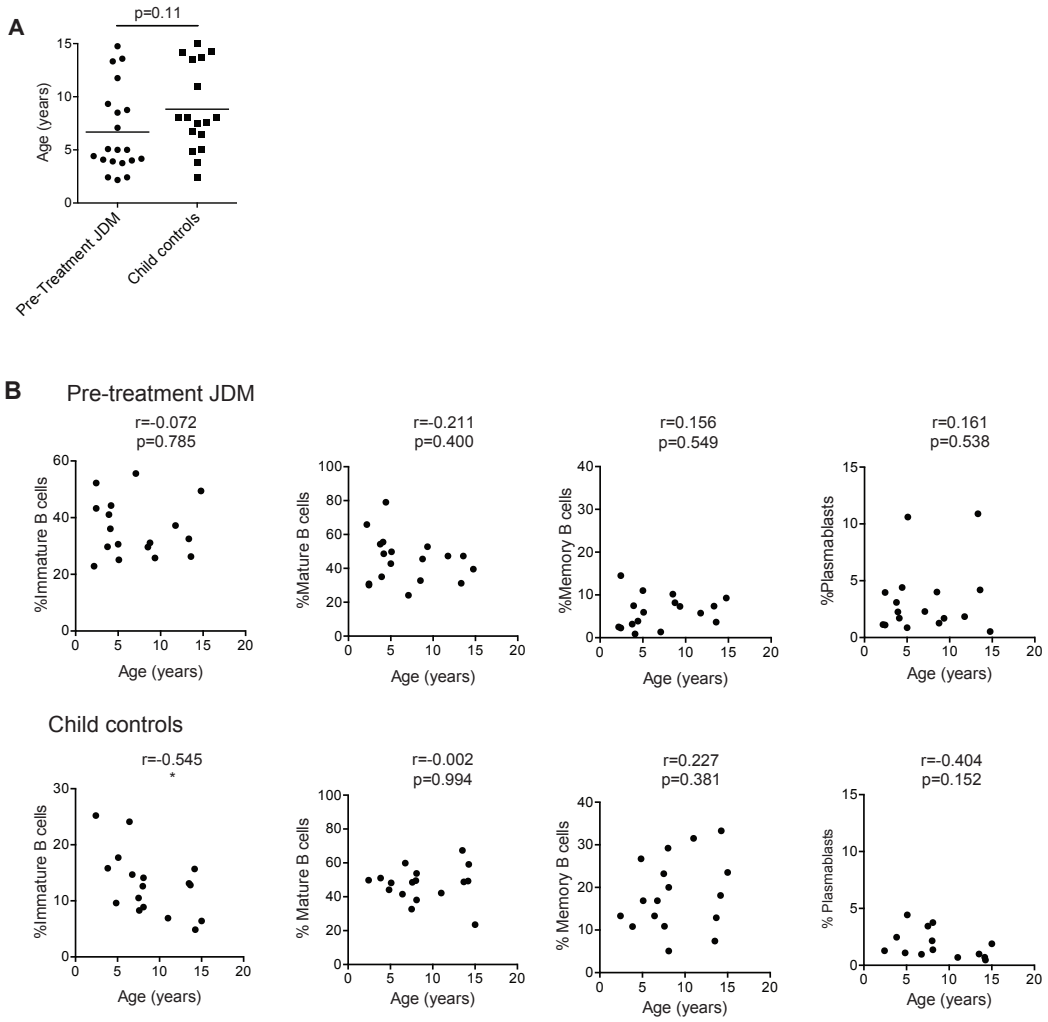

Figure III.3 Immature B cell population reduces with age in child healthy controls but not JDM. ***(A)*** *Scatter graph of age at sample of JDM pre-treatment (n=20) and child controls (17).* ***(B)*** *Frequencies of immature, mature, memory B cells and plasmablasts (left to right) analysed for correlation with age in pre-treatment patients (top row) and child controls (bottom row). For figure A student t-test was used to measure significance. Pearson correlation was used to measure significance and r values for B. *p<0.05, **p<0.01, ***p<0.001*

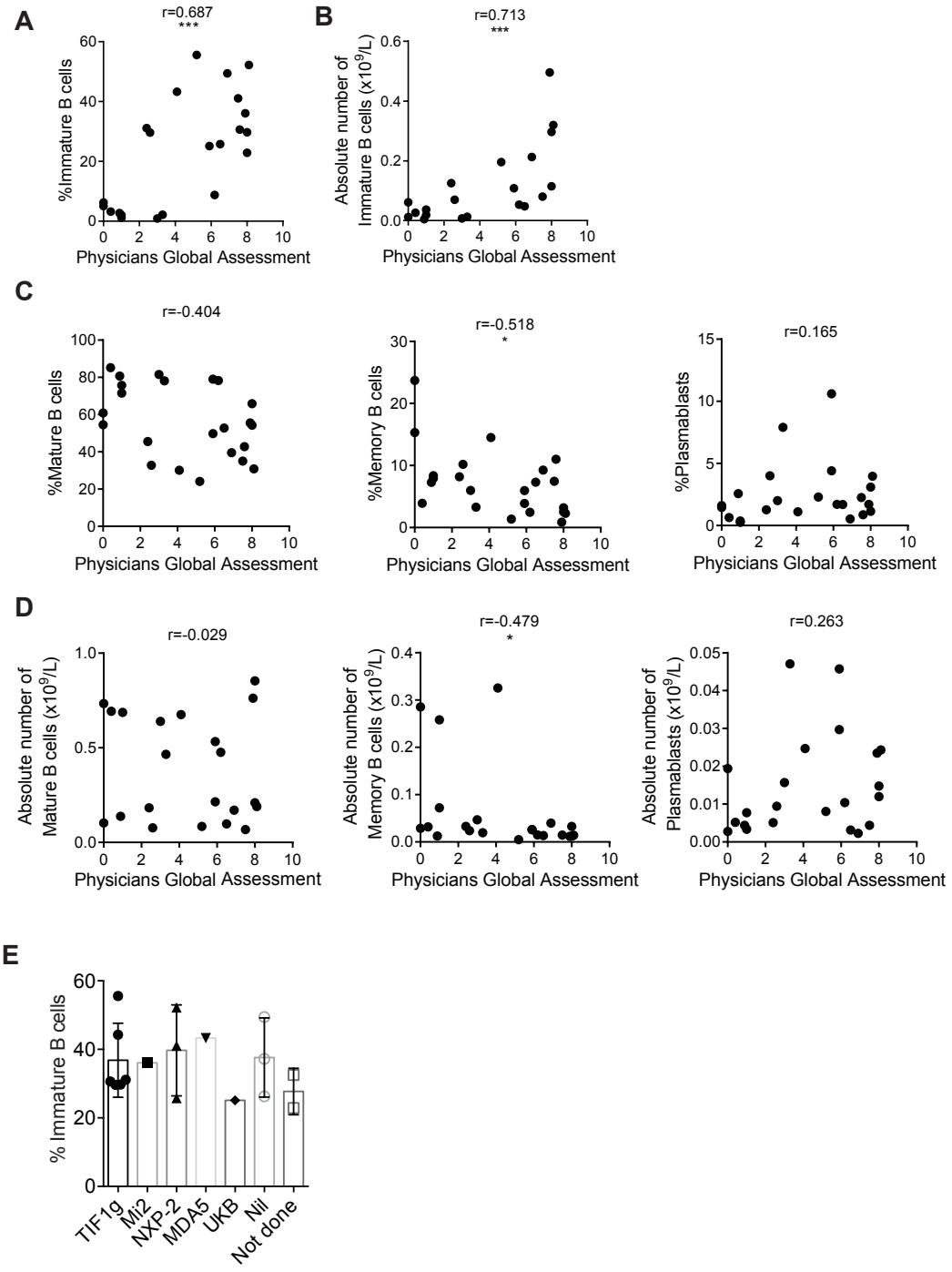

Figure III.4 Expanded immature B cell population correlates with increased disease activity in JDM*. For patients, up to 6 months into treatment (n=22),* ***(A)*** *frequency and* ***(B)*** *absolute numbers of immature B cells were correlated to Physician's Global Assessment (PGA). For patients, up to 6 months into treatment (including pre-treatment), the* ***(C)*** *frequency and* ***(D)*** *absolute number of cells were correlated to PGA for mature, memory and plasmablasts (left to right).* ***(E)*** *Frequencies of immature B cells plotted against autoantibody subtype for pre-treatment patients. Pearson correlation with significance and r values are shown for A-D. *p<0.05, **p<0.01, ***p<0.001*

As immature B cells were significantly expanded pre-treatment compared to CHC, we analysed cell proliferation in immature B cells and compared the results to other B cell subsets. Ki-67 identifies cells in all stages of cell division, except the resting G_0 phase. Increased proliferation was specifically seen in the immature population in pre-treatment patients (***Figure III.5A-B***). KREC were generated following rearrangement of the Ig kappa chain locus of the B cell receptor. As KREC DNA is not replicated, every cycle of division leads to a halving in the daughter cell's KREC content (van Zelm et al., 2007). Thus, KREC measurement allows the quantification of cell division from B cells, providing insight into the replication history of a cell population. We sorted B cells subsets from patients and CHC to measure KREC content. Patient immature B cells had a significantly lower KREC content compared to CHC. No difference was observed in mature B cells (***Figure III.5C***). KREC content was undetectable in memory B cells and plasmablasts (data not shown). Taken collectively, these data suggest that immature B cells from pre-treatment JDM patients proliferate more than their child healthy control counterparts and that is phenomenon is specific to immature B cells.

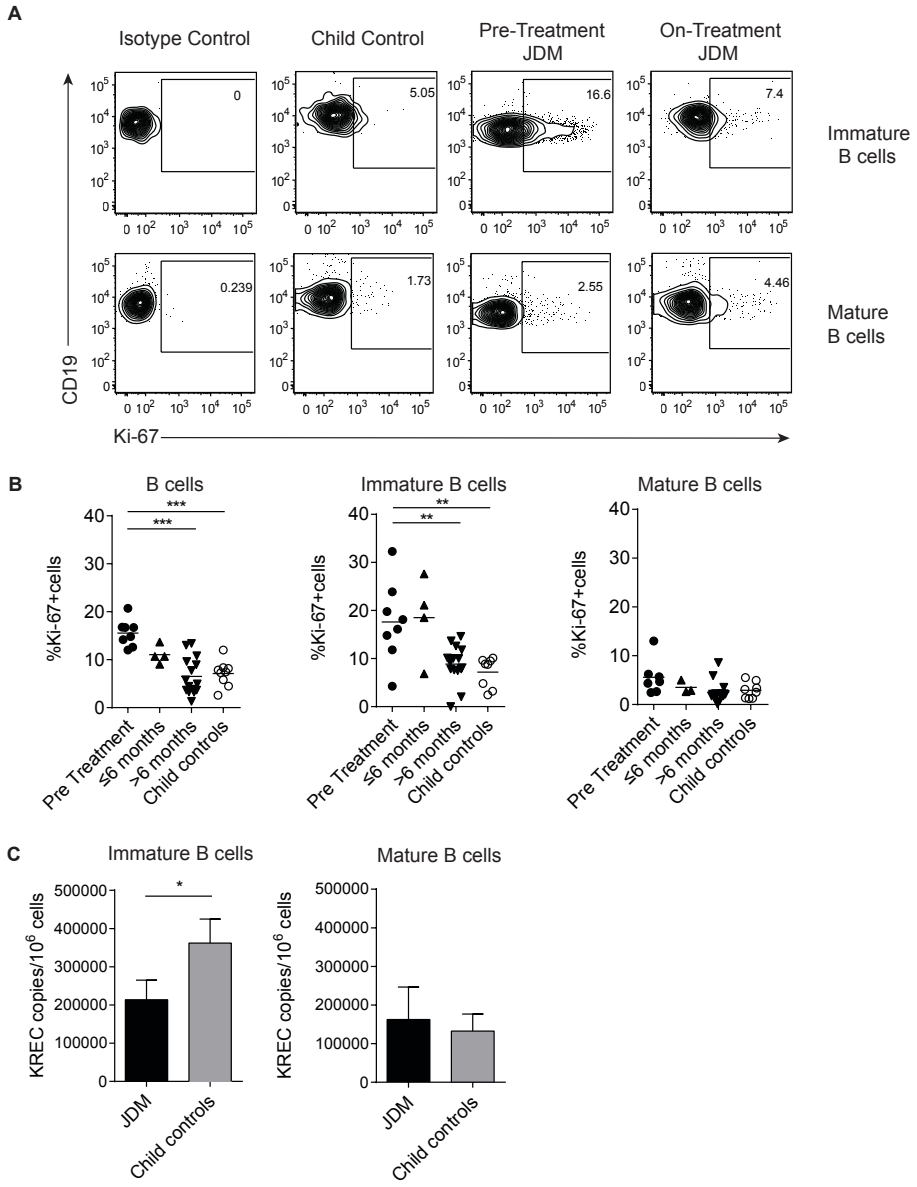

Figure III.5 Immature B cells are highly proliferative in JDM patients prior to treatment. *PBMC samples were stained ex-vivo for the B cell surface markers CD19, CD24 and CD38 and the intra-nuclear marker for proliferation, Ki-67.* ***(A)*** *Representative flow cytometry plots of Ki-67 expression in immature (top row) and mature B cells (bottom row), in patients and controls.* ***(B)*** *The frequency of Ki-67+ B cells were summarised for total B cells, immature B cells and mature B cells (left-right) for patients (n=8 pre-treatment, 4 ≤6 months, 14 ≥6 months) split according to time from treatment start, and for child controls.* ***(C)*** *B cell sub-populations were sorted from patients on-treatment (n=3) and child controls (n=3) PBMC. DNA extracted from immature ($CD19^{+}CD24^{hi}CD38^{hi}CD27^{-}$) and mature B cells ($CD19^{+}CD24^{int}CD38^{int}CD27^{-}$) were assessed for the levels of kappa-deleting recombination excision circles (KRECs). KREC copies per 10^{6} cells were calculated for immature and mature B cells. Values represent mean ± SEM for figures B-C.* For figure B one-way ANOVA was used to measure significance. For figure C the student t-test was used to measure significance. **p<0.05, **p<0.01, ***p<0.001*

Upregulation of the type I interferon signature in JDM B cells

To understand what drives B cell expansion in patients, we carried out RNA sequencing of B cells isolated from 9 pre- and 9 on-treatment patients (median time on-treatment 11 months) and 4 CHC (refer to specific demographics in ***Table V.1***). Gene set enrichment analysis of Hallmark pathways in the ranked gene lists revealed that the IFN-α response was the most upregulated pathway in pre- vs. on-treatment isolated B cells (***Figure III.6A***). The normalized enrichment score was 3.03 with a FDR q-value of <0.0001 (***Figure III.6B***). The 20 most significant differentially expressed genes between pre- vs. on-treatment patients and pre-treatment vs CHC are summarised (***Table III.2-3***).

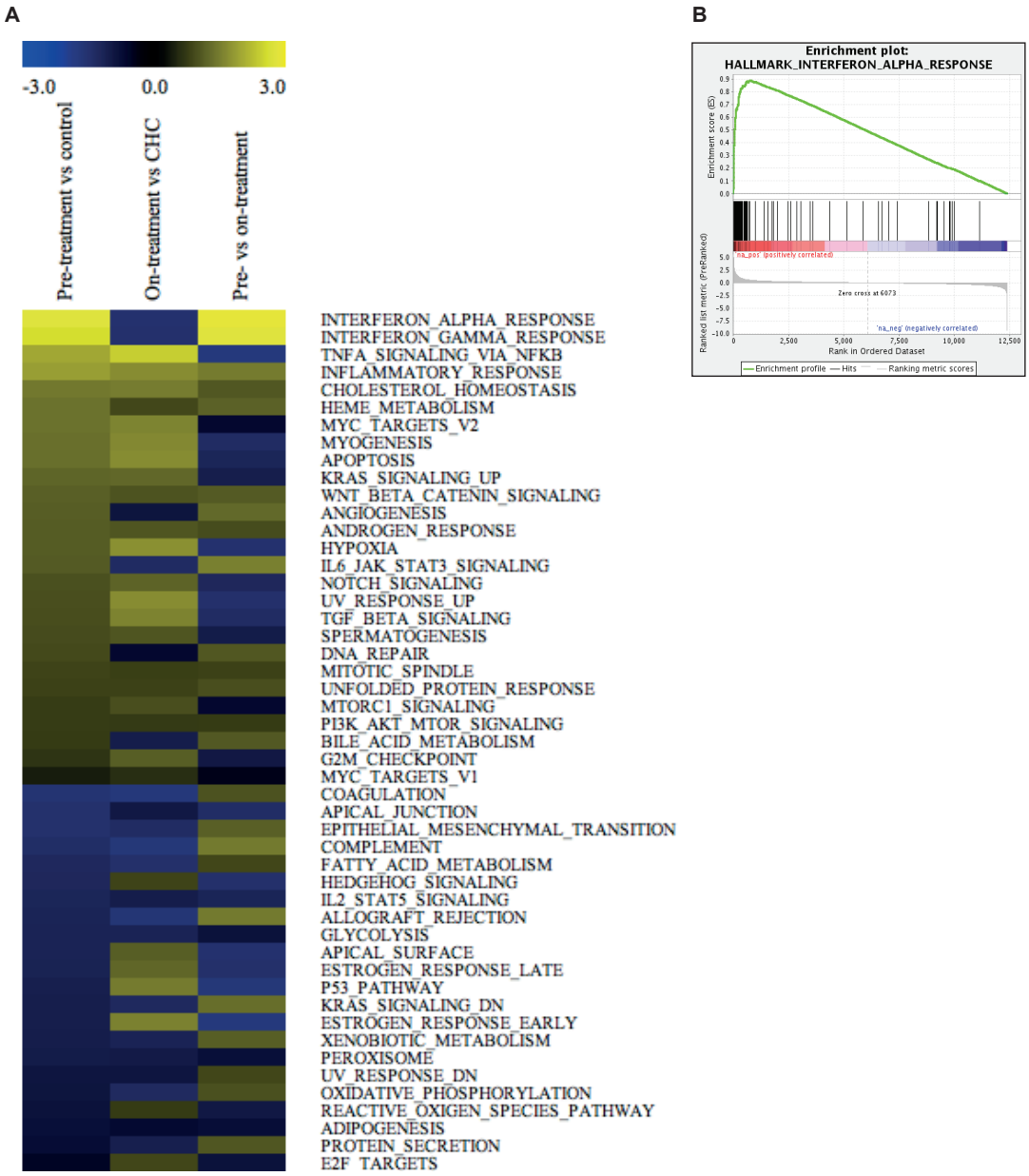

Figure III.6 Pre-treatment JDM B cells have up-regulated type I interferon signature. *JDM B cells have a prominent IFNα and TLR7 pathway signature.* ***(A)*** *Heatmap showing the normalized enrichment score (NES) for B cells when JDM pre-/on-treatment were compared with child healthy control (CHC) from gene set enrichment analysis (GSEA) hallmark analysis. Yellow represents significantly up-regulated pathways and blue represents significantly down-regulated pathways.* ***(B)*** *Gene set enrichment analysis (GSEA) plot showing the hallmark IFN-α response gene-set in pre- vs on-treatment patient B cells.*

Table III.2 20 most significantly expressed genes in a comparison of B cells from pre- and on-treatment JDM patients.

hgnc_symbol	Description	Log fold change	p adjusted value
CMPK2	cytidine/uridine monophosphate kinase 2 [Source:HGNC Symbol;Acc:HGNC:27015]	5.015845164	1.17E-24
EIF2AK2	eukaryotic translation initiation factor 2 alpha kinase 2 [Source:HGNC Symbol;Acc:HGNC:9437]	2.204637499	5.82E-19
RSAD2	radical S-adenosyl methionine domain containing 2 [Source:HGNC Symbol;Acc:HGNC:30908]	4.495877258	7.51E-19
HERC6	HECT and RLD domain containing E3 ubiquitin protein ligase family member 6 [Source:HGNC Symbol;Acc:HGNC:26072]	2.999681795	1.94E-18
OASL	2'-5'-oligoadenylate synthetase like [Source:HGNC Symbol;Acc:HGNC:8090]	5.175624818	3.63E-17
IFI44	interferon induced protein 44 [Source:HGNC Symbol;Acc:HGNC:16938]	3.619703923	6.44E-17
OAS3	2'-5'-oligoadenylate synthetase 3 [Source:HGNC Symbol;Acc:HGNC:8088]	3.759215718	6.44E-17
IFIT1	interferon induced protein with tetratricopeptide repeats 1 [Source:HGNC Symbol;Acc:HGNC:5407]	5.661457062	2.58E-16
IFITM1	interferon induced transmembrane protein 1 [Source:HGNC Symbol;Acc:HGNC:5412]	2.65927262	3.71E-16
MX2	MX dynamin like GTPase 2 [Source:HGNC Symbol;Acc:HGNC:7533]	2.075976163	5.91E-16
USP18	ubiquitin specific peptidase 18 [Source:HGNC Symbol;Acc:HGNC:12616]	4.478369432	1.71E-15
DDX60	DExD/H-box helicase 60 [Source:HGNC Symbol;Acc:HGNC:25942]	2.502981805	3.81E-15
IFI44L	interferon induced protein 44 like [Source:HGNC Symbol;Acc:HGNC:17817]	4.3932757	4.30E-15
NRIR	negative regulator of interferon response (non-protein coding) [Source:HGNC Symbol;Acc:HGNC:51269]	4.367969389	7.08E-15
HERC5	HECT and RLD domain containing E3 ubiquitin protein ligase 5 [Source:HGNC Symbol;Acc:HGNC:24368]	3.122510334	2.81E-14
IFIT3	interferon induced protein with tetratricopeptide repeats 3 [Source:HGNC Symbol;Acc:HGNC:5411]	5.203493029	3.65E-14
PLSCR1	phospholipid scramblase 1 [Source:HGNC Symbol;Acc:HGNC:9092]	2.422234425	4.44E-14
IFI6	interferon alpha inducible protein 6 [Source:HGNC Symbol;Acc:HGNC:4054]	3.059370394	1.51E-13
SLFN5	schlafen family member 5 [Source:HGNC Symbol;Acc:HGNC:28286]	2.935522167	1.81E-13
STAT1	signal transducer and activator of transcription 1 [Source:HGNC Symbol;Acc:HGNC:11362]	2.412777888	1.13E-12

Table III.31 20 most significantly expressed genes in a comparison of B cells from pre-treatment JDM patients and child healthy controls

hgnc_symbol	Description	Log fold change	p adjusted value
CMPK2	cytidine/uridine monophosphate kinase 2 [Source:HGNC Symbol;Acc:HGNC:27015]	4.125949196	2.77E-07
EIF2AK2	eukaryotic translation initiation factor 2 alpha kinase 2 [Source:HGNC Symbol;Acc:HGNC:9437]	2.022581215	2.77E-07
OASL	2'-5'-oligoadenylate synthetase like [Source:HGNC Symbol;Acc:HGNC:8090]	5.097639577	8.76E-07
ADAR	adenosine deaminase, RNA specific [Source:HGNC Symbol;Acc:HGNC:225]	1.079673516	1.99E-06
TGFBI	transforming growth factor beta induced [Source:HGNC Symbol;Acc:HGNC:11771]	-2.889143829	2.50E-06
IFITM1	interferon induced transmembrane protein 1 [Source:HGNC Symbol;Acc:HGNC:5412]	2.429796925	5.49E-06
MX2	MX dynamin like GTPase 2 [Source:HGNC Symbol;Acc:HGNC:7533]	1.875673164	5.49E-06
NRIR	negative regulator of interferon response (non-protein coding) [Source:HGNC Symbol;Acc:HGNC:51269]	4.217600512	8.35E-06
CD4	CD4 molecule [Source:HGNC Symbol;Acc:HGNC:1678]	-2.522215473	8.35E-06
HERC5	HECT and RLD domain containing E3 ubiquitin protein ligase 5 [Source:HGNC Symbol;Acc:HGNC:24368]	2.967715524	1.16E-05
HERC6	HECT and RLD domain containing E3 ubiquitin protein ligase family member 6 [Source:HGNC Symbol;Acc:HGNC:26072]	2.434812047	1.21E-05
BAHCC1	BAH domain and coiled-coil containing 1 [Source:HGNC Symbol;Acc:HGNC:29279]	3.539876725	1.28E-05
SLFN5	schlafen family member 5 [Source:HGNC Symbol;Acc:HGNC:28286]	2.861670142	1.29E-05
LGALS3BP	galectin 3 binding protein [Source:HGNC Symbol;Acc:HGNC:6564]	2.671699546	1.29E-05
IL2RA	interleukin 2 receptor subunit alpha [Source:HGNC Symbol;Acc:HGNC:6008]	-2.202209619	1.52E-05
OAS3	2'-5'-oligoadenylate synthetase 3 [Source:HGNC Symbol;Acc:HGNC:8088]	3.143704429	1.81E-05
IFI44	interferon induced protein 44 [Source:HGNC Symbol;Acc:HGNC:16938]	3.00981476	1.96E-05
STAT1	signal transducer and activator of transcription 1 [Source:HGNC Symbol;Acc:HGNC:11362]	2.361882153	1.96E-05
DDX60	DExD/H-box helicase 60 [Source:HGNC Symbol;Acc:HGNC:25942]	2.179692129	1.96E-05
MDFIC	MyoD family inhibitor domain containing [Source:HGNC Symbol;Acc:HGNC:28870]	-1.257982447	3.17E-05

**A positive log fold change signifies up-regulation and negative a down-regulation of gene expression in pre-compared to on-treatment JDM.*

We validated the IFN-α signature at protein level using Luminex (de Jager et al., 2007) multiplex array (Trinchieri, 2010). Pre-treatment patients had high serum concentrations of CXCL10, CXCL11, MCP-1 and MCP-2, which reduced in patients on treatment for >6 months (***Figure III.7A***). Serum and PBMC were isolated on the same day. Serum levels of chemokines were also significantly associated with the frequency of immature B cells (***Figure III.7B***) in all patients. Conversely, no significant association was seen with mature or memory B cells (***Figure III.7C-D***).

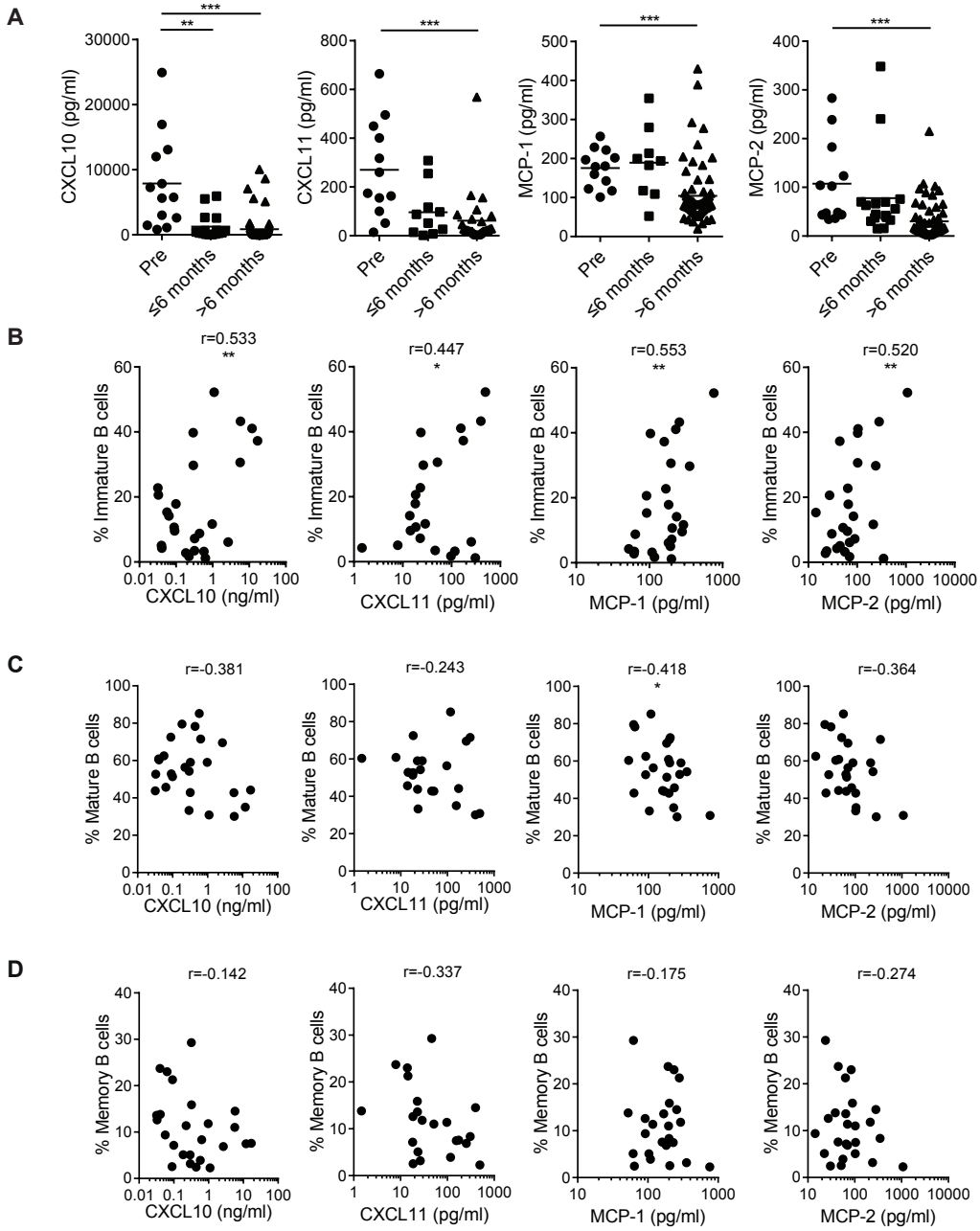

Figure III.7 IFNα signature validated at a protein level by Luminex multiplex array. ***(A)****Patient sera from pre- (n=13) and on-treatment (n=14, =14 ≤6 months, =25 ≥6 months) JDM patients were analysed for chemokines known to be downstream of the IFNα response. Serum concentrations of CXCL10, CXCL11, MCP-1 and MCP-2 (left-right) measured by Luminex multiplex array are summarised according to time since treatment start. Patient sera and PBMC were collected on the same day.* ***(B)*** *Immature B cell frequency and serum levels of CXCL10, CXCL11, MCP-1 and MCP-2 (left-right) were correlated in all JDM patients (pre/on treatment, n=25). Patient sera and PBMC collected on the same day were used to assess correlations between* ***(C)*** *Mature and* ***(D)*** *memory B cell frequency and serum concentrations of CXCL10, CXCL11, MCP-1 and MCP-2 (left to right) for all JDM patients (pre/on-treatment). For figure A one-way ANOVA was used to measure significance. Pearson correlation with significance and r values are shown for B-D. *p<0.05, **p<0.01, ***p<0.001*

IFNα regulates the expression of TLR7 and enhances the response to endogenous TLR7 ligands by B cells and, if overexpressed, can lead to the development of autoreactive B cells and autoantibody production (Green et al., 2009, Kiefer et al., 2012). It was hypothesised that the TLR7 pathway is important to B cell pathology in JDM. RNAseq identified upregulation of TLR7 and interferon-regulatory factor 7 (IRF7) in pre- vs. on-treatment patients (***Figure III.8A***). Normalised counts (Reads Per Kilobase of transcript per Million mapped reads - RPKM) for TLR7 and IRF7 were significantly higher in pre-treatment patients (***Figure III.8B***).

Patients with NXP2 autoantibodies often develop a more severe and prolonged disease course (Espada et al., 2009) and patients with autoantibodies against TIF1γ develop severe cutaneous disease (Gunawardena et al., 2008). Interestingly, when stratified according to autoantibody status, patients with the TIF1γ and NXP2 autoantibodies trended towards higher TLR7 and IRF7 expression (***Figure III.8C-D***).

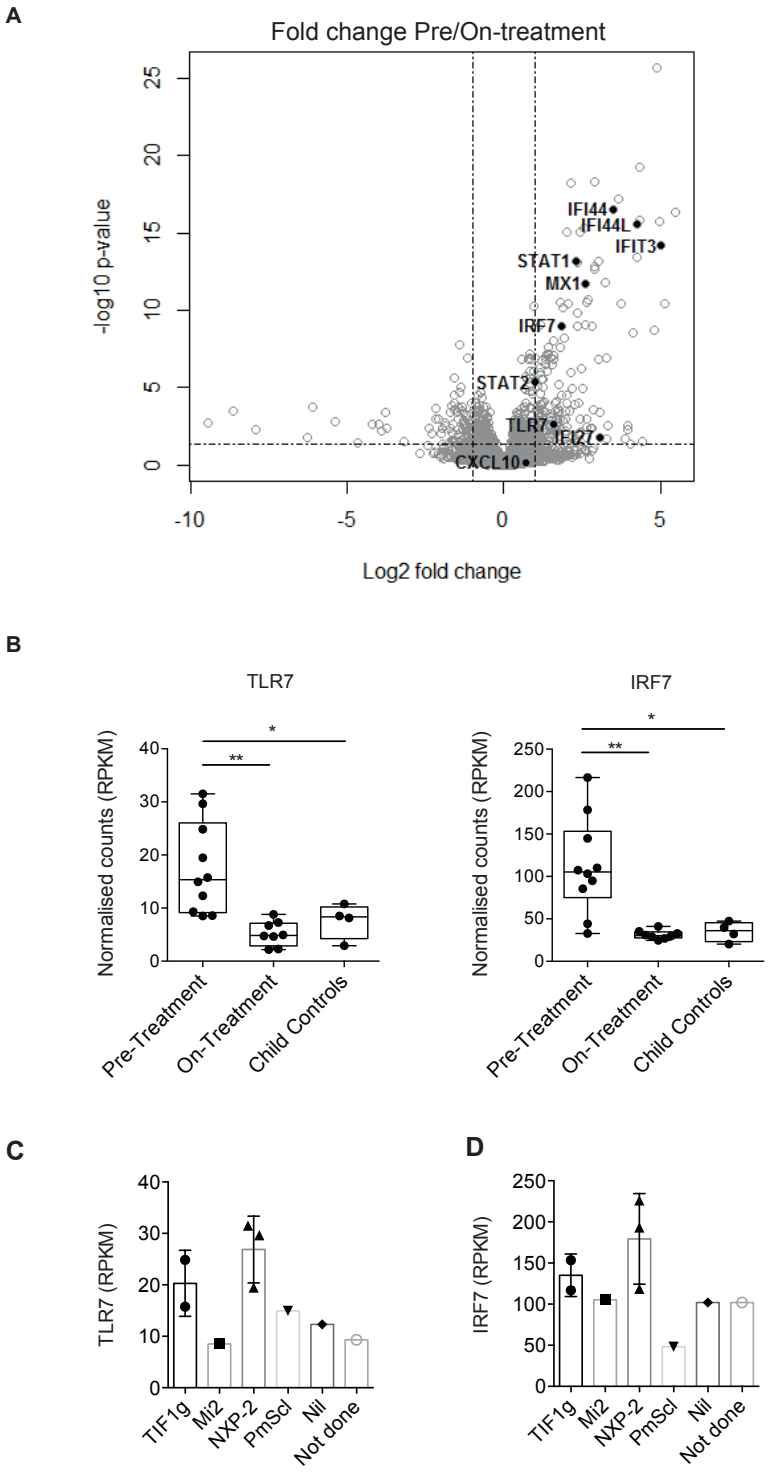

Figure III.8 RNA sequencing identified upregulation of TLR7 and IRF7 in pre- vs. on-treatment JDM patients. ***(A)*** *Volcano plot highlighting differentially expressed genes downstream of the IFN-α pathway in pre- vs on-treatment patients.* ***(B)*** *Normalised counts (RPKM) for pre-treatment, on-treatment patients and child controls are shown for TLR7 and IRF7. Figure B, N=10 for pre-treatment, 9 for on-treatment and 4 for child controls. Normalised counts (RPKM) for* ***(C)*** *TLR7 and* ***(D)*** *IRF7, in B cells isolated from pre-treatment patients, stratified according to autoantibody status. For figure B-D one-way ANOVA was used to measure significance. *p<0.05, **p<0.01, ***p<0.001*

TLR7 and IFNα promotes IL-6, but not IL-10 production in B cells from JDM patients

To assess B cell response to TLR7 ligation, I cultured purified B cells for 48 hours with or without IFN-α and quantified IL-6 and IL-10 expression. It has been shown previously that culturing healthy control B cells with IFN-α increases the $CD19^{+}CD24^{hi}CD38^{hi}$ population (Menon et al., 2016). Stimulating B cells with R848 and IFN-α increased the percentage of $CD19^{+}CD24^{hi}CD38^{hi}$ cells from CHC, but not in active on-treatment patients (PGA>3.5). The data did not reach significance (***Figure III.9A-B***).

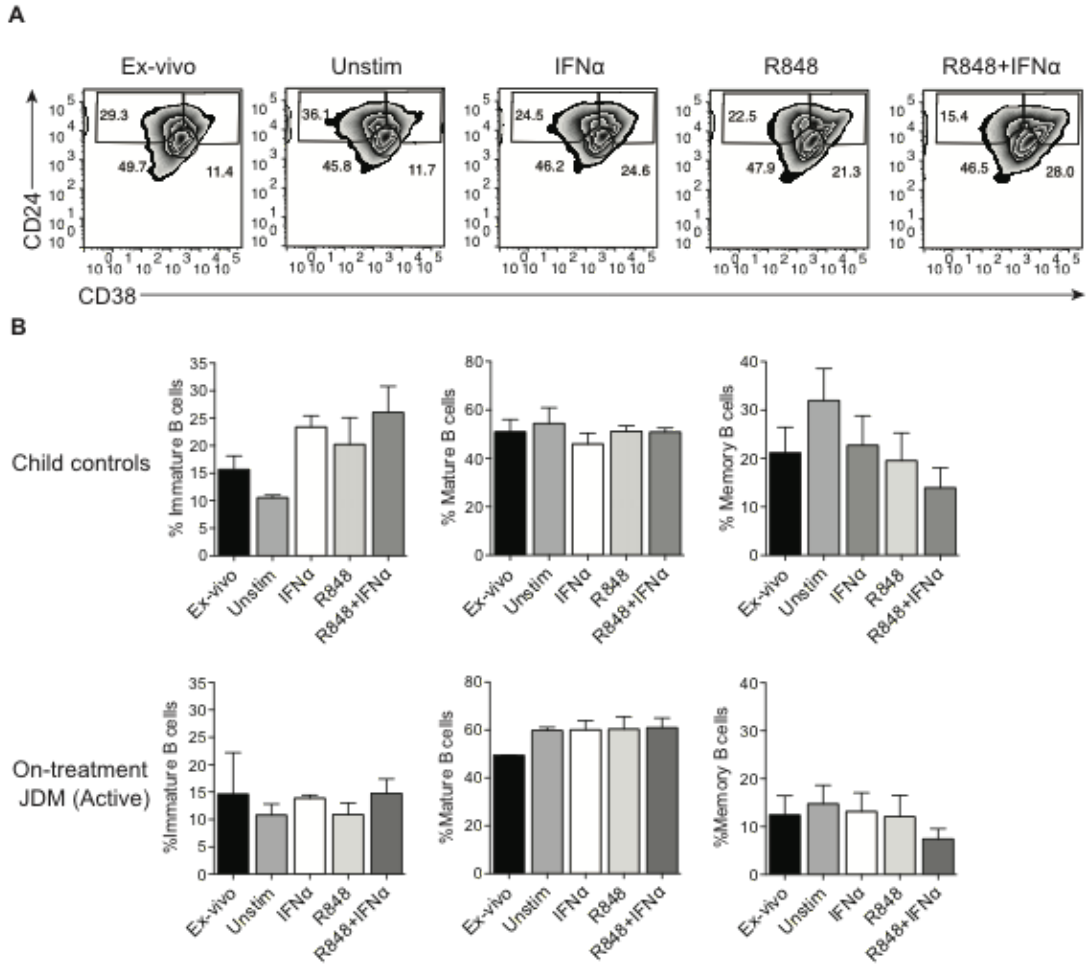

Figure III.9 IFNα may increase the immature B cell population in samples from child healthy controls but not JDM patients*. B cells were purified from active on-treatment patients (patients with flares in disease activity (PGA >3.5) and were >6months into treatment) and age-matched child control PBMC were stimulated with IFN-α (1000 IU/ml), 1μg/ml R848 (a TLR7/8 agonist) or a combination of both for 48h. B cells were stained for CD24 and CD38 expression.* ***(A)*** *Representative flow cytometry plots showing B cells subset gating for each of the conditions are shown (left to right: Isotype control, unstimulated, IFNα, R848, R848+IFNα) using child control sample.* ***(B)*** *Percentage of immature, mature and memory B cells (left-right) are summarised for each culture condition for child controls (top row) and JDM patients on-treatment (bottom row). For figure B, N=3 for patients and child controls. Two-way ANOVA with Sidak multiple comparisons test was used for figure B. Bars represent mean ± SEM.*

Concentrations of IL-6 and IL-10 were quantified from cell culture supernatants. TLR7 ligation induced IL-10 in CHC, but was significantly diminished in patients on treatment (***Figure III.10A, C&D***). No difference between patients and controls was

observed in TLR7-induced IL-6. Furthermore, addition of IFNα increased B cell IL-6 expression (***Figure III.10B, E&F***).

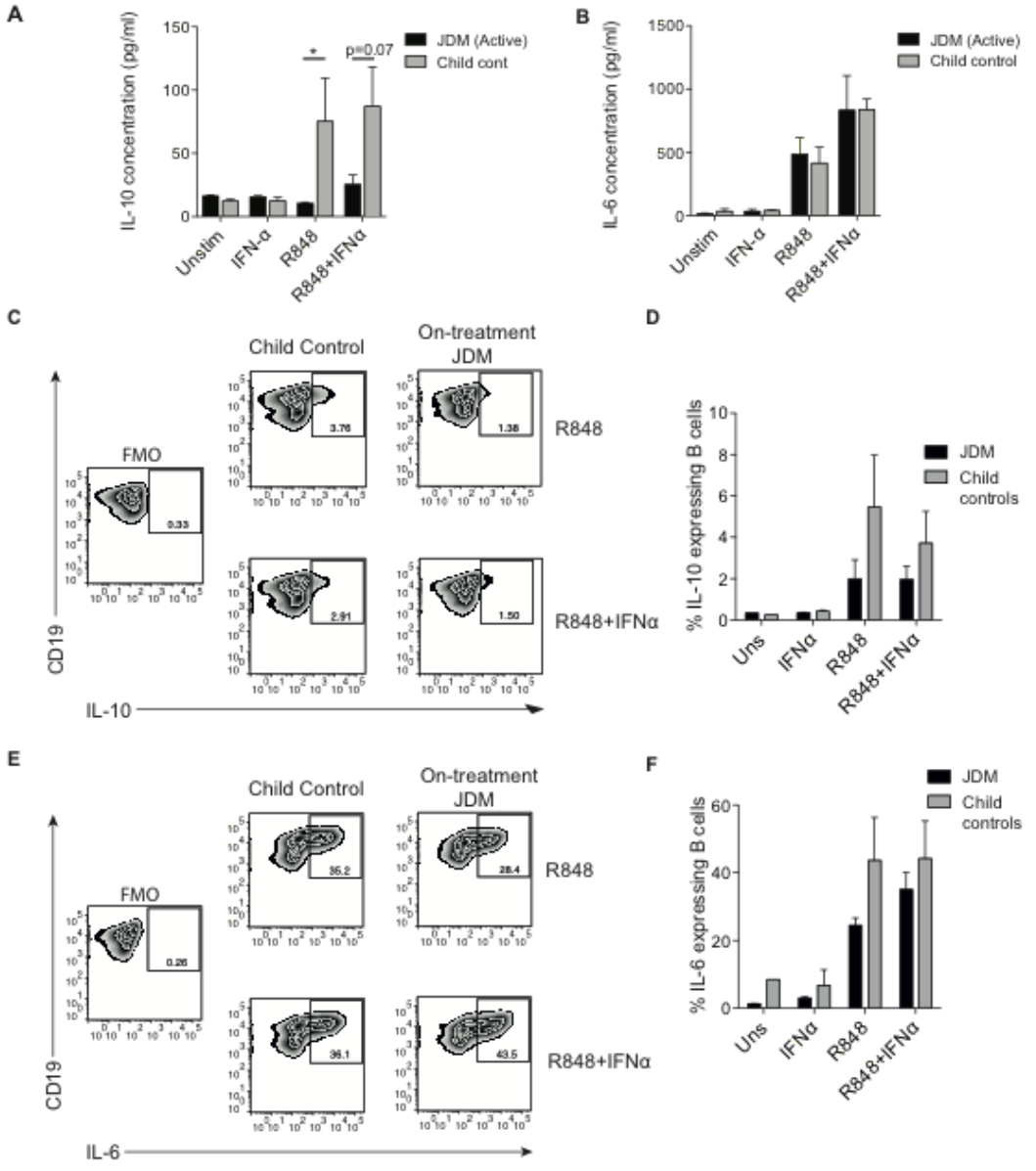

Figure III.10 JDM B cells fail to induce IL-10 after TLR7 stimulation. *B cells were isolated from on-treatment JDM patients (patients with flares in disease activity (PGA >3.5) and were >6months into treatment) and child controls and were stimulated for 48h with R848+/- IFN-α. Culture supernatants taken from total B cells at 48h were analysed for* ***(A)*** *IL-10 and* ***(B)*** *IL-6 concentrations for patients and controls. Representative FACS plots of* ***(C)*** *IL-10 and* ***(E)*** *IL-6 expression in B cells after 48h stimulation with R848 (top row) and R848+ IFNα (bottom row).* ***(D)*** *Total B cell IL-10 and* ***(F)*** *IL-6 expression are summarised by flow cytometry for child controls and on-treatment JDM patients. N=3 per group. Two-way ANOVA with Sidak multiple comparisons test was used for figures A, B, D & F. Bars represent mean ± SEM.*

CD40L stimulated JDM B cells have no defect in IL-10 production

I next assessed if the reduction in B cell IL-10 was an intrinsic defect in JDM patients or a signal-specific phenomenon. I used CD40-CD40 ligand (CD40L) interactions to assess IL-10 production. Using a well-established co-culture assay, CD40L-expressing CHO cells were co-cultured with PBMC, and B cell IL-10 expression analysed after 72 hours (Blair et al., 2010). I observed no significant difference in IL-10 expression between pre-treatment patients and CHC. However, IL-10+ cells were significantly decreased in patients within the first 6 months of treatment compared to pre-treatment patients (***Figure III.11A-B***). Immature B cells from on-treatment patients were the main source of IL-10 and IL-6 upon stimulation with CD40L (***Figure III.11C-D***). No IL-10 was detected in B cells stimulated with PMA and Ionomycin alone (***Figure III.11E***).

In addition, PBMC from patients' pre-treatment and on-treatment samples were stimulated with PMA and Ionomycin for 4hours and the frequency of total B cells expressing IL-6 was measured. There was no significant difference in IL-6 expression between pre-treatment patients and CHC (***Figure III.11F-G***). Of note, immature B cell IL-6 did not correlate to PGA (***Figure III.11H***).

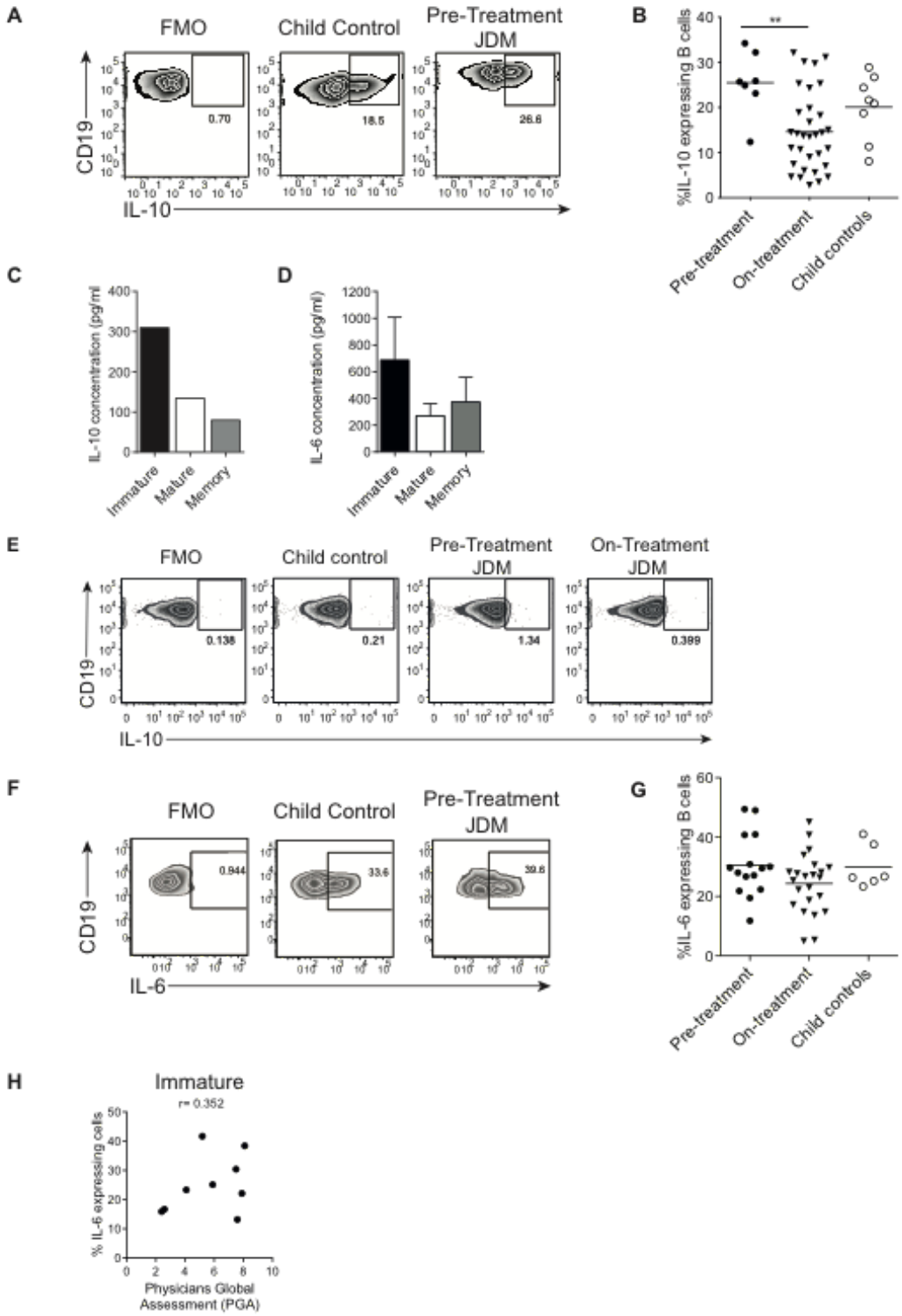
A
FMO
Child Control
Pre-Treatment JDM
CD19
IL-10
0.70
18.5
26.6
B
%IL-10 expressing B cells
**
Pre-treatment
On-treatment
Child controls
C
IL-10 concentration (pg/ml)
Immature
Mature
Memory
D
IL-6 concentration (pg/ml)
Immature
Mature
Memory
E
FMO
Child control
Pre-Treatment JDM
On-Treatment JDM
CD19
IL-10
0.138
0.21
1.34
0.389
F
FMO
Child Control
Pre-Treatment JDM
CD19
IL-6
0.944
33.6
39.6
G
%IL-6 expressing B cells
Pre-treatment
On-treatment
Child controls
H
Immature
r= 0.352
% IL-6 expressing cells
Physicians Global Assessment (PGA)

Figure III.11 B cells from JDM patients can express IL-10 upon CD40 stimulation. *PBMC were stimulated with CD40L-expressing CHO cells for 72h and B cell IL-10 expression was analysed by flow cytometry, following the addition of PMA, Ionomycin and brefeldin A for the last 4 hours of culture.* ***(A)*** *Representative flow cytometry plots of B cell IL-10 expression are shown for JDM pre-treatment, on-treatment and child controls.* ***(B)*** *Percentage of IL-10 expressing B cells after 72h culture with CD40L stimulation are summarised for each of the groups (n=7 pre-treatment, =33 on-treatment and =8 CHC). Purified B cells subsets from on-treatment JDM patients were sorted and stimulated with CD40L CHO for 72h and concentrations of* ***(C)*** *IL-10 and* ***(D)*** *IL-6 were quantified from the cell culture supernatants (N of 1 and 2 respectively).* ***(E)*** *IL-10 expression was assessed by flow cytometry. Representative FACS plots of IL-10 expression are shown for patients and controls. PBMC were stimulated for 4h with PMA/Ionomycin* ***(F)*** *Representative FACS plots of total B cell IL-6 staining are shown (left-right: Isotype control, JDM pre-treatment, JDM on-treatment and child control).* ***(G)*** *IL-6 expression by B cells are summarised for JDM subgroups (n=15 pre-treatment and =23 on-treatment) and child controls (n=6).* ***(H)*** *Analysis of the correlation between IL-6 expression by immature B cells and PGA. B, C, D and G were analysed by One-way ANOVA for significance. Pearson correlation was used to measure significance and r values for H. Values represent mean ± SEM. *p<0.05, **p<0.01, ***p<0.001*

DISCUSSION

It is known that B cells are expanded in peripheral blood (PB) of JDM (Strelkauskas et al., 1976, Eisenstein et al., 1997) and to have an important role in JDM pathology, primarily via the production of MSA. However, to my knowledge, no studies have characterised 2B cell phenotype in JDM in detail. I have shown that the immature B cells were expanded in the blood of JDM patients pre-treatment and importantly correlated with clinical severity. RNAseq analysis revealed that the B cell compartment in JDM exhibited a strong IFN gene signature and which was associated with an increase of immature B cells.

Studies examining B cell phenotype in patients with autoimmune diseases such as systemic sclerosis (Matsushita et al., 2015, Mavropoulos et al., 2015) and neuromyelitis optica (Quan et al., 2015), report a reduction in the number of immature B cells ($CD19^{+}CD24^{hi}CD38^{hi}$). Recently Li *et al* showed that immature B cells are decreased in adult DM (Li et al., 2016). However, I now report a significantly expanded immature population specifically in pre-treatment JDM. This trend has also been documented in SLE patients, which shares some features of aetiopathogenesis with DM (Blair et al., 2010). To my knowledge, this is the first report demonstrating an expansion of immature B cells in JDM. Immature B cell frequencies in the periphery decrease with age, with the frequency highest in infancy (Morbach et al., 2010). The cohort of CHC further confirms these findings. However, immature B cell frequency does not correlate with age in active JDM patients pre-treatment, suggesting that normal B cell development is disturbed in patients following the onset of autoimmunity. Interestingly, immature B cell frequency directly correlates with disease activity, suggesting that these cells are intrinsically linked to the development

of disease. The data showed that immature B cells, specifically in patients pre-treatment, are proliferating and have undergone more cell divisions *in-vivo* than age matched CHC, as determined by their lower KREC content. While these results indicate a replication history of a subset of B cells (van Zelm et al., 2007), it would be important in future work to distinguish whether there is a higher output of immature B cells from the bone marrow, and to determine the site of proliferation.

It has been previously reported that TLR-9 activated pDC, which produce IFNα, expand immature B cells *in vitro*. Interestingly, RNA sequencing analysis comparing gene expression between pre-, on-treatment patients and CHC, identified a strong IFN-α signature, with molecules downstream of IFN-α receptor signalling being highly expressed in pre-treatment patient B cells versus controls (Ng et al., 2016). These data suggest that the interferonopathy could be driving the expansion of immature B cells in JDM *in vivo*. Indeed, my analysis found that there was a strong positive correlation between interferon-driven chemokines and the frequency of immature B cells in JDM patients. Previous studies have also identified a strong IFN-α signature in muscle (Fall et al., 2005, Baechler et al., 2011), skin (Wenzel et al., 2006), PBMC and serum of DM and JDM patients (Baechler et al., 2007, Bilgic et al., 2009); a feature shared with other autoimmune diseases (Higgs et al., 2011). Furthermore, pDC, which are the major producers of IFN-α are known to be abundant in skin (McNiff and Kaplan, 2008, Wenzel et al., 2006, Lopez De Padilla et al., 2009) and muscle (Lopez de Padilla et al., 2007, Lopez De Padilla et al., 2009) in DM and JDM patients where they could potentially crosstalk with B cells that have also infiltrated inflamed muscle tissue (Lopez De Padilla et al., 2009). More recently, the role of IFN-β has been suggested to be pivitol in the pathogenesis of adult DM.

Elevated serum levels of IFN-β was associated with an elevated type I interferon gene signature and, moreover, correlated with skin disease activity in DM (Huard et al., 2017). However, the role of IFN-β in JDM disease pathology remains less well characterised. It would be important to dissect the relative contributions of IFN-α and IFN-β in JDM disease pathogenesis and how this affects B cell function.

Clinical trials testing anti-IFN-α biologics in the treatment of rheumatological diseases have started to gain traction (Kalunian et al., 2016). Sifalimumab, a human IgG1κ monoclonal antibody has been trialled in a phase 1b study in dermatomyositis patients (Higgs et al., 2014) and, successfully in phase IIb trial in SLE (Khamashta et al., 2016). In addition, Anifrolumab, an anti-interferon-alpha receptor monoclonal antibody has been found effective against SLE in a phase IIb trial (Furie et al., 2017). My work provides further evidence that anti- IFN-α biologics could be efficacious in the treatment of JDM.

Of particular interest, gene expression of TLR7 and its associated downstream signalling molecule IRF7 was significantly higher in pre- versus on-treatment B cells. It has been previously reported that activation of cells with IFN-α induces IRF7 expression in multiple cell types (Sato et al., 1998), and can directly induce TLR7 expression in naïve B cells (Bekeredjian-Ding et al., 2005). Importantly, overexpression of TLR7 has been shown to increase susceptibility to autoimmunity (Deane et al., 2007) and has a role in disease pathogenesis in mouse models of lupus (Celhar et al., 2012). Furthermore, overexpression of TLR7 in murine B cells promotes expansion and autoantibody production in the transitional 1 population (Giltiay et al., 2013). In this study, whilst TLR7 and IFN-α stimulation increased the

$CD19^{+}CD24^{hi}CD38^{hi}$ population in controls, this expansion was not observed in patients possibly due to conic activation of this pathway *in vivo*. Furthermore, TLR7 ligation in healthy B cells induces IL-6 and IL-10 production in child controls resembling previous studies using B cells isolated from healthy adults (Liu et al., 2014). However, in JDM patients stimulation with the TLR7 agonist R848 in JDM patients favoured IL-6 production over IL-10. Notably, IL-6 has been linked to disease activity in JDM (Bilgic et al., 2009), and is detectable in serum. Given the pre-disposition of autoantibody production in JDM (Tansley and McHugh, 2014) and that IL-6 is an important growth factor for plasmablast generation (Jego et al., 2001), it is possible that immature B cells receive the required signals to differentiate to plasmablasts in muscle tissue (Menon et al., 2016).

The final investigation was whether there was an intrinsic IL-10 defect in patient B cells using the CD40-CD40L interaction which is key for B cell development and induce IL-10 in B cells (Elgueta et al., 2009). Contrary to Kalampokis *et al*, who reported a reduction in Breg IL-10 in JDM patients (Kalampokis et al., 2016), I did not observe a difference in JDM patients pre-treatment and controls with the CD40L stimulus. However, the cohort in Kalampokis *et al* contained patients already on treatment and different stimuli (CD40L+CpG-B) were used which could account for the differences seen in both studies. We show that patients on treatment with prednisolone and methotrexate have reduced IL-10 production and immature B cell frequency; both of which are proportional to each other. We propose that the immature B cell population is capable of producing IL-10, given the right signals *in-vivo*, but are skewed away from Breg differentiation and towards a pro-inflammatory phenotype by over-activation with IFN-α and TLR7 agonists in B cells.

In conclusion, the data shows that immature B cells are greatly expanded in JDM pre-treatment, correlate with disease activity, and decrease upon treatment with prednisolone and methotrexate. This is likely to be caused by a reduction in inflammation, which drives the expansion of immature B cells. Notably, immature B cells from patients re-populate to equivalent levels seen in CHC after >6months on treatment. I propose a model whereby TLR7 ligation and stimulation via IFN-α lead to the expansion of immature B cells, and prime them towards a pro-inflammatory state in JDM. These data support a growing body of evidence that targeting the TLR7 and IFN-α response in autoimmune disease may be novel therapeutic pathways to target in dermatomyositis.

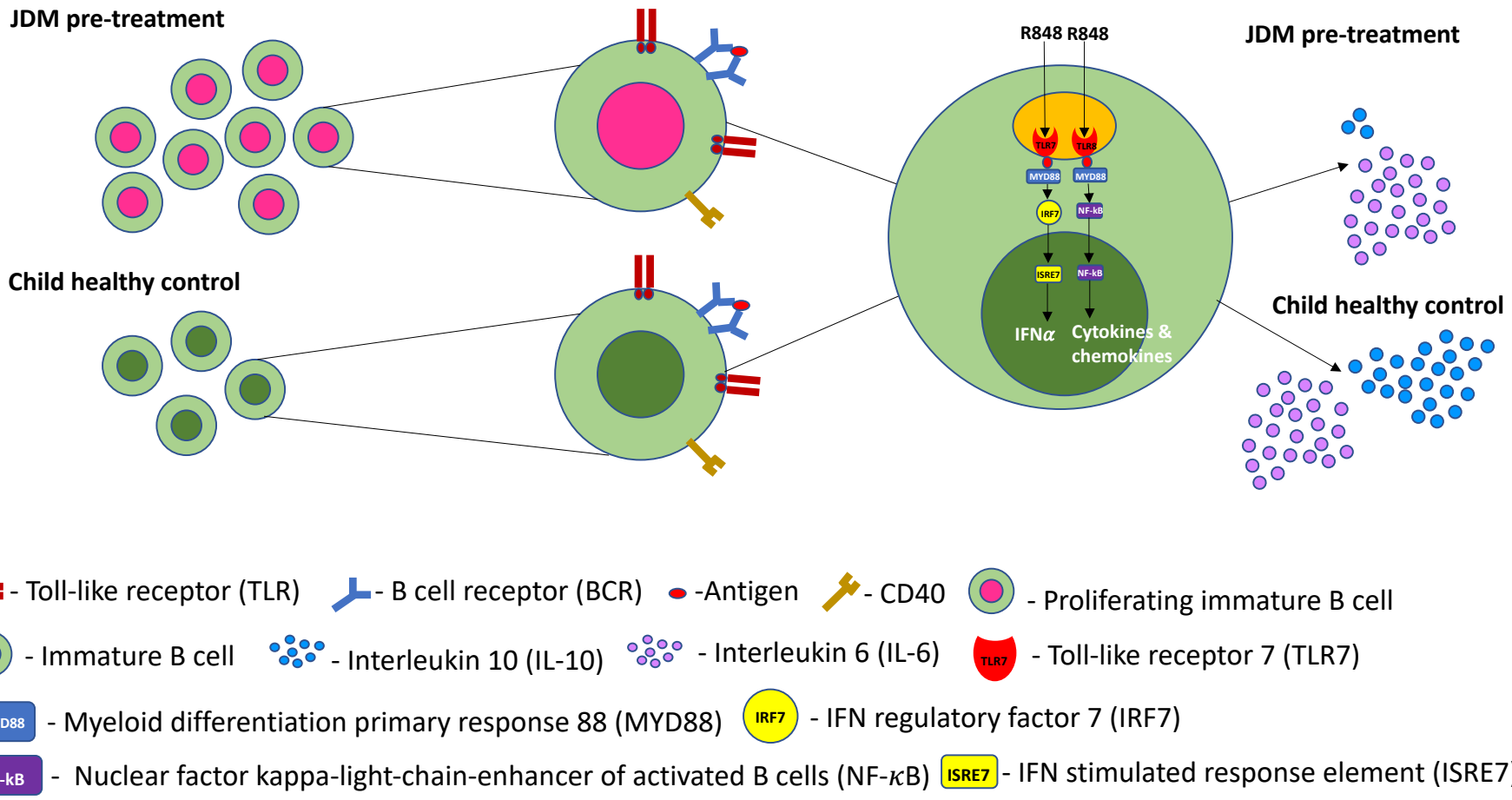

Figure III.12 Immature B cells are expanded in juvenile dermatomyositis and are skewed towards a pro-inflammatory phenotype by Toll-Like Receptor 7 (TLR7) and Interferon-α (IFN-α)

Chapter IV

Th17 cells are increased in adult dermatomyositis: a developing immune signature for the inflammatory myopathies

Results (section 2)

INTRODUCTION

The Inflammatory Idiopathic Myopathies (IIM) are a rare group of myopathic autoimmune diseases diagnosed in both adults and children. Patients may present with a variety of features including proximal muscle weakness and Gottron's papules. Immunohistochemical analysis of muscle tissue from these patients has identified immune cell infiltrate and the expression of pro-inflammatory cytokines however, little is known about the peripheral immunological profile in juvenile and adult patient groups.

There is clear evidence that the adaptive immune system plays an active role in the pathogenesis of IIM (Ceribelli et al., 2017). There are immune cellular infiltrates found in tissue biopsy and up to 80% of patients have specific clinical features correlated to detectable serum autoantibodies (Venalis and Lundberg, 2014). The endomysial cellular infiltrates most commonly detected in PM, constitute of CD8+ T cells, CD4+ T cells, dendritic cells (DCs) and macrophages. These cells localise around the muscle fibres. In DM, the perivascular infiltrates consist of CD4+ T cells, DCs, macrophages and B cells. Unlike PM, these cells are found around the inflamed blood vessels (Reed and Ernste, 2009).

T cells have been identified as dysfunctional in the context of IIM. CD4+CD25+FOXP3+ T cells were shown to have lost their ability to regulate the immune system with functional impairment in active JDM (Klein et al., 2010). Th17 cells have been found in tissue biopsy and an increased dysfunction positively correlated to disease activity (Banica et al., 2009). B cells have not been thought to be as vital as T cells in the pathogenesis of IIM, but do play an important role. Not only

are B cells found in the perivascular infiltrates of muscle tissue in DM patients, there is a high detection of myositis associated (MSA) and specific (MSS) autoantibodies (Greenberg et al., 2005a). The expression of B cell activating factor (BAFF) has been associated with anti-Jo-1 antibodies in DM muscle tissue, specifically in the perifascicular area (Baek et al., 2012).

Most studies on IIM have focused on the inflammatory milieu found within the tissue biopsy. The biopsy is a key diagnostic tool, but is rarely repeated past initial presentation, thus little is known about the histological changes during the disease course. This component of my thesis aims to investigate the peripheral blood immunological profile from adult and juvenile patients. Comparison will be made between adult and juvenile disease, PM and DM subsets, disease activity and autoantibody expression.

RESULTS

The sample groups included; 44 adult myositis (AM) patients (including DM and PM), 15 adolescent-onset juvenile dermatomyositis (JDM) patients, 25 age-matched adult healthy controls (AHC), and 15 age-matched teenage healthy controls (THC) were recruited with appropriate ethical approval after obtaining written informed consent (***Chapter II***). Demographic and clinical information was gathered for all patients and controls including; specific diagnosis, age at diagnosis, age at sample, gender, ethnicity, medication, measures of disease activity, autoantibody status and medications at time of sample (***Table IV.1-2***).

Comparing the demographics of all the AM to all the JDM patients, these cohorts had a similar sex distribution. The ethnicity distribution was different between the two groups primarily the increased representation of south Asian and white other patients within the AM cohort, though this did not reach statistical significance. This difference may be a reflection of the small sample size or the population demographics for that age group. Both cohorts had similar overall clinical findings. There were more AM than JDM patients that had had an increase in treatment at time of sample and therefore were deemed more active, but again this was not statistically significant. There was a difference in medication taken, AM patients were treated with a broader spectrum of drugs including tacrolimus, cyclosporine and IVIG. Methotrexate and hydroxychloroquine were more common treatments used in the JDM compared to AM cohort. The use of biologics was highest in the JDM cohort. Rituximab was the only biologic used in the AM cohort, where infliximab and adalimumab were used as well as rituximab in the JDM cohort.

The AM cohort was split by IIM subgroups including, dermatomyositis (DM), polymyositis (PM), DM with cancer, DM/PM with overlap autoimmune rheumatic diseases (e.g. SLE, scleroderma and RA)). Detailed analysis of the subgroups of the AM cohort identified differences in the demographics. The PM patients were all female whereas the DM patient group was constituted of 63.2% female. More DM patients were of white British ethnicity than the PM patients. More PM patients were of black Caribbean ethnicity than the DM patients. Clinically the DM with cancer patients had the highest median ESR (40 mm/hour) and MITAX scores (9.50). The higher ESR values were likely to be increased due to the cancer. The PM group had the highest percentage of patients with an increase in treatment at time of sample. DM patients had the greatest spread of singularly detected auto-antibodies, whereas the PM group only possessed anti-Jo-1 and anti-SRP. Hydroxychloroquine and mycophenolate mofetil (MMF) were more commonly used in DM compared to the other subgroups. Equally cyclosporine and IVIG were only used to treat DM and DM with cancer. Though there were differences in clinical data between sub-groups, none of the results reached statistical significance and may be not as apparent in a larger cohort.

Table IV.1 Demographic features of the adult myositis, JDM, adult and teenage healthy control cohorts at time of sample. *44 adult myositis (AM) patients, 15 adolescent onset-juvenile dermatomyositis (JDM) patients, 25 adult healthy controls (AHC) and 15 teenage healthy controls (THC) were recruited. The AM group was divided into subgroups; dermatomyositis (ADM), polymyositis (APM), dermatomyositis with cancer, dermatomyositis with overlap and polymyositis with overlap. For each group, the demographics were recorded including; age at diagnosis, age at samples, time since diagnosis, sex ratio and ethnicity. The binary measures were analysed by Chi-square test and the continuous variables were analysed by one-way ANOVA. A significant p-value was reached between AM and JDM for age at diagnosis and age at sample. $p \leq 0.05$ for significance.*

	Patients						**Controls**		
Patient characteristics	**Adult Myositis samples (n=44)**						**Juvenile DM (adolescent onset) samples (n=15)**	**Adult healthy control samples (n=25)**	**Adolescent healthy control samples (n=15)**
Sub-types of myositis	**All**	**Dermatomyositis**	**Polymyositis**	**Dermatomyositis with cancer**	**Dermatomyositis with overlap syndrome**	**Polymyositis with overlap syndrome**	**All**	**All**	**All**
Number of patients	**44**	**19**	**9**	**4**	**7**	**5**	**15**	**25**	**15**
Age at diagnosis (years), median [IQR] (p=0.0632)	39.82 [31.65-49.00]	34.02 [30.33-48.96]	41.29 [34.10-44.07]	47.83 [27.65-60.62]	39.87 [31.30-45.80]	39.64 [32.47-43.04]	14.78 [14.02-16.01]		
Age at sample (years), median [IQR] (p=0.2194)	55.48 [47.59-60.33]	55.80 [46.21-59.99]	52.37 [48.35-53.10]	63.04 [59.81-67.99]	49.20 [46.82-53.47]	59.72 [55.96-66.73]	21.48[19.07-23.19]	51.26[43.23-58.31]	20.11[17.40-22.28]
Time since diagnosis (years), median [IQR] (p=0.5453)	9.64 [3.39-23.13]	12.39 [4.61-22.29]	6.43 [5.15-10.97]	0.34 [0-6.23]	11.02 [1.02-24.86]	23.48 [7.98-23.69]	6.09 [5.28-7.82]		
Sex, (F/M) [p=0.3013]	34/10	12/7	9/0	4/0	5/2	4/1	11/4	14/11	11/4
Ethnicty, n (%) [0.0968]									
White British	17 (38.64)	10 (52.63)	1 (11.11)	2 (50.00)	3 (42.86)	1 (20)	9 (60.00)	14 (56.00)	6 (40.00)
Black Carribean	9 (20.45)	1 (5.26)	5 (55.56)	1 (25)	1 (14.29)	1 (20)	2 (13.33)	0 (0.00)	0 (0.00)
Black African	3 (6.81)	1 (5.26)	0 (0.00)	0 (0.00)	1 (14.29)	1 (20)	1 (6.67)	0 (0.00)	1 (6.67)
South Asian	7 (15.91)	2 (10.53)	1 (11.11)	0 (0.00)	2 (28.57)	2 (40.00)	0 (0.00)	2 (8.00)	5 (33.33)
East Asian	0 (0.00)	0 (0.00)	0 (0.00)	0 (0.00)	0 (0.00)	0 (0.00)	0 (0.00)	0 (0.00)	1 (6.67)
White other	7 (15.91)	4 (21.05)	2 (22.22)	1 (25)	0 (0.00)	0 (0.00)	0 (0.00)	7 (28.00)	0 (0.00)
South American	0 (0.00)	0 (0.00)	0 (0.00)	0 (0.00)	0 (0.00)	0 (0.00)	0 (0.00)	0 (0.00)	0 (0.00)
Other	1 (2.27)	1 (5.26)	0 (0.00)	0 (0.00)	0 (0.00)	0 (0.00)	3 (20.00)	0 (0.00)	1 (6.67)
Unknown	0 (0.00)	0 (0.00)	0 (0.00)	0 (0.00)	0 (0.00)	0 (0.00)	0 (0.00)	2 (8.00)	0 (0.00)

Table IV.2 Clinical and serological features of the adult myositis, JDM, adult and teenage healthy control cohorts at time of sample. *44 adult myositis (AM) patients and 15 adolescent onset-juvenile dermatomyositis (JDM) patients were recruited. The AM group was divided into subgroups; dermatomyositis (ADM), polymyositis (APM), dermatomyositis with cancer, dermatomyositis with overlap and polymyositis with overlap. For each group, the clinical and serological data were recorded including; erythrocyte sedimentation rate (ESR) [normal range <20mm/hour], C-reactive protein (CRP) [normal range <5mg/L], lymphocyte count [normal range 1.5-2x10⁹/L], creatine kinase (CK) [normal range <150U/L], MITAX score, MMT8 score [normal range >78], clinician's decision on treatment, auto-antibodies and medication. The binary measures were analysed by Chi-square test and the continuous variables were analysed by one-way ANOVA. p≤0.05 for significance.*

Patient characteristics	**Adult Myositis samples (n=44)**						**Juvenile DM (adolescent onset) samples (n=15)**	**Adult healthy control samples (n=25)**	**Adolescent healthy control samples (n=15)**
Sub-types of myositis	**All**	**Dermatomyositis**	**Polymyositis**	**Dermatomyositis with cancer**	**Dermatomyositis with overlap syndrome**	**Polymyositis with overlap syndrome**	**All**	**All**	**All**
Number of patients	**44**	**19**	**9**	**4**	**7**	**5**	**15**	**25**	**15**
Age at diagnosis (years), median [IQR] (p=0.0632)	39.82 [31.65-49.00]	34.02 [30.33-48.96]	41.29 [34.10-44.07]	47.83 [27.65-60.62]	39.87 [31.30-45.80]	39.64 [32.47-43.04]	14.78 [14.02-16.01]		
Age at sample (years), median [IQR] (p=0.2194)	55.48 [47.59-60.33]	55.80 [46.21-59.99]	52.37 [48.35-53.10]	63.04 [59.81-67.99]	49.20 [46.82-53.47]	59.72 [55.96-66.73]	21.48[19.07-23.19]	51.26[43.23-58.31]	20.11[17.40-22.28]
Time since diagnosis (years), median [IQR] (p=0.5453)	9.64 [3.39-23.13]	12.39 [4.61-22.29]	6.43 [5.15-10.97]	0.34 [0-6.23]	11.02 [1.02-24.86]	23.48 [7.98-23.69]	6.09 [5.28-7.82]		
Sex, (F/M) [p=0.3013]	34/10	12/7	9/0	4/0	5/2	4/1	11/4	14/11	11/4
Ethnicty, n (%) [0.0968]									
White British	17 (38.64)	10 (52.63)	1 (11.11)	2 (50.00)	3 (42.86)	1 (20)	9 (60.00)	14 (56.00)	6 (40.00)
Black Carribean	9 (20.45)	1 (5.26)	5 (55.56)	1 (25)	1 (14.29)	1 (20)	2 (13.33)	0 (0.00)	0 (0.00)
Black African	3 (6.81)	1 (5.26)	0 (0.00)	0 (0.00)	1 (14.29)	1 (20)	1 (6.67)	0 (0.00)	1 (6.67)
South Asian	7 (15.91)	2 (10.53)	1 (11.11)	0 (0.00)	2 (28.57)	2 (40.00)	0 (0.00)	2 (8.00)	5 (33.33)
East Asian	0 (0.00)	0 (0.00)	0 (0.00)	0 (0.00)	0 (0.00)	0 (0.00)	0 (0.00)	0 (0.00)	1 (6.67)
White other	7 (15.91)	4 (21.05)	2 (22.22)	1 (25)	0 (0.00)	0 (0.00)	0 (0.00)	7 (28.00)	0 (0.00)
South American	0 (0.00)	0 (0.00)	0 (0.00)	0 (0.00)	0 (0.00)	0 (0.00)	0 (0.00)	0 (0.00)	0 (0.00)
Other	1 (2.27)	1 (5.26)	0 (0.00)	0 (0.00)	0 (0.00)	0 (0.00)	3 (20.00)	0 (0.00)	1 (6.67)
Unknown	0 (0.00)	0 (0.00)	0 (0.00)	0 (0.00)	0 (0.00)	0 (0.00)	0 (0.00)	2 (8.00)	0 (0.00)
Clinical features, median [IQR]									
Erythrocyte sedimentation rate (ESR) mm/hour (measured at time of sample)[p=0.0394]	18.5 [8.00-28.25]	9.00 [5.75-17.50]	25.00 [22.5-30.00]	40.00 [33.00-43.50]	23.00 [16.50-37.50]	24.5 [16.25-36.25]	16.5 [7.50-22.50]		
C-reactive protein (CRP) mg/L <3.0mg/L (measured in serum at time of sample) [p=0.7019]	2 [0.70-5.80]	1.60 [0.78-2.65]	2.3 [0.70-6.48]	3.00 [1.88-28.45]	4.45 [1.73-17.90]	4.90 [1.65-10.05]	2.75 [2.23-5.00]		
Lymphocyte count (1-4x10^9 /L of blood) (taken at time of sample)	1.35 [0.65-1.67]	1.5 [1.38-1.65]	1.66 [0.81-2.13]	0.46 [0.40-0.57]	0.56 [0.52-0.62]	1.62 [1.44-1.90]	1.72 [1.06-1.85]		
Creatinine Kinase (CK) U/L - (>0) (meaured in serum at time of PBMC sample) [p=0.6966]	147 [93-364]	195 [125-301]	230.5 [142-308]	116 [107.75-696.50]	100 [92.25-949.25]	87 [75.5-192.25]	106 [76.50-464.75]		
MITAX score	1.50 [0.00-9.00]	1.00 [0.00-9.00]	3.00 [1.00-9.00]	9.50 [1.75-19.00]	2.00 [0.50-10.50]	0.00 [0.00-2.25]	0.00 [0.00-4.00]		
MMT8 (0-80)	Not done	Not done	Not done	Not done	Not done	Not done	80 [77-80]		
Clinicians decision on treatment, n(%)									
Decreased	6 (13.63)	2 (10.53)	1 (11.11)	0 (0.00)	2 (28.57)	1 (20.0)	3 (20.00)		
Stable	28 (63.63)	13 (68.42)	5 (55.56)	3 (75.00)	3 (42.86)	4 (80.00)	10 (66.67)		
Increased	10 (22.73)	4 (21.05)	3 (33.33)	1 (25.00)	2 (28.57)	0 (0.00)	2 (13.33)		
Myositis-specific autoantibodies, n (%) [0.3022]									
Anti-Jo-1	5 (11.36)	1 (5.26)	3(33.33)	0 (0.00)	1(14.29)	0 (0.00)	0 (0.00)		
Anti-Ro	3 (6.81)	2 (10.53)	0 (0.00)	1 (25)	0 (0.00)	0 (0.00)	1 (13.33)		
Anti-PL12	1 (2.27)	1 (5.26)	0 (0.00)	0 (0.00)	0 (0.00)	0 (0.00)	0 (0.00)		
Anti-PM-Scl75	1 (2.27)	1 (5.26)	0 (0.00)	0 (0.00)	0 (0.00)	0 (0.00)	0 (0.00)		
Anti-Mi2	3 (6.81)	3 (15.78)	0 (0.00)	0 (0.00)	0 (0.00)	0 (0.00)	1 (6.67)		
Anti-SRP	1 (2.27)	0 (0.00)	1 (11.11)	0 (0.00)	0 (0.00)	0 (0.00)	0 (0.00)		
Anti-NXP2	1 (2.27)	1 (5.26)	0 (0.00)	0 (0.00)	0 (0.00)	0 (0.00)	0 (0.00)		
TIF1-y	3 (6.81)	2 (10.53)	0 (0.00)	1 (25)	0 (0.00)	0 (0.00)	0 (0.00)		
ANA	2 (4.55)	1 (5.26)	1 (11.11)	0 (0.00)	0 (0.00)	0 (0.00)	5 (33.33)		
RF	2 (4.55)	1 (5.26)	1 (11.11)	0 (0.00)	0 (0.00)	0 (0.00)	0 (0.00)		
Multiple	11 (25.00)	2 (10.53)	1 (11.11)	0 (0.00)	4 (57.14)	4 (80)	5 (33.33)		
Negative	5 (11.36)	3 (15.78)	1 (11.11)	1 (25)	0 (0.00)	0 (0.00)	0 (0.00)		
Not done	6 (13.63)	1 (5.26)	1 (11.11)	1 (25)	2 (28.57)	1 (20)	3 (20.00)		
Unknown	0 (0.00)	0 (0.00)	0 (0.00)	0 (0.00)	0 (0.00)	0 (0.00)	0 (0.00)		
Medications (at time of sample) n(%): [p=0.3237]									
Prednisolone	28 (63.63)	10 (52.63)	4 (44.44)	3 (75)	7 (100)	4 (80)	8 (53.33)		
Methotrexate	5 (11.36)	2 (10.53)	2 (22.22)	0 (0.00)	1 (14.29)	0 (0.00)	10 (66.67)		
Azathioprine	9 (20.45)	2 (10.53)	2 (22.22)	1(25.00)	4 (57.14)	0 (0.00)	2 (13.33)		
Rituximab past	7 (15.91)	2 (10.53)	2 (22.22)	0 (0.00)	1 (14.29)	2 (40.00)	1 (13.33)		
Hydroxychloriquine	5 (11.36)	3 (15.78)	1 (11.11)	0 (0.00)	1 (14.29)	0 (0.00)	6 (40.00)		
MMF	8 (18.18)	5 (26.32)	1 (11.11)	0 (0.00)	1 (14.29)	1 (20)	2 (13.33)		
Tacrolimus	3 (6.812)	1 (5.26)	1 (11.11)	0 (0.00)	1 (14.29)	0 (0.00)	0 (0.00)		
Cyclosporine	2 (4.54)	2 (10.53)	0 (0.00)	0 (0.00)	0 (0.00)	0 (0.00)	0 (0.00)		
IVIG	3 (6.82)	2 (10.53)	0 (0.00)	1 (25)	0 (0.00)	0 (0.00)	0 (0.00)		
Infliximab	0 (0.00)	0 (0.00)	0 (0.00)	0 (0.00)	0 (0.00)	0 (0.00)	2 (13.33)		
Adalimumab	0 (0.00)	0 (0.00)	0 (0.00)	0 (0.00)	0 (0.00)	0 (0.00)	1 (6.67)		

PBMC from all sample groups were analysed by flow cytometry to quantify 33 lymphocyte populations including; T-cell, B-cell and monocyte subsets. Total T cell and 16 T cell sub-populations were categorized and measured *ex-vivo* (***Figure IV.1*** and ***Table IV.3***) (McGowan et al., 2015). Total B cell, 8 B cell sub-populations, total monocytes, 3 monocyte sub-populations and natural killer (NK) cells were categorized and measured *ex-vivo* (***Figure IV.2*** and ***Table IV.4***) (Lima et al., 2016, Lee et al., 2017). In addition to defining these populations, the expression of CD69 from each population was measured as a recording of cellular activity (***Figure IV.3*** and ***5***). The expression of IL-6 from monocyte, T and B cell populations and subsets were measured from PBMC from all sample groups after a 4hour culture in the presence of PMA, ionomycin and golgi plug (***Figure IV.4*** and ***5***). The expression of IL-17 was measured to identify the Th17 population after the same 4hour culture in the presence of PMA, ionomycin and golgi plug (***Figure IV.6***).

Flow cytometry gating

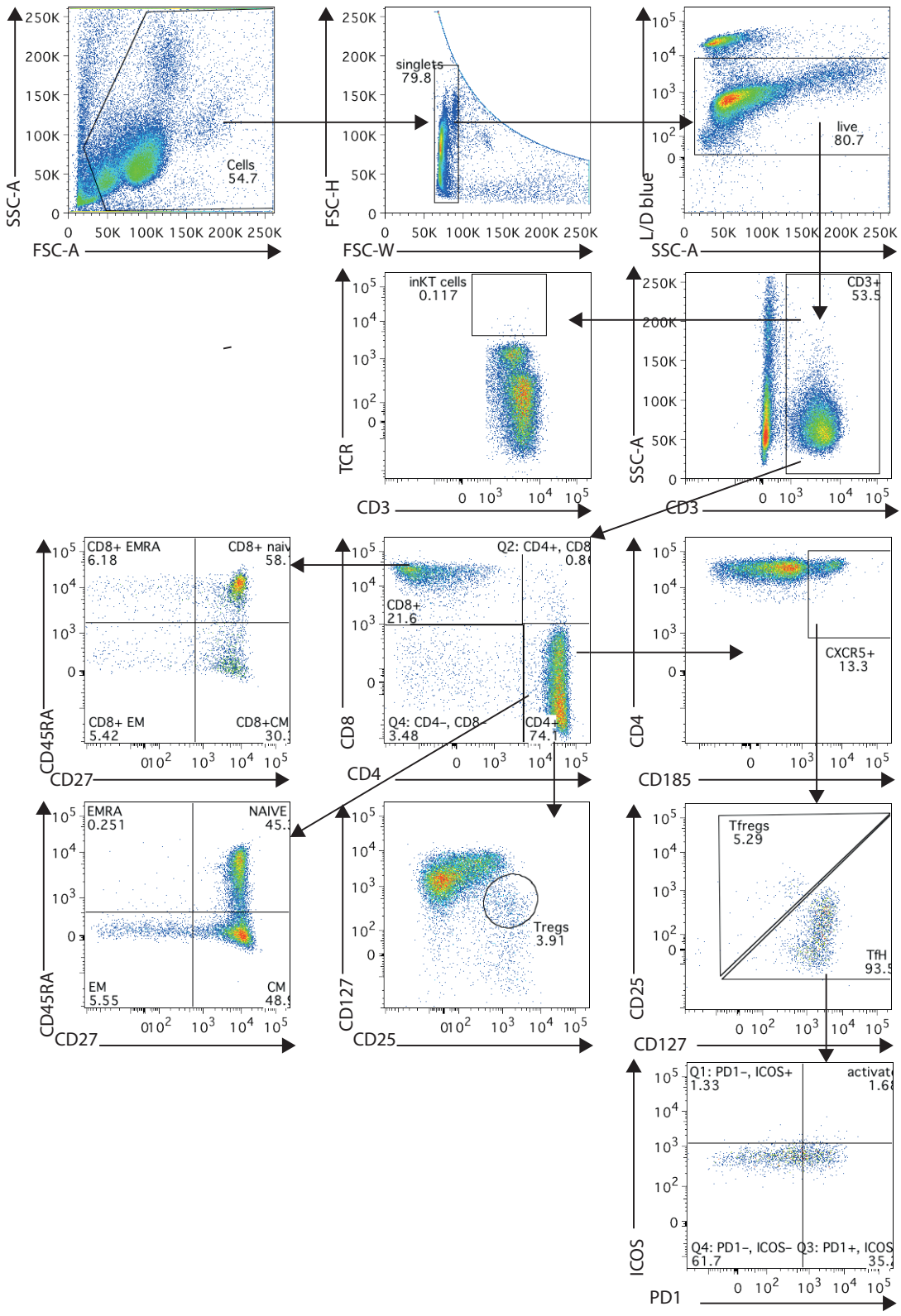

Figure IV.1 Flow cytometry gating strategy for T cells and subsets

Table IV.3 T cell panel with defined sub-population by surface cell markers

Cell type	Markers
T cell	CD3+
Invariant killer T cells (inKT)	CD3+γδTCR+
CD8+ T cell	CD3+CD8+
C8+ Effector memory (EM)	CD3+CD8+CD45RA-CD27-
C8+ Central memory (CM)	CD3+CD8+CD45RA-CD27+
C8+ CD45RA+ Effector memory (EMRA)	CD3+CD8+CD45RA+CD27-
C8+ naïve	CD3+CD8+CD45RA+CD27+
CD4+ T cell	CD3+CD8+
C4+ Effector memory (EM)	CD3+CD4+CD45RA-CD27-
C4+ Central memory (CM)	CD3+CD4+CD45RA-CD27+
C4+ CD45RA+ Effector memory (EMRA)	CD3+CD4+CD45RA+CD27-
C4+ naïve	CD3+CD4+CD45RA+CD27+
Tregs	CD3+CD4+CD127^{low}CD25+
CXCR5+ T cell	CD3+CD4+CD185+
Tfregs	CD3+CD4+CD185+CD25+CD127^{low}
TfH	CD3+CD4+CD185+ CD25^{low}CD127+
Activated T cells	CD3+CD4+CD185+ CD25^{low}CD127+PD1+ICOS+

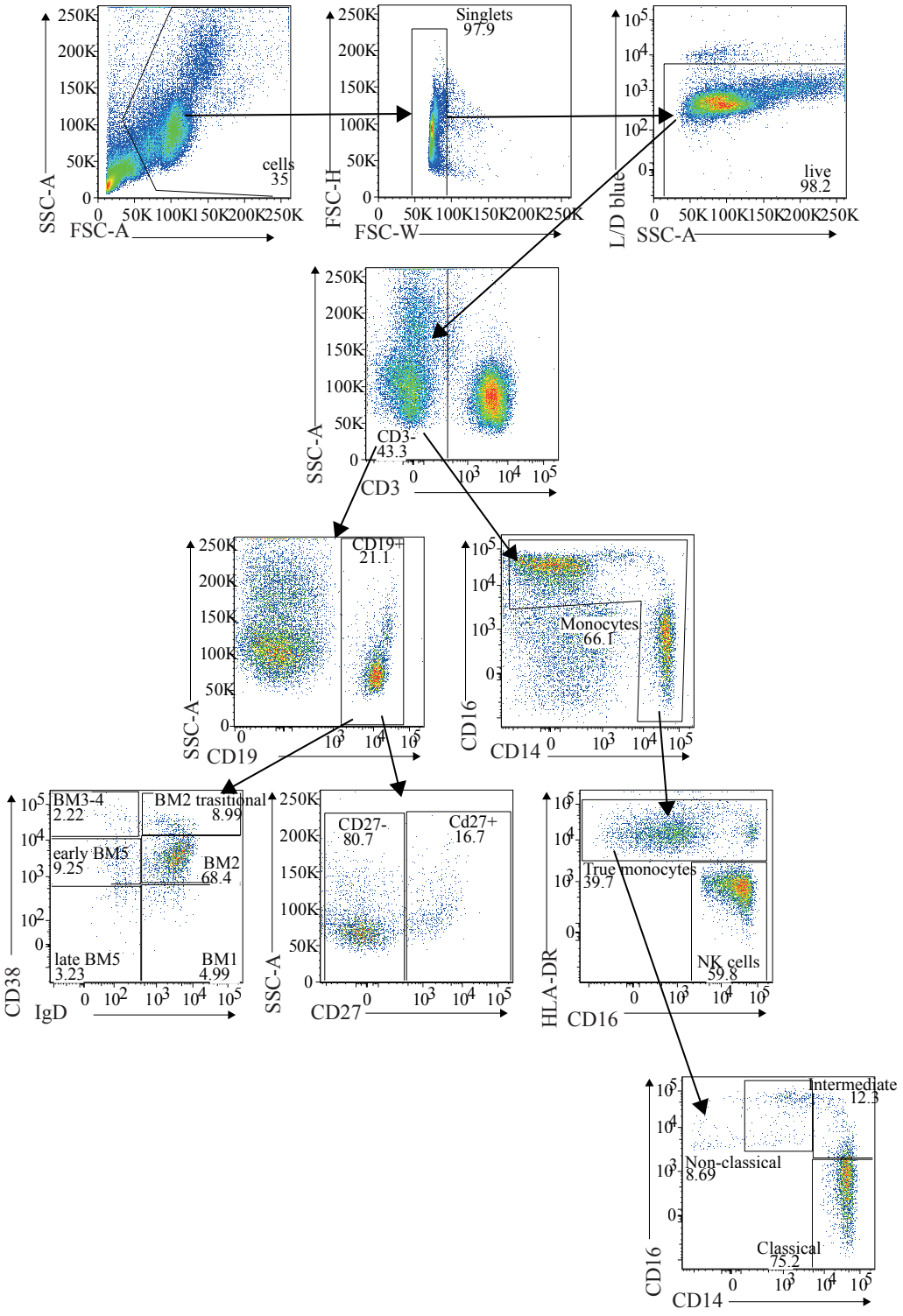

Figure IV.2 Flow cytometry gating strategy for B cells and subsets

Table IV.4 B cell and monocyte ex-vivo panel with defined sub-population by surface cell markers

Cell type	Markers
B cell	CD3-CD19+
CD27+ B cells	CD3-CD19+CD27+
CD27- B cells	CD3-CD19+CD27-
BM1	CD3-CD19+IgD+CD38-
BM2	CD3-CD19+IgD+CD38+
BM2 transitional	CD3-CD19+IgD^{hi}CD38^{hi}
BM3-4	CD3-CD19+IgD-CD38^{hi}
BM5 early	CD3-CD19+IgD-CD38+
BM5 late	CD3-CD19+IgD+CD38-
Monocytes	CD3-HLA-DR+
Natural killer cells (NK)	CD3-HLA-DR-CD16+
Non-classical monocytes	CD3-HLA-DR+CD14-CD16+
Intermediate monocytes	CD3-HLA-DR+CD14+CD16+
Classical monocytes	CD3-HLA-DR+CD14+CD16-

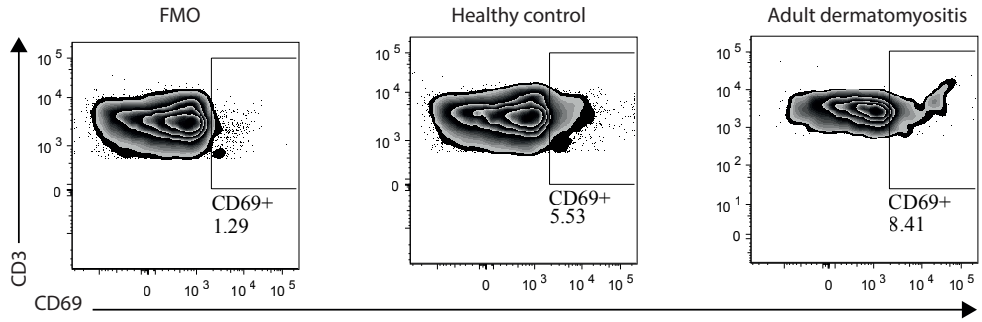

Figure IV.3 Flow cytometry gating strategy for CD69 expression

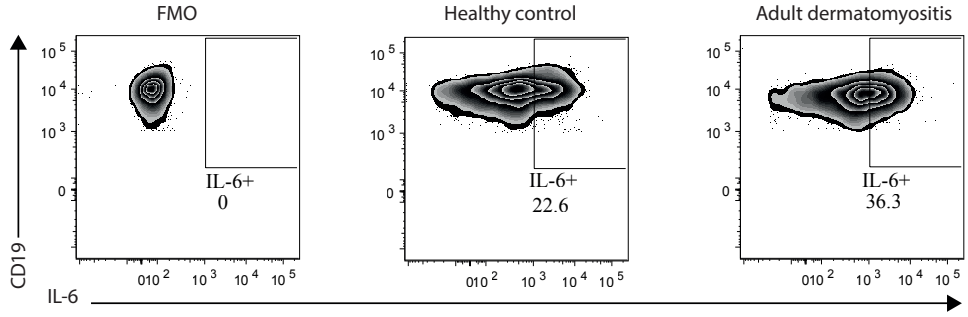

Figure IV.4 Flow cytometry gating strategy for IL-6 expression

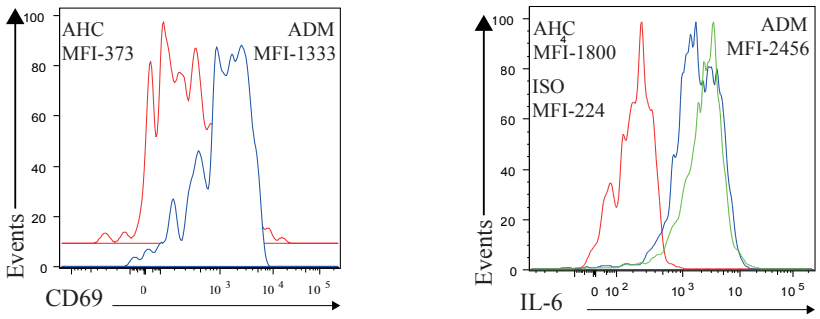

Figure IV.5 Flow cytometry histograms of CD69 and IL-6 median fluorescence intensity (MFI)

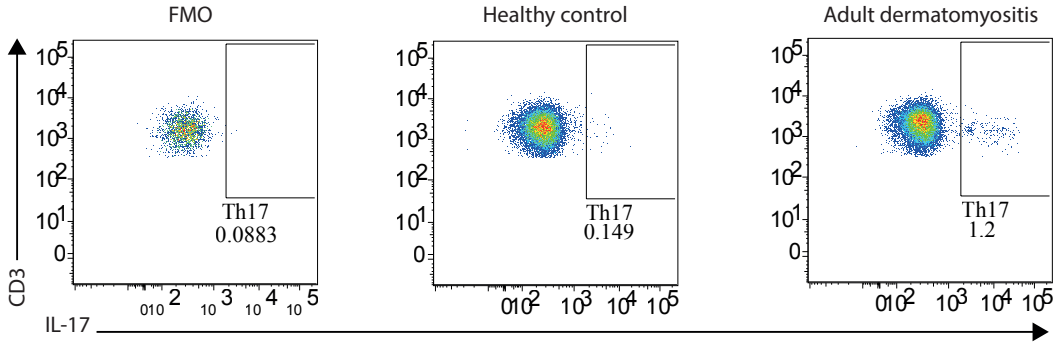

Figure IV.6 Flow cytometry gating strategy for Th17 cells

Distinct changes of the immune cell signature with age and key differences between adult and juvenile disease

All the categorised cell populations were compared between sample groups, AM, JDM, AHC and THC, which were demonstrated in a heatmap of p-values (***Figure IV.7***). Clear differences in the immune cell signature between patients and age-matched healthy donors for both AM and JDM were identified. However, the immune signature was altered in adults (AM vs AHC) compared to juveniles (JDM vs THC) suggesting an influence of age and/or that the immunopathogensis was different between AM and JDM.

Volcano plots (fold changes vs p-value) were used to further visualise the multiple differences in the immune cell populations between patients and healthy donors (***Figure IV.8***). When AM was compared to AHC memory B and T cell populations (CD27+ve B cells, CD4+ CM, CD8+ CM) and total B cells were significantly decreased, whereas CD27-ve B cells and intermediate monocytes were significantly increased (***Figure IV.8A***). However, in JDM patients BM2, CD8+ and CD8+CM populations were significantly decreased and CD4+ T cells were increased compared to THC (***Figure IV.8B***). This finding suggested that ADM and JDM patients had unique phenotypes compared to age matched controls. This was supported when the immune phenotype of AM patients was compared to that of JDM. A significant decrease in CD27+ve B cells and CD8+ naïve cell populations was identified in AM compared to JDM, however CD27-ve B cells were increased (***Figure IV.8C***).

Finally, when AHC was compared to THC the CD4+ naïve, CD8+ naïve and classical monocyte populations were increased, whilst the BM2 and intermediate monocytes

were decreased (***Figure IV.8D***). These data showed that the immune system changes with age which in turn may influence the differences in immunopathogenesis between adult and juvenile disease.

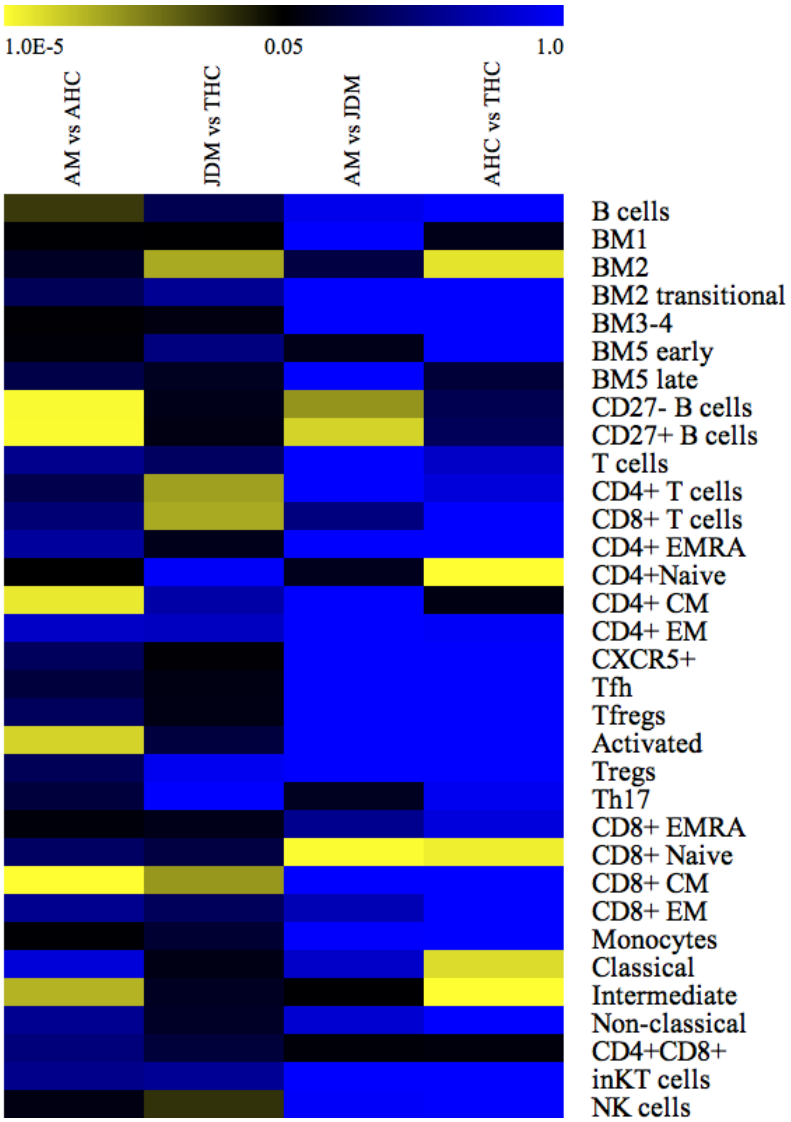

Figure IV.7 Heat map identifying significant differences in cell populations, a comparison of IIM to healthy samples. *The frequency of 33 PBMC populations were measured by flow cytometry from 44 adult myositis (AM) patients, 25 adult healthy controls (AHC), 15 adolescent-onset juvenile dermatomyositis (JDM) patients and 15 teenage healthy controls (THC). This heat map demonstrates the statistical difference between each cell population by comparing the mean of each group of samples; AM vs. AHC, JDM vs. THC, AM, vs. JDM and AHC vs. THC. A student t-test calculated the p-values. Black to yellow - $p \leq 0.05$. Blue to black - $p \geq 0.05$.*

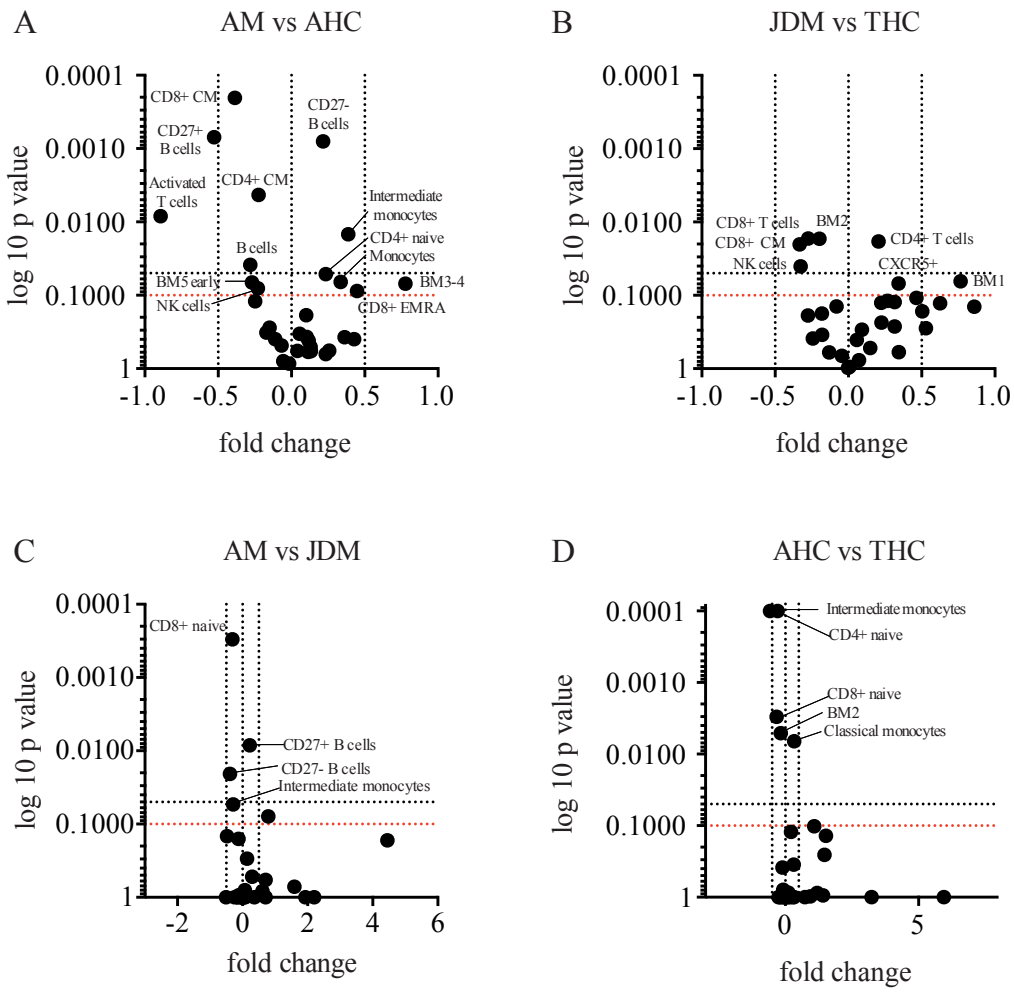

Figure IV.8 Volcano plots identifying significant differences and fold change of cell populations, a comparison of IIM to healthy samples. *Volcano plots represent the fold change and p value for each cell population when sample groups were compared.* ***A)*** *AM vs. AHC,* ***B)*** *JDM vs. THC,* ***C)*** *ADM vs. JDM,* ***D)*** *AHC, THC. The p values were calculated by one-way ANOVA. All p-values represent adjusted p-value calculated by Tukey's multiple comparison. Stringent significance p≤0.05 (black dotted line). Adjusted significance for small sample size p≤0.1 (red dotted line)*

A T cell signature in ADM and B cell signature in APM

Immune signatures in the IIM patient subgroups were also compared to the AHCs. Patients with ADM had increased Th17 and Treg T cell populations and decreased BM5 early B cells compared to AHC (***Figure IV.9A***). When the ADM with overlap patients were compared to the AHC group an increase in Th17 T cells was also identified (***Figure IV.9E***). However, the APM signature was characterised by a

change in the CD27+ve/-ve ratio, with an increase of CD27-ve and there by a decrease in CD27+ve B cells. In addition, there was also a decrease in the CD8+ CM T cell population (***Figure IV.9B***).

T follicular regulatory (Tfreg) and CD4+ EMRA T cells were increased in the ADM with cancer compared to AHC group (***Figure IV.9C***). There were no significant differences in immune cell populations between the APM with overlap and AHC groups (***Figure IV.9D***). Finally, the ADM group was compared to the JDM group as the most comparable disease groups. This comparison identified key differences in the immune signature. The ADM group showed an increase of the Th17 and Treg T cell populations and a decrease in BM5 early, CD8+ naïve and intermediate monocyte cell populations when compared to the JDM group (***Figure IV.9F***). Thus, confirming the association between ADM and increased Th17 and Treg populations.

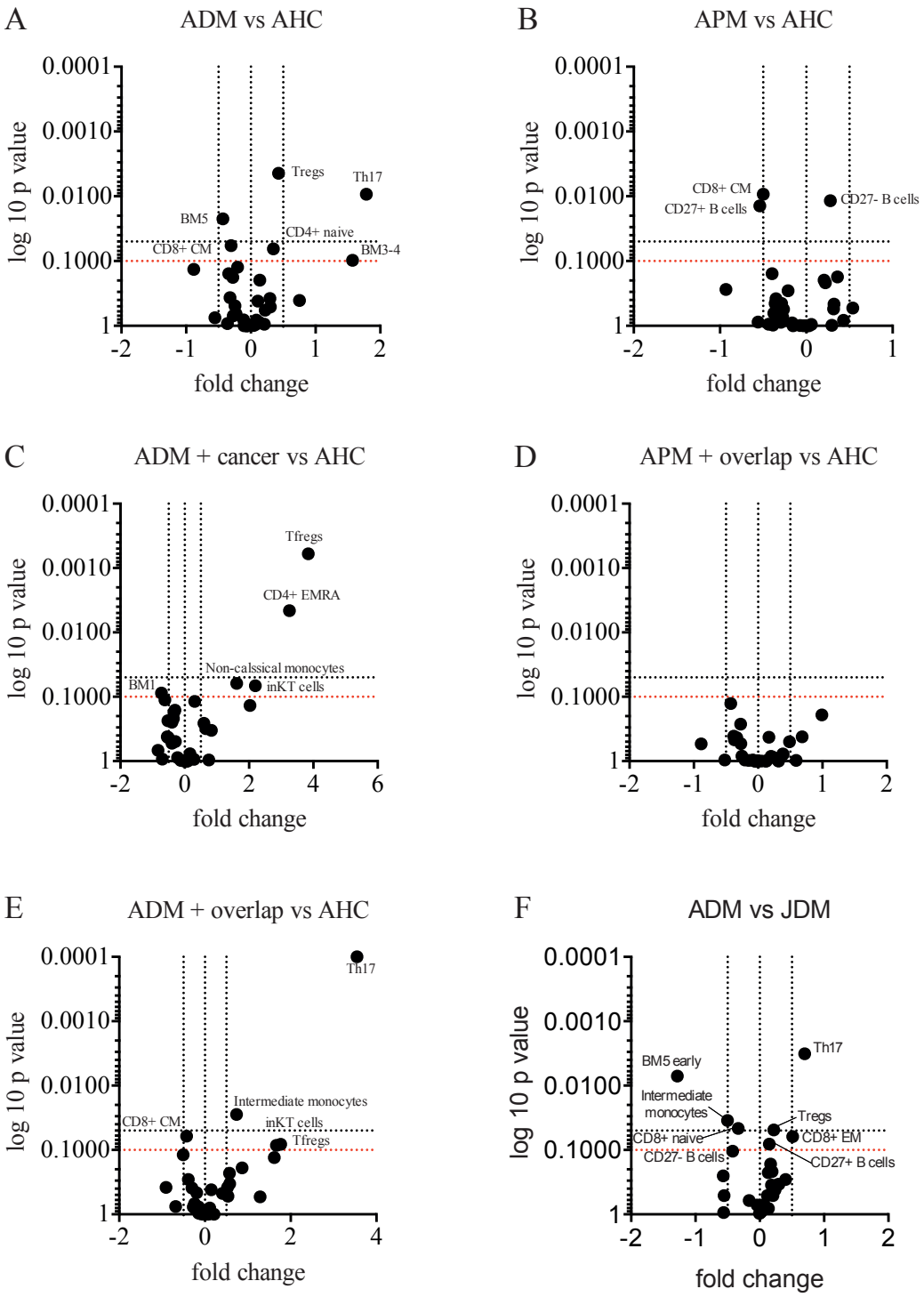

Figure IV.9 Volcano plots identifying significant differences and fold change of cell populations, a comparison of AM disease subgroups, JDM and AHC. *Volcano plots represent the fold change and p value for each cell population when sample groups were compared.* ***A)*** *ADM (n=19) vs. AHC (n=25),* ***B)*** *APM (n=9) vs. AHC,* ***C)*** *ADM + cancer (n=4) vs. AHC,* ***D)*** *APM + overlap (n=7) vs. AHC,* ***E)*** *ADM + overlap (n=5) vs. AHC,* ***F)*** *ADM vs. JDM (n=15). The p values were calculated by one-way ANOVA. All p-values represent adjusted p-values calculated by Tukey's multiple comparison. Stringent significance p≤0.05 (black dotted line). Adjusted significance for small sample size p≤0.1 (red dotted line).*

Autoantibody groups highlight unique immune signatures

Previous groups have used the autoantibody profile to discriminate between AM patient subtypes (Habers et al., 2016). Therefore, the immune phenotype in patients with AM was assessed according to autoantibody status. Similar cell types appeared in these signatures that had already been observed, but were unique to different autoantibody groups. When the anti-synthetase (anti-Jo-1 and anti-Pl-12) group was compared to AHC there was a strong B cell signature which suggested a change in the CD27-/+ve ratio (***Figure IV.10A***). The autoimmune rheumatic disease (ARD) overlap (anti-Ro, anti-PmSCL and anti-RNP) group demonstrated a T cell signature with increased Th17 and decreased CD8+ CM T cell populations (***Figure IV.10B***). There were no significant differences between the individual populations when the severe skin (anti-Mi2) group was compared to AHC (***Figure IV.10C***). The cancer associated (anti-NXP2 and anti-TIF1γ) group showed increased monocyte, intermediate monocyte and BM3-4 B cell populations, but a decreased T cell population (***Figure IV.10D***). Those patients that had multiple auto-antibodies had increased Th17 T cell and intermediate monocyte populations (***Figure IV.10E***). The only significantly increased population seen when the negative group were compared to AHC was CD8+ naïve T cells (***Figure IV.10F***).

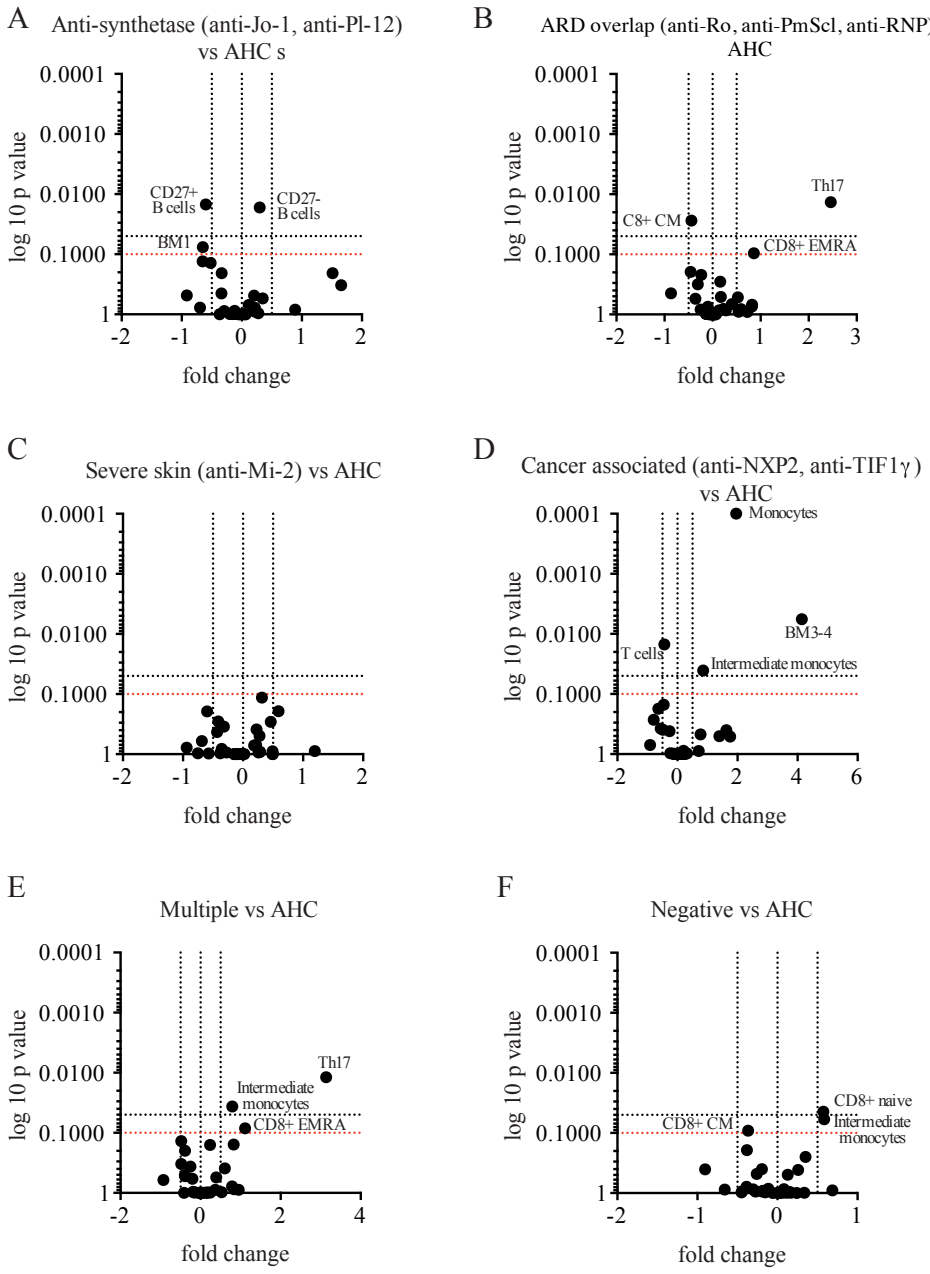

Figure IV.10 Volcano plots demonstrating the significantly different cell populations comparing AM autoantibody grouped samples with AHC. *Volcano plots represent the fold change and p value for each cell population when AM autoantibody groups were compared with AHC samples.* ***A)*** *Anti-synthetase group (anti-Jo-1 and anti-Pl-12) (n=7) compared to AHC (n=25).* ***B)*** *Autoimmune rheumatic disease overlap (ARD) group (anti-Ro, anti-PmScl and anti-RNP) (n=9) compared to AHC.* ***C)*** *Severe skin group (anti-Mi2) (n=3) compared to AHC.* ***D)*** *Cancer associated group (anti-NXP2 and anti-TIF1γ) (n=4) compared to AHC.* ***E)*** *Multiple autoantibodies group (n=5) compared to AHC.* ***F)*** *Negative for autoantibodies tested group (n=9) compared to AHC. The p values were calculated by one-way ANOVA. All p-values represent adjusted p-values calculated by Tukey's multiple comparison. Stringent significance p≤0.05 (black dotted line). Adjusted significance for small sample size p≤0.1 (red dotted line).*

AM immune signature most distinct from patients in remission

The AM group was further divided by disease activity status and compared to each other and the AHC group to identify changes in the immune signature linked to the activity of the disease. I distinguished four groups including, active, mildly active, remission on treatment and remission off treatment. The most differences seen were between the remission off treatment group when compared to each other group (***Figure IV.11A***). The consistent difference observed was an increase of non-classical monocytes, but when compared to AHC an increase of CD27-ve, BM2 and a decrease in CD27+ve B cells was also identified. Th17 cells were increased in the remission on treatment compared to AHC group (***Figure IV.11B***), and the CD8+CM T cells were decreased from the active compared to AHC group (***Figure IV.11D***). Table 4 shows that there were more differences with less stringent statistical testing which may be more applicable for the small sample sizes. These data showed that AM patients in remission off treatment have the most striking altered immune signature compared to AHC. Therefore, this signature may reflect the true immune changes that occur in AM that continue into remission and no longer masked by treatment.

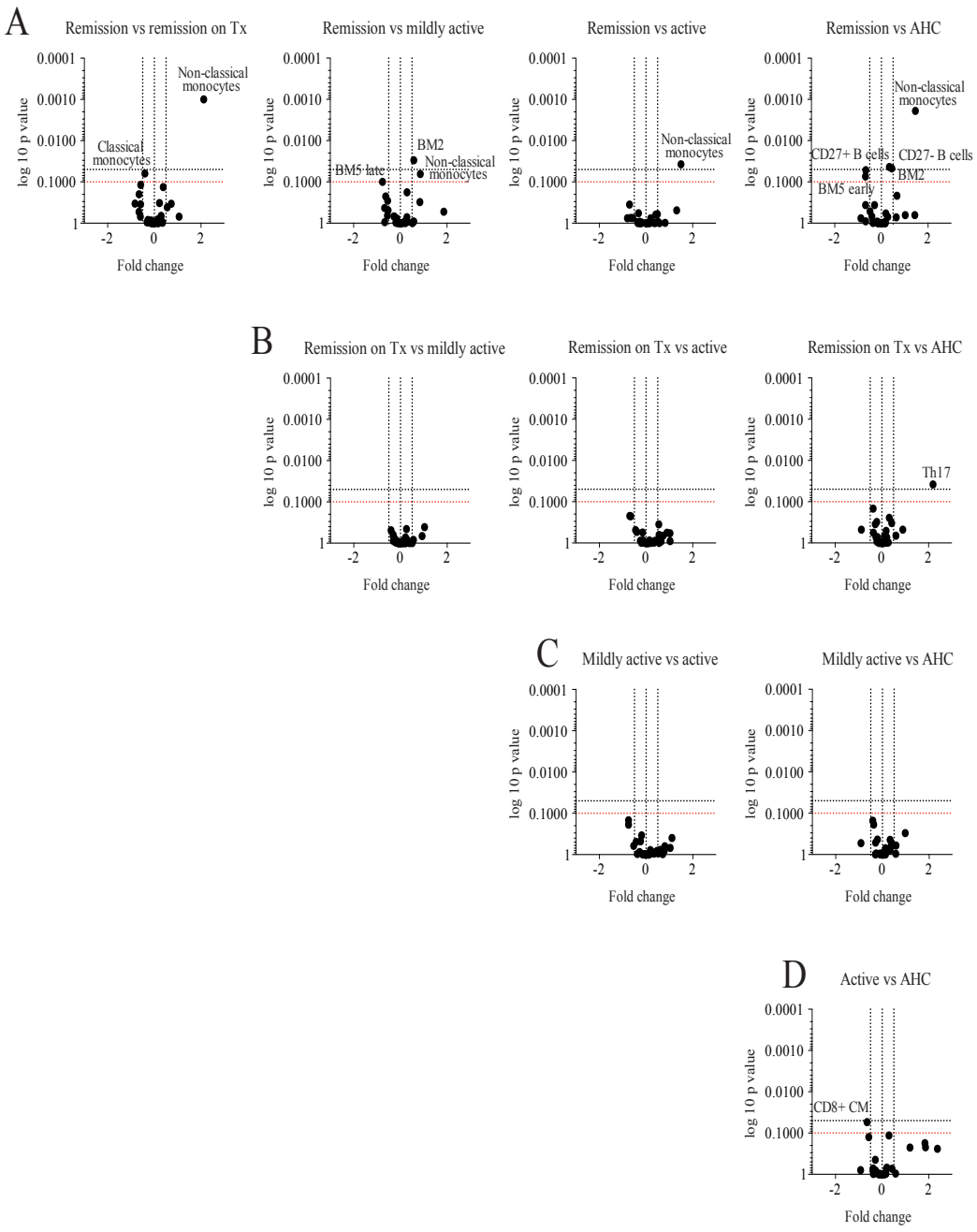

Figure IV.11 Volcano plots identifying significant differences and fold change of cell populations, a comparison of AM disease activity subgroups and AHC. *Volcano plots represent the fold change and p value for each cell population when AM disease activity groups were compared. Patients' with cancer, pregnant, treated with rituximab or diagnosed in childhood were removed from this analysis.* ***A)*** *Remission (n=5) compared to remission on treatment (Tx) (n=12), mildly active (n=9), active (n=4) and AHC (n=25).* ***B)*** *remission on Tx compared to mildly active, active and AHC.* ***C)*** *Mildly active compared to active and AHC.* ***D)*** *Active compared to AHC. The p values were calculated by one-way ANOVA. All p-values represent adjusted p-values calculated by Tukey's multiple comparison. Stringent significance p≤0.05 (black dotted line). Adjusted significance for small sample size p≤0.1 (red dotted line).*

Table IV.5 A comparison of AM disease activity groups; significantly different cell populations by student t-test

Comparison	Increased significantly	Decreased significantly
Remission vs remission on Treatment	Non-classical monocytes, B cells	Classical monocytes
Remission vs mildly active	BM2, non-classical monocytes, CD27- B cells	BM5 late, Monocytes
Remission vs active	Non-classical monocytes	BM5 early
Remission vs AHC	Non-classical monocytes, CD27- B cells, BM2, Th17	CD27+ B cells, BM5 early, BM5 late
Remission on Treatment vs mildly active	None	None
Remission on Treatment vs active	None	None
Remission on Treatment vs AHC	Th17, Monocytes	B cells
Mildly active vs active	None	CD4+ EMRA
Mildly active vs AHC	None	B cells, CD8+ CM, BM5 early
Active vs AHC	CD27+ B cells, Tfregs, Th17	CD8+ CM, CD27- B cells

CD8+CM T cells were decreased in active disease

Continued exploration of the correlation between disease activity and an immune cell signature revealed that specific markers of disease activity and treatment used were correlated to individual cell populations for AM and JDM. This confirmed the findings from the previous figures. In particular an increase in CRP showed a positive correlation to the Th17 and Tfreg T cell populations, and a decrease of the non-classical monocyte populations from the AM group. When the MITAX score increased so did the BM3-4 B cell population, but the CD8+ CM T cell population decreased from the AM group (***Figure IV.12A*** *and* ***Table IV.6***). For patients with JDM an increased CK was linked to a decrease in CD27+ve B cells, the MITAX positively correlated to an increase of the BM2 transitional B cell population, and an

increase in the MMT8 score was associated with an increased CD8+CM and a decreased Tfreg T cell population (***Figure IV.12B*** *and* ***Table IV.6***). When the medications were correlated to the cell populations, this highlighted that some of the previous observations may be due to medication. In particular the use of prednisolone correlated to a decrease of the B cell and CD8+ CM populations in the AM group (***Figure IV.12C*** *and* ***Table IV.7***).

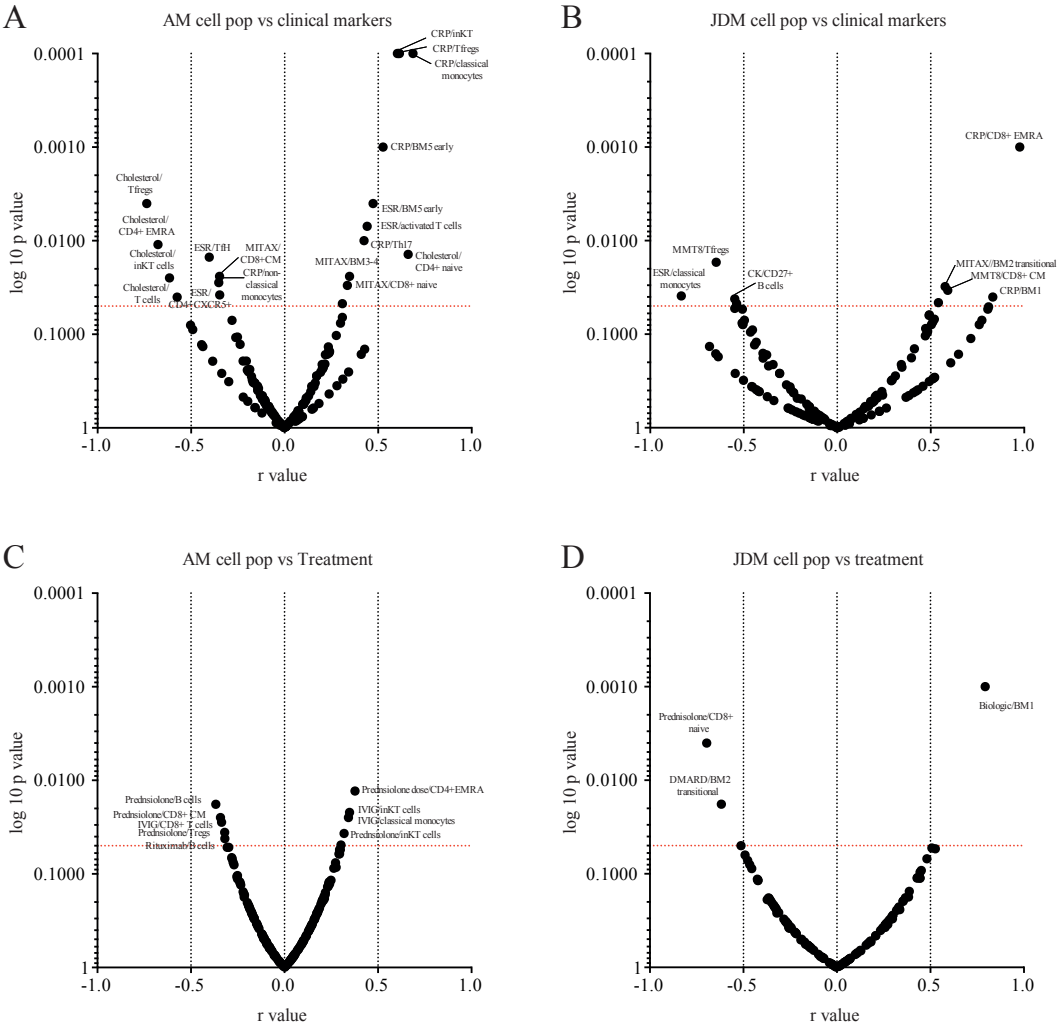

Figure IV.12 Volcano plots showing correlations between cell populations and clinical markers or treatment. *Volcano plots show statistical difference by p value and r value for directional change of correlation. The correlation between cell populations and clinical markers from* ***A)*** *AM (n=44) samples and* ***B)*** *JDM (n=15) samples. The correlation between cell populations and medication from* ***C)*** *AM samples and* ***D)*** *JDM samples. Pearson's correlation was conducted. Significance reached p≤0.05 (dotted red line).*

Table IV.6 Identified cell populations that correlate with myositis clinical markers

Myositis clinical markers	Positive correlation	Negative correlation
AM:		
CRP	iNKT, Tfregs, classical monocytes, BM5 early, Th17	Non-classical monocytes
ESR	BM5 early, activated T cells	TfH, CD4+CXCR5+
Cholesterol	CD4+ naive	Tfregs, CD4+ EMRA, inKT, T cells
MITAX	BM3-4, CD8+ naive	CD8+ CM
JDM:		
CRP	CD8+ EMRA, BM1	None
ESR	None	Classical monocytes
CK	None	CD27+ B cells
MITAX	BM2 transitional	None
MMT8	CD8+ CM	Tfregs

Table IV.7 Identified cell populations that correlate with treatment

Treatment	Positive correlation	Negative correlation
AM:		
Prednisolone	iNKT cells	B cells, CD8+ CM, Tregs
Prednisolone dose	CD4+ EMRA	None
IVIG	iNKT cells, classical monocytes	CD8+ T cells
Rituximab	B cells	None
JDM:		
Prednisolone	None	CD8+ naive
DMARDs	None	BM2 transitional
Biologics	BM1	None

Activated immune cells and IL-6 signature in AM

To assess whether the correlation between disease activity scores were matched by immune cell activation the expression of IL-6 and CD69 in immune cell subsets were compared between sample groups, AM, JDM, AHC and THC. ***Figure IV.13*** shows clear differences in the immune cell signature expression of IL-6 and CD69 between

disease and healthy individuals in the adult comparison. IL-6 was measured as it was a pro-inflammatory cytokine that has been detected at high levels in the serum and muscle of IIM and has been linked to active disease (Bilgic et al., 2009, Yang et al., 2013, Lundberg et al., 1997). There was an increased expression of IL-6 from monocytes, B cells and CD8+ T cells when AM was compared to AHC group, this was not observed in the JDM and THC comparisons (***Figure IV.14A*** *and* ***B)***. However, there was an increased expression of IL-6 from the BM2 transitional B cell population when JDM was compared to THC (***Figure IV.14B)***. Similarly, the AM group had a pan increased CD69 expression across all cell types when compared to AHC, but there were no observed differences between JDM and THC apart from a decreased expression from classical monocytes (***Figure IV.14C*** *and* ***D)***.

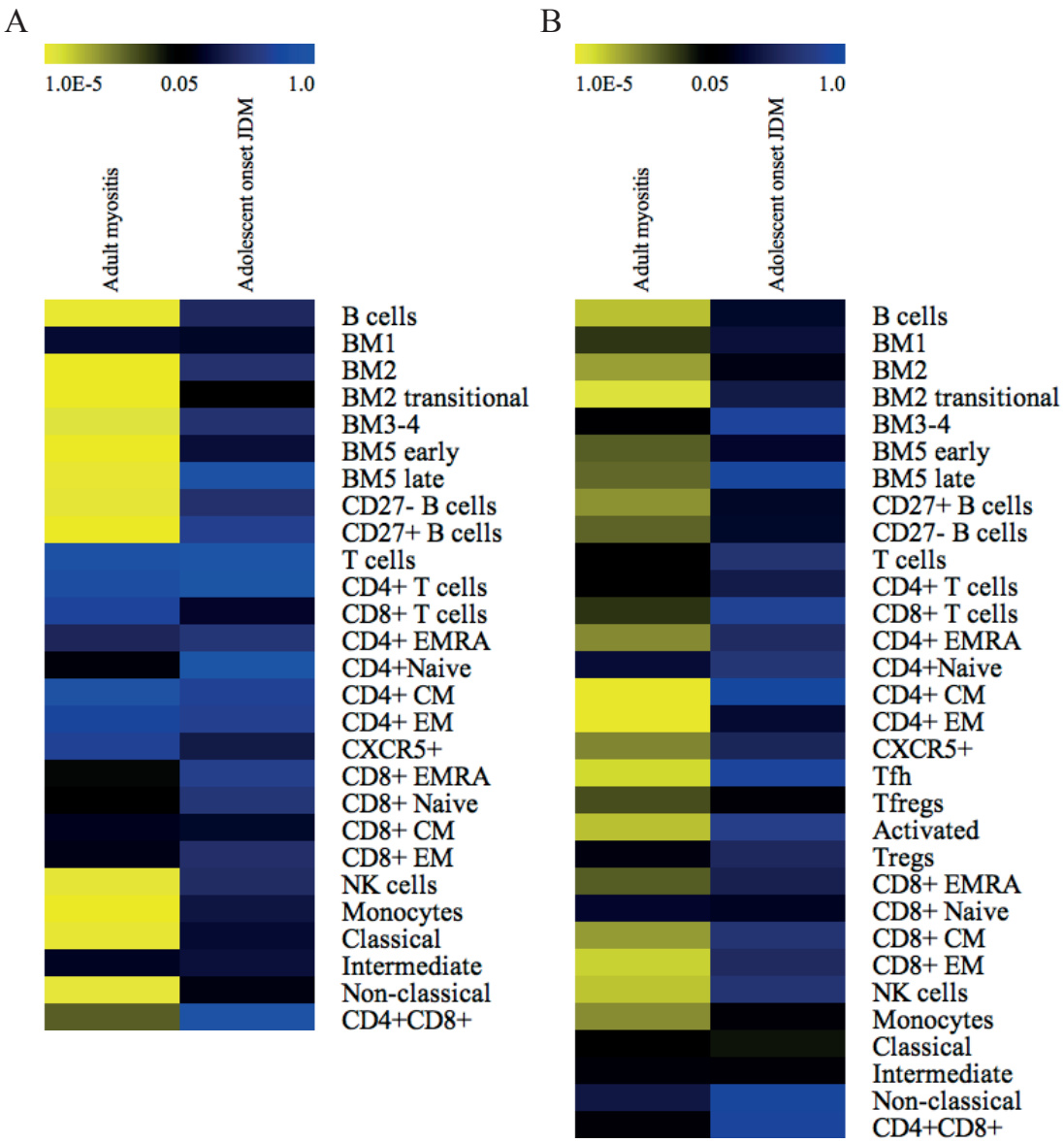

Figure IV.13 Heat map identifying significant differences in cell populations expression of IL-6 and CD69, a comparison of IIM to healthy samples. *The expression of* ***A)*** *IL-6 and* ***B)*** *CD69 from PBMC populations were measured by flow cytometry from 44 adult myositis (AM) patients, 25 adult healthy controls (AHC), 15 adolescent-onset juvenile dermatomyositis (JDM) patients and 15 teenage healthy controls (THC). This heat map demonstrates the statistical difference between each cell population by comparing the mean of each group of samples; AM vs. AHC, and JDM vs. THC. A student t-test calculated the p-values. Black to yellow - $p \leq 0.05$. Blue to black - $p \geq 0.05$.*

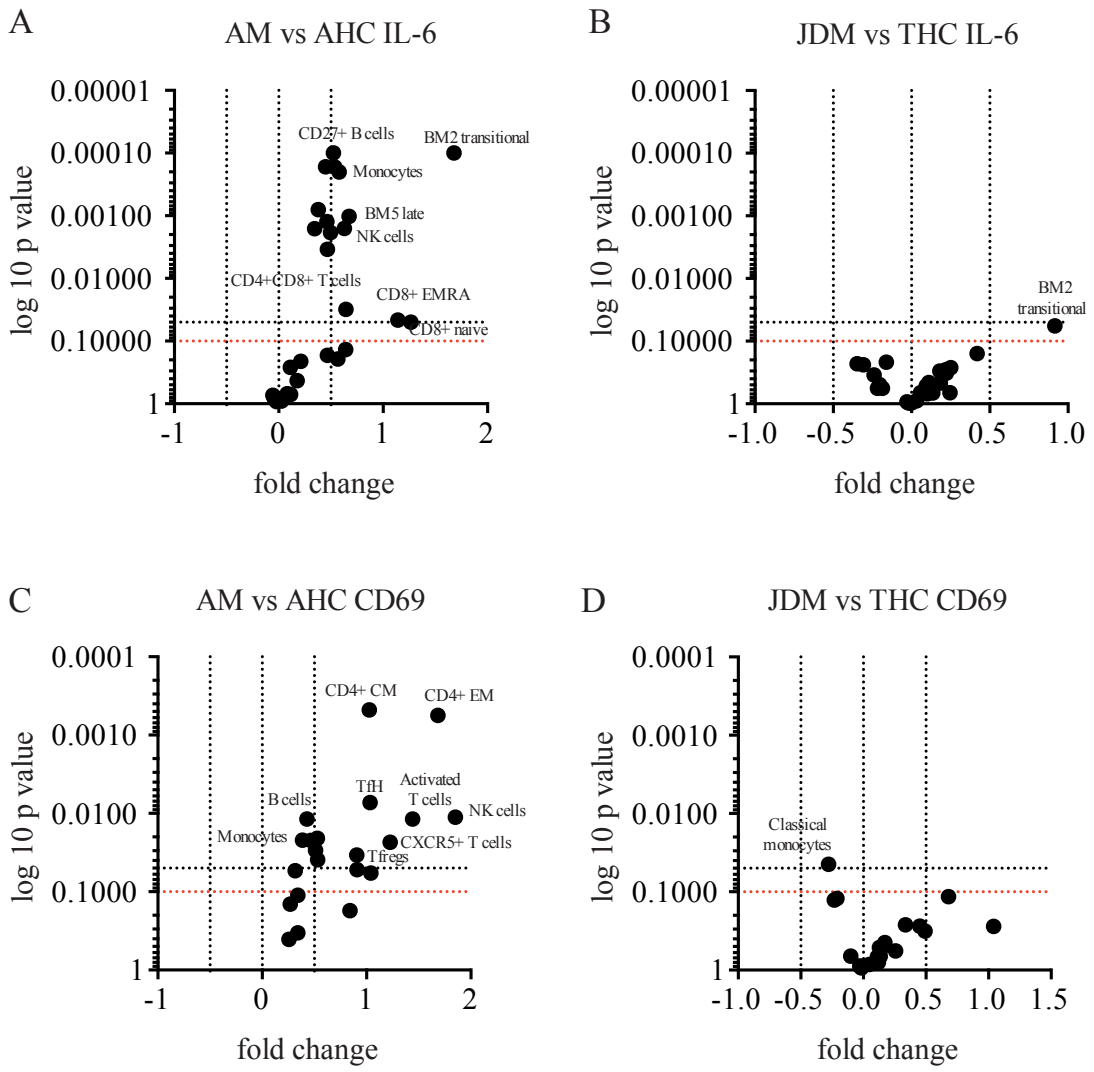

Figure IV.14 Volcano plots identifying significant differences and fold change of cell population expression of IL-6 and CD69, a comparison of IIM to healthy samples*. Volcano plots represent the fold change and p value for each cell populations expression of IL-6 (**A** and **B**) and CD69 (**C** and **D**) when sample groups were compared. **A)** AM vs. AHC (IL-6 expression), **B)** JDM vs. THC (IL-6 expression), **C)** AM vs. AHC (CD69 expression), **D)** JDM vs. THC (CD69 expression). The p values were calculated by one-way ANOVA. All p-values represent adjusted p-value calculated by Tukey's multiple comparison. Stringent significance p≤0.05 (black dotted line). Adjusted significance for small sample size p≤0.1 (red dotted line).*

The IL-6 signature unique to ADM

The IL-6 signature appeared to be strongest from B cells and monocytes. When the AM group was sub-divided into the IIM sub-groups, ADM, APM, ADM with cancer, ADM with overlap and APM with overlap, it was clear that this IL-6 signature was

sub-group specific. When ADM was compared to the AHC group the B cell and monocyte sub-population expression of IL-6 was increased *(**Figure IV.15A**)*. These differences were lost in the comparison between APM and AHC *(**Figure IV.15B**)*. When ADM with cancer was compared to AHC, the positive increase of IL-6 expression was from T cells *(**Figure IV.15C**)*. The signature of an increased B cell expression of IL-6 reappeared when ADM with overlap was compared to AHC *(**Figure IV.15D**)*. Then disappeared again for APM with overlap compared to AHC *(**Figure IV.15E**)*. The comparison of ADM compared to the JDM group showed that there was an increased expression of IL-6 from CD8+ T cell subsets and B cell subsets *(**Figure IV.15F**)*. The final comparison of ADM compared to the APM group showed that there was an increased expression of IL-6 from memory B cells *(**Figure IV.15G**)*.

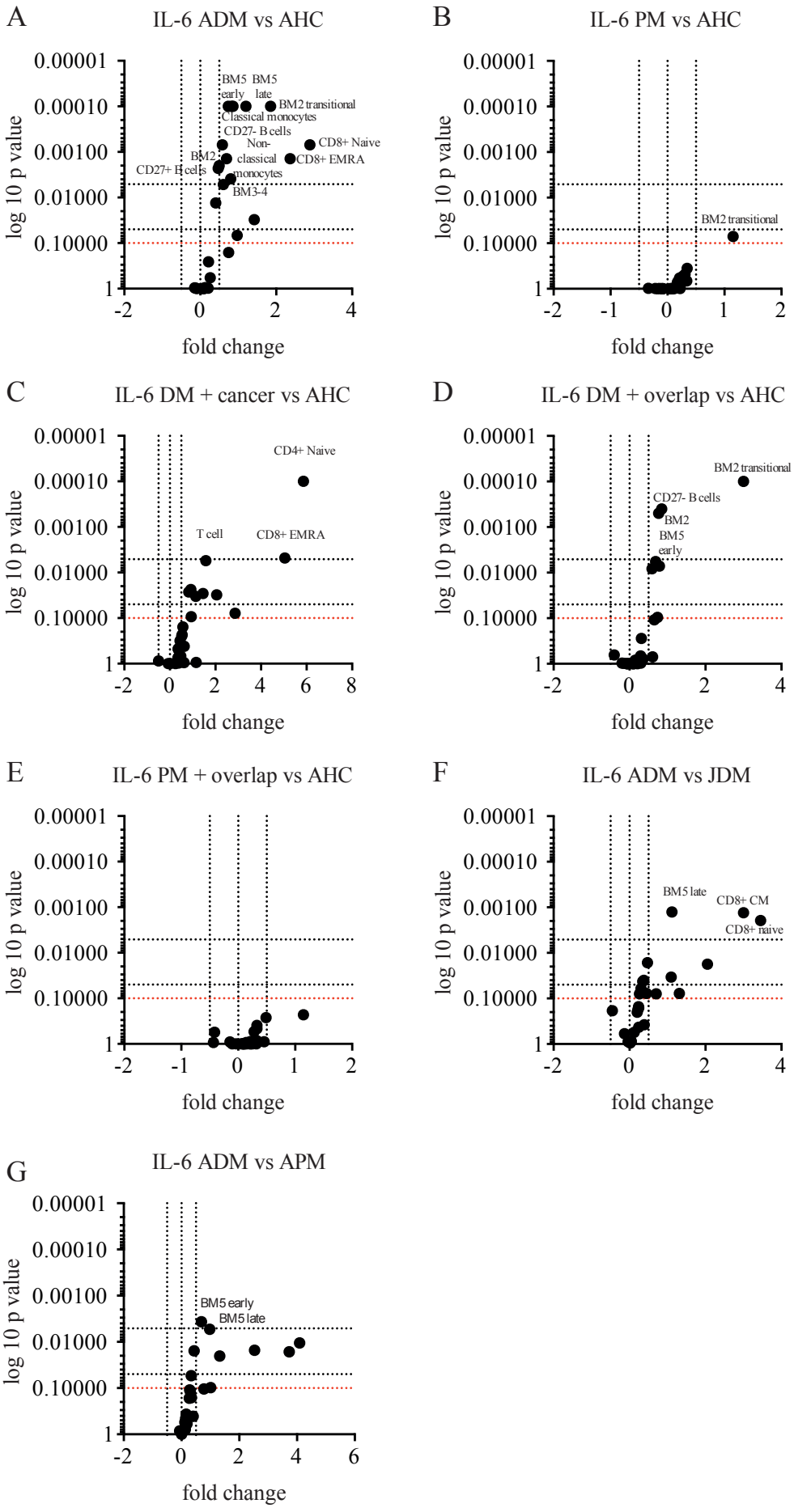
A
IL-6 ADM vs AHC
log 10 p value
fold change
BM5 early
BM5 late
BM2 transitional
Classical monocytes
CD27- B cells
Non-classical monocytes
CD8+ Naive
CD8+ EMRA
BM2
CD27+ B cells
BM3-4
B
IL-6 PM vs AHC
BM2 transitional
C
IL-6 DM + cancer vs AHC
CD4+ Naive
T cell
CD8+ EMRA
D
IL-6 DM + overlap vs AHC
BM2 transitional
CD27- B cells
BM2
BM5 early
E
IL-6 PM + overlap vs AHC
F
IL-6 ADM vs JDM
BM5 late
CD8+ CM
CD8+ naive
G
IL-6 ADM vs APM
BM5 early
BM5 late

Figure IV.15 Volcano plots identifying significant differences and fold change of cell population expression of IL-6, a comparison of AM disease subgroups to AHC and JDM samples. *Volcano plots represent the fold change and p value for each cell populations expression of IL-6 when AM sample disease sub-groups were compared with AHC and JDM samples.* ***A)*** *ADM (n=19) compared to AHC (n=25) (IL-6 expression),* ***B)*** *APM (n=9) compared to THC (IL-6 expression),* ***C)*** *ADM + cancer (n=4) compared to AHC (IL-6 expression),* ***D)*** *ADM+ overlap (n=7) compared to AHC (IL-6 expression),* ***E)*** *PM + overlap (n=5) compared to AHC (IL-6 expression),* ***F)*** *ADM compared to JDM (n=15) (IL-6 expression), and* ***G)*** *ADM compared to APM (IL-6 expression). The p values were calculated by multiple t-test, significance p≤ 0.05 (bottom dotted black line). Multiple comparison was calculated by the Holm-Sidak method, therefore adjusted p value significance p≤0.005116 (top dotted black line). Adjusted significance for small sample size p≤0.1 (red dotted line).*

The expression of IL-6 and CD69 from each cell population was correlated to clinical markers. Positive correlations were observed between CRP and IL-6 production by T cell sub-populations including; total T cells, CD4+ naïve and EMRA (***Figure IV.16A***). Only Il-6 production in BM2 transitional cells showed a positive correlation with CRP and ESR from the B cell IL-6 expression signature. The JDM group had only four significant correlations each different clinical markers and cell populations (***Figure IV.16B***). Again, from the AM group the CRP and ESR markers correlated with a T cell CD69 expression signature (***Figure IV.16C***). The JDM group had a wider spectrum of cell type CD69 expression correlation to clinical markers including; CD27-/+ve to CRP (***Figure IV.16D***).

Immune cell activation assessed by expression of IL-6 and CD69 also appeared to be influenced by treatment (***Figure IV.17*** and ***Table IV.8***). The analysis of the AM group showed that treatment with prednisolone correlated to an increased IL-6 expression from total CD4+ naïve and total T cell populations. This was similar for IVIG with additional populations including; BM2 transitional and CD4+ EMRA T cells. In contrast, treatment with cyclosporine and hydroxychloroquine correlated to a decreased IL-6 expression from CD8+ cells (***Figure IV.17A***). There was no

significant correlation between treatments and cellular expression of IL-6 from the JDM group (***Figure IV.17B***). The use of prednisolone and an increasing dose positively correlated to an increased T cell CD69 expression in the AM group. Conversely, the use of hydroxychloroquine and MMF correlated to a decreased expression of CD69 from B cells and monocytes (***Figure IV.17C***). In the JDM group, treatment with prednisolone and biologics correlated with an increased expression of CD69 from B cells and CXCR5+ T cells (***Figure IV.17D***).

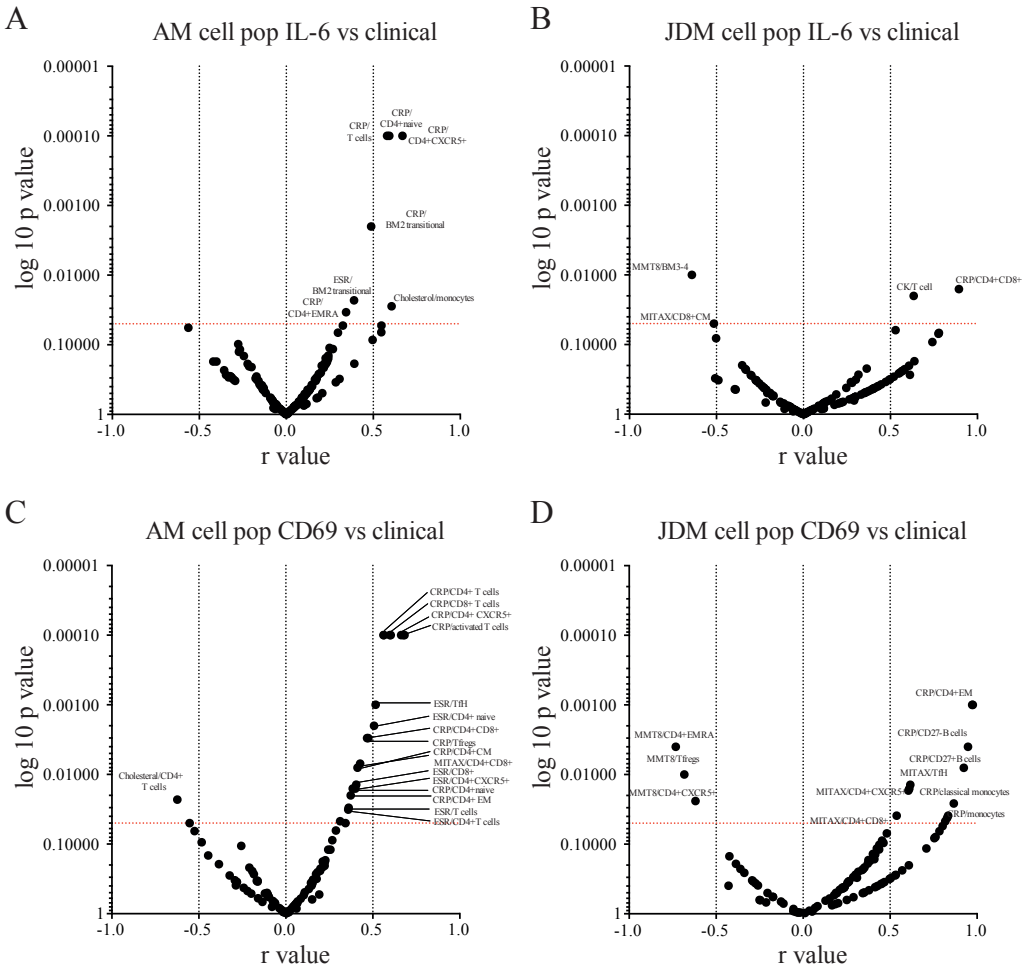

Figure IV.16 Volcano plots showing correlations between myositis clinical markers and cell population expression of IL-6 and CD69*. Volcano plots show statistical difference by p value and r value for directional change of correlation. The correlation between cell population expression of IL-6 and myositis clinical markers from **A)** AM samples and **B)** JDM samples. The correlation between cell population expression of CD69 and myositis clinical markers from **C)** AM samples and **D)** JDM samples. Pearson's correlation was conducted. Significance reached $p \leq 0.05$ (dotted red line).*

Table IV.8 – Summary of positive and negative correlations of myositis clinical markers to cell population expression of IL-6 or CD69

Myositis clinical markers	**Positively correlated**	**Negatively correlated**
AM (IL-6):		
CRP	CD4+ naïve, T cells, CXCR5+, BM2 transitional, CD4+ EMRA	None
ESR	BM2 transitional	None
Cholesterol	Monocytes	None
AM (CD69):		
CRP	CD4+, CD8+, CXCR5+, activated T cells, CD4+CD8+, Tfregs, CD4+ CM, CD4+ naïve, CD4+ EM	None
ESR	TfH, CD4+ naïve, CD4+, CD8+, CXCR5+, T cells	None
Cholesterol	CD4+ T cells	None
MITAX	CD4+CD8+	None
JDM (IL-6):		
CK	T cell	None
CRP	CD4+CD8+	None
MITAX	None	CD8+ CM
MMT8	None	BM3-4
JDM (CD69):		
CRP	CD4+ EM, CD27- B cells, CD27+ B cells, classical, monocytes	None
MITAX	CXCR5+, CD4+CD8+, TfH	None
MMT8	None	CD4+ EMRA, Tfregs, CXCR5+

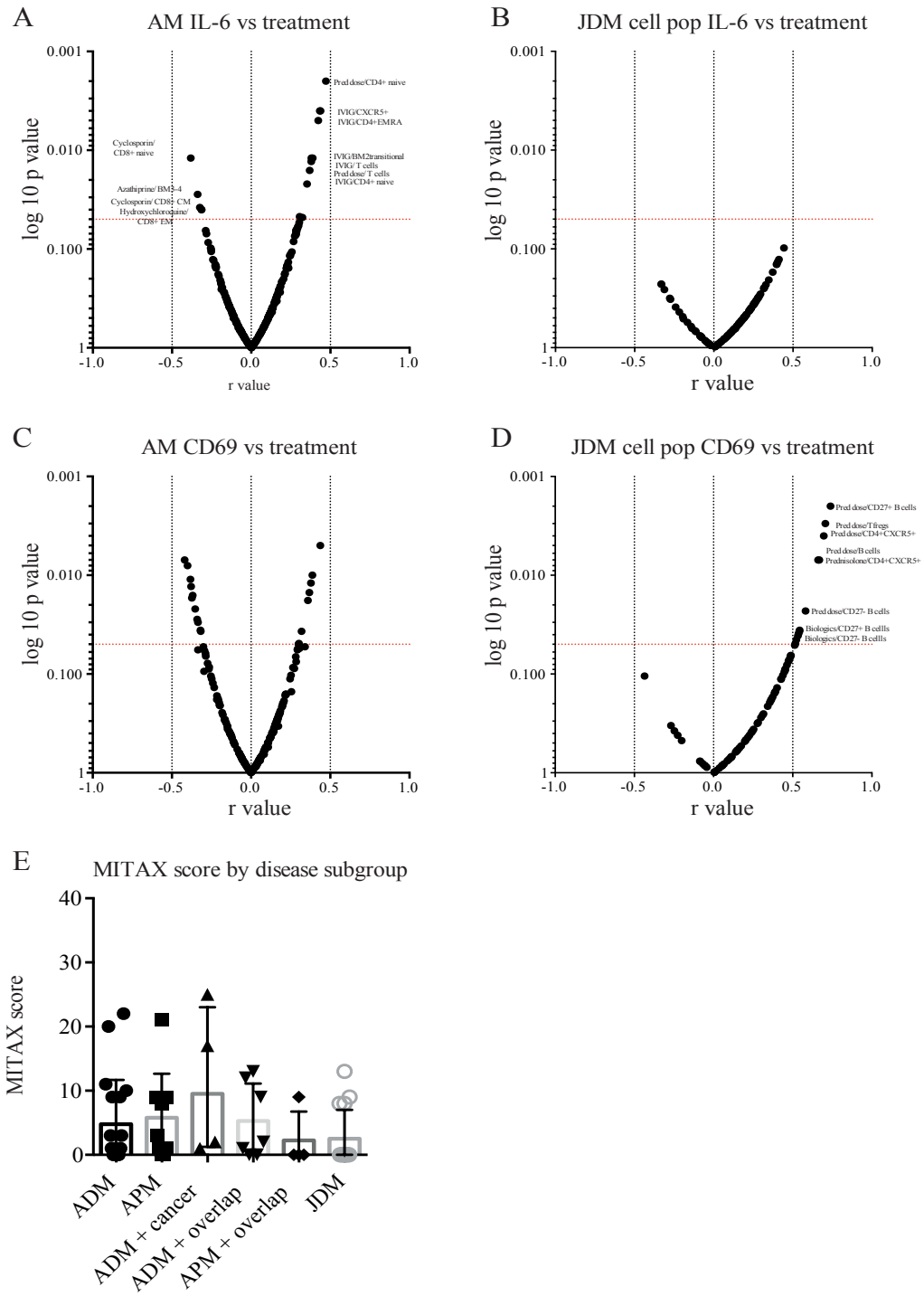

Figure IV.17 Volcano plots showing correlations between treatments and cell population expression of IL-6 and CD69. *Volcano plots show statistical difference by p value and r value for directional change of correlation. The correlation between cell population expression of IL-6 and treatment from* ***A)*** *AM samples and* ***B)*** *JDM samples. The correlation between cell population expression of CD69 and treatment from* ***C)*** *AM samples and* ***D)*** *JDM samples. Pearson's correlation was conducted. Significance reached p≤0.05 (dotted red line).* ***E)*** *Scatter plot showing MITAX scores for each IIM sample split into subgroups; ADM, APM, ADM + cancer, ADM + overlap, APM + overlap and JDM. Represented mean average with standard deviation.*

Table IV.9 Summary of positive and negative correlations of treatments to cell population expression of IL-6 or CD69

Treatment	Positively correlated	Negatively correlated
AM (IL-6):		
Prednisolone dose	CD4+ naïve, T cells	None
Azathioprine	None	BM3-4
IVIG	CXCR5+, CD4+ EMRA, CD4+ naive	None
Cyclosporin	None	CD8+naïve, CD8+ CM
AM (CD69):		
Prednisolone dose	CD4+CD8+, T cells, CD8+, CD4+ EM	None
Prednisolone	CD8+	None
Azathioprine	None	Tregs,
Hydroxychloriquine	None	Non-classical, TfH, CD27- B cells
MMF	None	Classical, B cells, non-classical, CD27- B cells
JDM (CD69):		
Prednisolone dose	Tfregs, CXCR5+, B cells, CD27- B cells	None
Prednisolone	CD27+ B cells, CXCR5+	None
Biologics	CD27+ B cells, CD27- B cells	None

Th17 cells; an expanded population in ADM that correlated to an expansion of activated T cells

Increased expression of the Th17 population was identified in the AM group, specifically in the ADM sub-group, compared to AHC and JDM. AM patients that were in remission on treatment, had the strongest association with an increased Th17 population. Equally the auto-antibody ARD overlap (anti-Ro, anti-PmSCL and anti-RNP) group and the group expressing multiple auto-antibodies demonstrated an increased Th17 population. Furthermore, a significant positive correlation between serum CRP levels and Th17 expression was identified in AM patients ***(Figure IV.18A)***. The expansion of the Treg, iNKT and CD4+ EMRA T cell populations correlated with the increased expression of Th17 cells ***(Figure IV.18B)***. Finally, there

was a positive correlation between Th17 expansion and the expression of CD69 from T cell subsets and IL-6 from BM5 early B cells in Am patients *(**Figure IV.18C**)*. In summary, the expansion of Th17 expression associated with the ADM sub-group and aligned with an expansion of activated T cells.

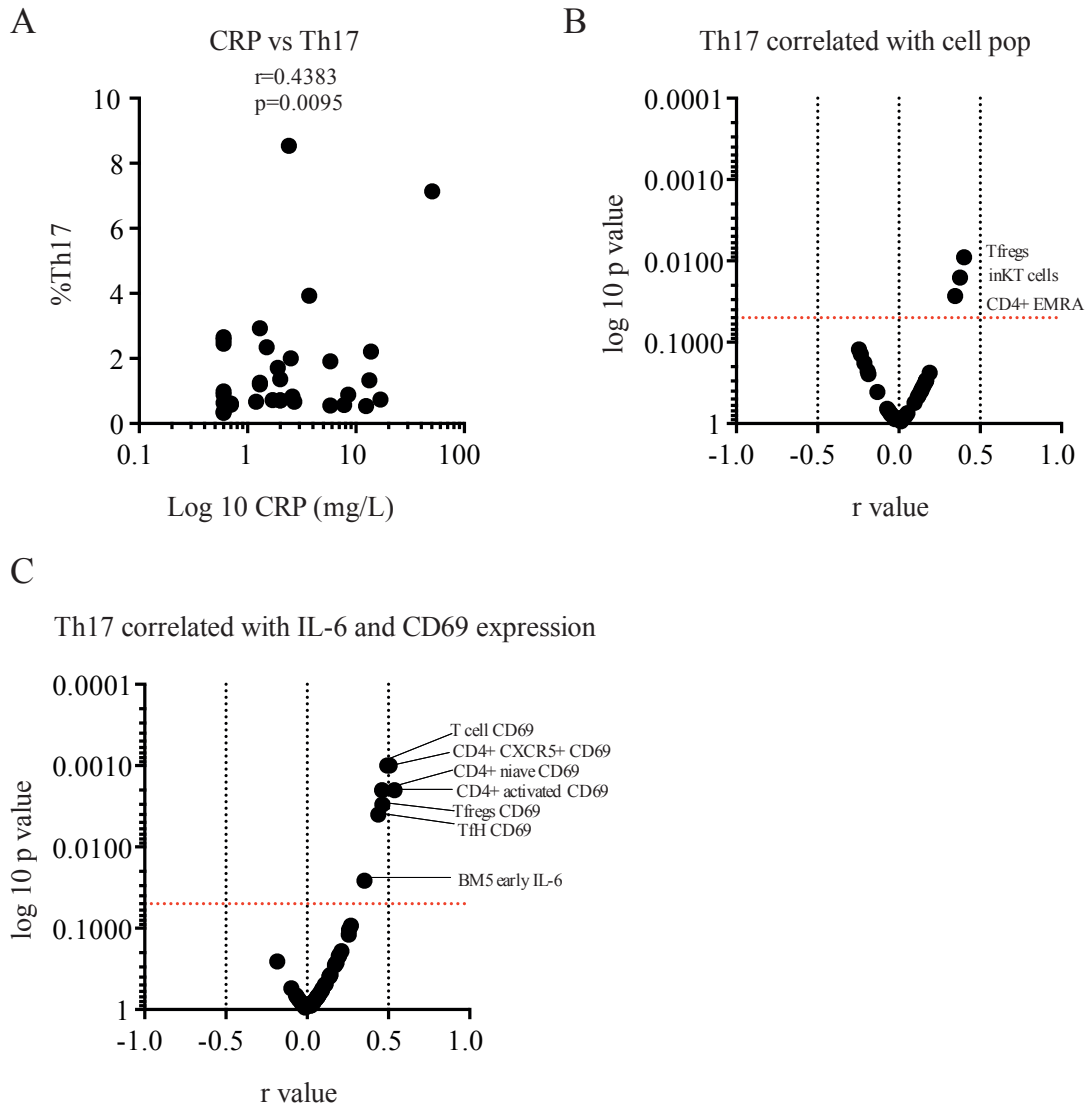

Figure IV.18 The Th17 population correlated to CRP, other PBMC populations, and cell populations expressing CD69 and IL-6*. The Th17 population was expanded in the AM population compared to JDM and AHC samples.* ***A)*** *A scatter graph showing that CRP positively correlated to Th17 frequency.* ***B)*** *A volcano plot showing all PBMC population frequencies correlation to Th17 frequency.* ***C)*** *A volcano plot showing all PBMC population expression of CD69 and IL-6 correlation to Th17 frequency. Pearson's correlation was conducted. Significance reached $p \leq 0.05$ (dotted red line).*

DISCUSSION

These results represent a novel in-depth immunophenotyping of patients with myositis. This was conducted to record differences in PBMC populations present in these patients. Previous studies have highlighted changes in total populations of monocytes, T and B lymphocytes, but to my knowledge none have correlated changes across such a large number of different lymphocyte sub-populations (O'Gorman et al., 1995, Behan et al., 1987). The analyses were conducted across multiple levels of comparison to observe changes between ages, disease and healthy, disease sub-groups, auto-antibody status, changes in disease activity and with different treatment. Activation status and the expression of the pro-inflammatory cytokine IL-6 was also measured to characterise the behaviour of these cells within the disease states.

The adult and juvenile patients were recruited from rheumatology out-patient clinics and in-patient wards at UCLH. There was no known selection bias for the patients with dermatomyositis or polymyositis, therefore the numbers in this cohort were a fair representation of the overall cohort seen at UCLH. Dermatomyositis has been identified as the most frequently diagnosed IIM in both adult and juvenile groups, with polymyositis more commonly diagnosed in adults. These findings were reflected in the cohorts used in this study. The results also identified a trend for a difference in sex demographics between IIM subgroups; both DM and PM groups had more females than males, but PM seemed to have the highest occurrence in females. Previous studies have identified that there was a higher incidence of DM and PM in females (Mastaglia and Phillips, 2002). The inflammatory idiopathic myopathies have been reported to occur in all ethnic groups (Mantegazza R, 2000-2013, Dalakas and Hohlfeld, 2003). Immune-response genes have been identified in genetically defined

ethnic groups which may predispose certain populations to polymyositis or dermatomyositis (Reed, 2001, Shamim et al., 2002). Equally, studies have reported a higher incidence of the IIMs in black men and women compared to white Caucasian's (Oddis et al., 1990, Medsger et al., 1970). The JDM and AM cohorts used in this study confirmed the spread of ethnicities previously observed. The small sample size and the restriction of the cohort recruitment to one hospital, UCLH, impacted the ethnic distribution, especially within the JDM cohort.

Generally, all IIM patients are treated with prednisolone on diagnosis (Dalakas, 2015). If they are responsive then disease modifying anti-rheumatic drugs (DMARDs) are introduced including; methotrexate, azathioprine, MMF or cyclosporine (Ernste and Reed, 2013). When ILD is also diagnosed cyclophosphamide or tacrolimus can be given (Oddis et al., 1999, Dalakas, 2010). Intravenous immunoglobulin (IVIG) is often considered in severe and rapidly progressive disease. When the disease is irresponsive to the above treatments, biologics approved for use in more commonly diagnosed immune conditions, can be introduced as experimental therapies. These drugs include; anti-CD20 (rituximab), anti-IL-6 (tocilizumab) and anti-interleukin-1 receptor (anakinra) (Oddis et al., 2013, Narazaki et al., 2011, Zong et al., 2014). The ADM, APM and JDM cohorts in this study demonstrated a difference in their use of treatments. Disease activity was highest in the AM compared to JDM, which may reflect the broader spectrum of DMARDs used. However, the patients with the most severe disease from the JDM cohort had received treatment with the TNF inhibitors, infliximab and adalimumab. These therapies were not used in the adult cohort. Infliximab was shown to be ineffective and may worsen disease in adults (Dastmalchi

et al., 2008). The AM cohort could have a higher rate of ILD which would reflect the use of tacrolimus (data not reported).

The MSA are detected in both DM and PM, but there is a wider range found in DM. The anti-Jo1 and anti-SRP autoantibodies are more common in PM. However, anti-Mi2, anti-TIF1γ, and anti-NXP2 are rarely detected in PM but more commonly in DM and JDM (Ghirardello et al., 2013). The AM cohort for this study displayed comparable prevalence of MSA's to that previously reported. In particular, PM patients were only positive for anti-Jo1 and anti-SRP. Unfortunately, accurate data was not available for the JDM cohort.

Ageing is a complex process that impacts immunosenescence. T cells have been identified to be particular vulnerable to the effects of ageing. This is thought to be attributed to age-induced thymic atrophy and the decreased output of naïve T cells (Gruver et al., 2007). The comparison of the AHC to THC samples identified decreased naïve T cell populations in the older control group. This result implied that this was an effect of ageing. B cells have also been shown to decrease with age, the BM2 population proportionally makes up the highest sub-population of the B cells and therefore would be relatively less the older the population (Morbach et al., 2010). The differences seen with the monocyte subset populations do not relate to the literature, as previous studies have found that CD16+ monocytes increased with age and proportionally the CD16- monocytes decreased (Nyugen et al., 2010). An expansion of the B cell population in active PM and DM has been identified, although this was not apparent in the cohorts for this study (Ishii et al., 2008, Wang et al., 2012). However, there was an apparent change in the proportion of CD27ve-/+ B

cells. All the patients from this study had received prednisolone and some methotrexate, these treatments may impact the B cell expression of CD27. Early studies of the use of prednisolone in healthy adults and in SLE patients showed that the frequency of B cells reduced in a time and dose dependant manner (Yu et al., 1974, Chatham and Kimberly, 2001). A recent study showed that both B cells and the immature B cell subset were reduced in frequency in JIA patients treated with methotrexate alone in comparison to patients who did not receive treatment (Glaesener et al., 2014). There have been reports of decreased CD4+ and CD8+ populations from active ADM samples when compared to healthy controls, but there has been no data on JDM samples that reported similar decreased CD8+ and increased CD4+ T cell populations (Wang et al., 2012). CD8+ CM T cells were decreased in both adult and juvenile disease in comparison to healthy controls, previous studies that have investigated the effects of immunosuppressive agents on this lymphocyte population have shown that they remained in a steady state (Meyer et al., 2015).

A particular aim was to report unique immune signatures of the peripheral blood for each subtype of AM. The increased population of Th17 cells was specific to ADM and ADM with overlap. In addition, this signature was observed in patients with the CTD overlap (anti-Ro, anti-PmSCL and anti-RNP) group of autoantibodies and also those patients that were in remission on treatment. Th17 cells were recognised as CD4 expressing T-helper cells that selectively expressed IL-17 over interferon (IFN)- γ (Tournadre and Miossec, 2012). The differentiation of these cells is dependent on IL-6, IL-21, IL-23 and transforming-growth factor (TGF)-β (Miossec et al., 2009). The IL-23-Th17 pathway has been extensively explored and reported to play a critical role in the induction and maintenance of chronic inflammation and autoimmunity,

specifically in RA (Miossec, 2017). Th17 cells have been found in the muscle tissue from both DM and PM patients (Chevrel et al., 2003, Page et al., 2004, Tournadre et al., 2009). IL-17 has a central role in the migration and differentiation of mononuclear cells, it does this by inducing IL-6 and β chemokines. Chevrel et al showed that IL-17 in conjunction with IL-1 and TNF-α increased the expression of MHC class I on muscle cells (Chevrel et al., 2003). This is relevant in the context of IIM as the overexpression of MHC class I is a common trait (Rowe et al., 1981, Nagaraju et al., 2005). An inflammatory loop in inflamed muscles exists; this is sustained by interactions between IL-17, IL-1, TNF-α and toll-like receptor (TLR) 3 expressed by muscle. The induction of IL-6 by IL-17 may also be involved in the dysfunctional repair of inflamed muscle (Tournadre and Miossec, 2012).

There are multiple biologic drugs that target the IL-17 pathway. The targets include; Il-17, IL-17A, IL-17R, IL17RA and the potential for bispecific in combination with TNF-α. Some of these drugs, secukinumab, ixekizumab, and brodalumab, have been approved and are in phase 3 trials for the treatment of psoriasis (Langley et al., 2014, Gordon et al., 2016, Lebwohl et al., 2015). There were no previous reports of an expanded Th17 population in the peripheral blood of IIM patients, or a correlation between the periphery and tissue. The identification in muscle and exploration of the pathological mechanisms has prompted the potential for using IL-17 targeting agent in the treatment of IIM (Tournadre and Miossec, 2012). The preliminary findings from this study suggest that ADM was more an IL-17 driven disease than APM or JDM. This heterogeneity would imply that not all IIM patients would be responsive to an IL-17 targeting drug. Extrapolating from these results, it would be important to establish a correlation between the proportion of Th17 cells in the periphery and

inflamed tissue at diagnosis and to monitor the change over time on treatment with disease progression.

In addition to an expanded Th17 population specifically seen in ADM there was also an expansion of T regulatory (Treg) cells. There was a positive correlation identified between these T cell populations. FOXP3+ Tregs have been identified as part of the infiltrating immune cell mileau detected in muscle biopsies, but the main T cells were CD4+/CD8+ memory and Th1 (Malmstrom et al., 2012). The Treg population has been noted to reduce with glucocorticoid therapy, where CD4+CD28null T cells are persistent on biopsy (Loell, 2011). A recent study identified that Tregs directly contributed to muscle damage in infection induced myositis, they were thought to promote macrophage homeostatic dysfunction (Jin et al., 2017). The expansion of Tregs that was noted reflect a reduction in the prednisolone dose, though there was no noted correlation. There was no correlation between the Treg population and disease activity either.

Conversely there was a decrease of the CD8+ central memory (CM) T cell population in AM and JDM when compared to the age-matched healthy control samples. The decrease was most obvious in the APM group. The analysis of muscle biopsies from both ADM and APM patients has identified a CD8+ cytotoxic T cell phenotype from APM samples, whereas ADM samples portrayed a CD4+ driven inflammation (Benveniste et al., 2004, Amemiya et al., 2000). A study that analysed the immune infiltrate from two JDM patient biopsies revealed, an oligoclonal expansion of CD8+ T cells surrounding inflamed vessels that expressed a characteristic phenotype of memory/effector T cells with killer functions (Mizuno et al., 2004). The decrease of

the CD8+CM cell population identified from the AM and JDM PBMC samples, could be a reflection that these cells were tissue residing in disease and therefore there were lower numbers than seen in healthy controls in the periphery. In both AM and JDM, the patients with the most active disease had the lowest circulating peripheral population of these cells, suggesting that the recruitment to tissue pathway was switched off with suppression of disease activity. To investigate this hypothesis further, it would be important to correlate the population of tissue residing CD8+CM to the PBMC population at time of biopsy. From there, the mechanism of CD8+CM migration to tissue, such as complement activation, could be delineated (Dalakas and Hohlfeld, 2003).

B cells have also been detected within the inflamed muscle of AM and JDM patients, suggesting that B cells exert a pathological function on muscles (Shah et al., 2013, Greenberg et al., 2005a). A strong autoantibody profile can be detected in most IIM patients implying one function of B cells in this group of diseases is the production of autoantibodies (Nistala and Wedderburn, 2013). My results provided an insight into the phenotype and function of B cells within the peripheral blood of both AM and JDM patients. I found that the B cell compartment was dysregulated in the peripheral blood; the AM patients had a lower proportion of CD27- and BM5 early (IgD-CD38+) B cells than JDM and AHC groups, and the JDM group had an increased BM2 transitional ($IgD^{hi}CD38^{hi}$) population. However, studies in SLE have identified that the memory B cell populations, both CD27+ and -, were expanded and immunosuppressive resistant (Dorner et al., 2011). The decrease of the CD27+ and BM5 B cell populations was most evident in the AM patients expressing anti-synthetase (anti-Jo-1 and anti-Pl-12) autoantibodies and those that were classified as

in remission off treatment. Interestingly, the results from chapter III, which detailed an in-depth investigation of B cell populations in JDM from pre- and on-treatment patients, showed that the memory B cell population was lowest in pre-treatment patients. The low memory B cell population identified in IIM may be a coincidental non-pathogenic finding which better reflects changes in related populations. Conversely in JDM, the BM2 transitional population positively correlated to an increase of disease activity (MITAX score). This result was comparable to those reported in chapter III, which suggested a pathological role for immature/BM2 transitional B cells.

One way to measure the pathogenic potential of immune cells is to examine the expression of pro-inflammatory cytokines. Interleukin (IL) 6 is a pro-inflammatory cytokine that has been detected at high levels in the serum of IIM and other autoimmune diseases and has been linked to active disease (Bilgic et al., 2009). This cytokine has also been detected in the muscle (Yang et al., 2013, Salomonsson and Lundberg, 2006). Suppression of IL-6 with prednisolone has also been shown to be dose dependant (de Kruif et al., 2007). A multi-centre pilot study at the University of Pittsburgh has begun recruitment to determine if the monoclonal antibody against the IL-6 receptor, tocilizumab, is an effective treatment for adult polymyositis and dermatomyositis. This study has been set up from the evidence that tocilizumab is an effective treatment in other rheumatological conditions, including RA and systemic JIA, and that serum levels of IL-6 significantly correlated with disease activity in both adult and juvenile DM (Okuda, 2008, Bilgic et al., 2009).

My data showed that the frequency of B cells, monocytes and CD8+ T cells expressing IL-6 was higher in AM compared to both JDM and adult healthy control samples. This trend was particularly clear in the ADM samples. The differences identified could be a reflection of disease activity; there were more active patients in the AM group compared to JDM. The use of prednisolone has been shown to suppress IL-6. Treatment of childhood primary nephrotic syndrome with prednisolone suppressed the levels of serum IL-6 in a steroid-responsive patient group (Yu and Zhang, 2005).The only noted IL-6 signature for the JDM group was an increased expression from BM2 transitional cells which were identified to be expanded and correlate with an increase in disease activity. However, there was no noted difference in disease activity between the ADM and APM disease groups, yet there was an IL-6 signature in uniquely the ADM patients. Equally, the expression of IL-6 did not correlate with disease activity or use of different therapeutic agents. These results would suggest that the IL-6 signature observed in ADM maybe ancillary to a pathological mechanism not yet identified. Without further exploration of this signature it is unclear whether IL-6 would be a useful therapeutic target in the context of IIM, and specifically ADM.

Not only was an IL-6 signature noted in the AM patients it was also observed that there was increased immune cell activation determined by the expression of CD69, a type II C-lectin membrane receptor (Gonzalez-Amaro et al., 2013). Previous studies have reported that CD69 had an important role in the activation of leukocytes that exert a pro-inflammatory effect (Sancho et al., 2005). However, more recently it has been identified that CD69 employs a complex immune-regulatory role in humans and animal models by the inhibition of Th17 differentiation and function (Martin et al.,

2010, Cruz-Adalia et al., 2010). In systemic sclerosis (SSc) an association was found in the skin between infiltrating Th17 cells, CD69+ leucocytes and enhanced synthesis of transforming growth factor (TGF)-β (Kalogerou et al., 2005, Radstake et al., 2009). The increased population of Th17 cells reported from the ADM group correlated to an increased expression of CD69 from Treg, iNKT and CD4+ EMRA T cells. These results support the evidence that CD69+ T cells may exert an immune-regulatory role in the context of ADM.

The immune cell signatures identified in this study would need further investigation to substantiate their accuracy and relevance in disease pathogenesis. My work was restricted by a small sample size for each disease group, and therefore was low-powered. Preferably each sub-group would have the same number of samples, similar time points since diagnosis and a cross-comparison between treatments. The IIMs are a very rare group of diseases and are heterogeneous in nature, specifically in their clinical presentation and expression of autoantibodies. Each confounder provided a new way to cross-compare the disease and identified new signatures. The main statistical methods used to analyse the comparisons were multiple *t* tests with Holm-Sidak method of correction or one-way ANOVA with a calculated adjusted p value by Tukey's multiple comparison test. Due to low levels of and a discrepancy in the sample size, the adjusted p value significance level was likely too stringent, but for consistency was applied throughout.

This study provided an insight into the peripheral immune cell signatures of IIM patients on treatment. To substantiate these data, it would be useful to observe changes in the signature over time, preferably from pre-treatment to remission off

treatment. Equally, to correlate the peripheral signature to that found in the muscle tissue immune cell milieu. A potential therapeutic target identified from this study is Th17 cells and thus IL-17, but this is likely to be confined to ADM patients. IL-6 may also be a possible target, but as the data showed no clinical correlation this would require further investigation.

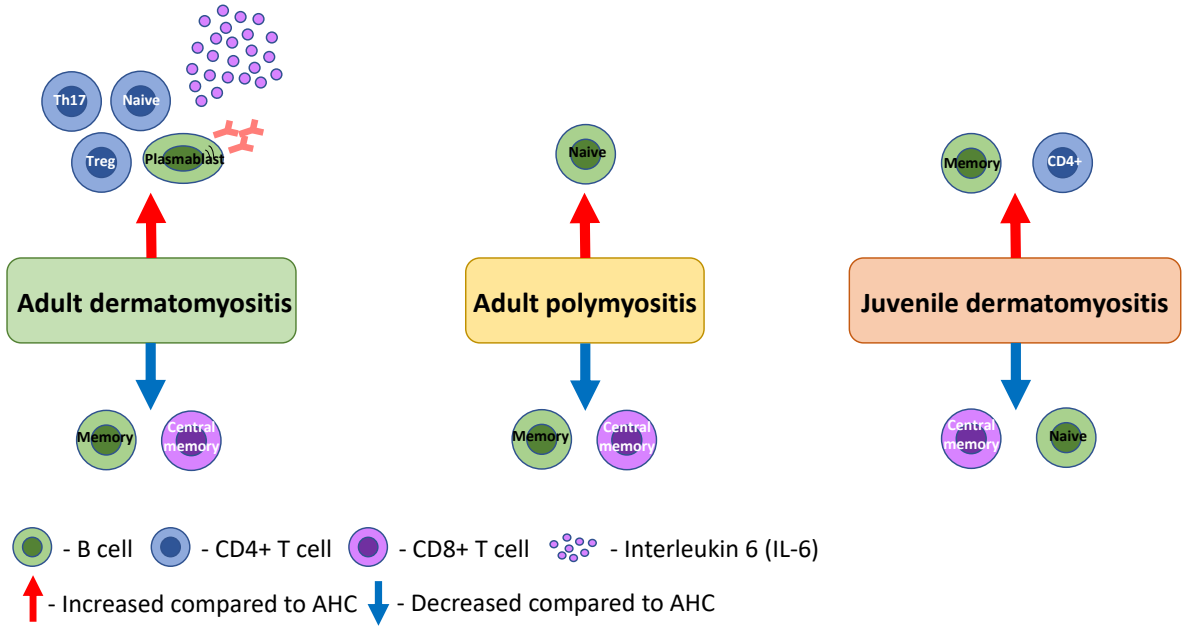

Figure IV.19 Different immune signatures in adult dermatomyositis, polymyositis and juvenile dermatomyositis*. ADM was characterised by an increase of CD4+ T cells including; Th17, naïve T cells and Tregs, but also plasmablasts and an increased cellular expression of IL-6. Common to both ADM and APM there was a decrease of memory B cells and central memory CD8+ T cells. This decrease in central memory CD8+ T cells was also noted in JDM.*

Chapter V

To investigate the effects of type I interferon on immune cell lipid membranes

Results (section 3)

INTRODUCTION

Type I interferons constitute a large subgroup of interferon proteins involved in immune regulation. An up-regulation of the type I interferon signature has been described in autoimmune diseases, and in the myopathies correlates with disease activity (Bilgic et al., 2009). The type I IFN signature has been shown to be involved in the immunopathology of both juvenile and adult IIM, indicated by gene expression profiling of muscle tissue and peripheral blood. The signature has been confirmed by the detection of IFN producing cells, such as pDCs, in the muscle and skin tissue, and the presence of the IFN inducible protein, MxA, in muscle tissue (Lundberg and Helmers, 2010). This signature was also identified to be up-regulated in the JDM cohort RNA-sequencing data shown in Chapter III.

A study by Tisseverasinghe et al suggested that patients with DM and PM have a significantly increased risk of incurring a cardiovascular event (CV). They also showed that CV events were strongly associated with dyslipidemia (Tisseverasinghe et al., 2009). Changes in cholesterol homeostasis and fatty acid metabolism have been related to the IFN pathway. York et al showed with isotype tracer analysis, that type I IFN signalling shifts the balance of the biosynthesis and import of cellular lipids by decreasing cholesterol and long chain fatty acids. An upregulation of the type I IFN signature correlated with a reduction in the pool size of synthesized cholesterol, that in turn could be inhibited by replenishing cells with free cholesterol. They showed that limiting the flux through the cholesterol biosynthetic pathway engaged the type I IFN response in a stimulator of interferon genes (STING)-dependent manner. Overall these studies demonstrated a metabolic-inflammatory circuit that links fluctuations in

cholesterol biosynthesis with an upregulation of the type I IFN pathway (York et al., 2015).

The aim of this chapter was to explore the relationship between the type I IFN pathway and cholesterol homeostasis. To investigate this relationship, gene mining of RNA-seq data was performed to identify specific cholesterol pathway genes with altered expression in JDM. Cell culture with IFN-α was performed to identify changes in the selected gene, and markers of plasma membrane-associated lipid glycosphingolipids (measured by cholera-toxin-B binding, CTB) and cholesterol (measured using filipin binding) in healthy control PBMC and isolated T and B cells.

RESULTS

The type I IFN signature was confirmed by analysis of RNA-seq data carried out on JDM and CHC samples. ***Table V.1*** highlights the demographics, clinical and serological features of both the JDM pre- and on- treatment patient and CHC cohorts. This table shows that the JDM samples were age matched to the CHC samples, but the female predominance seen in the JDM cohort was not proportionally reflected in the CHC cohort. The JDM pre-treatment patients had worse disease than on-treatment patients which was confirmed by significantly higher PGA score and CK levels, but significantly lower MMT8 and CMAS scores. A broad spectrum of autoantibodies was represented in the JDM cohort, however there were no patients with anti-MDA5. The majority of the on-treatment samples were taken from patients on methotrexate and oral prednisolone, which suggests that this cohort was relatively responsive to treatment with DMARDs.

Table V.1 *Demographic, clinical and serological features of the JDM cohort and child healthy controls used in RNA-sequencing data set. The median and interquartile range (IQR) was represented for patient characteristics and clinical features. Student t-test was used to test the significance between JDM pre- and on-treatment groups for PGA, manual muscle testing of 8 groups (MMT8), and childhood myositis Assessment Scale (CMAS). Mann-Whitney test was used to test the significance between JDM pre- and on-treatment groups for creatine kinase (CK). The number of patients (percentage)were shown for autoantibody status and medication taken. Autoantibodies included; anti–transcription intermediary factor 1γ (anti–TIF-1γ), anti–nuclear matrix protein 2 (anti–NXP-2), anti-75-and 100kDa polymyositis/systemic sclerosis proteins (anti-PmScl), Nucleosome-remodeling deactulase complex (anti–Mi2), Signal recognition particle (anti-SRP), and Unknown bands (UKB)*

	JDM patients			Controls
Patient characteristics	**Pre-treatment samples (n=13)**	**On- treatment samples (n=13)**	**All JDM samples (n=26)**	**Child healthy control (n=8)**
Number of patients	**13**	**13**	**16**	
Age at onset (years), median [IQR]			7.52 [4.32-12.58]	
Age at diagnosis (years), median [IQR]			7.81 [4.74-12.74]	
Age at sample (years), median [IQR]	7.34 [5.00-12.62]	10.4 [5.94-14.32]	8.84 [5.20-13.74]	8.06 [6.00-13.83]
Sex, (F/M)	10/3	8/5	11/5	4/4
Clinical features, median [IQR]				
Physician's Global Assessment (PGA) - (0-10) [p<0.0001]	7.00 [5.20-7.60]	1.1 [0.90-1.30]		
MMT8 - (0-80) [p<0.0001]	35.00 [25.00-44.50]	80 [79-80]		
CMAS - (0-53) [p<0.0001]	15.5 [6.50-23.00]	49 [45-52]		
Creatine Kinase (CK) U/L - (>0) (meaured in serum at time of PBMC sample) [p=0.01]	2981 [254.00-7176.00]	105.50 [86.25-117.00]		
Myositis-specific autoantibodies, n (%)				
Anti-TIF1 gamma			3 (18.75)	
Anti-SRP			1 (6.25)	
Anti-NXP2			4 (25.00)	
Anti-Mi2			3 (18.75)	
Anti-PmScl			1 (6.25)	
UKB			2 (12.50)	
No detectable autoantibodies			2 (12.50)	
Medications (at time of sample) n(%):				
Azathioprine		1 (7.69)		
Cyclophosphamide		0 (0.00)		
Oral Prednisolone		9 (69.23)		
Methotrexate		12 (92.31)		
IV Prednisolone		0 (0.00)		
Other drugs		6 (46.15)		

Up-regulation of the type I interferon alpha signature in JDM

Gene set enrichment analysis (GSEA) revealed significant differences in the fifty Hallmark pathways (***Figure V.1***). GSEA ranked the pathway associated list of genes,

comparing between cell types (PBMC, CD19+, CD8+, CD4+, CD14+) and between JDM pre/on treatment and child healthy control (CHC) samples. The interferon alpha response Hallmark pathway was one of the most up-regulated across all cell types when comparing JDM pre- to on-treatment and JDM pre-treatment to CHC. These results confirmed previous findings that JDM has a significant IFNα gene signature in the peripheral blood (Baechler et al., 2011, Bilgic et al., 2009). These data enhanced the results by identifying the signature across multiple cell types including, CD14+ monocytes, C19+ B cells, CD8+ and CD4+ T cells. We focused on the gene expression from CD19+ B cells, CD8+ and CD4+ T cells (***Figure V.2***). When JDM pre- to on-treatment and JDM pre-treatment to CHC were compared a high proportion of the interferon alpha response Hallmark pathway genes were significantly upregulated in all three cell types (***Table V.2***). When JDM on-treatment to CHC were compared this up-regulation was lost.

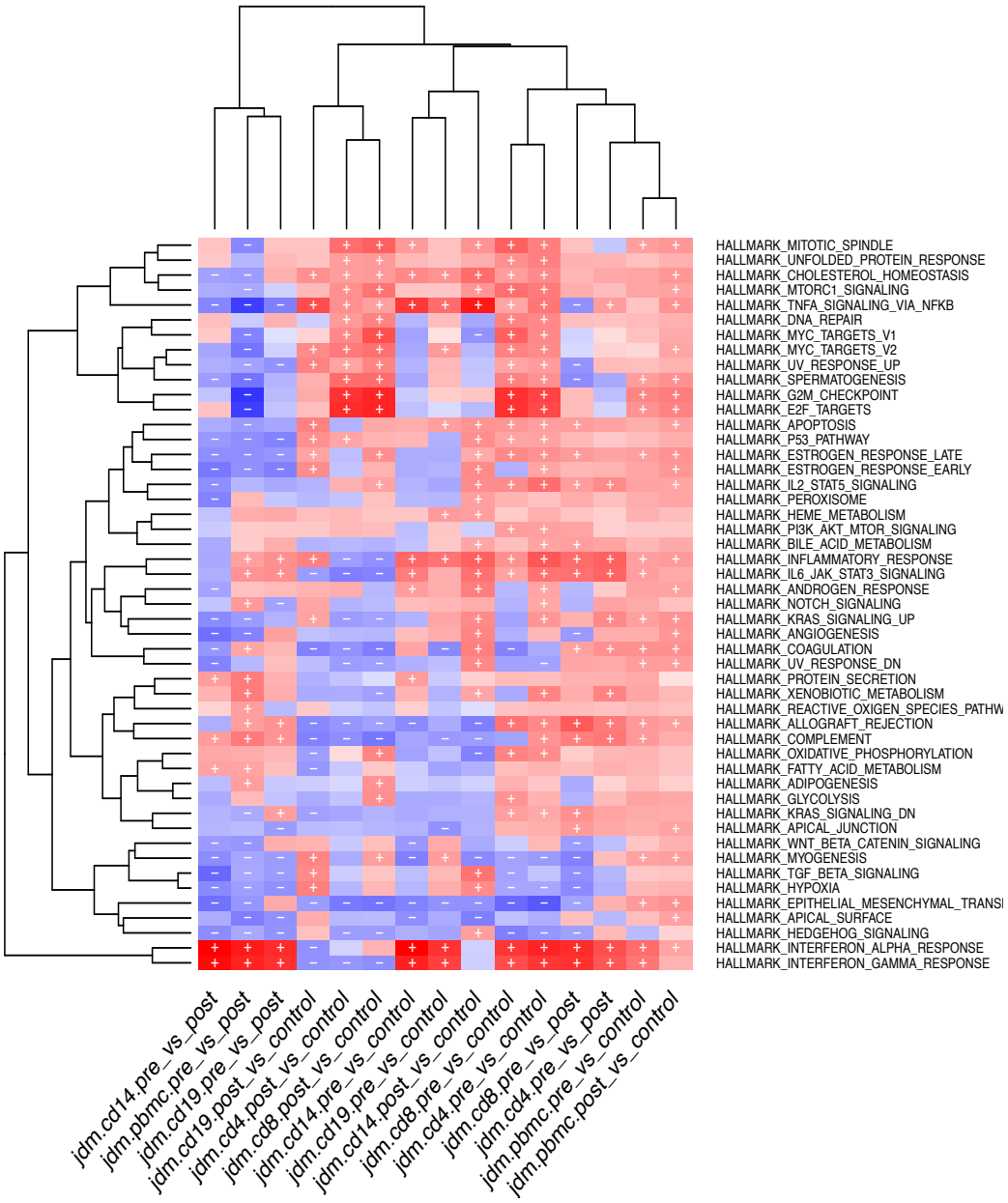

Figure V.1 Heatmap of GSEA enriched Hallmark gene sets for JDM and control PBMC subsets. *Heatmap demonstrating the up-regulation and down-regulation of GSEA Hallmark pathways from RNA-sequencing data. Total PBMC, CD19+ B cells, CD14+ monocytes, CD4+ T cells, and CD8+ T cells were sorted from JDM pre-/on-treatment JDM and child healthy controls samples. Gene expression was measured by RNA-sequencing. For each cell type every gene was ranked comparing pre-treatment JDM to on-treatment JDM, pre-treatment JDM to child healthy control and on-treatment JDM to child healthy control. Red represents an up-regulated pathway and blue a down-regulated pathway. + = significantly up-regulated. - = significantly downregulated.*

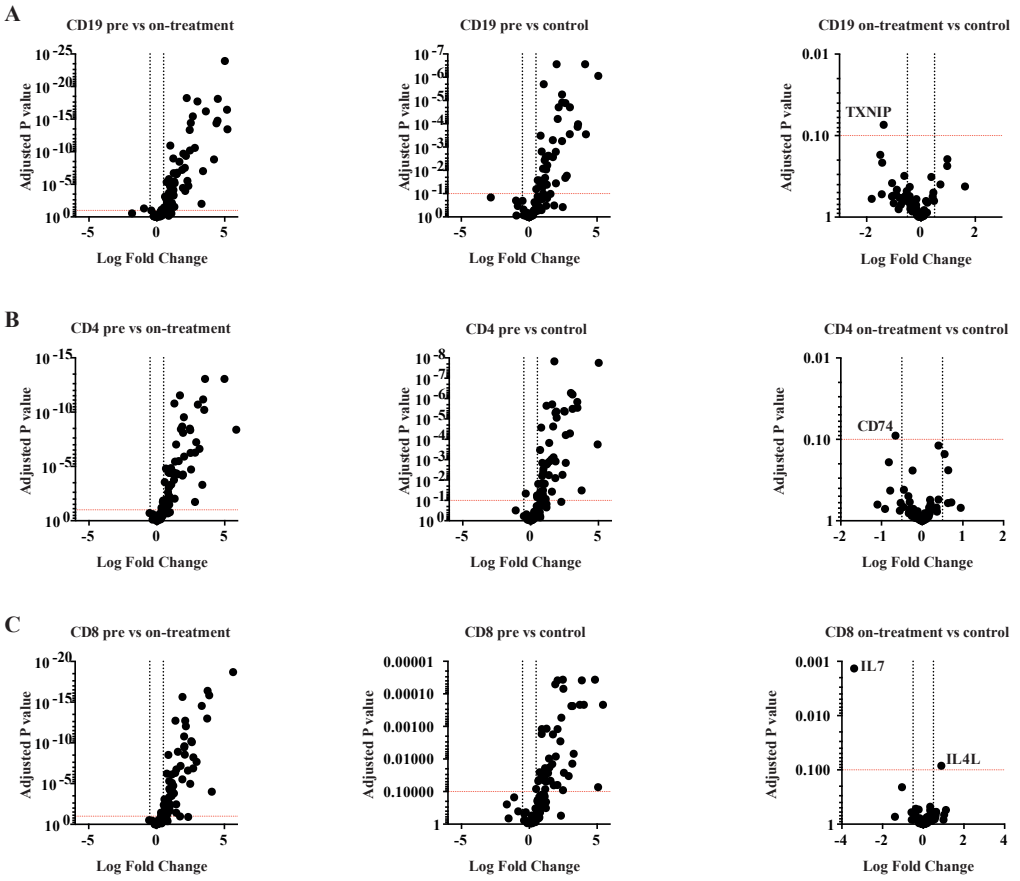

Figure V.2 IFN Alpha response hallmark gene set pre, on-treatment and CHC. *Volcano plots representing the log fold change and adjusted p value for the genes present in the GSEA Hallmark interferon alpha response pathway. A) CD19+ B cells, B) CD4+ T cells, and C) CD8+ T cells were sorted from JDM pre-/on-treatment JDM and child healthy controls samples. Gene expression was measured by RNA-sequencing and adjusted p value (by Bonferroni) and log fold change was calculated comparing pre-treatment JDM to on-treatment JDM, pre-treatment JDM to child healthy control and on-treatment JDM to child healthy control. For Bonferroni multiple comparison the adjusted p value significance level was 0.1. The fold change significance was +/-0.5.*

Table V.2 A list of upregulated IFN signature genes in all cell types

IFN gene	Description
OAS1	2'-5'-oligoadenylate synthetase 1 [Source:HGNC Symbol;Acc:HGNC:8086]
IFIT3	interferon induced protein with tetratricopeptide repeats 3 [Source:HGNC Symbol;Acc:HGNC:5411]
RSAD2	radical S-adenosyl methionine domain containing 2 [Source:HGNC Symbol;Acc:HGNC:30908]
USP18	ubiquitin specific peptidase 18 [Source:HGNC Symbol;Acc:HGNC:12616]
CMPK2	cytidine/uridine monophosphate kinase 2 [Source:HGNC Symbol;Acc:HGNC:27015]
IFI44L	interferon induced protein 44 like [Source:HGNC Symbol;Acc:HGNC:17817]
ISG15	ISG15 ubiquitin-like modifier [Source:HGNC Symbol;Acc:HGNC:4053]
OASL	2'-5'-oligoadenylate synthetase like [Source:HGNC Symbol;Acc:HGNC:8090]
SAMD9L	sterile alpha motif domain containing 9 like [Source:HGNC Symbol;Acc:HGNC:1349]
HERC6	HECT and RLD domain containing E3 ubiquitin protein ligase family member 6 [Source:HGNC Symbol;Acc:HGNC:26072]
IFI27	interferon alpha inducible protein 27 [Source:HGNC Symbol;Acc:HGNC:5397]
IFI44	interferon induced protein 44 [Source:HGNC Symbol;Acc:HGNC:16938]

Up-regulation of the cholesterol homeostasis pathway in JDM

The GSEA also highlighted that the cholesterol homeostasis Hallmark pathway was up-regulated across cell types and sample group comparisons (***Figure V.1***). This pathway was up-regulated in JDM pre-treatment and on-treatment compared to CHC, suggesting that medication within the first year of treatment does not restore cholesterol homeostasis to comparative levels seen in CHC. However, the significant gene expression changed between cell types and across sample comparison (***Figure V.3***). Phospholipid scramblase 1 (PLSCR1) and F-box O6 (FBXO6) protein coding genes were up-regulated in all cell types when JDM pre-treatment was compared to both JDM on-treatment and CHC samples. This up-regulation was lost after treatment, but in CD4+ T cells the JDM on-treatment compared to CHC samples had an up-regulation of fatty acid synthase (FASN) and 7-Dehydrocholesterol reductase (DHCR7) protein coding genes. When JDM pre-treatment were compared to CHC a high proportion of the cholesterol homeostasis Hallmark pathway genes were upregulated in all three cell types (***Table V.3***). As both the interferon and cholesterol pathways were up-regulated, especially in JDM pre-treatment compared to CHC samples, I wanted to investigate the relationship between them.

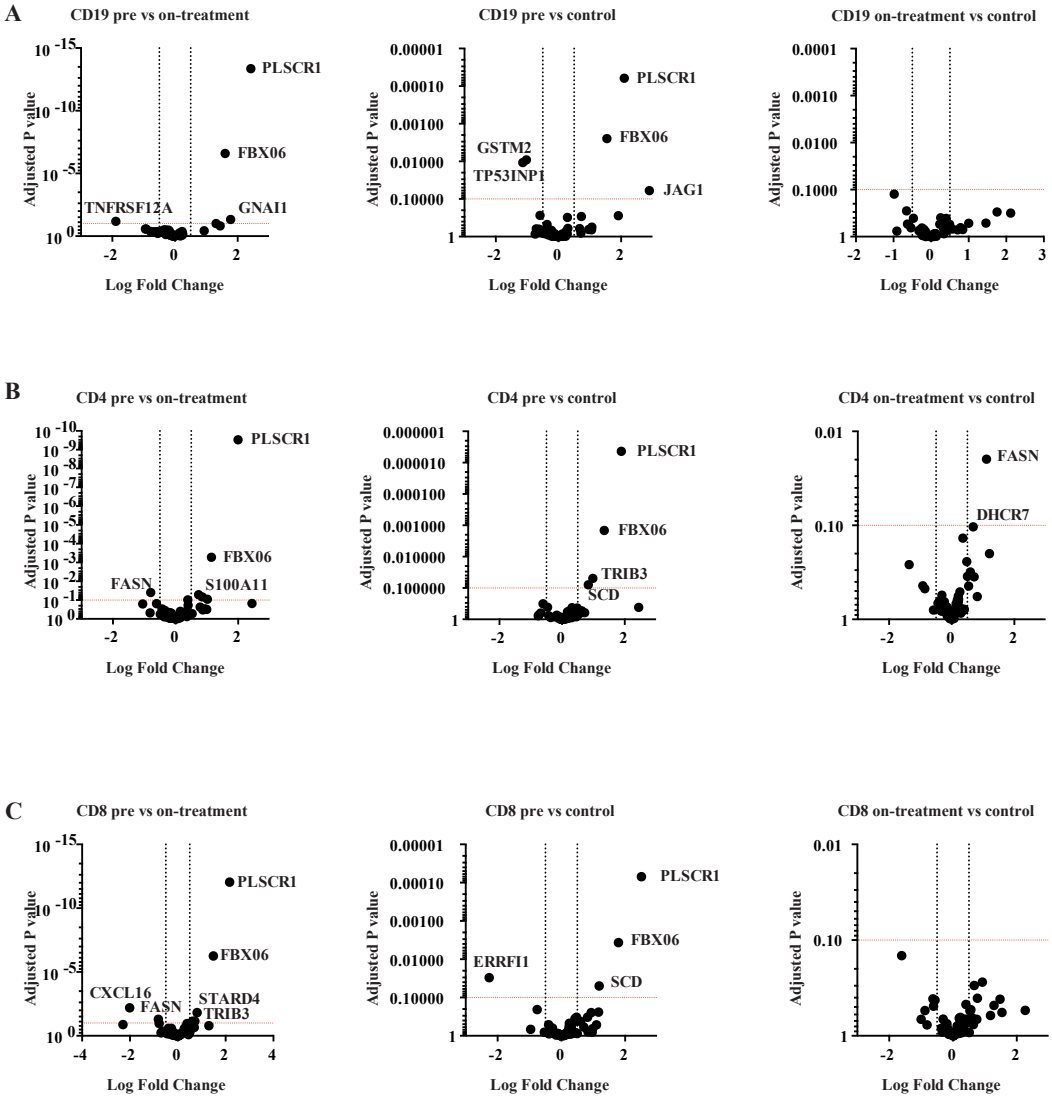

Figure V.3 Volcano plots representing the log fold change and adjusted p value for the genes present in the GSEA Hallmark cholesterol homeostasis pathway*. A) CD19+ B cells, B) CD4+ T cells, and C) CD8+ T cells were sorted from JDM pre-/on-treatment JDM and child healthy controls samples. Gene expression was measured by RNA-sequencing and adjusted p value (by Bonferroni) and log fold change was calculated comparing pre-treatment JDM to on-treatment JDM, pre-treatment JDM to child healthy control and on-treatment JDM to child healthy control. For Bonferroni multiple comparison the adjusted p value significance level was 0.1. The fold change significance was +/-0.5.*

Table V.3 A list of upregulated cholesterol homeostasis genes in all cell types

Cholesterol homeostasis gene	Description
JAG1	jagged 1 [Source:HGNC Symbol;Acc:HGNC:6188]
PLSCR1	phospholipid scramblase 1 [Source:HGNC Symbol;Acc:HGNC:9092]
GNAI1	G protein subunit alpha i1 [Source:HGNC Symbol;Acc:HGNC:4384]
FBXO6	F-box protein 6 [Source:HGNC Symbol;Acc:HGNC:13585]
ATF3	activating transcription factor 3 [Source:HGNC Symbol;Acc:HGNC:785]
SCD	stearoyl-CoA desaturase [Source:HGNC Symbol;Acc:HGNC:10571]
LDLR	low density lipoprotein receptor [Source:HGNC Symbol;Acc:HGNC:6547]
HMGCS1	3-hydroxy-3-methylglutaryl-CoA synthase 1 [Source:HGNC Symbol;Acc:HGNC:5007]
STX5	syntaxin 5 [Source:HGNC Symbol;Acc:HGNC:11440]
FASN	fatty acid synthase [Source:HGNC Symbol;Acc:HGNC:3594]
NSDHL	NAD(P) dependent steroid dehydrogenase-like [Source:HGNC Symbol;Acc:HGNC:13398]
ACTG1	actin gamma 1 [Source:HGNC Symbol;Acc:HGNC:144]
SREBF2	sterol regulatory element binding transcription factor 2 [Source:HGNC Symbol;Acc:HGNC:11290]
MVK	mevalonate kinase [Source:HGNC Symbol;Acc:HGNC:7530]
TRIB3	tribbles pseudokinase 3 [Source:HGNC Symbol;Acc:HGNC:16228]
ECH1	enoyl-CoA hydratase 1 [Source:HGNC Symbol;Acc:HGNC:3149]
CYP51A1	cytochrome P450 family 51 subfamily A member 1 [Source:HGNC Symbol;Acc:HGNC:2649]

I mined the GSEA and gene expression data to select a profile of cholesterol pathway genes; UPD-Glucose ceramide glucosyltransferase (UGCG), ELOVL fatty acid elongase 5 (ELOV5), stearoyl-CoA desaturase (SCD), F-box 06 (FBX06), syntaxin 5 (STX5) and malic enzyme 1 (ME1). JDM pre- and on-treatment CD19+ B cells had significantly decreased expression of ELOV5 than CHC (***Figure V.4A***). JDM pre-treatment CD4+ T cells had significantly increased expression of UGCG than JDM on-treatment and CHC (***Figure V.4B***). JDM pre- treatment CD4+ and CD8+ T cells had significantly increased expression of SCD than JDM on-treatment and CHC (***Figure V.4B***). JDM pre- treatment CD19+ B cells, CD8+ and CD4+ T cells had significantly increased expression of FBX06 than JDM on-treatment and CHC (***Figure V.4A-B***). JDM pre- treatment CD8+ T cells had significantly decreased expression of ME1 than JDM on-treatment and CHC (***Figure V4B***). The selected genes were used to investigate the effect of IFNα stimulation on B and T cell expression of cholesterol related genes.

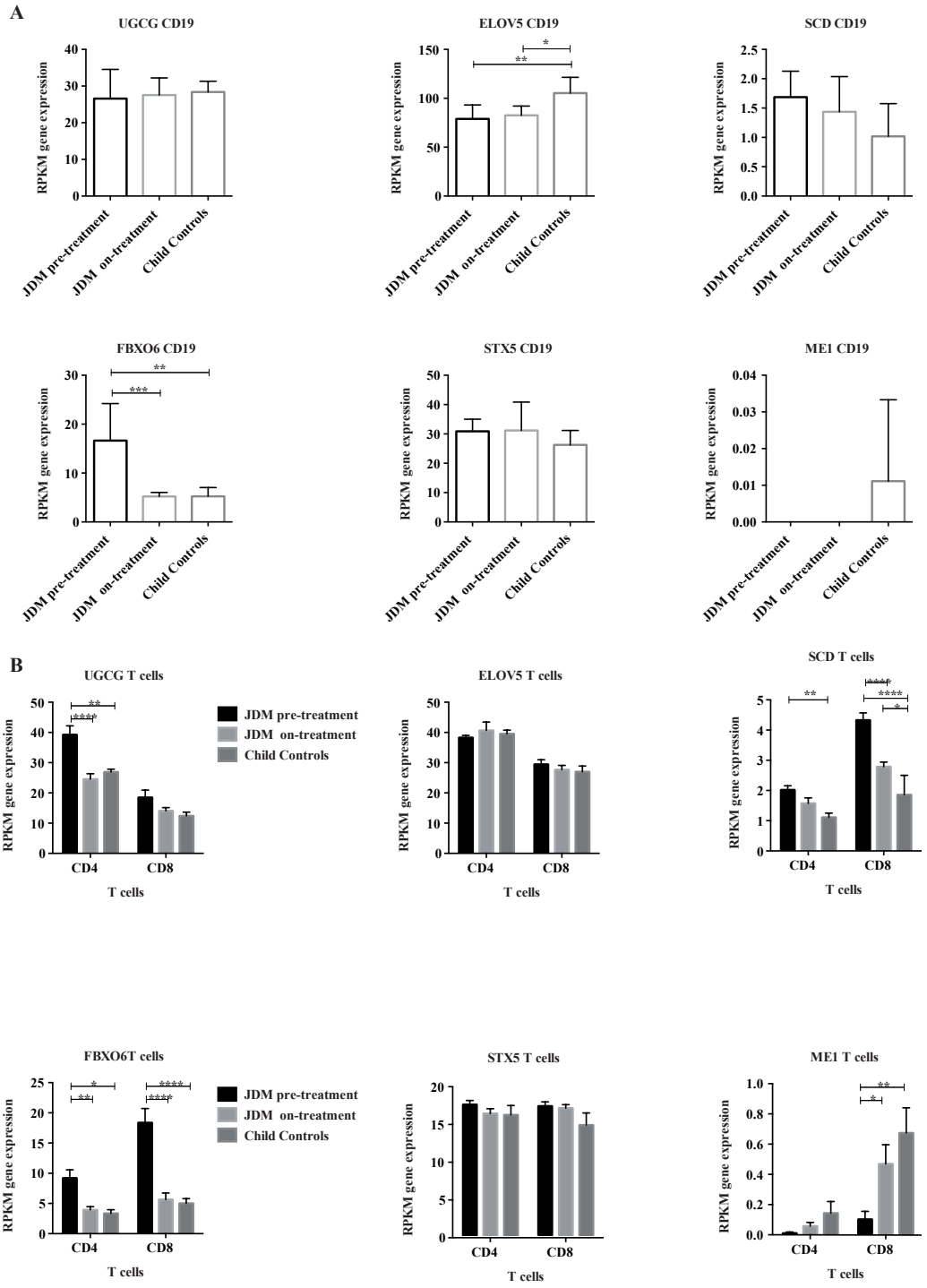

Figure V.4 A comparison of the expression of selected genes from the GSEA Hallmark cholesterol homeostasis pathway from B cells and CD4+/8+ T cells sorted from JDM pre-/on- treatment and child healthy control samples*. Scatter plots showing the reads per kilobase per million mapped reads (RPKM) of the genes UGCG, ELOVL5, FBXO6, STX5 and ME1 for A) B cells and B) T cells from pre- and on-treatment JDM and child healthy control (CHC) samples. Values represent mean ± SEM. *p<0.05, **p<0.01, ***p<0.001*

Change in expression of cholesterol related genes from B and T cells after IFNα stimulation

Isolated B and T cells from adult healthy control PBMC samples were stimulated for 2hours, 6hours and 24hours with IFN-α. After stimulation, we isolated the RNA and measured gene expression by qPCR. There was not a significant change in the expression of UGCG or SCD from either cell type after stimulation with IFNα for any time point. After 24hours of stimulation with IFN-α there was a trend towards a decrease in expression of ELOVL5 from the B cells (***Figure V.5A***) comparative to the expression results seen in JDM pre-treatment (***Figure V.4A***). There was significant increase in FBX06 expression from T cells after a 2hr stimulation with IFN-α, there was a trend for a maintained increase at 6hours and 24hours (***Figure V.5B***). There was no significant change in the expression of STX5 or ME1 from T cells after stimulation with IFN-α for any time point (***Figure V.5B***). These results suggest that ELOVL5 expression from B cells and FBX06 expression from T cells were influenced by IFN-α. Due to limitations in the quantity of B cell cDNA the number of genes analysed by qPCR was limited, therefore I can only hypothesise that FBX06 expression from B cells would also be increased.

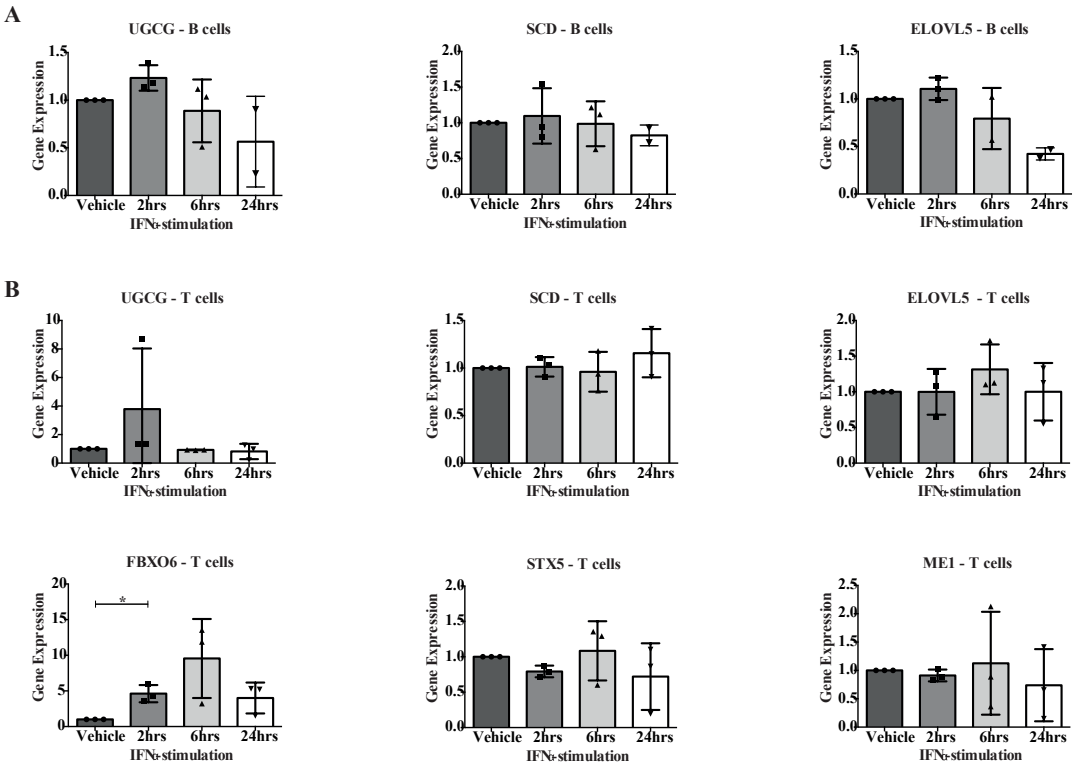

Figure V.5 IFN stimulation over time; gene expression from B and T cells. *T cell and B cell expression of cholesterol homeostatic genes after 2hour, 6hour and 24hour culture, stimulated +/- IFN-α. A) Scatter plots showing the B cell relative gene expression of UGCG, SCD and ELOVL5. B) Scatter plots showing the T cell relative gene expression of UGCG, ELOVL5, FBX60, STX5 and ME1. Values represent mean ± SEM. *p<0.05, **p<0.01, ***p<0.001*

Lymphocyte membrane glycosphingolipids decreased after IFNα stimulation

Since plasma membrane lipid composition is known to influence immune cell function I also assessed whether IFN-α stimulation influenced plasma membrane lipid expression. I analysed the frequency expression of glycosphingolipid (GSL) (using CTB binding) and cholesterol (filipin binding) in CD19+ B cells, CD4+ and CD8+ T cells after culture with IFNα for 2hours, 6hours and 24hours. CTB is a surrogate marker for GSL expression (McDonald et al., 2014) and are markers of plasma membrane associated lipids and cholesterol. The gating strategy used is shown in ***Figure V.6***. Both B cells and CD8+ T cells had a significant decrease in CTB binding after 24 hours of IFNα stimulation (***Figure V.7A***). There was also a trend towards a

decrease in CTB expression from CD4+ T cells but it did not reach significance. No change in filipin expression was seen in any of the cell types (***Figure V.7B***). Therefore IFNα stimulation did not alter PM cholesterol levels but did influence GSL content.

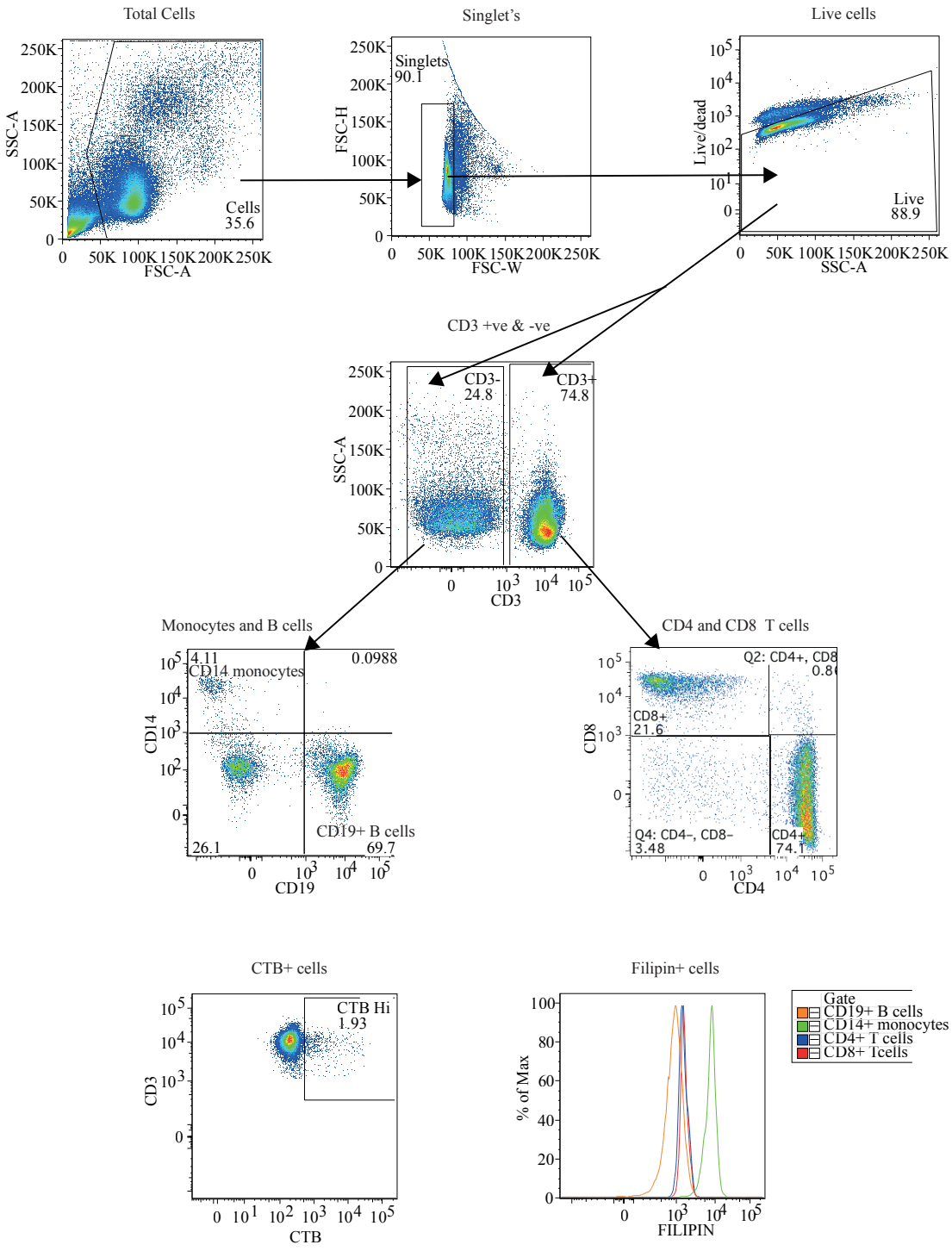

Figure V.6 Flow cytometry gating strategy for surface markers, CTB and filipin expression

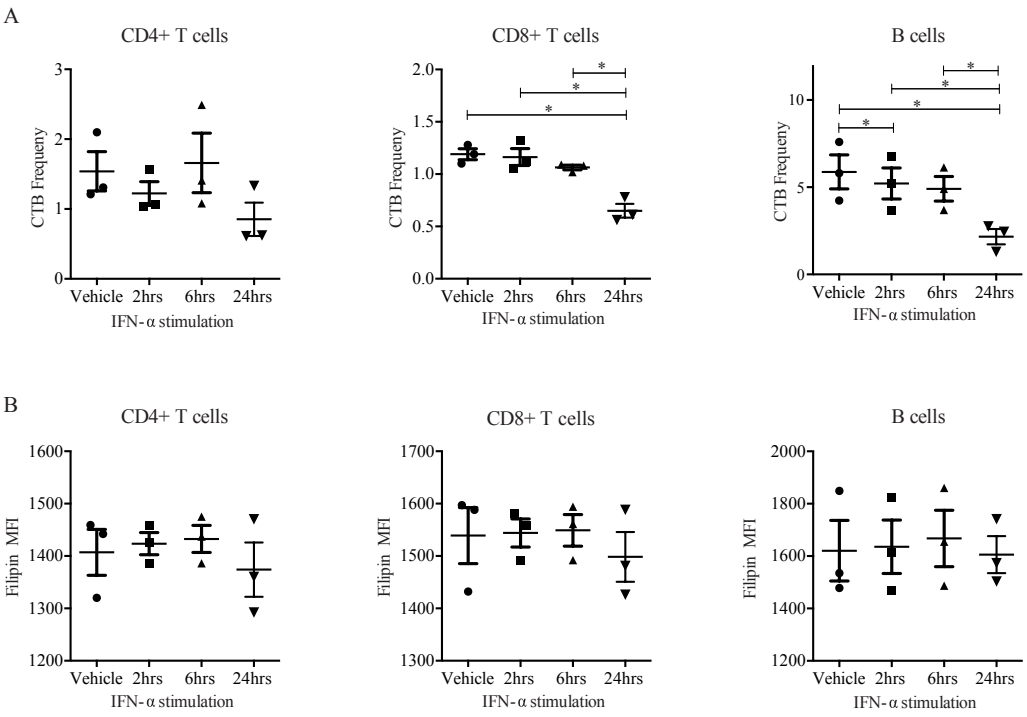

Figure V.7 - CD4/8+ T cell and B cell expression of CTB and filipin after 2hour, 6hour and 24hour culture, stimulated +/- IFN-α. *A) Scatter plots showing the frequency of CD4+, CD8+ T cells and B cells expressing CTB. B) Scatter plots showing the filipin MFI from CD4+, CD8+ T cells and B cells. Values represent mean ± SEM. *p<0.05, **p<0.01, ***p<0.001*

ADM patients have a high B cell expression of HMGCR

A sub-group of adult myositis patients develop an auto-antibody against 3-hydroxy-3-methylglutaryl-CoA reductase (HMGCR), this is most commonly induced by statin use as HMGCR is the pharmacological target for statins. I investigated the B cell expression of HMGCR and the related genes FASN, sterol regulatory element-binding protein 1 (SREBP1) and SREBP2. In JDM compared to CHC there was no change in HMGCR expression, but a trend emerged towards an increased expression of FASN from JDM on-treatment samples (***Figure V.8A***). In adult DM (ADM) compared to adult HC (AHC) samples there was a significant increase of HMGCR expression. No change in expression of FASN or SREBP2 were noted. A significant decrease in expression of SREBP1 was seen in ADM compared to AHC, but the n

number was two (***Figure V.8B***). The final experiment repeated the design from figure 5, taking four AHC PBMC samples and isolated the B cells. We stimulated the B cells with IFN-α for 6hours and 24hours, isolated RNA and analysed for gene expression by qPCR (***Figure V.8C***). A significant difference was not identified for any of the four genes. There was however a trend towards an increase in HMGCR and FASN expression, but a decrease in SREBP2 expression.

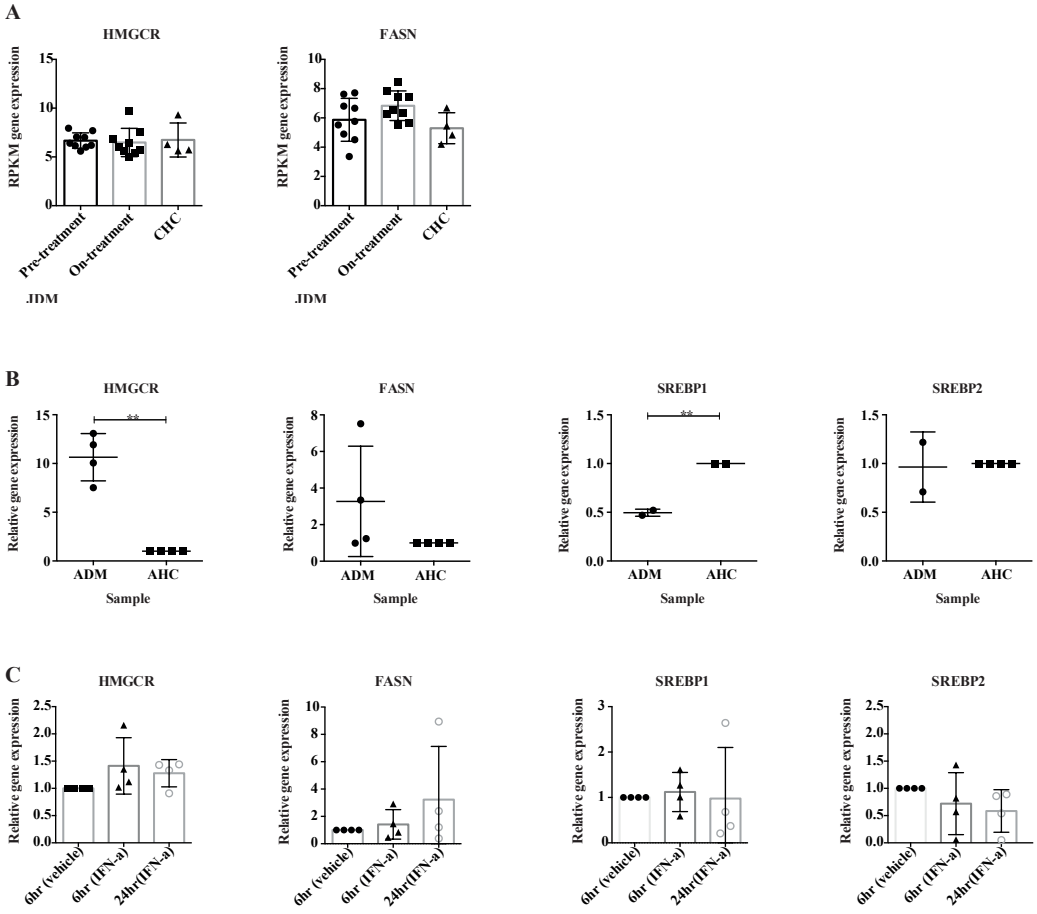

Figure V.8 B cell expression of cholesterol associated genes in patients and healthy controls. *A) Scatter plots showing the reads per kilobase per million mapped reads (RPKM) of the genes HMGCR and FASN for B cells from pre- and on-treatment JDM and child healthy control (CHC) samples. B) Scatter plots showing the relative gene expression of HMGCR, FASN, SREPB1 and SREBP2 for B cells from adult DM and adult healthy control (AHC) samples. C) Scatter plots showing relative gene expression of HMGCR, FASN, SREPB1 and SREBP2 for B cells from AHC samples cultured for 6hours and 24hours +/- IFN-α. Values represent mean ± SEM. *p<0.05, **p<0.01, ***p<0.001*

DISCUSSION

These results confirmed that the type I IFN pathway genes were up-regulated in all cell types in samples taken from JDM patients pre-treatment compared to both JDM on-treatment and healthy child controls. The cholesterol homeostasis pathway genes were also up-regulated in all cell types in samples taken from JDM patients pre-treatment compared to both JDM on-treatment and CHC. However the genes were also up-regulated when JDM on-treatment was compared to CHC. These findings suggest that the dysregulation of cholesterol homeostasis was not corrected by a year on treatment with prednisolone and methotrexate, unlike the type I IFN pathway. As both these pathways were up-regulated in JDM, I explored the relationship between IFN-α stimulation and the dysregulation of lipid rafts and cholesterol related genes.

Previous studies have identified a mechanism by which changes in cholesterol biosynthesis were linked to an increase in type I IFN expression (York et al., 2015). My data showed that although there was a trend towards a decrease in B cell UGCG expression in response to stimulation with IFN-α, this was not seen for the T cells. UGCG is a gene that encodes an enzyme that catalyses the first glycosylation step in the biosynthesis of glycosphingolipids. GSL expression can be detected using the specific association of CTB with the ganglioside GM1 (Waddington and Jury, 2015). The UGCG gene expression data correlated to the significantly decreased B cell expression of CTB after stimulation with IFN-α. A possible mechanism could be that type I IFN inhibits UGCG expression, which in turn inhibits the production of glycosphingolipids in the lipid rafts and leads to abnormal levels. A reduction of glycosphingolipids could lead to aberrant BCR signalling between immune cells. When exposed to an antigen the BCR has been shown to associate with the lipid rafts.

The lipid rafts aid amplification of BCR signalling after ligand binding. Increasing evidence highlights the process of initial endocytosis of antigens and the presentation onto a MHC-II receptor are coordinated within membrane domains (Gupta and DeFranco, 2007). Therefore, a disruption in lipid rafts would affect the antigen presentation between immune cells, especially in B cells.

ELOVL5 was another gene whose expression in B cells was decreased from both the RNA-seq JDM pre-treatment data and from the healthy control samples stimulated with IFN-α. This gene codes for elongation of very long chain fatty acid protein 5, catalysing the formation of very long-chain fatty acids. The fatty acids are components of membrane lipids, including the sphingolipids (Kihara, 2012). A study has shown that the expression of this gene was up-regulated after treatment with atorvastatin (Ishihara et al., 2017). This study suggests that statins increase the plasma concentration of arachidonic acid, an ω-6 long-chained polyunsaturated fatty acid (LCPUFA), but decrease the concentrations of eicosapentaenoic acid and docosahexaenoic acid, which are ω-3 LCPUFAs. Schwartz et al. reported that JDM patients with active disease, high eotaxin and MCP-1 and cholesterol levels in the upper normal range may have an increased risk of cardiac dysfunction (Schwartz et al., 2014). Therefore, if JDM patients have decreased expression of ELOVL5 they may be more susceptible to higher cholesterol which could be induced by the type I IFN pathway.

Myositis is known to be associated with a dysregulation of the cholesterol pathway (Tisseverasinghe et al., 2009). There is an identified sub-group of adult patients that test positive for the anti-HMGCR antibody. These patients are most commonly

associated with statin use (Mohassel and Mammen, 2013). The results showed that HMGCR expression was increased in B cells from adult but not JDM patient samples. HMGCR is a transmembrane glycoprotein that acts as the rate-limiting enzyme in cholesterol biosynthesis and the biosynthesis of non-sterol isoprenoids, both pathways are essential for normal cell function. HMGCR function is inhibited by the pharmacological agent, statins. This inhibition in the liver stimulates the low-density lipoprotein (LDL)-receptors, and in turn there is increased clearance of the LDL from the bloodstream and a decrease in blood cholesterol levels (Brown and Goldstein, 1980). The results from this study suggest that ADM patients have higher expression of HMGCR, which could alter cholesterol homeostasis. However, as statins have known myopathic side effects it may not be advisable to use them as cholesterol lowering preventative treatment in this disease.

Abnormal levels of glycosphingolipids in T cells have been identified to lead to abnormal T cell function, specifically in SLE (Kidani and Bensinger, 2014, McDonald et al., 2014). It was shown that by culturing healthy control T cells with SLE patient serum there was an increase in glycosphingolipids, this was comparative to the levels seen in T cells from SLE patients. These results suggest that SLE patients over-express a protein pathway within the serum that up-regulates T cell glycosphingolipids. A possible pathway would be type I IFN which is known to be up-regulated in SLE and other autoimmune diseases (Bilgic et al., 2009). The RNA-seq data supported this hypothesis in the context of JDM. FBX06, a gene identified within the Hallmark cholesterol homeostasis pathway, has been shown to be important for the controlled degradation on cellular regulatory proteins (Cenciarelli et al., 1999). FBX06 was significantly increased in B cells and T cells from JDM pre-

treatment samples, but also in HC T cells after stimulation with IFN-α. This gene showed an opposite trend to that seen of UGCG, and therefore CTB expression. The data showed no change in cholesterol by filipin expression over time after stimulation with IFN-α. Previous data collected by my laboratory group suggested that cholesterol should increase after 72hour of stimulation with IFN-α. The time points used for these experiments appeared too short to observe changes in cholesterol, but were correct for detecting changes in gene expression. This highlights the importance of ascertaining the correct time point to detect important changes in gene expression and phenotypic changes, which are likely to be different between cell types and within sub-populations.

The SCD gene codes for an endoplasmic reticulum enzyme that catalyses the formation of monounsaturated fatty acids. This enzyme has been identified to play an important role in the biogenesis of the plasma membrane, and for cell proliferation and survival of certain types of cancer (Belkaid et al., 2015). The RNA-seq data showed that the expression of SCD was significantly higher in all T cells, particularly CD8+ T cells, from JDM patients on-treatment, and there was a trend for this in B cells. There was a possible trend for an increased expression of SCD from HC T cells after 24hour of stimulation with IFN-α, but again this induction may be more pronounced after longer stimulation. If IFN-α affects the expression of SCD from T cells this could lead to an increase of monounsaturated fatty acids and in turn disrupting the plasma membrane. Further experimentation would be required.

I have shown that IFN-α stimulation of T and B cells does change the expression of some genes that are part of the Hallmark cholesterol homeostasis pathway. This

stimulation also altered lipid rafts. These data were only preliminary as most results were dependent upon just three or four healthy controls. To confirm the findings, it would be important to repeat this set of experiments with an increased number of samples. The results showed a change of CTB expression and thus lipid rafts for the time points used, but no change in cholesterol was observed. It would be useful to repeat the experiments for gene, CTB and filipin expression at longer time points. Also, an altered CTB:filipin ration could be important as it may reflect changes in membrane fluidity.

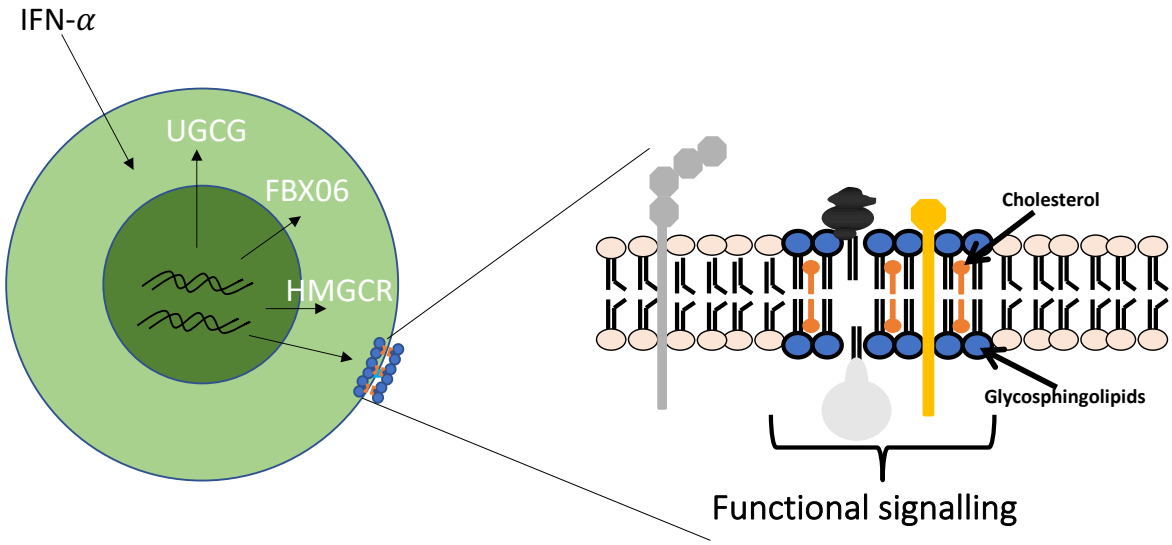

Figure V.9 IFN-α stimulation of T and B cells does change the expression of some genes that are part of the Hallmark cholesterol homeostasis pathway.
Stimulation of B and T cells with IFN-α recapitulated the increase in expression of certain cholesterol homeostasis pathway genes that were seen in IIM including; UGCG, FBX06 and HMGCR. Equally at a more functional level there were changes in glycosphingolipids and cholesterol at the lipid bilayer.

Chapter VI

Discussion Summary

My thesis has explored the immunopathogenesis of IIM in both adult and juvenile patients. It has addressed three main aims. Firstly, the investigation of the mechanisms driving B cell lymphocytosis and to define pathological features of B cells in the blood of JDM patients. The identification of specific immune cell signatures and cytokine profiles for myositis disease subtypes and correlation of this data with measurements of disease activity. Finally, delineation of a correlation between the up-regulated type I interferon signature and dysfunction of cholesterol homeostasis in immune cells.

The results identified that JDM patients with active disease had a significantly expanded immature B cell population which was correlated with the type I IFN signature. The expanded population and up-regulated type I IFN signature resolved after the patients received treatment with prednisolone and methotrexate. Activation through TLR7 and IFN-α may drive the expansion of immature B cells in JDM and skew the cells towards a more pro-inflammatory phenotype. To proceed with this work, it would be important to untangle the mechanism by which these interpretations are linked.

To establish, whether the expanded immature B cell population is skewed towards a pro-inflammatory phenotype, it would be important to delineate which IL-10 inducing pathway is dominant in the context of JDM. I propose further experimentation whereby by B cells taken from JDM pre- and on-treatment patients and CHC samples are stimulated with vehicle, IFN-α, R848 and cultured with or without CD40L CHO

cells for 72 hours. This experiment could be taken further by which immature B cells are isolated from each sample group. This may be required as after 72 hours of culture it is difficult to identify B cell subsets by flow cytometry due to down-regulation of cell surface markers. However, due to small PBMC numbers it can be difficult to isolate enough immature B cells. It would also be useful to repeat this experiment using ADM samples both pre- and on-treatment comparing with AHC to establish if the same mechanisms are apparent in adult disease.

My hypothesis would be that under dual stimulation the TLR7 would override that of the CD40-CD40L pathway, and that the JDM B cells would express less IL-10 than that of the CHC B cells. This would suggest that the immature B cell population in JDM are skewed away from B regulatory cell differentiation and towards a pro-inflammatory phenotype due to the over-activation of the type I IFN pathway. With further investigation, these data support a growing body of evidence that novel therapeutic agents that target the TLR7 and IFN-α response pathways could be useful for the treatment of dermatomyositis.

The novel in-depth immunophenotyping of patients with myositis showed that there were unique immune signatures in adult disease sub-types and this highlighted the heterogeneous nature of the myopathies. There were changes in cell populations between DM, PM and JDM, but also with changes in disease activity, treatment and auto-antibody presence. One particular signature was of an expanded Th17 T cell population in the peripheral blood of ADM patients. To expand on this result, it would be important to establish this signature in a larger cohort and confirm that it was specific to DM rather than PM. Equally, it is known that Th17 cells are tissue

residing in the biopsies from IIM patients (Chevrel et al., 2003, Page et al., 2004, Tournadre et al., 2009). Therefore, it would be useful to correlate the proportion of Th17 cells in the peripheral blood with that found in the inflamed muscle tissue at diagnosis. This ratio could be used establish a biomarker for monitoring disease progression. The use of IL-17A inhibitors could be efficacious to treat patients with a Th17 signature, but further exploration of the mechanism would be required.

My results demonstrated that the expanded Th17 population correlated with an expansion of activated T cells and also increased IL-6 expression from memory B cells. The highest immune cell expression of IL-6 and CD69 was noted in the ADM group. This would suggest that the Th17 expansion seen in the peripheral blood of ADM patients is linked with the activated cellular IL-6 signature. It has been identified that CD69 employs a complex immune-regulatory role in humans and animal models by the inhibition of Th17 differentiation and function (Martin et al., 2010, Cruz-Adalia et al., 2010). This would suggest that the increased activated Treg population found in the ADM group may be exerting an immune-regulatory role in response to the expanded Th17 population. IL-17 is a known inducer of IL-6 as part of its central role in the migration and differentiation of mononuclear cells. An increase in Th17 cells could lead to an increased expression of IL-6 by B cells. To investigate this mechanism PBMC from ADM and AHC could be cultured in the presence or absence of an IL-17A inhibitor, then the expression of IL-6 from B cells could be measured by flow cytometry and ELISA. If the IL-17A inhibitor did reduce the expression of IL-6 from B cells this would form supporting evidence for the use of IL-17A inhibitors in the treatment of ADM.

Lastly, I showed that IFN-α stimulation of T and B cells does change the expression of some genes that are part of the Hallmark cholesterol homeostasis pathway and that this pathway was up-regulated in JDM patients compared to CHC. IFN-α stimulation also altered lipid rafts. Changes in cholesterol, cholesterol homeostasis gene expression and membrane fluidity may affect T cell signalling and antigen presentation between immune cells, which are noted changes in autoimmune disease (Baechler et al., 2003, Cedeno et al., 2003). If type I IFNs do alter lipid rafts in autoimmune disease then, diseases like myositis, may require lipid raft modulating therapeutic agents. These would work in conjunction with existing agents such as anti-CD20 antibodies (rituximab) and statins that exert their effect in part via the lipid raft (Kabouridis and Jury, 2008). Further experimentation would be required to establish this mechanism.

In conclusion, the study provides further evidence that anti- IFNα biologics could be efficacious in the treatment of JDM. That unique cell signatures could help to choose treatments and assess disease outcomes. Also, the need for further investigation for the use of IL-17A inhibitors in the treatment of IIM.

Future work aims

1. Further delineate the pathogenic role of immature B cells in IIM
    a. Does type I IFN blockade increase IL-10 expression and restore the regulatory nature of immature B cells?
    b. Are these immature B cells infiltrating muscle tissue and exerting a pathogenic effect?
    c. Is the expansion of pro-inflammatory immature B cells in pre-treatment patients a common trait in IIM or is it unique to JDM?
2. Re-capitulate the immune signatures found in the IIM sub-groups in a defined cohort
3. Investigate the immunopathogenesis of the specific cell types found to be associated with disease e.g. B cells , Th17 and C8+CM
    a. Are they found to infiltrate inflamed muscle tissue?
    b. What is driving these changes in immune cell type?
4. Establish mechanisms by which type I IFN alters cholesterol and lipid metabolism in immune cells
    a. Is this pathway a potential therapeutic target?

References

ABDULAHAD, W. H., BOOTS, A. M. & KALLENBERG, C. G. 2011. FoxP3+ CD4+ T cells in systemic autoimmune diseases: the delicate balance between true regulatory T cells and effector Th-17 cells. *Rheumatology (Oxford),* 50**,** 646-56.

ALBEROLA-ILA, J., HOGQUIST, K. A., SWAN, K. A., BEVAN, M. J. & PERLMUTTER, R. M. 1996. Positive and negative selection invoke distinct signaling pathways. *J Exp Med,* 184**,** 9-18.

AMEMIYA, K., GRANGER, R. P. & DALAKAS, M. C. 2000. Clonal restriction of T-cell receptor expression by infiltrating lymphocytes in inclusion body myositis persists over time. Studies in repeated muscle biopsies. *Brain,* 123 (Pt 10)**,** 2030-9.

ANDREOLI, L., NALLI, C., MOTTA, M., NORMAN, G. L., SHUMS, Z., ENCABO, S., BINDER, W. L., NUZZO, M., FRASSI, M., LOJACONO, A., AVCIN, T., MERONI, P. L. & TINCANI, A. 2011. Anti-beta(2)-glycoprotein I IgG antibodies from 1-year-old healthy children born to mothers with systemic autoimmune diseases preferentially target domain 4/5: might it be the reason for their 'innocent' profile? *Ann Rheum Dis,* 70**,** 380-3.

ARAHATA, K. & ENGEL, A. G. 1984. Monoclonal antibody analysis of mononuclear cells in myopathies. I: Quantitation of subsets according to diagnosis and sites of accumulation and demonstration and counts of muscle fibers invaded by T cells. *Ann Neurol,* 16**,** 193-208.

AUFFRAY, C., SIEWEKE, M. H. & GEISSMANN, F. 2009. Blood monocytes: development, heterogeneity, and relationship with dendritic cells. *Annu Rev Immunol,* 27**,** 669-92.

BAECHLER, E. C., BATLIWALLA, F. M., KARYPIS, G., GAFFNEY, P. M., ORTMANN, W. A., ESPE, K. J., SHARK, K. B., GRANDE, W. J., HUGHES, K. M., KAPUR, V., GREGERSEN, P. K. & BEHRENS, T. W. 2003. Interferon-inducible gene expression signature in peripheral blood cells of patients with severe lupus. *Proc Natl Acad Sci U S A,* 100**,** 2610-5.

BAECHLER, E. C., BAUER, J. W., SLATTERY, C. A., ORTMANN, W. A., ESPE, K. J., NOVITZKE, J., YTTERBERG, S. R., GREGERSEN, P. K., BEHRENS, T. W. & REED, A. M. 2007. An interferon signature in the peripheral blood of dermatomyositis patients is associated with disease activity. *Mol Med,* 13**,** 59-68.

BAECHLER, E. C., BILGIC, H. & REED, A. M. 2011. Type I interferon pathway in adult and juvenile dermatomyositis. *Arthritis Res Ther,* 13**,** 249.

BAEK, A., PARK, H. J., NA, S. J., SHIM, D. S., MOON, J. S., YANG, Y. & CHOI, Y. C. 2012. The expression of BAFF in the muscles of patients with dermatomyositis. *J Neuroimmunol,* 249**,** 96-100.

BAIRD, G. S. & MONTINE, T. J. 2008. Multiplex immunoassay analysis of cytokines in idiopathic inflammatory myopathy. *Arch Pathol Lab Med,* 132**,** 232-8.

BANCHEREAU, J. & STEINMAN, R. M. 1998. Dendritic cells and the control of immunity. *Nature,* 392**,** 245-52.

BANICA, L., BESLIU, A., PISTOL, G., STAVARU, C., IONESCU, R., FORSEA, A. M., TANASEANU, C., DUMITRACHE, S., OTELEA, D., TAMSULEA, I., TANASEANU, S., CHITONU, C., PARASCHIV, S., BALTEANU, M., STEFANESCU, M. & MATACHE, C. 2009. Quantification and molecular characterization of regulatory T cells in connective tissue diseases. *Autoimmunity,* 42**,** 41-9.

BARTLETT, H. S. & MILLION, R. P. 2015. Targeting the IL-17-T(H)17 pathway. *Nat Rev Drug Discov,* 14**,** 11-2.

BEHAN, W. M., BEHAN, P. O., DURWARD, W. F. & MCQUEEN, A. 1987. The inflammatory process in polymyositis: monoclonal antibody analysis of muscle and peripheral blood immunoregulatory lymphocytes. *J Neurol Neurosurg Psychiatry,* 50**,** 1468-74.

BEKEREDJIAN-DING, I. B., WAGNER, M., HORNUNG, V., GIESE, T., SCHNURR, M., ENDRES, S. & HARTMANN, G. 2005. Plasmacytoid dendritic cells control TLR7 sensitivity of naive B cells via type I IFN. *J Immunol,* 174**,** 4043-50.

BELKAID, A., DUGUAY, S. R., OUELLETTE, R. J. & SURETTE, M. E. 2015. 17beta-estradiol induces stearoyl-CoA desaturase-1 expression in estrogen receptor-positive breast cancer cells. *BMC Cancer,* 15**,** 440.

BELLUTTI ENDERS, F., VAN WIJK, F., SCHOLMAN, R., HOFER, M., PRAKKEN, B. J., VAN ROYEN-KERKHOF, A. & DE JAGER, W. 2014. Correlation of CXCL10, tumor necrosis factor receptor type II, and galectin 9 with disease activity in juvenile dermatomyositis. *Arthritis Rheumatol,* 66**,** 2281-9.

BENDEWALD, M. J., WETTER, D. A., LI, X. & DAVIS, M. D. 2010. Incidence of dermatomyositis and clinically amyopathic dermatomyositis: a population-based study in Olmsted County, Minnesota. *Arch Dermatol,* 146**,** 26-30.

BENVENISTE, O., HERSON, S., SALOMON, B., DIMITRI, D., TREBEDEN-NEGRE, H., JEAN, L., BON-DURAND, V., ANTONELLI, D., KLATZMANN, D. & BOYER, O. 2004. Long-term persistence of clonally expanded T cells in patients with polymyositis. *Ann Neurol,* 56**,** 867-72.

BERGGREN, O., HAGBERG, N., WEBER, G., ALM, G. V., RONNBLOM, L. & ELORANTA, M. L. 2012. B lymphocytes enhance interferon-alpha production by plasmacytoid dendritic cells. *Arthritis Rheum,* 64**,** 3409-19.

BETTELLI, E., CARRIER, Y., GAO, W., KORN, T., STROM, T. B., OUKKA, M., WEINER, H. L. & KUCHROO, V. K. 2006. Reciprocal developmental pathways for the generation of pathogenic effector TH17 and regulatory T cells. *Nature,* 441**,** 235-8.

BETTERIDGE, Z. & MCHUGH, N. 2016. Myositis-specific autoantibodies: an important tool to support diagnosis of myositis. *J Intern Med,* 280**,** 8-23.

BILGIC, H., YTTERBERG, S. R., AMIN, S., MCNALLAN, K. T., WILSON, J. C., KOEUTH, T., ELLINGSON, S., NEWMAN, B., BAUER, J. W., PETERSON, E. J., BAECHLER, E. C. & REED, A. M. 2009. Interleukin-6 and type I interferon-regulated genes and chemokines mark disease activity in dermatomyositis. *Arthritis Rheum,* 60**,** 3436-46.

BINGHAM, A., MAMYROVA, G., ROTHER, K. I., ORAL, E., COCHRAN, E., PREMKUMAR, A., KLEINER, D., JAMES-NEWTON, L., TARGOFF, I. N., PANDEY, J. P., CARRICK, D. M., SEBRING, N., O'HANLON, T. P., RUIZ-HIDALGO, M., TURNER, M., GORDON, L. B., LABORDA, J., BAUER, S. R., BLACKSHEAR, P. J., IMUNDO, L., MILLER, F. W., RIDER, L. G. & CHILDHOOD MYOSITIS HETEROGENEITY STUDY, G. 2008. Predictors of acquired lipodystrophy in juvenile-onset dermatomyositis and a gradient of severity. *Medicine (Baltimore),* 87**,** 70-86.

BLACK, R. A., RAUCH, C. T., KOZLOSKY, C. J., PESCHON, J. J., SLACK, J. L., WOLFSON, M. F., CASTNER, B. J., STOCKING, K. L., REDDY, P., SRINIVASAN, S., NELSON, N., BOIANI, N., SCHOOLEY, K. A., GERHART, M., DAVIS, R., FITZNER, J. N., JOHNSON, R. S., PAXTON, R. J., MARCH, C. J. & CERRETTI, D. P. 1997. A metalloproteinase disintegrin that releases tumour-necrosis factor-alpha from cells. *Nature,* 385**,** 729-33.

BLAIR, P. A., NORENA, L. Y., FLORES-BORJA, F., RAWLINGS, D. J., ISENBERG, D. A., EHRENSTEIN, M. R. & MAURI, C. 2010. CD19(+)CD24(hi)CD38(hi) B cells exhibit regulatory capacity in healthy individuals but are functionally impaired in systemic Lupus Erythematosus patients. *Immunity,* 32**,** 129-40.

BLANK, N., SCHILLER, M., KRIENKE, S., WABNITZ, G., HO, A. D. & LORENZ, H. M. 2007. Cholera toxin binds to lipid rafts but has a limited specificity for ganglioside GM1. *Immunol Cell Biol,* 85**,** 378-82.

BOHAN, A. & PETER, J. B. 1975a. Polymyositis and dermatomyositis (first of two parts). *N Engl J Med,* 292**,** 344-7.

BOHAN, A. & PETER, J. B. 1975b. Polymyositis and dermatomyositis (second of two parts). *N Engl J Med,* 292**,** 403-7.

BOHAN, A., PETER, J. B., BOWMAN, R. L. & PEARSON, C. M. 1977. Computer-assisted analysis of 153 patients with polymyositis and dermatomyositis. *Medicine (Baltimore),* 56**,** 255-86.

BOUWMEESTER, T., BAUCH, A., RUFFNER, H., ANGRAND, P. O., BERGAMINI, G., CROUGHTON, K., CRUCIAT, C., EBERHARD, D., GAGNEUR, J., GHIDELLI, S., HOPF, C., HUHSE, B., MANGANO, R., MICHON, A. M., SCHIRLE, M., SCHLEGL, J., SCHWAB, M., STEIN, M. A., BAUER, A., CASARI, G., DREWES, G., GAVIN, A. C., JACKSON, D. B., JOBERTY, G., NEUBAUER, G., RICK, J.,

KUSTER, B. & SUPERTI-FURGA, G. 2004. A physical and functional map of the human TNF-alpha/NF-kappa B signal transduction pathway. *Nat Cell Biol,* 6**,** 97-105.

BRACK, C., HIRAMA, M., LENHARD-SCHULLER, R. & TONEGAWA, S. 1978. A complete immunoglobulin gene is created by somatic recombination. *Cell,* 15**,** 1-14.

BRADLEY, J. R. 2008. TNF-mediated inflammatory disease. *J Pathol,* 214**,** 149-60.

BRAUN, D., CARAMALHO, I. & DEMENGEOT, J. 2002. IFN-alpha/beta enhances BCR-dependent B cell responses. *Int Immunol,* 14**,** 411-9.

BROERE, F. A., S. G.; SITKOVSKY, M. V.; VAN EDEN, W.; 2011. T cell subsets and T cell-mediated immunity. *Principles of Immunopharmacology, Springer basel AG,* 3rd revised and extended edition**,** 15-26.

BROWN, M. S. & GOLDSTEIN, J. L. 1980. Multivalent feedback regulation of HMG CoA reductase, a control mechanism coordinating isoprenoid synthesis and cell growth. *J Lipid Res,* 21**,** 505-17.

BUCKNER, J. H. 2010. Mechanisms of impaired regulation by CD4(+)CD25(+)FOXP3(+) regulatory T cells in human autoimmune diseases. *Nat Rev Immunol,* 10**,** 849-59.

CARSETTI, R., ROSADO, M. M. & WARDMANN, H. 2004. Peripheral development of B cells in mouse and man. *Immunol Rev,* 197**,** 179-91.

CASCIOLA-ROSEN, L., NAGARAJU, K., PLOTZ, P., WANG, K., LEVINE, S., GABRIELSON, E., CORSE, A. & ROSEN, A. 2005. Enhanced autoantigen expression in regenerating muscle cells in idiopathic inflammatory myopathy. *J Exp Med,* 201**,** 591-601.

CEDENO, S., CIFARELLI, D. F., BLASINI, A. M., PARIS, M., PLACERES, F., ALONSO, G. & RODRIGUEZ, M. A. 2003. Defective activity of ERK-1 and ERK-2 mitogen-activated protein kinases in peripheral blood T lymphocytes from patients with systemic lupus erythematosus: potential role of altered coupling of Ras guanine nucleotide exchange factor hSos to adapter protein Grb2 in lupus T cells. *Clin Immunol,* 106**,** 41-9.

CELHAR, T., MAGALHAES, R. & FAIRHURST, A. M. 2012. TLR7 and TLR9 in SLE: when sensing self goes wrong. *Immunol Res,* 53**,** 58-77.

CENCIARELLI, C., CHIAUR, D. S., GUARDAVACCARO, D., PARKS, W., VIDAL, M. & PAGANO, M. 1999. Identification of a family of human F-box proteins. *Curr Biol,* 9**,** 1177-9.

CEREDIG, R. & ROLINK, T. 2002. A positive look at double-negative thymocytes. *Nat Rev Immunol,* 2**,** 888-97.

CERIBELLI, A., DE SANTIS, M., ISAILOVIC, N., GERSHWIN, M. E. & SELMI, C. 2017. The Immune Response and the Pathogenesis of Idiopathic Inflammatory Myositis: a Critical Review. *Clin Rev Allergy Immunol,* 52**,** 58-70.

CHAN, H. L. 1985. Dermatomyositis and cancer in Singapore. *Int J Dermatol,* 24**,** 447-50.

CHARLES-SCHOEMAN, C., AMJADI, S. S., PAULUS, H. E., INTERNATIONAL MYOSITIS, A. & CLINICAL STUDIES, G. 2012. Treatment of dyslipidemia in idiopathic inflammatory myositis: results of the International Myositis Assessment and Clinical Studies Group survey. *Clin Rheumatol,* 31**,** 1163-8.

CHATHAM, W. W. & KIMBERLY, R. P. 2001. Treatment of lupus with corticosteroids. *Lupus,* 10**,** 140-7.

CHEN, Y. J., WU, C. Y., HUANG, Y. L., WANG, C. B., SHEN, J. L. & CHANG, Y. T. 2010. Cancer risks of dermatomyositis and polymyositis: a nationwide cohort study in Taiwan. *Arthritis Res Ther,* 12**,** R70.

CHEN, Y. J., WU, C. Y. & SHEN, J. L. 2001. Predicting factors of malignancy in dermatomyositis and polymyositis: a case-control study. *Br J Dermatol,* 144**,** 825-31.

CHEVREL, G., PAGE, G., GRANET, C., STREICHENBERGER, N., VARENNES, A. & MIOSSEC, P. 2003. Interleukin-17 increases the effects of IL-1 beta on muscle cells: arguments for the role of T cells in the pathogenesis of myositis. *J Neuroimmunol,* 137**,** 125-33.

CHINOY, H., SALWAY, F., FERTIG, N., SHEPHARD, N., TAIT, B. D., THOMSON, W., ISENBERG, D. A., ODDIS, C. V., SILMAN, A. J., OLLIER, W. E., COOPER, R. G. & COLLABORATION, U. K. A. O. M. I. C. 2006. In adult onset myositis, the presence of interstitial lung disease and myositis specific/associated antibodies are governed by HLA class II haplotype, rather than by myositis subtype. *Arthritis Res Ther,* 8**,** R13.

CHOW, W. H., GRIDLEY, G., MELLEMKJAER, L., MCLAUGHLIN, J. K., OLSEN, J. H. & FRAUMENI, J. F., JR. 1995. Cancer risk following polymyositis and dermatomyositis: a nationwide cohort study in Denmark. *Cancer Causes Control,* 6**,** 9-13.

CHRISTEN-ZAECH, S., SESHADRI, R., SUNDBERG, J., PALLER, A. S. & PACHMAN, L. M. 2008. Persistent association of nailfold capillaroscopy changes and skin involvement over thirty-six months with duration of untreated disease in patients with juvenile dermatomyositis. *Arthritis Rheum,* 58**,** 571-6.

CHRISTENSEN, M. L., PACHMAN, L. M., SCHNEIDERMAN, R., PATEL, D. C. & FRIEDMAN, J. M. 1986. Prevalence of Coxsackie B virus antibodies in patients with juvenile dermatomyositis. *Arthritis Rheum,* 29**,** 1365-70.

COLONNA, M., TRINCHIERI, G. & LIU, Y. J. 2004. Plasmacytoid dendritic cells in immunity. *Nat Immunol,* 5**,** 1219-26.

CONNORS, G. R., CHRISTOPHER-STINE, L., ODDIS, C. V. & DANOFF, S. K. 2010. Interstitial lung disease associated with the idiopathic inflammatory myopathies: what progress has been made in the past 35 years? *Chest,* 138**,** 1464-74.

CORCORAN, L., FERRERO, I., VREMEC, D., LUCAS, K., WAITHMAN, J., O'KEEFFE, M., WU, L., WILSON, A. & SHORTMAN, K. 2003. The lymphoid past of mouse plasmacytoid cells and thymic dendritic cells. *J Immunol,* 170**,** 4926-32.

COTTIN, V., THIVOLET-BEJUI, F., REYNAUD-GAUBERT, M., CADRANEL, J., DELAVAL, P., TERNAMIAN, P. J., CORDIER, J. F. & GROUPE D'ETUDES ET DE RECHERCHE SUR LES MALADIES "ORPHELINES, P. 2003. Interstitial lung disease in amyopathic dermatomyositis, dermatomyositis and polymyositis. *Eur Respir J,* 22**,** 245-50.

CROW, M. K. 2014. Type I interferon in the pathogenesis of lupus. *J Immunol,* 192**,** 5459-68.

CROW, M. K. 2016. Autoimmunity: Interferon alpha or beta: which is the culprit in autoimmune disease? *Nat Rev Rheumatol,* 12**,** 439-40.

CROW, Y. J. & CASANOVA, J. L. 2014. STING-associated vasculopathy with onset in infancy--a new interferonopathy. *N Engl J Med,* 371**,** 568-71.

CRUZ-ADALIA, A., JIMENEZ-BORREGUERO, L. J., RAMIREZ-HUESCA, M., CHICO-CALERO, I., BARREIRO, O., LOPEZ-CONESA, E., FRESNO, M., SANCHEZ-MADRID, F. & MARTIN, P. 2010. CD69 limits the severity of cardiomyopathy after autoimmune myocarditis. *Circulation,* 122**,** 1396-404.

DALAKAS, M. C. 1991. Polymyositis, dermatomyositis and inclusion-body myositis. *N Engl J Med,* 325**,** 1487-98.

DALAKAS, M. C. 2006. Mechanisms of disease: signaling pathways and immunobiology of inflammatory myopathies. *Nat Clin Pract Rheumatol,* 2**,** 219-27.

DALAKAS, M. C. 2010. Inflammatory muscle diseases: a critical review on pathogenesis and therapies. *Curr Opin Pharmacol,* 10**,** 346-52.

DALAKAS, M. C. 2015. Inflammatory muscle diseases. *N Engl J Med,* 372**,** 1734-47.

DALAKAS, M. C. & HOHLFELD, R. 2003. Polymyositis and dermatomyositis. *Lancet,* 362**,** 971-82.

DANOFF, S. K. & CASCIOLA-ROSEN, L. 2011. The lung as a possible target for the immune reaction in myositis. *Arthritis Res Ther,* 13**,** 230.

DASTMALCHI, M., GRUNDTMAN, C., ALEXANDERSON, H., MAVRAGANI, C. P., EINARSDOTTIR, H., HELMERS, S. B., ELVIN, K., CROW, M. K., NENNESMO, I. & LUNDBERG, I. E. 2008. A high incidence of disease flares in an open pilot study of infliximab in patients with refractory inflammatory myopathies. *Ann Rheum Dis,* 67**,** 1670-7.

DE JAGER, W., HOPPENREIJS, E. P., WULFFRAAT, N. M., WEDDERBURN, L. R., KUIS, W. & PRAKKEN, B. J. 2007. Blood and synovial fluid cytokine signatures in patients with juvenile idiopathic arthritis: a cross-sectional study. *Ann Rheum Dis,* 66**,** 589-98.

DE KRUIF, M. D., LEMAIRE, L. C., GIEBELEN, I. A., VAN ZOELEN, M. A., PATER, J. M., VAN DEN PANGAART, P. S., GROOT, A. P., DE VOS, A. F., ELLIOTT, P. J., MEIJERS, J. C., LEVI, M. & VAN DER POLL, T. 2007. Prednisolone dose-dependently influences inflammation and coagulation during human endotoxemia. *J Immunol,* 178**,** 1845-51.

DE PAEPE, B., CREUS, K. K. & DE BLEECKER, J. L. 2007. Chemokine profile of different inflammatory myopathies reflects humoral versus cytotoxic immune responses. *Ann N Y Acad Sci,* 1109**,** 441-53.

DE VISSER, M., EMSLIE-SMITH, A. M. & ENGEL, A. G. 1989. Early ultrastructural alterations in adult dermatomyositis. Capillary abnormalities precede other structural changes in muscle. *J Neurol Sci,* 94**,** 181-92.

DEAKIN, C. T., YASIN, S. A., SIMOU, S., ARNOLD, K. A., TANSLEY, S. L., BETTERIDGE, Z. E., MCHUGH, N. J., VARSANI, H., HOLTON, J. L., JACQUES, T. S., PILKINGTON, C. A., NISTALA, K., WEDDERBURN, L. R. & GROUP, U. K. J. D. R. 2016a. Muscle Biopsy Findings in Combination With Myositis-Specific Autoantibodies Aid Prediction of Outcomes in Juvenile Dermatomyositis. *Arthritis Rheumatol,* 68**,** 2806-2816.

DEANE, J. A., PISITKUN, P., BARRETT, R. S., FEIGENBAUM, L., TOWN, T., WARD, J. M., FLAVELL, R. A. & BOLLAND, S. 2007. Control of toll-like receptor 7 expression is essential to restrict autoimmunity and dendritic cell proliferation. *Immunity,* 27**,** 801-10.

DORNER, T., GIESECKE, C. & LIPSKY, P. E. 2011. Mechanisms of B cell autoimmunity in SLE. *Arthritis Res Ther,* 13**,** 243.

DUDDY, M. E., ALTER, A. & BAR-OR, A. 2004. Distinct profiles of human B cell effector cytokines: a role in immune regulation? *J Immunol,* 172**,** 3422-7.

EISENSTEIN, D. M., O'GORMAN, M. R. & PACHMAN, L. M. 1997. Correlations between change in disease activity and changes in peripheral blood lymphocyte subsets in patients with juvenile dermatomyositis. *J Rheumatol,* 24**,** 1830-2.

ELGUETA, R., BENSON, M. J., DE VRIES, V. C., WASIUK, A., GUO, Y. & NOELLE, R. J. 2009. Molecular mechanism and function of CD40/CD40L engagement in the immune system. *Immunol Rev,* 229**,** 152-72.

ELORANTA, M. L., BARBASSO HELMERS, S., ULFGREN, A. K., RONNBLOM, L., ALM, G. V. & LUNDBERG, I. E. 2007. A possible mechanism for endogenous activation of the type I interferon system in myositis patients with anti-Jo-1 or anti-Ro 52/anti-Ro 60 autoantibodies. *Arthritis Rheum,* 56**,** 3112-24.

EMSLIE-SMITH, A. M., ARAHATA, K. & ENGEL, A. G. 1989. Major histocompatibility complex class I antigen expression, immunolocalization of interferon subtypes, and T cell-mediated cytotoxicity in myopathies. *Hum Pathol,* 20**,** 224-31.

ERNSTE, F. C. & REED, A. M. 2013. Idiopathic inflammatory myopathies: current trends in pathogenesis, clinical features, and up-to-date treatment recommendations. *Mayo Clin Proc,* 88**,** 83-105.

ESPADA, G., MALDONADO COCCO, J. A., FERTIG, N. & ODDIS, C. V. 2009. Clinical and serologic characterization of an Argentine pediatric myositis cohort: identification of a novel autoantibody (anti-MJ) to a 142-kDa protein. *J Rheumatol,* 36**,** 2547-51.

FACCHETTI, F. & VERGONI, F. 2000. The plasmacytoid monocyte: from morphology to function. *Adv Clin Path,* 4**,** 187-90.

FALL, N., BOVE, K. E., STRINGER, K., LOVELL, D. J., BRUNNER, H. I., WEISS, J., HIGGINS, G. C., BOWYER, S. L., GRAHAM, T. B., THORNTON, S. & GROM, A. A. 2005. Association between lack of angiogenic response in muscle tissue and high expression of angiostatic ELR-negative CXC chemokines in patients with juvenile dermatomyositis: possible link to vasculopathy. *Arthritis Rheum,* 52**,** 3175-80.

FATHI, M., DASTMALCHI, M., RASMUSSEN, E., LUNDBERG, I. E. & TORNLING, G. 2004. Interstitial lung disease, a common manifestation of newly diagnosed polymyositis and dermatomyositis. *Ann Rheum Dis,* 63**,** 297-301.

FENG, D. & BARNES, B. J. 2013. Bioinformatics analysis of the factors controlling type I IFN gene expression in autoimmune disease and virus-induced immunity. *Front Immunol,* 4**,** 291.

FILLATREAU, S., SWEENIE, C. H., MCGEACHY, M. J., GRAY, D. & ANDERTON, S. M. 2002. B cells regulate autoimmunity by provision of IL-10. *Nat Immunol,* 3**,** 944-50.

FIORENTINO, D. F., CHUNG, L. S., CHRISTOPHER-STINE, L., ZABA, L., LI, S., MAMMEN, A. L., ROSEN, A. & CASCIOLA-ROSEN, L. 2013. Most patients with cancer-associated dermatomyositis have antibodies to nuclear matrix protein NXP-2 or transcription intermediary factor 1gamma. *Arthritis Rheum,* 65**,** 2954-62.

FIORENTINO, D. F., KUO, K., CHUNG, L., ZABA, L., LI, S. & CASCIOLA-ROSEN, L. 2015. Distinctive cutaneous and systemic features associated with antitranscriptional intermediary factor-1gamma antibodies in adults with dermatomyositis. *J Am Acad Dermatol,* 72**,** 449-55.

FLORES-BORJA, F., BOSMA, A., NG, D., REDDY, V., EHRENSTEIN, M. R., ISENBERG, D. A. & MAURI, C. 2013. CD19+CD24hiCD38hi B cells maintain regulatory T cells while limiting TH1 and TH17 differentiation. *Sci Transl Med,* 5**,** 173ra23.

FURIE, R., KHAMASHTA, M., MERRILL, J. T., WERTH, V. P., KALUNIAN, K., BROHAWN, P., ILLEI, G. G., DRAPPA, J., WANG, L., YOO, S. & INVESTIGATORS, C. D. S. 2017. Anifrolumab, an Anti-Interferon-alpha Receptor Monoclonal Antibody, in Moderate-to-Severe Systemic Lupus Erythematosus. *Arthritis Rheumatol,* 69**,** 376-386.

GASPAR, H. B., COORAY, S., GILMOUR, K. C., PARSLEY, K. L., ZHANG, F., ADAMS, S., BJORKEGREN, E., BAYFORD, J., BROWN, L., DAVIES, E. G., VEYS, P., FAIRBANKS, L., BORDON, V., PETROPOULOU, T., KINNON, C. & THRASHER, A. J. 2011. Hematopoietic stem cell gene therapy for adenosine deaminase-deficient severe combined immunodeficiency leads to long-term immunological recovery and metabolic correction. *Sci Transl Med,* 3**,** 97ra80.

GEISSMANN, F., MANZ, M. G., JUNG, S., SIEWEKE, M. H., MERAD, M. & LEY, K. 2010. Development of monocytes, macrophages, and dendritic cells. *Science,* 327**,** 656-61.

GHIRARDELLO, A., BASSI, N., PALMA, L., BORELLA, E., DOMENEGHETTI, M., PUNZI, L. & DORIA, A. 2013. Autoantibodies in polymyositis and dermatomyositis. *Curr Rheumatol Rep,* 15**,** 335.

GILTIAY, N. V., CHAPPELL, C. P., SUN, X., KOLHATKAR, N., TEAL, T. H., WIEDEMAN, A. E., KIM, J., TANAKA, L., BUECHLER, M. B., HAMERMAN, J. A., IMANISHI-KARI, T., CLARK, E. A. & ELKON, K. B. 2013. Overexpression of TLR7 promotes cell-intrinsic expansion and autoantibody production by transitional T1 B cells. *J Exp Med,* 210**,** 2773-89.

GLAESENER, S., QUACH, T. D., ONKEN, N., WELLER-HEINEMANN, F., DRESSLER, F., HUPPERTZ, H. I., THON, A. & MEYER-BAHLBURG, A. 2014. Distinct effects of methotrexate and etanercept on the B cell compartment in patients with juvenile idiopathic arthritis. *Arthritis Rheumatol,* 66**,** 2590-600.

GODFREY, D. I., KENNEDY, J., SUDA, T. & ZLOTNIK, A. 1993. A developmental pathway involving four phenotypically and functionally distinct subsets of CD3-CD4-CD8- triple-negative adult mouse thymocytes defined by CD44 and CD25 expression. *J Immunol,* 150**,** 4244-52.

GONO, T., KANEKO, H., KAWAGUCHI, Y., HANAOKA, M., KATAOKA, S., KUWANA, M., TAKAGI, K., ICHIDA, H., KATSUMATA, Y., OTA, Y., KAWASUMI, H. & YAMANAKA, H. 2014. Cytokine profiles in polymyositis and dermatomyositis complicated by rapidly progressive or chronic interstitial lung disease. *Rheumatology (Oxford),* 53**,** 2196-203.

GONZALEZ-AMARO, R., CORTES, J. R., SANCHEZ-MADRID, F. & MARTIN, P. 2013. Is CD69 an effective brake to control inflammatory diseases? *Trends Mol Med,* 19**,** 625-32.

GORDON, K. B., BLAUVELT, A., PAPP, K. A., LANGLEY, R. G., LUGER, T., OHTSUKI, M., REICH, K., AMATO, D., BALL, S. G., BRAUN, D. K., CAMERON, G. S., ERICKSON, J., KONRAD, R. J., MURAM, T. M., NICKOLOFF, B. J., OSUNTOKUN, O. O., SECREST, R. J., ZHAO, F., MALLBRIS, L., LEONARDI, C. L., GROUP, U.-S., GROUP, U.-S. & GROUP, U.-S. 2016. Phase 3 Trials of Ixekizumab in Moderate-to-Severe Plaque Psoriasis. *N Engl J Med,* 375**,** 345-56.

GORDON, S. 2002. Pattern recognition receptors: doubling up for the innate immune response. *Cell,* 111**,** 927-30.

GRASSI, M., CAPELLO, F., BERTOLINO, L., SEIA, Z. & PIPPIONE, M. 2009. Identification of granzyme B-expressing CD-8-positive T cells in lymphocytic inflammatory infiltrate in cutaneous lupus erythematosus and in dermatomyositis. *Clin Exp Dermatol,* 34**,** 910-4.

GRAY, D., GRAY, M. & BARR, T. 2007. Innate responses of B cells. *Eur J Immunol,* 37**,** 3304-10.

GREEN, N. M., LAWS, A., KIEFER, K., BUSCONI, L., KIM, Y. M., BRINKMANN, M. M., TRAIL, E. H., YASUDA, K., CHRISTENSEN, S. R., SHLOMCHIK, M. J., VOGEL, S., CONNOR, J. H., PLOEGH, H., EILAT, D., RIFKIN, I. R., VAN SEVENTER, J. M. & MARSHAK-ROTHSTEIN, A. 2009. Murine B cell response to TLR7 ligands depends on an IFN-beta feedback loop. *J Immunol,* 183**,** 1569-76.

GREENBERG, S. A., BRADSHAW, E. M., PINKUS, J. L., PINKUS, G. S., BURLESON, T., DUE, B., BREGOLI, L., O'CONNOR, K. C. & AMATO, A. A. 2005a. Plasma cells in muscle in inclusion body myositis and polymyositis. *Neurology,* 65**,** 1782-7.

GREENBERG, S. A., PINKUS, J. L., PINKUS, G. S., BURLESON, T., SANOUDOU, D., TAWIL, R., BAROHN, R. J., SAPERSTEIN, D. S., BRIEMBERG, H. R., ERICSSON, M., PARK, P. & AMATO, A. A. 2005b. Interferon-alpha/beta-mediated innate immune mechanisms in dermatomyositis. *Ann Neurol,* 57**,** 664-78.

GRUVER, A. L., HUDSON, L. L. & SEMPOWSKI, G. D. 2007. Immunosenescence of ageing. *J Pathol,* 211**,** 144-56.

GUNAWARDENA, H., WEDDERBURN, L. R., CHINOY, H., BETTERIDGE, Z. E., NORTH, J., OLLIER, W. E., COOPER, R. G., ODDIS, C. V., RAMANAN, A. V., DAVIDSON, J. E., MCHUGH, N. J., JUVENILE DERMATOMYOSITIS RESEARCH GROUP, U. K. & IRELAND 2009. Autoantibodies to a 140-kd protein in juvenile dermatomyositis are associated with calcinosis. *Arthritis Rheum,* 60**,** 1807-14.

GUNAWARDENA, H., WEDDERBURN, L. R., NORTH, J., BETTERIDGE, Z., DUNPHY, J., CHINOY, H., DAVIDSON, J. E., COOPER, R. G., MCHUGH, N. J. & JUVENILE DERMATOMYOSITIS RESEARCH GROUP, U. K. 2008. Clinical associations of autoantibodies to a p155/140 kDa doublet protein in juvenile dermatomyositis. *Rheumatology (Oxford),* 47**,** 324-8.

GUPTA, N. & DEFRANCO, A. L. 2007. Lipid rafts and B cell signaling. *Semin Cell Dev Biol,* 18**,** 616-26.

GUSEINOVA, D., CONSOLARO, A., TRAIL, L., FERRARI, C., PISTORIO, A., RUPERTO, N., BUONCOMPAGNI, A., PILKINGTON, C., MAILLARD, S., OLIVEIRA, S. K., SZTAJNBOK, F., CUTTICA, R., CORONA, F., KATSICAS, M. M., RUSSO, R., FERRIANI, V., BURGOS-VARGAS, R., SOLIS-VALLEJO, E., BANDEIRA, M., BACA, V., SAAD-MAGALHAES, C., SILVA, C. A., BARCELLONA, R., BREDA, L., CIMAZ, R., GALLIZZI, R., GAROZZO, R., MARTINO, S., MEINI, A., STABILE, A., MARTINI, A. & RAVELLI, A. 2011.

Comparison of clinical features and drug therapies among European and Latin American patients with juvenile dermatomyositis. *Clin Exp Rheumatol,* 29**,** 117-24.

HABERS, G. E., HUBER, A. M., MAMYROVA, G., TARGOFF, I. N., O'HANLON, T. P., ADAMS, S., PANDEY, J. P., BOONACKER, C., VAN BRUSSEL, M., MILLER, F. W., VAN ROYEN-KERKHOF, A., RIDER, L. G. & CHILDHOOD MYOSITIS HETEROGENEITY STUDY, G. 2016. Brief Report: Association of Myositis Autoantibodies, Clinical Features, and Environmental Exposures at Illness Onset With Disease Course in Juvenile Myositis. *Arthritis Rheumatol,* 68**,** 761-8.

HARMAN, B. C., JENKINSON, E. J. & ANDERSON, G. 2003. Microenvironmental regulation of Notch signalling in T cell development. *Semin Immunol,* 15**,** 91-7.

HARRIS, D. P., HAYNES, L., SAYLES, P. C., DUSO, D. K., EATON, S. M., LEPAK, N. M., JOHNSON, L. L., SWAIN, S. L. & LUND, F. E. 2000. Reciprocal regulation of polarized cytokine production by effector B and T cells. *Nat Immunol,* 1**,** 475-82.

HASHIZUME, M. & MIHARA, M. 2011. The roles of interleukin-6 in the pathogenesis of rheumatoid arthritis. *Arthritis,* 2011**,** 765624.

HIGGS, B. W., LIU, Z., WHITE, B., ZHU, W., WHITE, W. I., MOREHOUSE, C., BROHAWN, P., KIENER, P. A., RICHMAN, L., FIORENTINO, D., GREENBERG, S. A., JALLAL, B. & YAO, Y. 2011. Patients with systemic lupus erythematosus, myositis, rheumatoid arthritis and scleroderma share activation of a common type I interferon pathway. *Ann Rheum Dis,* 70**,** 2029-36.

HIGGS, B. W., ZHU, W., MOREHOUSE, C., WHITE, W. I., BROHAWN, P., GUO, X., REBELATTO, M., LE, C., AMATO, A., FIORENTINO, D., GREENBERG, S. A., DRAPPA, J., RICHMAN, L., GRETH, W., JALLAL, B. & YAO, Y. 2014. A phase 1b clinical trial evaluating sifalimumab, an anti-IFN-alpha monoclonal antibody, shows target neutralisation of a type I IFN signature in blood of dermatomyositis and polymyositis patients. *Ann Rheum Dis,* 73**,** 256-62.

HILL, C. L., ZHANG, Y., SIGURGEIRSSON, B., PUKKALA, E., MELLEMKJAER, L., AIRIO, A., EVANS, S. R. & FELSON, D. T. 2001. Frequency of specific cancer types in dermatomyositis and polymyositis: a population-based study. *Lancet,* 357**,** 96-100.

HOFBAUER, M., WIESENER, S., BABBE, H., ROERS, A., WEKERLE, H., DORNMAIR, K., HOHLFELD, R. & GOEBELS, N. 2003. Clonal tracking of autoaggressive T cells in polymyositis by combining laser microdissection, single-cell PCR, and CDR3-spectratype analysis. *Proc Natl Acad Sci U S A,* 100**,** 4090-5.

HOWARD, O. M., DONG, H. F., YANG, D., RABEN, N., NAGARAJU, K., ROSEN, A., CASCIOLA-ROSEN, L., HARTLEIN, M., KRON, M., YANG, D., YIADOM, K., DWIVEDI, S., PLOTZ, P. H. & OPPENHEIM, J. J. 2002. Histidyl-tRNA synthetase and asparaginyl-tRNA synthetase, autoantigens in myositis, activate chemokine receptors on T lymphocytes and immature dendritic cells. *J Exp Med,* 196**,** 781-91.

HUANG, E. Y., GALLEGOS, A. M., RICHARDS, S. M., LEHAR, S. M. & BEVAN, M. J. 2003. Surface expression of Notch1 on thymocytes: correlation with the double-negative to double-positive transition. *J Immunol,* 171**,** 2296-304.

HUANG, Y. L., CHEN, Y. J., LIN, M. W., WU, C. Y., LIU, P. C., CHEN, T. J., CHEN, Y. C., JIH, J. S., CHEN, C. C., LEE, D. D., CHANG, Y. T., WANG, W. J. & LIU, H. N. 2009. Malignancies associated with dermatomyositis and polymyositis in Taiwan: a nationwide population-based study. *Br J Dermatol,* 161**,** 854-60.

HUARD, C., GULLA, S. V., BENNETT, D. V., COYLE, A. J., VLEUGELS, R. A. & GREENBERG, S. A. 2017. Correlation of cutaneous disease activity with type 1 interferon gene signature and interferon beta in dermatomyositis. *Br J Dermatol,* 176**,** 1224-1230.

HUBER, A. M., FELDMAN, B. M., RENNEBOHM, R. M., HICKS, J. E., LINDSLEY, C. B., PEREZ, M. D., ZEMEL, L. S., WALLACE, C. A., BALLINGER, S. H., PASSO, M. H., REED, A. M., SUMMERS, R. M., WHITE, P. H., KATONA, I. M., MILLER, F. W., LACHENBRUCH, P. A., RIDER, L. G. & JUVENILE DERMATOMYOSITIS DISEASE ACTIVITY COLLABORATIVE STUDY, G. 2004. Validation and clinical significance of the Childhood Myositis Assessment Scale for assessment of muscle function in the juvenile idiopathic inflammatory myopathies. *Arthritis Rheum,* 50**,** 1595-603.

HUIZINGA, T. W., AMOS, C. I., VAN DER HELM-VAN MIL, A. H., CHEN, W., VAN GAALEN, F. A., JAWAHEER, D., SCHREUDER, G. M., WENER, M., BREEDVELD, F. C., AHMAD, N., LUM, R. F., DE VRIES, R. R., GREGERSEN, P. K., TOES, R. E. & CRISWELL, L. A. 2005. Refining the complex rheumatoid arthritis phenotype based on specificity of the HLA-DRB1 shared epitope for antibodies to citrullinated proteins. *Arthritis Rheum,* 52**,** 3433-8.

HUNTER, C. A. & JONES, S. A. 2015. IL-6 as a keystone cytokine in health and disease. *Nat Immunol,* 16**,** 448-57.

ICHIMURA, Y., MATSUSHITA, T., HAMAGUCHI, Y., KAJI, K., HASEGAWA, M., TANINO, Y., INOKOSHI, Y., KAWAI, K., KANEKURA, T., HABUCHI, M., IGARASHI, A., SOGAME, R., HASHIMOTO, T., KOGA, T., NISHINO, A., ISHIGURO, N., SUGIMOTO, N., AOKI, R., ANDO, N., ABE, T., KANDA, T., KUWANA, M., TAKEHARA, K. & FUJIMOTO, M. 2012. Anti-NXP2 autoantibodies in adult patients with idiopathic inflammatory myopathies: possible association with malignancy. *Ann Rheum Dis,* 71**,** 710-3.

ILLERA, V. A., PERANDONES, C. E., STUNZ, L. L., MOWER, D. A., JR. & ASHMAN, R. F. 1993. Apoptosis in splenic B lymphocytes. Regulation by protein kinase C and IL-4. *J Immunol,* 151**,** 2965-73.

ISHIHARA, N., SUZUKI, S., TANAKA, S., WATANABE, Y., NAGAYAMA, D., SAIKI, A., TANAKA, T. & TATSUNO, I. 2017. Atorvastatin increases Fads1, Fads2 and Elovl5 gene expression via the geranylgeranyl pyrophosphate-dependent Rho kinase pathway in 3T3-L1 cells. *Mol Med Rep,* 16**,** 4756-4762.

ISHII, W., MATSUDA, M., SHIMOJIMA, Y., ITOH, S., SUMIDA, T. & IKEDA, S. 2008. Flow cytometric analysis of lymphocyte subpopulations and TH1/TH2 balance in patients with polymyositis and dermatomyositis. *Intern Med,* 47**,** 1593-9.

IVASHKIV, L. B. & DONLIN, L. T. 2014. Regulation of type I interferon responses. *Nat Rev Immunol,* 14**,** 36-49.

JACOB, J., KELSOE, G., RAJEWSKY, K. & WEISS, U. 1991. Intraclonal generation of antibody mutants in germinal centres. *Nature,* 354**,** 389-92.

JEGO, G., BATAILLE, R. & PELLAT-DECEUNYNCK, C. 2001. Interleukin-6 is a growth factor for nonmalignant human plasmablasts. *Blood,* 97**,** 1817-22.

JIN, R. M., BLAIR, S. J., WARUNEK, J., HEFFNER, R. R., BLADER, I. J. & WOHLFERT, E. A. 2017. Regulatory T Cells Promote Myositis and Muscle Damage in Toxoplasma gondii Infection. *J Immunol,* 198**,** 352-362.

JONES, S. A., SCHELLER, J. & ROSE-JOHN, S. 2011. Therapeutic strategies for the clinical blockade of IL-6/gp130 signaling. *J Clin Invest,* 121**,** 3375-83.

JURY, E. C., FLORES-BORJA, F. & KABOURIDIS, P. S. 2007. Lipid rafts in T cell signalling and disease. *Semin Cell Dev Biol,* 18**,** 608-15.

KABOURIDIS, P. S. & JURY, E. C. 2008. Lipid rafts and T-lymphocyte function: implications for autoimmunity. *FEBS Lett,* 582**,** 3711-8.

KALAMPOKIS, I., VENTURI, G. M., POE, J. C., DVERGSTEN, J. A., SLEASMAN, J. W. & TEDDER, T. F. 2016. The regulatory B cell compartment expands transiently during childhood and is contracted in children with autoimmunity. *Arthritis Rheumatol*.

KALOGEROU, A., GELOU, E., MOUNTANTONAKIS, S., SETTAS, L., ZAFIRIOU, E. & SAKKAS, L. 2005. Early T cell activation in the skin from patients with systemic sclerosis. *Ann Rheum Dis,* 64**,** 1233-5.

KALUNIAN, K. C., MERRILL, J. T., MACIUCA, R., MCBRIDE, J. M., TOWNSEND, M. J., WEI, X., DAVIS, J. C., JR. & KENNEDY, W. P. 2016. A Phase II study of the efficacy and safety of rontalizumab (rhuMAb interferon-alpha) in patients with systemic lupus erythematosus (ROSE). *Ann Rheum Dis,* 75**,** 196-202.

KARPATI, G., POULIOT, Y. & CARPENTER, S. 1988. Expression of immunoreactive major histocompatibility complex products in human skeletal muscles. *Ann Neurol,* 23**,** 64-72.

KHAMASHTA, M., MERRILL, J. T., WERTH, V. P., FURIE, R., KALUNIAN, K., ILLEI, G. G., DRAPPA, J., WANG, L., GRETH, W. & INVESTIGATORS, C. D. S. 2016. Sifalimumab, an anti-interferon-alpha monoclonal antibody, in moderate to severe systemic lupus erythematosus: a randomised, double-blind, placebo-controlled study. *Ann Rheum Dis,* 75**,** 1909-1916.

KIDANI, Y. & BENSINGER, S. J. 2014. Lipids rule: resetting lipid metabolism restores T cell function in systemic lupus erythematosus. *J Clin Invest,* 124**,** 482-5.

KIEFER, K., OROPALLO, M. A., CANCRO, M. P. & MARSHAK-ROTHSTEIN, A. 2012. Role of type I interferons in the activation of autoreactive B cells. *Immunol Cell Biol,* 90**,** 498-504.

KIHARA, A. 2012. Very long-chain fatty acids: elongation, physiology and related disorders. *J Biochem,* 152**,** 387-95.

KIM, D., PERTEA, G., TRAPNELL, C., PIMENTEL, H., KELLEY, R. & SALZBERG, S. L. 2013. TopHat2: accurate alignment of transcriptomes in the presence of insertions, deletions and gene fusions. *Genome Biol,* 14**,** R36.

KISSEL, J. T., MENDELL, J. R. & RAMMOHAN, K. W. 1986. Microvascular deposition of complement membrane attack complex in dermatomyositis. *N Engl J Med,* 314**,** 329-34.

KLEIN, R., ROSENBACH, M., KIM, E. J., KIM, B., WERTH, V. P. & DUNHAM, J. 2010. Tumor necrosis factor inhibitor-associated dermatomyositis. *Arch Dermatol,* 146**,** 780-4.

KLEIN, U. & DALLA-FAVERA, R. 2008. Germinal centres: role in B-cell physiology and malignancy. *Nat Rev Immunol,* 8**,** 22-33.

KONDO, M., MURAKAWA, Y., HARASHIMA, N., KOBAYASHI, S., YAMAGUCHI, S. & HARADA, M. 2009. Roles of proinflammatory cytokines and the Fas/Fas ligand interaction in the pathogenesis of inflammatory myopathies. *Immunology,* 128**,** e589-99.

KORESSAAR, T. & REMM, M. 2007. Enhancements and modifications of primer design program Primer3. *Bioinformatics,* 23**,** 1289-91.

KURASAWA, K., NAWATA, Y., TAKABAYASHI, K., KUMANO, K., KITA, Y., TAKIGUCHI, Y., KURIYAMA, T., SUEISHI, M., SAITO, Y. & IWAMOTO, I. 2002. Activation of pulmonary T cells in corticosteroid-resistant and -sensitive interstitial pneumonitis in dermatomyositis/polymyositis. *Clin Exp Immunol,* 129**,** 541-8.

LAM, K. P., KUHN, R. & RAJEWSKY, K. 1997. In vivo ablation of surface immunoglobulin on mature B cells by inducible gene targeting results in rapid cell death. *Cell,* 90**,** 1073-83.

LANGLEY, R. G., ELEWSKI, B. E., LEBWOHL, M., REICH, K., GRIFFITHS, C. E., PAPP, K., PUIG, L., NAKAGAWA, H., SPELMAN, L., SIGURGEIRSSON, B., RIVAS, E., TSAI, T. F., WASEL, N., TYRING, S., SALKO, T., HAMPELE, I., NOTTER, M., KARPOV, A., HELOU, S., PAPAVASSILIS, C., GROUP, E. S. & GROUP, F. S. 2014. Secukinumab in plaque psoriasis--results of two phase 3 trials. *N Engl J Med,* 371**,** 326-38.

LAU, C. M., BROUGHTON, C., TABOR, A. S., AKIRA, S., FLAVELL, R. A., MAMULA, M. J., CHRISTENSEN, S. R., SHLOMCHIK, M. J., VIGLIANTI, G. A., RIFKIN, I. R. & MARSHAK-ROTHSTEIN, A. 2005. RNA-associated autoantigens activate B cells by combined B cell antigen receptor/Toll-like receptor 7 engagement. *J Exp Med,* 202**,** 1171-7.

LEBIEN, T. W. & TEDDER, T. F. 2008. B lymphocytes: how they develop and function. *Blood,* 112**,** 1570-80.

LEBWOHL, M., STROBER, B., MENTER, A., GORDON, K., WEGLOWSKA, J., PUIG, L., PAPP, K., SPELMAN, L., TOTH, D., KERDEL, F., ARMSTRONG, A. W., STINGL, G., KIMBALL, A. B., BACHELEZ, H., WU, J. J., CROWLEY, J., LANGLEY, R. G., BLICHARSKI, T., PAUL, C., LACOUR, J. P., TYRING, S., KIRCIK, L., CHIMENTI, S., CALLIS DUFFIN, K., BAGEL, J., KOO, J., ARAS, G., LI, J., SONG, W., MILMONT, C. E., SHI, Y., ERONDU, N., KLEKOTKA, P., KOTZIN, B. & NIRULA, A. 2015. Phase 3 Studies Comparing Brodalumab with Ustekinumab in Psoriasis. *N Engl J Med,* 373**,** 1318-28.

LEE, J., TAM, H., ADLER, L., ILSTAD-MINNIHAN, A., MACAUBAS, C. & MELLINS, E. D. 2017. The MHC class II antigen presentation pathway in human monocytes differs by subset and is regulated by cytokines. *PLoS One,* 12**,** e0183594.

LEE, S. W., JUNG, S. Y., PARK, M. C., PARK, Y. B. & LEE, S. K. 2006. Malignancies in Korean patients with inflammatory myopathy. *Yonsei Med J,* 47**,** 519-23.

LEGA, J. C., FABIEN, N., REYNAUD, Q., DURIEU, I., DURUPT, S., DUTERTRE, M., CORDIER, J. F. & COTTIN, V. 2014. The clinical phenotype associated with myositis-specific and associated autoantibodies: a meta-analysis revisiting the so-called antisynthetase syndrome. *Autoimmun Rev,* 13**,** 883-91.

LEGA, J. C., REYNAUD, Q., BELOT, A., FABIEN, N., DURIEU, I. & COTTIN, V. 2015. Idiopathic inflammatory myopathies and the lung. *Eur Respir Rev,* 24**,** 216-38.

LEVINE, S. M., RABEN, N., XIE, D., ASKIN, F. B., TUDER, R., MULLINS, M., ROSEN, A. & CASCIOLA-ROSEN, L. A. 2007. Novel conformation of histidyl-transfer RNA synthetase in the lung: the target tissue in Jo-1 autoantibody-associated myositis. *Arthritis Rheum,* 56**,** 2729-39.

LI, H., HANDSAKER, B., WYSOKER, A., FENNELL, T., RUAN, J., HOMER, N., MARTH, G., ABECASIS, G., DURBIN, R. & GENOME PROJECT DATA PROCESSING, S. 2009. The Sequence Alignment/Map format and SAMtools. *Bioinformatics,* 25**,** 2078-9.

LI, W., TIAN, X., LU, X., PENG, Q., SHU, X., YANG, H., LI, Y., WANG, Y., ZHANG, X., LIU, Q. & WANG, G. 2016. Significant decrease in peripheral regulatory B cells is an immunopathogenic feature of dermatomyositis. *Sci Rep,* 6**,** 27479.

LIAO, Y., SMYTH, G. K. & SHI, W. 2014. featureCounts: an efficient general purpose program for assigning sequence reads to genomic features. *Bioinformatics,* 30**,** 923-30.

LIMA, J., MARTINS, C., LEANDRO, M. J., NUNES, G., SOUSA, M. J., BRANCO, J. C. & BORREGO, L. M. 2016. Characterization of B cells in healthy pregnant women from late pregnancy to post-partum: a prospective observational study. *BMC Pregnancy Childbirth,* 16**,** 139.

LIU, B. S., CAO, Y., HUIZINGA, T. W., HAFLER, D. A. & TOES, R. E. 2014. TLR-mediated STAT3 and ERK activation controls IL-10 secretion by human B cells. *Eur J Immunol,* 44**,** 2121-9.

LOELL, I. M. P., J.; RAGHAVAN, S.; ZONG, M.; MALMSTROM, V.; LUNDBERG, IE. 2011. Persisting CD28(null) T cells, but not regulatory T cells, in muscle tissue of myositis patients after immunosuppressive therapy. *Arthritis Rheum,* 14**,** S86–S86.

LOPEZ DE PADILLA, C. M., VALLEJO, A. N., LACOMIS, D., MCNALLAN, K. & REED, A. M. 2009. Extranodal lymphoid microstructures in inflamed muscle and disease severity of new-onset juvenile dermatomyositis. *Arthritis Rheum,* 60**,** 1160-72.

LOPEZ DE PADILLA, C. M., VALLEJO, A. N., MCNALLAN, K. T., VEHE, R., SMITH, S. A., DIETZ, A. B., VUK-PAVLOVIC, S. & REED, A. M. 2007. Plasmacytoid dendritic cells in inflamed muscle of patients with juvenile dermatomyositis. *Arthritis Rheum,* 56**,** 1658-68.

LUNDBERG, I., ULFGREN, A. K., NYBERG, P., ANDERSSON, U. & KLARESKOG, L. 1997. Cytokine production in muscle tissue of patients with idiopathic inflammatory myopathies. *Arthritis Rheum,* 40**,** 865-74.

LUNDBERG, I. E. 2000. The role of cytokines, chemokines, and adhesion molecules in the pathogenesis of idiopathic inflammatory myopathies. *Curr Rheumatol Rep,* 2**,** 216-24.

LUNDBERG, I. E. & HELMERS, S. B. 2010. The type I interferon system in idiopathic inflammatory myopathies. *Autoimmunity,* 43**,** 239-43.

MALMSTROM, V., VENALIS, P. & ALBRECHT, I. 2012. T cells in myositis. *Arthritis Res Ther,* 14**,** 230.

MAMMEN, A. L. 2011. Autoimmune myopathies: autoantibodies, phenotypes and pathogenesis. *Nat Rev Neurol,* 7**,** 343-54.

MAMYROVA, G., O'HANLON, T. P., MONROE, J. B., CARRICK, D. M., MALLEY, J. D., ADAMS, S., REED, A. M., SHAMIM, E. A., JAMES-NEWTON, L., MILLER, F. W., RIDER, L. G. & CHILDHOOD MYOSITIS HETEROGENEITY COLLABORATIVE STUDY, G. 2006. Immunogenetic risk and protective factors for juvenile dermatomyositis in Caucasians. *Arthritis Rheum,* 54**,** 3979-87.

MAMYROVA, G., O'HANLON, T. P., SILLERS, L., MALLEY, K., JAMES-NEWTON, L., PARKS, C. G., COOPER, G. S., PANDEY, J. P., MILLER, F. W., RIDER, L. G. & CHILDHOOD MYOSITIS HETEROGENEITY COLLABORATIVE STUDY, G. 2008. Cytokine gene polymorphisms as risk and severity factors for juvenile dermatomyositis. *Arthritis Rheum,* 58**,** 3941-50.

MANTEGAZZA R, B. P. 2000-2013. Inflammatory Myopathies: Dermatomyositis, Polymyositis and Inclusion Body Myositis.

MARTIN, P., GOMEZ, M., LAMANA, A., MATESANZ MARIN, A., CORTES, J. R., RAMIREZ-HUESCA, M., BARREIRO, O., LOPEZ-ROMERO, P., GUTIERREZ-

VAZQUEZ, C., DE LA FUENTE, H., CRUZ-ADALIA, A. & SANCHEZ-MADRID, F. 2010. The leukocyte activation antigen CD69 limits allergic asthma and skin contact hypersensitivity. *J Allergy Clin Immunol,* 126**,** 355-65, 365 e1-3.

MASTAGLIA, F. L. & PHILLIPS, B. A. 2002. Idiopathic inflammatory myopathies: epidemiology, classification, and diagnostic criteria. *Rheum Dis Clin North Am,* 28**,** 723-41.

MATSUSHITA, T., HAMAGUCHI, Y., HASEGAWA, M., TAKEHARA, K. & FUJIMOTO, M. 2015. Decreased levels of regulatory B cells in patients with systemic sclerosis: association with autoantibody production and disease activity. *Rheumatology (Oxford).*

MAURI, C. & BOSMA, A. 2012. Immune regulatory function of B cells. *Annu Rev Immunol,* 30**,** 221-41.

MAURI, C., GRAY, D., MUSHTAQ, N. & LONDEI, M. 2003. Prevention of arthritis by interleukin 10-producing B cells. *J Exp Med,* 197**,** 489-501.

MAURI, C. & MENON, M. 2015. The many faces of type I interferon in systemic lupus erythematosus. *J Clin Invest,* 125**,** 2562-4.

MAVROPOULOS, A., SIMOPOULOU, T., VARNA, A., LIASKOS, C., KATSIARI, C., BOGDANOS, D. P. & SAKKAS, L. I. 2015. B regulatory cells are decreased and functionally impaired in patients with systemic sclerosis. *Arthritis Rheumatol.*

MAVROPOULOS, A., SIMOPOULOU, T., VARNA, A., LIASKOS, C., KATSIARI, C. G., BOGDANOS, D. P. & SAKKAS, L. I. 2016. Breg Cells Are Numerically Decreased and Functionally Impaired in Patients With Systemic Sclerosis. *Arthritis Rheumatol,* 68**,** 494-504.

MCCANN, L. J., JUGGINS, A. D., MAILLARD, S. M., WEDDERBURN, L. R., DAVIDSON, J. E., MURRAY, K. J., PILKINGTON, C. A. & JUVENILE DERMATOMYOSITIS RESEARCH, G. 2006. The Juvenile Dermatomyositis National Registry and Repository (UK and Ireland)--clinical characteristics of children recruited within the first 5 yr. *Rheumatology (Oxford),* 45**,** 1255-60.

MCDONALD, G., DEEPAK, S., MIGUEL, L., HALL, C. J., ISENBERG, D. A., MAGEE, A. I., BUTTERS, T. & JURY, E. C. 2014. Normalizing glycosphingolipids restores function in CD4+ T cells from lupus patients. *J Clin Invest,* 124**,** 712-24.

MCGOWAN, I., ANTON, P. A., ELLIOTT, J., CRANSTON, R. D., DUFFILL, K., ALTHOUSE, A. D., HAWKINS, K. L. & DE ROSA, S. C. 2015. Exploring the feasibility of multi-site flow cytometric processing of gut associated lymphoid tissue with centralized data analysis for multi-site clinical trials. *PLoS One,* 10**,** e0126454.

MCNIFF, J. M. & KAPLAN, D. H. 2008. Plasmacytoid dendritic cells are present in cutaneous dermatomyositis lesions in a pattern distinct from lupus erythematosus. *J Cutan Pathol,* 35**,** 452-6.

MEDSGER, T. A., JR., DAWSON, W. N., JR. & MASI, A. T. 1970. The epidemiology of polymyositis. *Am J Med,* 48**,** 715-23.

MELLMAN, I. & STEINMAN, R. M. 2001. Dendritic cells: specialized and regulated antigen processing machines. *Cell,* 106**,** 255-8.

MENON, M., BLAIR, P. A., ISENBERG, D. A. & MAURI, C. 2016. A Regulatory Feedback between Plasmacytoid Dendritic Cells and Regulatory B Cells Is Aberrant in Systemic Lupus Erythematosus. *Immunity,* 44**,** 683-97.

MEYER, C., WALKER, J., DEWANE, J., ENGELMANN, F., LAUB, W., PILLAI, S., THOMAS, C. R., JR. & MESSAOUDI, I. 2015. Impact of irradiation and immunosuppressive agents on immune system homeostasis in rhesus macaques. *Clin Exp Immunol,* 181**,** 491-510.

MILLER, F. W., COOPER, R. G., VENCOVSKY, J., RIDER, L. G., DANKO, K., WEDDERBURN, L. R., LUNDBERG, I. E., PACHMAN, L. M., REED, A. M., YTTERBERG, S. R., PADYUKOV, L., SELVA-O'CALLAGHAN, A., RADSTAKE, T. R., ISENBERG, D. A., CHINOY, H., OLLIER, W. E., O'HANLON, T. P., PENG, B., LEE, A., LAMB, J. A., CHEN, W., AMOS, C. I., GREGERSEN, P. K. & MYOSITIS GENETICS, C. 2013. Genome-wide association study of dermatomyositis reveals genetic overlap with other autoimmune disorders. *Arthritis Rheum,* 65**,** 3239-47.

MIOSSEC, P. 2017. Update on interleukin-17: a role in the pathogenesis of inflammatory arthritis and implication for clinical practice. *RMD Open,* 3**,** e000284.

MIOSSEC, P. & KOLLS, J. K. 2012. Targeting IL-17 and TH17 cells in chronic inflammation. *Nat Rev Drug Discov,* 11**,** 763-76.

MIOSSEC, P., KORN, T. & KUCHROO, V. K. 2009. Interleukin-17 and type 17 helper T cells. *N Engl J Med,* 361**,** 888-98.

MIZOGUCHI, A., MIZOGUCHI, E., TAKEDATSU, H., BLUMBERG, R. S. & BHAN, A. K. 2002. Chronic intestinal inflammatory condition generates IL-10-producing regulatory B cell subset characterized by CD1d upregulation. *Immunity,* 16**,** 219-30.

MIZUNO, K., YACHIE, A., NAGAOKI, S., WADA, H., OKADA, K., KAWACHI, M., TOMA, T., KONNO, A., OHTA, K., KASAHARA, Y. & KOIZUMI, S. 2004. Oligoclonal expansion of circulating and tissue-infiltrating CD8+ T cells with killer/effector phenotypes in juvenile dermatomyositis syndrome. *Clin Exp Immunol,* 137**,** 187-94.

MOHASSEL, P. & MAMMEN, A. L. 2013. Statin-associated autoimmune myopathy and anti-HMGCR autoantibodies. *Muscle Nerve,* 48**,** 477-83.

MORBACH, H., EICHHORN, E. M., LIESE, J. G. & GIRSCHICK, H. J. 2010. Reference values for B cell subpopulations from infancy to adulthood. *Clin Exp Immunol,* 162**,** 271-9.

NAGARAJU, K., CASCIOLA-ROSEN, L., LUNDBERG, I., RAWAT, R., CUTTING, S., THAPLIYAL, R., CHANG, J., DWIVEDI, S., MITSAK, M., CHEN, Y. W., PLOTZ, P., ROSEN, A., HOFFMAN, E. & RABEN, N. 2005. Activation of the endoplasmic reticulum stress response in autoimmune myositis: potential role in muscle fiber damage and dysfunction. *Arthritis Rheum,* 52**,** 1824-35.

NAGARAJU, K., RABEN, N., LOEFFLER, L., PARKER, T., ROCHON, P. J., LEE, E., DANNING, C., WADA, R., THOMPSON, C., BAHTIYAR, G., CRAFT, J., HOOFT VAN HUIJSDUIJNEN, R. & PLOTZ, P. 2000. Conditional up-regulation of MHC class I in skeletal muscle leads to self-sustaining autoimmune myositis and myositis-specific autoantibodies. *Proc Natl Acad Sci U S A,* 97**,** 9209-14.

NAGARAJU, K., RIDER, L. G., FAN, C., CHEN, Y. W., MITSAK, M., RAWAT, R., PATTERSON, K., GRUNDTMAN, C., MILLER, F. W., PLOTZ, P. H., HOFFMAN, E. & LUNDBERG, I. E. 2006. Endothelial cell activation and neovascularization are prominent in dermatomyositis. *J Autoimmune Dis,* 3**,** 2.

NARAZAKI, M., HAGIHARA, K., SHIMA, Y., OGATA, A., KISHIMOTO, T. & TANAKA, T. 2011. Therapeutic effect of tocilizumab on two patients with polymyositis. *Rheumatology (Oxford),* 50**,** 1344-6.

NEUFELD, K. M., KARUNANAYAKE, C. P., MAENZ, L. Y. & ROSENBERG, A. M. 2013. Stressful life events antedating chronic childhood arthritis. *J Rheumatol,* 40**,** 1756-65.

NG, C. T., MENDOZA, J. L., GARCIA, K. C. & OLDSTONE, M. B. 2016. Alpha and Beta Type 1 Interferon Signaling: Passage for Diverse Biologic Outcomes. *Cell,* 164**,** 349-52.

NIEWOLD, T. B., KARIUKI, S. N., MORGAN, G. A., SHRESTHA, S. & PACHMAN, L. M. 2009. Elevated serum interferon-alpha activity in juvenile dermatomyositis: associations with disease activity at diagnosis and after thirty-six months of therapy. *Arthritis Rheum,* 60**,** 1815-24.

NISTALA, K., VARSANI, H., WITTKOWSKI, H., VOGL, T., KROL, P., SHAH, V., MAMCHAOUI, K., BROGAN, P. A., ROTH, J. & WEDDERBURN, L. R. 2013. Myeloid related protein induces muscle derived inflammatory mediators in juvenile dermatomyositis. *Arthritis Res Ther,* 15**,** R131.

NISTALA, K. & WEDDERBURN, L. R. 2013. Update in juvenile myositis. *Curr Opin Rheumatol,* 25**,** 742-6.

NUTT, S. L., HEAVEY, B., ROLINK, A. G. & BUSSLINGER, M. 1999. Commitment to the B-lymphoid lineage depends on the transcription factor Pax5. *Nature,* 401**,** 556-62.

NYUGEN, J., AGRAWAL, S., GOLLAPUDI, S. & GUPTA, S. 2010. Impaired functions of peripheral blood monocyte subpopulations in aged humans. *J Clin Immunol,* 30**,** 806-13.

O'GORMAN, M. R., CORROCHANO, V., ROLECK, J., DONOVAN, M. & PACHMAN, L. M. 1995. Flow cytometric analyses of the lymphocyte subsets in peripheral blood of children with untreated active juvenile dermatomyositis. *Clin Diagn Lab Immunol,* 2**,** 205-8.

ODDIS, C. V. & AGGARWAL, R. 2018. Treatment in myositis. *Nat Rev Rheumatol,* 14**,** 279-289.

ODDIS, C. V., CONTE, C. G., STEEN, V. D. & MEDSGER, T. A., JR. 1990. Incidence of polymyositis-dermatomyositis: a 20-year study of hospital diagnosed cases in Allegheny County, PA 1963-1982. *J Rheumatol,* 17**,** 1329-34.

ODDIS, C. V., OKANO, Y., RUDERT, W. A., TRUCCO, M., DUQUESNOY, R. J. & MEDSGER, T. A., JR. 1992. Serum autoantibody to the nucleolar antigen PM-Scl. Clinical and immunogenetic associations. *Arthritis Rheum,* 35**,** 1211-7.

ODDIS, C. V., REED, A. M., AGGARWAL, R., RIDER, L. G., ASCHERMAN, D. P., LEVESQUE, M. C., BAROHN, R. J., FELDMAN, B. M., HARRIS-LOVE, M. O., KOONTZ, D. C., FERTIG, N., KELLEY, S. S., PRYBER, S. L., MILLER, F. W., ROCKETTE, H. E. & GROUP, R. I. M. S. 2013. Rituximab in the treatment of refractory adult and juvenile dermatomyositis and adult polymyositis: a randomized, placebo-phase trial. *Arthritis Rheum,* 65**,** 314-24.

ODDIS, C. V., SCIURBA, F. C., ELMAGD, K. A. & STARZL, T. E. 1999. Tacrolimus in refractory polymyositis with interstitial lung disease. *Lancet,* 353**,** 1762-3.

OGATA, A., KUMANOGOH, A. & TANAKA, T. 2012. Pathological role of interleukin-6 in psoriatic arthritis. *Arthritis,* 2012**,** 713618.

OKUDA, Y. 2008. Review of tocilizumab in the treatment of rheumatoid arthritis. *Biologics,* 2**,** 75-82.

PACHMAN, L. M., LIOTTA-DAVIS, M. R., HONG, D. K., KINSELLA, T. R., MENDEZ, E. P., KINDER, J. M. & CHEN, E. H. 2000. TNFalpha-308A allele in juvenile dermatomyositis: association with increased production of tumor necrosis factor alpha, disease duration, and pathologic calcifications. *Arthritis Rheum,* 43**,** 2368-77.

PACHMAN, L. M., LIPTON, R., RAMSEY-GOLDMAN, R., SHAMIYEH, E., ABBOTT, K., MENDEZ, E. P., DYER, A., CURDY, D. M., VOGLER, L., REED, A., CAWKWELL, G., ZEMEL, L., SANDBORG, C., RIVAS-CHACON, R., HOM, C., ILOWITE, N., GEDALIA, A., GITLIN, J. & BORZY, M. 2005. History of infection before the onset of juvenile dermatomyositis: results from the National Institute of Arthritis and Musculoskeletal and Skin Diseases Research Registry. *Arthritis Rheum,* 53**,** 166-72.

PAGE, G., CHEVREL, G. & MIOSSEC, P. 2004. Anatomic localization of immature and mature dendritic cell subsets in dermatomyositis and polymyositis: Interaction with chemokines and Th1 cytokine-producing cells. *Arthritis Rheum,* 50**,** 199-208.

PASSLICK, B., FLIEGER, D. & ZIEGLER-HEITBROCK, H. W. 1989. Identification and characterization of a novel monocyte subpopulation in human peripheral blood. *Blood,* 74**,** 2527-34.

PENG, J. C., SHEEN, T. S. & HSU, M. M. 1995. Nasopharyngeal carcinoma with dermatomyositis. Analysis of 12 cases. *Arch Otolaryngol Head Neck Surg,* 121**,** 1298-301.

PIKE, L. J. 2003. Lipid rafts: bringing order to chaos. *J Lipid Res,* 44**,** 655-67.

QUAN, C., ZHANGBAO, J., LU, J., ZHAO, C., CAI, T., WANG, B., YU, H., QIAO, J. & LU, C. 2015. The immune balance between memory and regulatory B cells in NMO and the changes of the balance after methylprednisolone or rituximab therapy. *J Neuroimmunol,* 282**,** 45-53.

RADSTAKE, T. R., VAN BON, L., BROEN, J., HUSSIANI, A., HESSELSTRAND, R., WUTTGE, D. M., DENG, Y., SIMMS, R., LUBBERTS, E. & LAFYATIS, R. 2009. The pronounced Th17 profile in systemic sclerosis (SSc) together with intracellular expression of TGFbeta and IFNgamma distinguishes SSc phenotypes. *PLoS One,* 4**,** e5903.

RAVELLI, A., TRAIL, L., FERRARI, C., RUPERTO, N., PISTORIO, A., PILKINGTON, C., MAILLARD, S., OLIVEIRA, S. K., SZTAJNBOK, F., CUTTICA, R., BELTRAMELLI, M., CORONA, F., KATSICAS, M. M., RUSSO, R., FERRIANI, V., BURGOS-VARGAS, R., MAGNI-MANZONI, S., SOLIS-VALLEOJ, E., BANDEIRA, M., ZULIAN, F., BACA, V., CORTIS, E., FALCINI, F., ALESSIO, M., ALPIGIANI, M. G., GERLONI, V., SAAD-MAGALHAES, C., PODDA, R., SILVA, C. A., LEPORE, L., FELICI, E., ROSSI, F., SALA, E. & MARTINI, A. 2010. Long-term outcome and prognostic factors of juvenile dermatomyositis: a multinational, multicenter study of 490 patients. *Arthritis Care Res (Hoboken),* 62**,** 63-72.

RAYAVARAPU, S., COLEY, W., KINDER, T. B. & NAGARAJU, K. 2013. Idiopathic inflammatory myopathies: pathogenic mechanisms of muscle weakness. *Skelet Muscle,* 3**,** 13.

REED, A. M. 2001. Myositis in children. *Curr Opin Rheumatol,* 13**,** 428-33.

REED, A. M. & ERNSTE, F. 2009. The inflammatory milieu in idiopathic inflammatory myositis. *Curr Rheumatol Rep,* 11**,** 295-301.

RICE, G. I., DEL TORO DUANY, Y., JENKINSON, E. M., FORTE, G. M., ANDERSON, B. H., ARIAUDO, G., BADER-MEUNIER, B., BAILDAM, E. M., BATTINI, R., BERESFORD, M. W., CASARANO, M., CHOUCHANE, M., CIMAZ, R., COLLINS, A. E., CORDEIRO, N. J., DALE, R. C., DAVIDSON, J. E., DE WAELE, L., DESGUERRE, I., FAIVRE, L., FAZZI, E., ISIDOR, B., LAGAE, L., LATCHMAN, A. R., LEBON, P., LI, C., LIVINGSTON, J. H., LOURENCO, C. M., MANCARDI, M. M., MASUREL-PAULET, A., MCINNES, I. B., MENEZES, M. P., MIGNOT, C., O'SULLIVAN, J., ORCESI, S., PICCO, P. P., RIVA, E., ROBINSON, R. A., RODRIGUEZ, D., SALVATICI, E., SCOTT, C., SZYBOWSKA, M., TOLMIE, J. L., VANDERVER, A., VANHULLE, C., VIEIRA, J. P., WEBB, K., WHITNEY, R. N., WILLIAMS, S. G., WOLFE, L. A., ZUBERI, S. M., HUR, S. & CROW, Y. J. 2014.

Gain-of-function mutations in IFIH1 cause a spectrum of human disease phenotypes associated with upregulated type I interferon signaling. *Nat Genet,* 46**,** 503-509.

RICHARDS, T. J., EGGEBEEN, A., GIBSON, K., YOUSEM, S., FUHRMAN, C., GOCHUICO, B. R., FERTIG, N., ODDIS, C. V., KAMINSKI, N., ROSAS, I. O. & ASCHERMAN, D. P. 2009. Characterization and peripheral blood biomarker assessment of anti-Jo-1 antibody-positive interstitial lung disease. *Arthritis Rheum,* 60**,** 2183-92.

RIDER, L. G., FELDMAN, B. M., PEREZ, M. D., RENNEBOHM, R. M., LINDSLEY, C. B., ZEMEL, L. S., WALLACE, C. A., BALLINGER, S. H., BOWYER, S. L., REED, A. M., PASSO, M. H., KATONA, I. M., MILLER, F. W. & LACHENBRUCH, P. A. 1997. Development of validated disease activity and damage indices for the juvenile idiopathic inflammatory myopathies: I. Physician, parent, and patient global assessments. Juvenile Dermatomyositis Disease Activity Collaborative Study Group. *Arthritis Rheum,* 40**,** 1976-83.

RIDER, L. G., KOZIOL, D., GIANNINI, E. H., JAIN, M. S., SMITH, M. R., WHITNEY-MAHONEY, K., FELDMAN, B. M., WRIGHT, S. J., LINDSLEY, C. B., PACHMAN, L. M., VILLALBA, M. L., LOVELL, D. J., BOWYER, S. L., PLOTZ, P. H., MILLER, F. W. & HICKS, J. E. 2010. Validation of manual muscle testing and a subset of eight muscles for adult and juvenile idiopathic inflammatory myopathies. *Arthritis Care Res (Hoboken),* 62**,** 465-72.

RIDER, L. G., LINDSLEY, C. B. & MILLER, F. W. 2016. Juvenile Dermatomyositis. *In:* PETTY, R. E., LAXER, R. M., LINDSLEY, C. B. & WEDDERBURN, L. R. (eds.) *Textbook of Pediatric Rheumatology*
. 7th ed. 1600 John F. Kennedy Blvd.
Ste 1800
Philadelphia
PA 19103-2899
: Elsevier.

RIDER, L. G., SHAH, M., MAMYROVA, G., HUBER, A. M., RICE, M. M., TARGOFF, I. N., MILLER, F. W. & CHILDHOOD MYOSITIS HETEROGENEITY COLLABORATIVE STUDY, G. 2013. The myositis autoantibody phenotypes of the juvenile idiopathic inflammatory myopathies. *Medicine (Baltimore),* 92**,** 223-43.

ROBINSON, M. D., MCCARTHY, D. J. & SMYTH, G. K. 2010. edgeR: a Bioconductor package for differential expression analysis of digital gene expression data. *Bioinformatics,* 26**,** 139-40.

ROGACEV, K. S., CREMERS, B., ZAWADA, A. M., SEILER, S., BINDER, N., EGE, P., GROSSE-DUNKER, G., HEISEL, I., HORNOF, F., JEKEN, J., REBLING, N. M., ULRICH, C., SCHELLER, B., BOHM, M., FLISER, D. & HEINE, G. H. 2012. CD14++CD16+ monocytes independently predict cardiovascular events: a cohort study of 951 patients referred for elective coronary angiography. *J Am Coll Cardiol,* 60**,** 1512-20.

RONNBLOM, L. & ELKON, K. B. 2010. Cytokines as therapeutic targets in SLE. *Nat Rev Rheumatol,* 6**,** 339-47.

RONNBLOM, L. & ELORANTA, M. L. 2013. The interferon signature in autoimmune diseases. *Curr Opin Rheumatol,* 25**,** 248-53.

ROSTASY, K. M., PIEPKORN, M., GOEBEL, H. H., MENCK, S., HANEFELD, F. & SCHULZ-SCHAEFFER, W. J. 2004. Monocyte/macrophage differentiation in dermatomyositis and polymyositis. *Muscle Nerve,* 30**,** 225-30.

ROSTASY, K. M., SCHMIDT, J., BAHN, E., PFANDER, T., PIEPKORN, M., WILICHOWSKI, E. & SCHULZ-SCHAEFFER, J. 2008. Distinct inflammatory properties of late-activated macrophages in inflammatory myopathies. *Acta Myol,* 27**,** 49-53.

ROWE, D. J., ISENBERG, D. A., MCDOUGALL, J. & BEVERLEY, P. C. 1981. Characterization of polymyositis infiltrates using monoclonal antibodies to human leucocyte antigens. *Clin Exp Immunol,* 45**,** 290-8.

SALAJEGHEH, M., RAKOCEVIC, G., RAJU, R., SHATUNOV, A., GOLDFARB, L. G. & DALAKAS, M. C. 2007. T cell receptor profiling in muscle and blood lymphocytes in sporadic inclusion body myositis. *Neurology,* 69**,** 1672-9.

SALOMONSSON, S. & LUNDBERG, I. E. 2006. Cytokines in idiopathic inflammatory myopathies. *Autoimmunity,* 39**,** 177-90.

SANCHO, D., GOMEZ, M. & SANCHEZ-MADRID, F. 2005. CD69 is an immunoregulatory molecule induced following activation. *Trends Immunol,* 26**,** 136-40.

SARAIVA, M. & O'GARRA, A. 2010. The regulation of IL-10 production by immune cells. *Nat Rev Immunol,* 10**,** 170-81.

SATO, J. O., SALLUM, A. M., FERRIANI, V. P., MARINI, R., SACCHETTI, S. B., OKUDA, E. M., CARVALHO, J. F., PEREIRA, R. M., LEN, C. A., TERRERI, M. T., LOTUFO, S. A., ROMANELLI, P. R., RAMOS, V. C., HILARIO, M. O., SILVA, C. A., CORRENTE, J. E., SAAD-MAGALHAES, C. & RHEUMATOLOGY COMMITTEE OF THE SAO PAULO PAEDIATRICS, S. 2009. A Brazilian registry of juvenile dermatomyositis: onset features and classification of 189 cases. *Clin Exp Rheumatol,* 27**,** 1031-8.

SATO, M., HATA, N., ASAGIRI, M., NAKAYA, T., TANIGUCHI, T. & TANAKA, N. 1998. Positive feedback regulation of type I IFN genes by the IFN-inducible transcription factor IRF-7. *FEBS Lett,* 441**,** 106-10.

SCHELLER, J., CHALARIS, A., SCHMIDT-ARRAS, D. & ROSE-JOHN, S. 2011. The pro- and anti-inflammatory properties of the cytokine interleukin-6. *Biochim Biophys Acta,* 1813**,** 878-88.

SCHETT, G., ELEWAUT, D., MCINNES, I. B., DAYER, J. M. & NEURATH, M. F. 2013. How cytokine networks fuel inflammation: Toward a cytokine-based disease taxonomy. *Nat Med,* 19**,** 822-4.

SCHMIDT, J., BARTHEL, K., WREDE, A., SALAJEGHEH, M., BAHR, M. & DALAKAS, M. C. 2008. Interrelation of inflammation and APP in sIBM: IL-1 beta induces accumulation of beta-amyloid in skeletal muscle. *Brain,* 131**,** 1228-40.

SCHWARTZ, T., SJAASTAD, I., FLATO, B., VISTNES, M., CHRISTENSEN, G. & SANNER, H. 2014. In active juvenile dermatomyositis, elevated eotaxin and MCP-1 and cholesterol levels in the upper normal range are associated with cardiac dysfunction. *Rheumatology (Oxford),* 53**,** 2214-22.

SEZGIN, E., LEVENTAL, I., MAYOR, S. & EGGELING, C. 2017. The mystery of membrane organization: composition, regulation and roles of lipid rafts. *Nat Rev Mol Cell Biol,* 18**,** 361-374.

SHAH, M., MAMYROVA, G., TARGOFF, I. N., HUBER, A. M., MALLEY, J. D., RICE, M. M., MILLER, F. W., RIDER, L. G. & CHILDHOOD MYOSITIS HETEROGENEITY COLLABORATIVE STUDY, G. 2013. The clinical phenotypes of the juvenile idiopathic inflammatory myopathies. *Medicine (Baltimore),* 92**,** 25-41.

SHAMIM, E. A., RIDER, L. G., PANDEY, J. P., O'HANLON, T. P., JARA, L. J., SAMAYOA, E. A., BURGOS-VARGAS, R., VAZQUEZ-MELLADO, J., ALCOCER-VARELA, J., SALAZAR-PARAMO, M., KUTZBACH, A. G., MALLEY, J. D., TARGOFF, I. N., GARCIA-DE LA TORRE, I. & MILLER, F. W. 2002. Differences in idiopathic inflammatory myopathy phenotypes and genotypes between Mesoamerican Mestizos and North American Caucasians: ethnogeographic influences in the genetics and clinical expression of myositis. *Arthritis Rheum,* 46**,** 1885-93.

SHAPIRO-SHELEF, M. & CALAME, K. 2005. Regulation of plasma-cell development. *Nat Rev Immunol,* 5**,** 230-42.

SIGURDSSON, S., NORDMARK, G., GORING, H. H., LINDROOS, K., WIMAN, A. C., STURFELT, G., JONSEN, A., RANTAPAA-DAHLQVIST, S., MOLLER, B., KERE, J., KOSKENMIES, S., WIDEN, E., ELORANTA, M. L., JULKUNEN, H., KRISTJANSDOTTIR, H., STEINSSON, K., ALM, G., RONNBLOM, L. & SYVANEN, A. C. 2005. Polymorphisms in the tyrosine kinase 2 and interferon regulatory factor 5 genes are associated with systemic lupus erythematosus. *Am J Hum Genet,* 76**,** 528-37.

SOLOMON, G. J. & MAGRO, C. M. 2008. Foxp3 expression in cutaneous T-cell lymphocytic infiltrates. *J Cutan Pathol,* 35**,** 1032-9.

SOTTINI, A., GHIDINI, C., ZANOTTI, C., CHIARINI, M., CAIMI, L., LANFRANCHI, A., MORATTO, D., PORTA, F. & IMBERTI, L. 2010. Simultaneous quantification of recent thymic T-cell and bone marrow B-cell emigrants in patients with primary immunodeficiency undergone to stem cell transplantation. *Clin Immunol,* 136**,** 217-27.

SPANN, N. J. & GLASS, C. K. 2013. Sterols and oxysterols in immune cell function. *Nat Immunol,* 14**,** 893-900.

STONE, R. C., FENG, D., DENG, J., SINGH, S., YANG, L., FITZGERALD-BOCARSLY, P., ELORANTA, M. L., RONNBLOM, L. & BARNES, B. J. 2012.

Interferon regulatory factor 5 activation in monocytes of systemic lupus erythematosus patients is triggered by circulating autoantigens independent of type I interferons. *Arthritis Rheum,* 64**,** 788-98.

STRELKAUSKAS, A. J., SCHAUF, V. & DRAY, S. 1976. Alterations in T, B, and null cells in children with autoimmune diseases. *Clin Immunol Immunopathol,* 6**,** 359-68.

SUBRAMANIAN, A., TAMAYO, P., MOOTHA, V. K., MUKHERJEE, S., EBERT, B. L., GILLETTE, M. A., PAULOVICH, A., POMEROY, S. L., GOLUB, T. R., LANDER, E. S. & MESIROV, J. P. 2005. Gene set enrichment analysis: a knowledge-based approach for interpreting genome-wide expression profiles. *Proc Natl Acad Sci U S A,* 102**,** 15545-50.

SULTAN, S. M., ALLEN, E., ODDIS, C. V., KIELY, P., COOPER, R. G., LUNDBERG, I. E., VENCOVSKY, J. & ISENBERG, D. A. 2008. Reliability and validity of the myositis disease activity assessment tool. *Arthritis Rheum,* 58**,** 3593-9.

SWIRSKI, F. K., NAHRENDORF, M., ETZRODT, M., WILDGRUBER, M., CORTEZ-RETAMOZO, V., PANIZZI, P., FIGUEIREDO, J. L., KOHLER, R. H., CHUDNOVSKIY, A., WATERMAN, P., AIKAWA, E., MEMPEL, T. R., LIBBY, P., WEISSLEDER, R. & PITTET, M. J. 2009. Identification of splenic reservoir monocytes and their deployment to inflammatory sites. *Science,* 325**,** 612-6.

TANAKA, Y. & MARTIN MOLA, E. 2014. IL-6 targeting compared to TNF targeting in rheumatoid arthritis: studies of olokizumab, sarilumab and sirukumab. *Ann Rheum Dis,* 73**,** 1595-7.

TANSLEY, S. L., BETTERIDGE, Z. E., GUNAWARDENA, H., JACQUES, T. S., OWENS, C. M., PILKINGTON, C., ARNOLD, K., YASIN, S., MORAITIS, E., WEDDERBURN, L. R., MCHUGH, N. J. & GROUP, U. K. J. D. R. 2014a. Anti-MDA5 autoantibodies in juvenile dermatomyositis identify a distinct clinical phenotype: a prospective cohort study. *Arthritis Res Ther,* 16**,** R138.

TANSLEY, S. L., BETTERIDGE, Z. E., SHADDICK, G., GUNAWARDENA, H., ARNOLD, K., WEDDERBURN, L. R., MCHUGH, N. J. & JUVENILE DERMATOMYOSITIS RESEARCH, G. 2014b. Calcinosis in juvenile dermatomyositis is influenced by both anti-NXP2 autoantibody status and age at disease onset. *Rheumatology (Oxford),* 53**,** 2204-8.

TANSLEY, S. L. & MCHUGH, N. J. 2014. Myositis specific and associated autoantibodies in the diagnosis and management of juvenile and adult idiopathic inflammatory myopathies. *Curr Rheumatol Rep,* 16**,** 464.

TEAM, R. C. 2015. R: A Language and Enviroment for Statistical Computing. *R Foundation for Statistical Computing*.

TISSEVERASINGHE, A., BERNATSKY, S. & PINEAU, C. A. 2009. Arterial events in persons with dermatomyositis and polymyositis. *J Rheumatol,* 36**,** 1943-6.

TODD, S. K., PEPPER, R. J., DRAIBE, J., TANNA, A., PUSEY, C. D., MAURI, C. & SALAMA, A. D. 2014. Regulatory B cells are numerically but not functionally deficient in anti-neutrophil cytoplasm antibody-associated vasculitis. *Rheumatology (Oxford),* 53**,** 1693-703.

TOURNADRE, A. & MIOSSEC, P. 2012. Interleukin-17 in inflammatory myopathies. *Curr Rheumatol Rep,* 14**,** 252-6.

TOURNADRE, A., PORCHEROT, M., CHERIN, P., MARIE, I., HACHULLA, E. & MIOSSEC, P. 2009. Th1 and Th17 balance in inflammatory myopathies: interaction with dendritic cells and possible link with response to high-dose immunoglobulins. *Cytokine,* 46**,** 297-301.

TRALLERO-ARAGUAS, E., RODRIGO-PENDAS, J. A., SELVA-O'CALLAGHAN, A., MARTINEZ-GOMEZ, X., BOSCH, X., LABRADOR-HORRILLO, M., GRAU-JUNYENT, J. M. & VILARDELL-TARRES, M. 2012. Usefulness of anti-p155 autoantibody for diagnosing cancer-associated dermatomyositis: a systematic review and meta-analysis. *Arthritis Rheum,* 64**,** 523-32.

TRINCHIERI, G. 2010. Type I interferon: friend or foe? *J Exp Med,* 207**,** 2053-63.

VAN FURTH, R. & COHN, Z. A. 1968. The origin and kinetics of mononuclear phagocytes. *J Exp Med,* 128**,** 415-35.

VAN ZELM, M. C., SZCZEPANSKI, T., VAN DER BURG, M. & VAN DONGEN, J. J. 2007. Replication history of B lymphocytes reveals homeostatic proliferation and extensive antigen-induced B cell expansion. *J Exp Med,* 204**,** 645-55.

VARSANI, H., CHARMAN, S. C., LI, C. K., MARIE, S. K., AMATO, A. A., BANWELL, B., BOVE, K. E., CORSE, A. M., EMSLIE-SMITH, A. M., JACQUES, T. S., LUNDBERG, I. E., MINETTI, C., NENNESMO, I., RUSHING, E. J., SALLUM, A. M., SEWRY, C., PILKINGTON, C. A., HOLTON, J. L., WEDDERBURN, L. R. & GROUP, U. K. J. D. R. 2015. Validation of a score tool for measurement of histological severity in juvenile dermatomyositis and association with clinical severity of disease. *Ann Rheum Dis,* 74**,** 204-10.

VENALIS, P. & LUNDBERG, I. E. 2014. Immune mechanisms in polymyositis and dermatomyositis and potential targets for therapy. *Rheumatology (Oxford),* 53**,** 397-405.

WADDINGTON, K. E. & JURY, E. C. 2015. Manipulating membrane lipid profiles to restore T-cell function in autoimmunity. *Biochem Soc Trans,* 43**,** 745-51.

WALSH, R. J., KONG, S. W., YAO, Y., JALLAL, B., KIENER, P. A., PINKUS, J. L., BEGGS, A. H., AMATO, A. A. & GREENBERG, S. A. 2007. Type I interferon-inducible gene expression in blood is present and reflects disease activity in dermatomyositis and polymyositis. *Arthritis Rheum,* 56**,** 3784-92.

WANG, D. X., LU, X., ZU, N., LIN, B., WANG, L. Y., SHU, X. M., MA, L. & WANG, G. C. 2012. Clinical significance of peripheral blood lymphocyte subsets in patients with polymyositis and dermatomyositis. *Clin Rheumatol,* 31**,** 1691-7.

WANG, Y. J., LII, Y. P., LAN, J. L., CHI, C. S., MAK, S. C. & SHIAN, W. J. 1993. Juvenile and adult dermatomyositis among the Chinese: a comparative study. *Zhonghua Yi Xue Za Zhi (Taipei),* 52**,** 285-92.

WASKOW, C., LIU, K., DARRASSE-JEZE, G., GUERMONPREZ, P., GINHOUX, F., MERAD, M., SHENGELIA, T., YAO, K. & NUSSENZWEIG, M. 2008. The receptor tyrosine kinase Flt3 is required for dendritic cell development in peripheral lymphoid tissues. *Nat Immunol,* 9**,** 676-83.

WEDDERBURN, L. R., VARSANI, H., LI, C. K., NEWTON, K. R., AMATO, A. A., BANWELL, B., BOVE, K. E., CORSE, A. M., EMSLIE-SMITH, A., HARDING, B., HOOGENDIJK, J., LUNDBERG, I. E., MARIE, S., MINETTI, C., NENNESMO, I., RUSHING, E. J., SEWRY, C., CHARMAN, S. C., PILKINGTON, C. A., HOLTON, J. L. & GROUP, U. K. J. D. R. 2007. International consensus on a proposed score system for muscle biopsy evaluation in patients with juvenile dermatomyositis: a tool for potential use in clinical trials. *Arthritis Rheum,* 57**,** 1192-201.

WENZEL, J., SCHMIDT, R., PROELSS, J., ZAHN, S., BIEBER, T. & TUTING, T. 2006. Type I interferon-associated skin recruitment of CXCR3+ lymphocytes in dermatomyositis. *Clin Exp Dermatol,* 31**,** 576-82.

YANG, M., CEN, X., XIE, Q., ZUO, C., SHI, G. & YIN, G. 2013. Serum interleukin-6 expression level and its clinical significance in patients with dermatomyositis. *Clin Dev Immunol,* 2013**,** 717808.

YE, J., COULOURIS, G., ZARETSKAYA, I., CUTCUTACHE, I., ROZEN, S. & MADDEN, T. L. 2012. Primer-BLAST: a tool to design target-specific primers for polymerase chain reaction. *BMC Bioinformatics,* 13**,** 134.

YEE, C. S., CRESSWELL, L., FAREWELL, V., RAHMAN, A., TEH, L. S., GRIFFITHS, B., BRUCE, I. N., AHMAD, Y., PRABU, A., AKIL, M., MCHUGH, N., D'CRUZ, D., KHAMASHTA, M. A., ISENBERG, D. A. & GORDON, C. 2010. Numerical scoring for the BILAG-2004 index. *Rheumatology (Oxford),* 49**,** 1665-9.

YORK, A. G., WILLIAMS, K. J., ARGUS, J. P., ZHOU, Q. D., BRAR, G., VERGNES, L., GRAY, E. E., ZHEN, A., WU, N. C., YAMADA, D. H., CUNNINGHAM, C. R., TARLING, E. J., WILKS, M. Q., CASERO, D., GRAY, D. H., YU, A. K., WANG, E. S., BROOKS, D. G., SUN, R., KITCHEN, S. G., WU, T. T., REUE, K., STETSON, D. B. & BENSINGER, S. J. 2015. Limiting Cholesterol Biosynthetic Flux Spontaneously Engages Type I IFN Signaling. *Cell,* 163**,** 1716-29.

YOUNG, M. D., WAKEFIELD, M. J., SMYTH, G. K. & OSHLACK, A. 2010. Gene ontology analysis for RNA-seq: accounting for selection bias. *Genome Biol,* 11**,** R14.

YU, D. T., CLEMENTS, P. J., PAULUS, H. E., PETER, J. B., LEVY, J. & BARNETT, E. V. 1974. Human lymphocyte subpopulations. Effect of corticosteroids. *J Clin Invest,* 53**,** 565-71.

YU, Y.-W. & ZHANG, Q.-Y. 2005. Serum and urinary interleukin 6 levels in children with primary nephrotic syndrome. *CJCP*
, 7**,** 493-494.

ZIEGLER-HEITBROCK, L. 2015. Blood Monocytes and Their Subsets: Established Features and Open Questions. *Front Immunol,* 6**,** 423.

ZIEGLER-HEITBROCK, L., ANCUTA, P., CROWE, S., DALOD, M., GRAU, V., HART, D. N., LEENEN, P. J., LIU, Y. J., MACPHERSON, G., RANDOLPH, G. J., SCHERBERICH, J., SCHMITZ, J., SHORTMAN, K., SOZZANI, S., STROBL, H., ZEMBALA, M., AUSTYN, J. M. & LUTZ, M. B. 2010. Nomenclature of monocytes and dendritic cells in blood. *Blood,* 116**,** e74-80.

ZONG, M., DORPH, C., DASTMALCHI, M., ALEXANDERSON, H., PIEPER, J., AMOUDRUZ, P., BARBASSO HELMERS, S., NENNESMO, I., MALMSTROM, V. & LUNDBERG, I. E. 2014. Anakinra treatment in patients with refractory inflammatory myopathies and possible predictive response biomarkers: a mechanistic study with 12 months follow-up. *Ann Rheum Dis,* 73**,** 913-20.

ZUNIGA-PFLUCKER, J. C. 2004. T-cell development made simple. *Nat Rev Immunol,* 4**,** 67-72.